

MID-MIOCENE RHYOLITE SEQUENCE, HIGHLAND RANGE, NV: RECORD OF
MAGMA EVOLUTION AND ERUPTION FROM THE SEARCHLIGHT PLUTON
MAGMA CHAMBER

By

Lindy Lee Colombini

Thesis

Submitted to the Faculty of the
Graduate School of Vanderbilt University
in partial fulfillment of the requirements
for the degree of

MASTER OF SCIENCE

In

Earth and Environmental Sciences

August, 2009

Nashville, Tennessee

Approved:

Professor Calvin F. Miller

Professor Guilherme Gualda

To God who gave me science.

ACKNOWLEDGMENTS

Above all I would like to thank Dr. Calvin Miller for his patience, understanding and guidance that made this project possible. When I would get discouraged with life and my surroundings, he was there, setting an example to show me how satisfying that can be to learn and think about anything, but mostly geology. Also, I am forever grateful of Calvin for showing me the best way to prepare grits.

I also would like to thank Dr. Guil Gaulda for his patience as well, and for taking the time to explain, in detail, the many concepts of magmas that I didn't have a strong grasp of. I also appreciate his flexibility in scheduling meetings and his ability to see the humor in many situations. Laughing always makes things easier.

A special thanks goes out to Nick Hinz for his observations and discussions in the field. I also want to thank my many field assistants, Jenny Murphy, Ayla Pamukcu, Prakash Dahkal, Tamara Carley, my brother Nathan Straathof, and my husband Josh Colombini. I received plenty of help at the SHRIMP lab and would like to thank Joe Wooden, Frank Mazdab, Ashley Bromley, Tamara Carley, Lily Claiborne, and Danny Flanagan.

Last, I would like to thank my husband, Josh Colombini for his unending support. When I was injured and couldn't walk, he never complained and was always happy to get up early, even on his days off, to help me get ready for school, and he even continued to help me after I healed. Without those happy mornings and his endless encouragement, I would never have been able to get through many days. Especially for his smile, I thank him.

TABLE OF CONTENTS

	Page
DEDICATION	ii
ACKNOWLEDGMENTS	iii
LIST OF TABLES	vii
LIST OF FIGURES	viii
Chapter	
I. INTRODUCTION	9
II. GEOLOGIC SETTING OF THE HIGHLAND RANGE, SOUTHERN NEVADA	11
III. METHODS	15
IV. HIGHLAND RANGE SILICIC SEQUENCE.....	19
Unit Descriptions	19
Contact Descriptions.....	34
Ages	37
Geochemistry	39
V. ERUPTION OF THE HIGHLAND RANGE SILICIC SEQUENCE	46
Unit Deposition.....	46
Eruptive Transition	48
Modern Analogue	51
VI. COMPOSITION OF HIGHLAND RANGE SPHENE AND ZIRCON: ZONING, ELEMENT PARTITIONING, ESTIMATED TEMPERATURES OF GROWTH, AND IMPLICATIONS FOR MELT EVOLUTION	56
Zircon	56
Sphene.....	57
Estimating Temperatures from Zircon and Sphene Thermometry	71
Implications of estimated temperatures	75
Sphene Effects on Magma Processes.....	81

VII. VOLCANO – PLUTON CONNECTION: RELATION BETWEEN SEARCHLIGHT PLUTON AND THE HIGHLAND RANGE SILICIC SEQUENCE	86
Searchlight Pluton	86
Searchlight pluton – Highland Range Connection.....	87
VIII. CONCLUSIONS.....	90
Appendix	
A. PETROGRAPHY AND PHOTOMICROGRAPHS OF THE HIGHLAND RANGE SILICIC SEQUENCE.....	92
B. WHOLE ROCK GEOCHEMISTRY OF THE HIGHLAND RANGE SILICIC SEQUENCE.....	168
C. U-PB GEOCHRONOLOGY, PROBABILITY DENSITY CURVES AND CATHODOLUMINESCENCE IMAGES OF ZIRCONS FROM THE HIGHLAND RANGE SILICIC SEQUENCE.....	177
D. ZIRCON ELEMENTAL DATA FROM THE HIGHLAND RANGE SILICIC SEQUENCE.....	211
E. SPHENE ELEMENTAL DATA AND BACKSCATTER ELECTRON EMAGES FROM THE HIGHLAND RANGE SILICIC SEQUENCE, SHRIMP-RG ANALYSIS.....	228
F. AR-AR DATA AND METHOD OF THE HIGHLAND RANGE SILICIC SEQUENCE.....	284
G. GLASS MAJOR ELEMENTAL DATA OF THE HIGHLAND RANGE SILICIC SEQUENCE, ELECTRON MICROPROBE ANALYSIS	289
H. OPERATING CONDITIONS, TRACE ELEMENTAL DATA OF GLASS FROM THE HIGHLAND RANGE SILICIC SEQUENCE, LASER ABLATION – INDUCTIVELY COUPLED PLASMA MASS SPECTROMETER.....	292
I. ESTIMATED TEMPERATURES FOR ZIRCON AND SPHENE SPOT ANALYSES OF THE HIGHLAND RANGE SILICIC SEQUENCE	310
REFERENCES	314

LIST OF TABLES

Table	Page
1. Ar-Ar and zircon ages for the Highland Range silicic sequence	40
2. Major and trace element abundances from whole rock analysis of lavas and pumices, separated by unit.....	41
3. Calculation of estimated partition coefficients (K) for REE in sphene	69
4. Activities of SiO ₂ and TiO ₂ and pressure values used to estimate the temperatures from the analysis of zircon and sphene.....	72
5. Zircon saturation temperatures	75

LIST OF FIGURES

Figure	Page
1. Geology of the northern Colorado River extensional corridor	12
2. Photograph and geologic map of the Highland Range silicic sequence	13
3. Photograph of the Highland Range silicic sequence, divided into units.....	20
4. Examples of enclaves from units Thr 1 and Thr 2.....	23
5. Field examples of flow banding and lava breccia.....	26
6. Block and ash flow of the north eastern section of Thr 3	27
7. Photograph examples of bedded tuffs from Tht 1 and Tht 2	30
8. Photomicrographs showing phenocrysts assemblages.....	33
9. Stratigraphic section of Highland Range silicic sequence.....	37
10. Contact of Thrd with Tht 2	38
11. Diagrams comparing TiO ₂ , K ₂ O, and Fe ₂ O ₃ (wt%), and Ba, Sr, and Gd (ppm) to SiO ₂ wt%	42
12. Diagram of volatile release from injected warmer mafic magma into the cooler siliceous magma.....	51
13. Examples of ash from Lipari volcano and the Highland Range silicic sequence	54
14. Representative images zircon and sphene.....	60
15. REE diagrams from zircon analysis.....	62
16. REE diagrams from sphene analysis.....	65
17. Partition coefficients for sphene REE.....	70
18. Average REE concentrations from glass analyses.....	71
19. Temperature histogram comparing sphene temperature estimates to zircon temperature estimates.....	76

20.	Histograms of temperature estimates of sphene sorted by sample	77
21.	REE diagrams from figure 1, Glazner <i>et al.</i> 2008	83
22.	Comparison of leucogranite REE concentrations from Searchlight pluton to the high silica rhyolite REE concentrations from the Highland Range silicic sequence and Gd anomaly vs. SiO ₂	84
23.	Reconstructed cross section of the Searchlight pluton divided into its three units, the Upper, Middle, and Lower Searchlight.....	87
24.	Suggested correlation between contacts in the Searchlight pluton and those in the Highland Range silicic sequence	89

CHAPTER I

INTRODUCTION

Understanding magmatic systems is important both because of their direct impacts on humans and because of their fundamental role in Earth processes. The more scientists know about how these systems work, the better they can predict volcanic eruptions and minimize their impacts on humans and society (Scandone *et al.* 2007). Beyond this practical impact, understanding how magmas form and evolve by melting in the deep crust and mantle and then ascend, are emplaced, exchange energy and mass with their host rocks, and in some cases erupt provides critical insights into the evolution of the Earth.

The products of a volcanic system can be split into two major parts, the volcanic rocks that form above ground and the plutonic rocks that form below ground. The pluton records events in the magma chamber that happen during the final stages of magma cooling, though it is possible that earlier events in the magma chamber's history are not completely erased by late stage events (Metcalf 2004; Miller and Miller 2002; Hawkins and Wiebe 2004; Bachmann *et al.* 2007). In contrast, volcanic rocks record an instantaneous "snapshot" of the state of the system during the eruption (Bachmann *et al.* 2007).

The purpose of this study is to better understand the geochemical "snapshot" provided by the silicic portion of the Miocene Highland Range volcanic sequence and how it relates to the nearby Searchlight plutonic rocks. I describe the petrology and

physical characteristics of the silicic portion of the Highland Range volcanic sequence to evaluate pre-eruptive chamber conditions and magma evolution and eruptive processes. I then compare these characteristics and evaluations to those existing data for the Searchlight pluton to evaluate connections between the two and refine understanding of the history of this system.

CHAPTER II

GEOLOGIC SETTING OF THE HIGHLAND RANGE, SOUTHERN NEVADA

Located in the western part of the northern Colorado River extensional corridor (CREC), the Highland Range is generally tilted about 70 degrees to the northwest (Olsen *et al.* 1999). The CREC is an extensional belt that is about 50-100 km wide, with extension starting at ~15.5-16.2 Ma and ending about 10-14 Ma (Faulds *et al.* 2001). Volcanism in the region started about 19 Ma, before the onset of extension, and slowed during peak extension or the period of maximum tilting (Faulds *et al.* 2001).

The 3.5 km thick, early to middle Miocene volcanic sequence of the Highland Range, rests upon Early Proterozoic gneiss and amphibolite (figure 1; Faulds *et al.* 2002a). The sequence can be divided into two parts: (1) the central domain comprised of thick mafic to intermediate lavas covered by two rhyolitic ash-flow tuffs, conglomerate, and isolated basalt lavas (Faulds *et al.* 2002a); and (2) the southern domain thought to be related to the nearby Searchlight pluton in the southern Eldorado Mountains. The southern domain is made up of, from bottom to top, a 1.5 km thick layer of trachyandesite lava, a 1 km thick section of trachydacite lava and rhyolitic lavas and tuffs, and topped by a thick layer of basaltic andesite, all covered by middle to late Miocene conglomerate and megabreccia (Faulds *et al.* 2002a) (figure 2). This sequence is exposed several times throughout the southern Highland Range as separate fault blocks. In this study we looked at the best exposure of the silicic part of the sequence (trachydacite-rhyolite, hereafter referred to as the Highland Range silicic sequence).

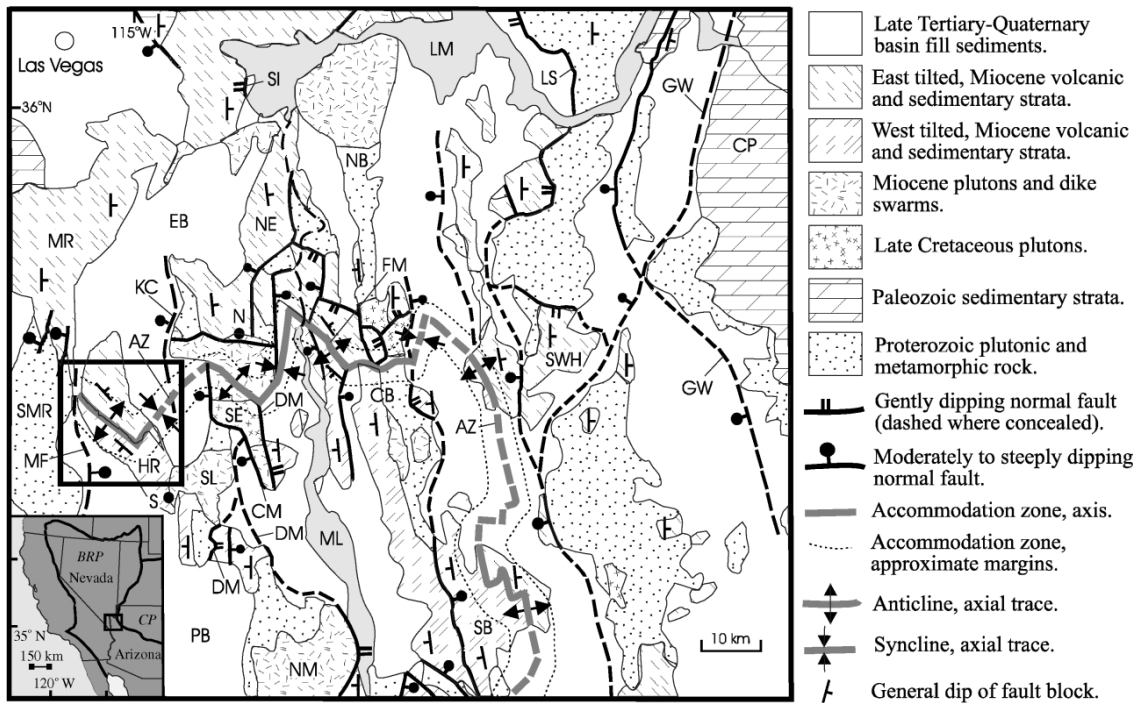


Figure 1. Geology of the northern Colorado River extensional corridor. Box outlines the Highland Range. Notice Searchlight pluton (SL) is located outside the southeast corner of the box. BRP, Basin and Range province (insert); CB, central Black Mountains; CM, Copper Mountian fault; CP, Colorado Plateau; DM, Dupont Mountain fault; EB, Eldorado basin; FM, Fire Mountain anticline; GW, Grand Wash fault zone; HR, Highland Range; KC, Keyhole Canyon fault; LM, Lake Mead; LS, Lakeside Mine-Salt Spring Wash fault; MF, McCullough Range fault; ML, Lake Mohave; MR, McCullough Range; N, Nelson, Nevada; NB, northern Black Mountains; NE, norhtern Eldorado Moutnains; NM, Newberry Mountains; PB, Piute basin; SB, southern Black Moutnains; S, Searchlight, Nevada; SE, southern Eldorado Mountains; SI, Saddle Island fault; SMR, southern McCullough Range; SWH, Southern White Hills (Faulds *et al.* 2002a).

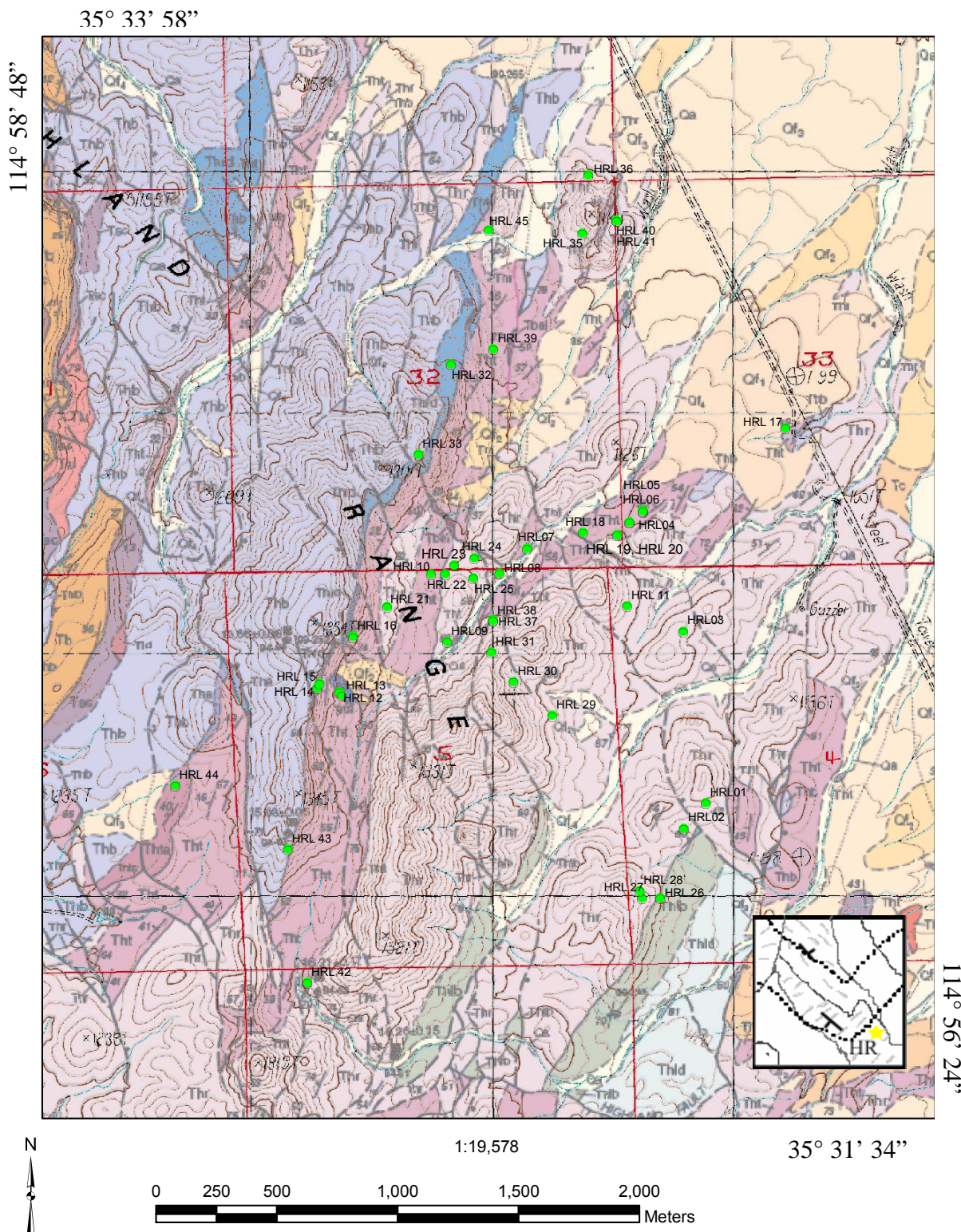
A)



Figure 2. A) Field view of the Highland Range silicic sequence, looking east. The light cream colored rocks are tuffs and the darker brown rocks in the center and right are silicic lavas. Dark gray rocks in foreground and at far left are overlying basalt. B) Geologic map of Highland Range silicic sequence. Inset refers to figure 1, and star represents location of map. The green symbols represent sample locations for this study. Map is adapted from Faulds *et al.* 2002b; details and unit descriptions can be found in Faulds *et al.* 2002c.

Figure 2, continued

B)



CHAPTER III

METHODS

I spent a total of 25 days in the field mostly studying the Highland Range volcanic sequence and a smaller amount of time in the Searchlight pluton collecting samples and making field observations. Field studies built upon those of Faulds *et al.* (2002b) excellent 1:24 000 map. My observations included contact relationships, enclave description and abundance, and rock unit descriptions. Stratigraphic-section notes were taken describing the tuff units in both small and large scale. A total of sixty-six samples were collected from the sequence, including 30 from lava and 36 from tuffs (including pumice samples).

Fifty four thin sections of representative samples were prepared by Idaho Petrographics. I then used thin section microscopy to describe mineral assemblages and textural relations (appendix A).

I selected and powdered 25 samples of rhyolite lava and pumice using an alumina ceramic shatterbox at Vanderbilt University. Twenty five grams of powder were mailed to Actlabs-Ancaster, Ontario, Canada where they were analyzed for their elemental compositions. Methods used at Actlabs include inductively coupled plasma mass spectrometry (ICP-MS), instrumental neutron activation analysis (INAA), and x-ray fluorescence (XRF). Appendix B presents the whole rock geochemistry results.

Three samples were selected for detailed zircon work, HRL 12a, HRL 14a, and HRL 27. I separated zircons from samples HRL 12a and HRL 14a at Vanderbilt

University by standard heavy mineral separation techniques. Ayla Pamukcu applied dissolution techniques to separate sparse zircons from sample HRL 27. She soaked 2-5 grams of rock sample in fluoroboric acid until the quartz and plagioclase dissolved and the rock sample broke down. She then used heavy liquids and hand picking to separate the zircons. Selected zircon grains from all three samples were mounted by Danny Flanagan in epoxy, polished, and imaged by cathodoluminescence using a scanning electron microscope at the USGS-Stanford SHRIMP lab. I performed elemental and U-Pb analyses of the mounted zircons using the USGS-Stanford reverse geometry sensitive high resolution ion microprobe (SHRIMP-RG). R33 (419 Ma) and CZ3 (U 550 ppm) were used as zircon standards (for details on techniques used see Claiborne *et al.* 2006; Walker *et al.* 2007). See appendix C for zircon U/Pb ages and appendix D for trace element results.

Sphene grains from 4 different samples were analyzed by me at the SHRIMP-RG for trace element compositions. I separated sphene phenocrysts from samples HRL 12a and HRL 14a by the same methods used for zircon separation from these samples. From samples HRL 21 and HRL 19a, I separated sphene phenocrysts by coarsely crushing the hand sample and hand picking out the grains. This allowed for the collection of whole sphene grains, including grains with glass still attached to the faces of the grain. Danny Flanagan mounted and imaged selected sphene grains at the SHRIMP lab by methods identical to the zircons, except that backscattered electron imaging rather than cathodoluminescence was used. I performed elemental analyses by SHRIMP-RG using methods developed by Mazdab *et al.* (2007), using standard BLR. See appendix E for sphene elemental results.

A set of five samples collected from key stratigraphic horizons were selected for Ar-Ar dating at the New Mexico Tech Geochronology Research center to provide highly precise eruption ages. There, alkali feldspars were heated with the CO₂ laser and analyzed by single crystal fusion (McDowell, McIntosh & Farley 2004). Abbreviated analytical methods and argon isotopic results for the samples are given in appendix F.

I used the a Cameca SX-50 electron microprobe(EMP) outfitted with an energy dispersive system (EDS) at the University of Tennessee-Knoxville EMP Laboratory to analyze glasses from seven samples for major and minor elements. Samples HRL 14a, HRL 12a, and HRL 27 were analyzed as thin sections. Samples HRL 10b, HRL 21, and HRL 16 were made into a single epoxy mount, which was analyzed. I picked the analysis spots in order to limit the amount of microlite contamination in the analyses. Any spurious data was removed. See appendix G for glass results and EMP operating conditions.

I determined trace element abundances of glasses by laser ablation-inductively coupled plasma mass spectrometry (LA-ICPMS) at Vanderbilt University (a New Wave/Merck UP-213 nm Laser Ablation unit connected to a Perkin Elmer Elan 6100 DRC ICPMS). I mounted small pieces (~1 cm³) of samples HRL 10b, HRL 16, HRL 21, and HRL 27 in epoxy and hand polished down to 1000 grit. We used a 60 µm spot, 10 Hz laser, and 0.85 L/min He flow, and counting times were 60s for background and 60s for signal. Detailed operating conditions can be found in appendix H, along with the results for the 43 analytes. NIST 610 was used as a primary standard, and NIST 612 as a secondary standard. We treated the data with Glitter data reduction software (Griffen *et al.*, 2008) developed by GEMOC (<http://www.glitter-gemoc.com>). Due to the possibility

of including microlites within the ablated volume, we analyzed between 10 and 20 spots per sample, and removed spurious data indicative of contamination by microlites. Averages presented in appendix H exclude these spurious data.

CHAPTER IV

HIGHLAND RANGE SILICIC SEQUENCE

Unit Descriptions

The Highland Range silicic sequence observed in this thesis is about 1700 m thick. Faulds *et al.* (2002b and 2002c) divided the silicic sequence into four rock units, Tht (tuff), Thr (rhyolite lava), Thrd (rhyodacite lava) (see descriptions and map in Faulds et al. 2002b and c) (figure 2,3). I further subdivided the units, Tht and Thr, into sub-units, Tht 1, Tht 2, Thr 1, Thr 2, and Thr 3. This chapter includes my description of all 7 of my units, plus brief descriptions of the immediately underlying and overlying units. Detailed descriptions of all the thin sections and samples collected can be found in appendix A.

Thlb

Faulds *et al.* (2002b and 2002c) describes this underlying unit as “biotite-rich trachydacite-trachyandesite lavas.” It underlies the silicic sequence that was the subject of this study. Lava near its top contains phenocrysts of euhedral biotite (1-2mm) and subhedral to euhedral plagioclase (0.7-1cm) that are visible in hand sample. In thin section a single sample contains phenocrysts of plagioclase, clinopyroxene, and biotite. About 70% of the sample is a devitrified glass groundmass, and the phenocrysts define a foliation (flow fabric?).

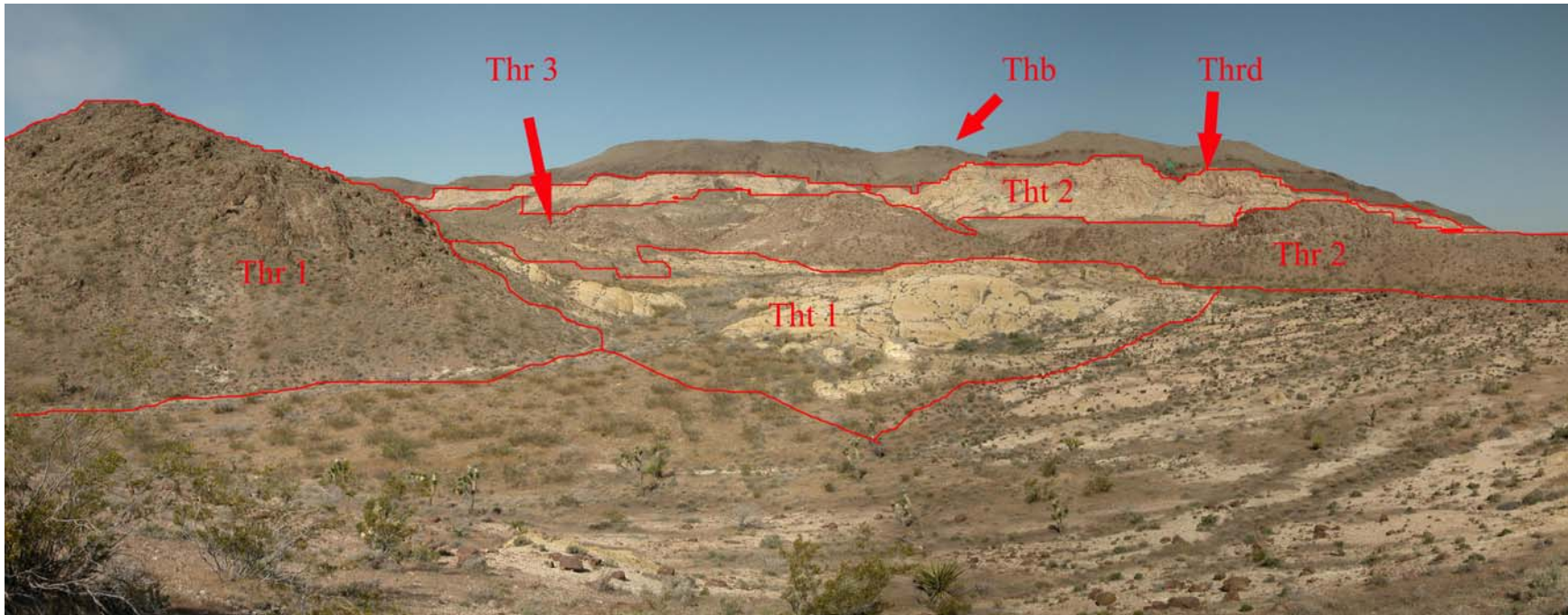


Figure 3. Photograph of the Highland Range silicic sequence, divided into units. Thr 1 and Thr 2 are trachydacite and rhyolite lavas, respectively; Tht 1 and Tht 2 are the tuffs; Thr 3 (upper rhyolite lava) is hidden behind Thr 2 and is not visible in the picture; Thrd is a thin layer of lava just above the red line of Tht 2; and Thb is the overlying basaltic andesite.

Thr

This unit was described by Faulds *et al.* (2002b and 2002c) as rhyolite lavas. I found it to include both silicic trachydacite lava in its lower portion and rhyolite lava in its upper portions and therefore have separated out unit Thr 1 (lower portion, trachydacite). I further subdivided the upper lavas into Thr 2 (lower rhyolite lava flows), and Thr 3 (upper high-silica rhyolite lava flows, enclosed within the upper tuffs, Tht 2).

Thr 1: trachydacite lavas

The trachydacite lava section is about 1350 m thick. These lavas exhibit strong flow banding locally throughout, especially in the upper part of the section. The thin sections (HRL 1, HRL 2, HRL 3, HRL 11, HRL 27, HRL 28, HRL 29, HRL 30, HRL 31, and HRL 42) from the unit show a phenocryst assemblage of plagioclase, clinopyroxene, and biotite, with 50-80% groundmass that is locally vitrophyric but generally devitrified. Microlites (probably mostly feldspar) are abundant. Inclusions are not abundant in thin section, but clumps of large plagioclase and clinopyroxene grains may represent portions of disaggregated enclaves.

We estimated that it contains <<0.01% of relatively mafic enclaves, based upon well-exposed, SE-NW (up-section) transect that appeared to be typical.¹¹ These small, round to angular enclaves (figure 4A) range from about 1-15 cm in maximum dimension, and are typically about 1 x 1 cm in exposed cross section.

¹¹ We noted 54 enclaves in the traverse, which focused on the best exposed meter wide zone within the canyon. The traverse was ~420 m long, and approximately half was covered by alluvium, thus yielding an investigated area of about ~210 m². Most enclaves were near 1 cm² or less in cross-sectional area, with few more than 2 cm² and a single outlier at 50 cm². We thus estimated that the total area of observed enclaves was very roughly 100 cm², or on the order of ~5 x 10⁻⁵ % or <<0.01%.

Thr 2: lower rhyolite lavas

Most of this unit in the study area has a thickness of about 250 m, but it pinches out near the southwestern end, and widens slightly at the northeastern end. The lava shows flow banding locally at the top and bottom parts of the unit, and also has a glassy texture in these areas. It was possibly emplaced as one, or possibly as several thick units.

Thin sections (HRL 23a, HRL 23b, HRL 24, and HRL 25) of Thr 2 have 0-10% quartz phenocrysts. Other phenocrysts include sanidine, plagioclase, biotite, sphene and in some cases, clinopyroxene and/or zircon. The groundmass consists of 70 – 85% variably devitrified glass.

Thr 2 rhyolite lavas contain more abundant enclaves, locally up to at least 10%, of exposed area (figure 4B). Most of the enclaves appear to be magmatic, with crenulate margins. The enclaves can be subdivided into two types. Mafic enclaves are smaller (5-7 cm) and more regular in shape and have a less crenulate margin; more silicic enclaves are larger (5-30 cm) and irregularly shaped and seem to be swirled into the host rhyolite. Mafic enclaves contain phenocrysts of plagioclase, clinopyroxene, and a heavily altered mineral that was mostly likely olivine.

Thr 3: upper rhyolite lavas

Lavas in the upper part of the section are high-silica rhyolites. This unit contains two different sections, though flow banding is evident throughout the unit (figure 5A). The lower, smaller section, composed of light grey obsidian, reaches a maximum thickness of about 130 m. It is completely surrounded by the rhyolite tuffs of Tht 2. Weathering and silicification is apparent near the contacts. The larger unit, in the northeastern part of the field area is ~ 280 m thick and is mostly composed of block-and-



Figure 4. A) Enclaves found in Thr 1 (trachydacite lava). The enclaves are small and angular to rounded. The large enclave in the picture is anomalous and not representative of the sizes of enclaves in the unit. The small enclave (arrow) is typical. B) Enclaves found in Thr 2 (high silica rhyolite). The enclaves are large and abundant with crenulated edges.

ash flows, with lesser flow banded lavas. The lavas grade into clast-rich block-and-ash flows, and blocks include both lava and weakly vesiculated lava/pumic. A thin lens of tuff (Tht 2) is exposed near the center of the unit (figure 6).

Sparse phenocrysts of quartz, sanidine, plagioclase, sphene and biotite constitute about 5% of the rocks. The glassy groundmass comprises the remaining 95%. Sphericalites (1 cm) are abundant throughout the unit.

Tht

This unit was described by Faulds *et al.* (2002b and 2002c) as tuffaceous sedimentary rocks and non-welded tuffs. I subdivided Tht into Tht 1 and Tht 2 (see figure 3). Tht 1 contains the lower tuffs that underlie Thr 2 and is non-cliff forming. Tht 2 contains the upper tuffs and overlies Thr 2 and in its upper portion is cliff forming.

Tht 1: lower tuffs

This rhyolite tuff is about 160 m thick, but pinches out at the southwestern end and widens at the northeastern end. The pumice and groundmass from this section both contain abundant quartz and plagioclase, as well as, less abundantly, sanidine, biotite, and clinopyroxene. Accessory minerals include, locally, sphene, zircon, opaques and apatite.

It can be split into two layer types: massive and finely bedded (figure 7A-D). The massive layers range from 1-6 m in thickness, are poorly sorted and are rich in lithic clasts. These clasts are all volcanic, and based on field identification and 7 thin sections, appear to range from basaltic andesite to trachydacite or low-silica rhyolite in composition. The clasts are angular to sub-rounded and range in size from about 3 mm (course sand) to 1 m boulders, with the majority being gravel size. The boulders commonly form horizons within the massive layers. Between the massive layers are

bedded layers that are about 20-40 cm thick. The bedding alternates from more massive beds with 3-10 mm clasts to planar laminated beds that contain smaller than 4 mm lithics and crystals. Some planar beds are lithic-free. There are very few pumice clasts found in either the massive or the bedded layers, and where present they are small (2-4 cm). Pumice clasts can get up to 10 cm at the contacts with the lavas (Thr 1 and Thr 2), but are generally absent. Locally, normal graded bedding is apparent in both types of layers.

Tht 2: upper tuffs

This rhyolite tuff is approximately 250 m thick at its southwestern end and thickness varies by about 100 m throughout the section. The tuffs and pumice samples contain abundant plagioclase, sanidine, and quartz, with clinopyroxene and biotite found in several samples. Of the tuffs, the glassy groundmass makes up ~15-20% of the sample in thin section. Of the pumice thin sections, the glassy groundmass is about 95% of the sample.

At its base, this unit is similar to Tht 1 with alternating poorly sorted massive layers and thinner, planar bedded layers. The lithics in the massive layers fine upwards in each layer, with the larger clasts at the bottom, slowly becoming smaller near the top of the layer. Moving up the section, the massive layers contain cobble-sized lithic clast horizons and no longer fine upwards. The upper part of the section lacks bedded layers. I split the massive layers into two types that alternate (figure 7E & F). One is about 5 m thick and contains coarse (gravel sized), sparse, well sorted lithic clasts. The second type of layer is ~ 2 m thick containing poorly sorted, darker colored, cobble-size clasts. Finally, the very top of the section is discontinuous tuffaceous sandstone up to at least 15 m thick. The



Figure 5. A) Flow banding from northeastern part of Thr 3. B) Flow banded lava breccia from the bottom of Thr 2.

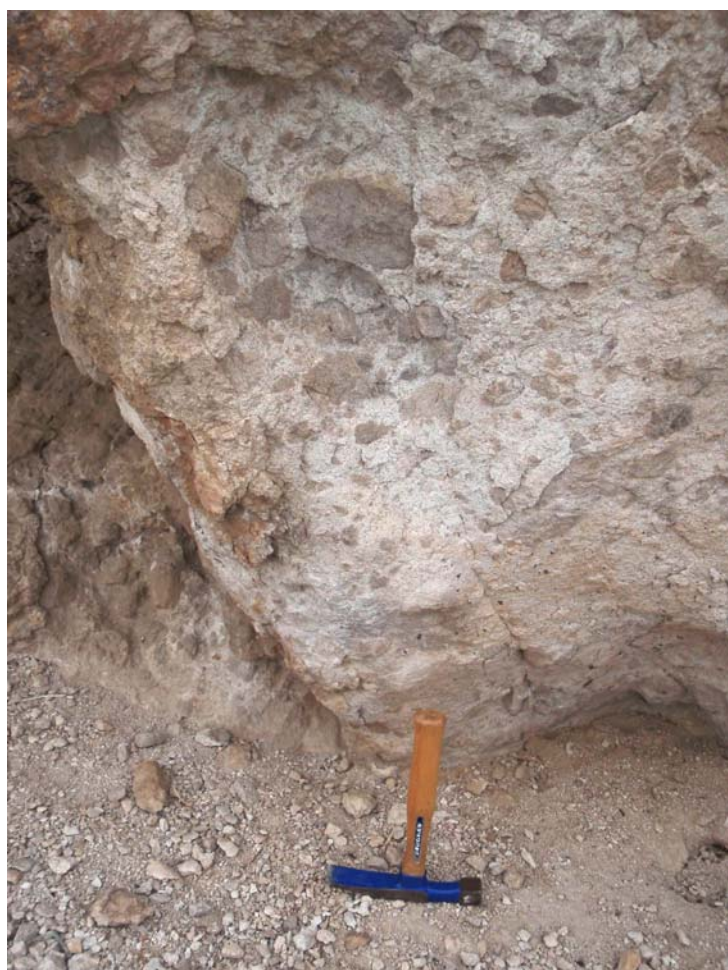


Figure 6. Block and ash flow of the north eastern section of Thr 3. Note how it grades upward from small to large pumice blocks.

abundance of pumice increases in this unit, with several layers that are dominated by large pumice blocks. Pumice fragments range from 2 to 15 cm.

Thrd

This unit was described by Faulds *et al.* (2002b and 2002c) as rhyodacite-rhyolite lavas. I describe it as a rhyolite breccia at the bottom meter that changes into glassy rhyolite lava. The unit ranges in thickness from ~25 m to ~50 m, being thinner and pinching out at the southwestern and northeastern parts of the section. The basal breccia contains clasts that are 5-20 cm in size in the form of lava blocks. The rhyolite lava contains phenocrysts of plagioclase, clinopyroxene, sanidine, quartz, biotite, and sphene, and has about 80% variably devitrified glass as groundmass.

There are two different types of very abundant enclaves throughout the unit. Both range from 5-10 cm. One enclave type is a dark gray, similar to the overlying basaltic andesite, and one is magenta in color, possibly more felsic. Both contain quartz and a dark mineral, possibly pyroxene or altered feldspar. Enclaves are both angular and ovoid with crenulate margins.

In addition to the abundant enclaves, Thrd shows clear textural evidence for open-system processes. This includes altered pseudomorphs after what appears to have been olivine and fragments of what appear to have disaggregated enclaves in the rhyolite host, and ubiquitous rounded, resorbed margins and reaction rims on sanidine, quartz, and sphene (figure 14E & F). This is consistent with the relatively low SiO₂ in the rhyolite glass – lower than expected for quartz-saturated melt.

Trdi

This unit was described by Faulds *et al.* (2002b and 2002c) as a rhyodacite plug. It is indeed a rhyolite porphyry plug intruded into the topmost part of Tht 2. It contains intermediate composition enclaves with crenulate edges that range from 1-15 cm. The margin of the intrusion is vitrophyric. The outcrop varies in color from lavender to dark red. Elsewhere, the porphyry contains ~75% devitrified groundmass and ~25% phenocrysts of sanidine, plagioclase, quartz, clinopyroxene, biotite and sphene.

The enclaves in this unit are ~5-15 cm in size with crenulate edges. There are two types, a darker type of enclave and a lighter type of enclave. These enclaves are similar to the ones found Thrd. This and identical mineral assemblage, age, and reaction textures in phenocrysts, very similar accessory mineral compositions (see chapter VI, figure 8), suggest that Trdi may be a source for Thrd. Their proximity to each other (~ 50 m) also is consistent with a relationship between the two units.

Thb

This unit was described by Faulds *et al.* (2002b and 2002c) as basaltic andesite lavas. Except for a brief inspection in the field, I did not study Thb, which overlies the silicic section. According to Faulds *et al.* (2002b and 2002c), it contains phenocrysts of plagioclase, clinopyroxene, and altered olivine (see Faulds 2002b and 2002c for more detailed description).

A)



B)



Figure 7. A) Tht 1 with the red arrows pointing to the massive tuffs and the green arrow pointing to the thinly bedded layers. B) Massive tuff found in Tht 1; note the slight internal bedding. C) Thinly bedded layers found in Tht 1; note the change in grain size and bedding from layer to layer. D) Fine-grained laminar bedded layers from Tht 1. The star indicates the poorly sorted lapilli massive layer with the fine grained ash fall layer (circle) on top. E) Massive tuffs of Tht 2. F) Individual massive tuff layers of Tht 2, red arrow points to an eagle's nest for scale.

Figure 7, continued

C)



D)

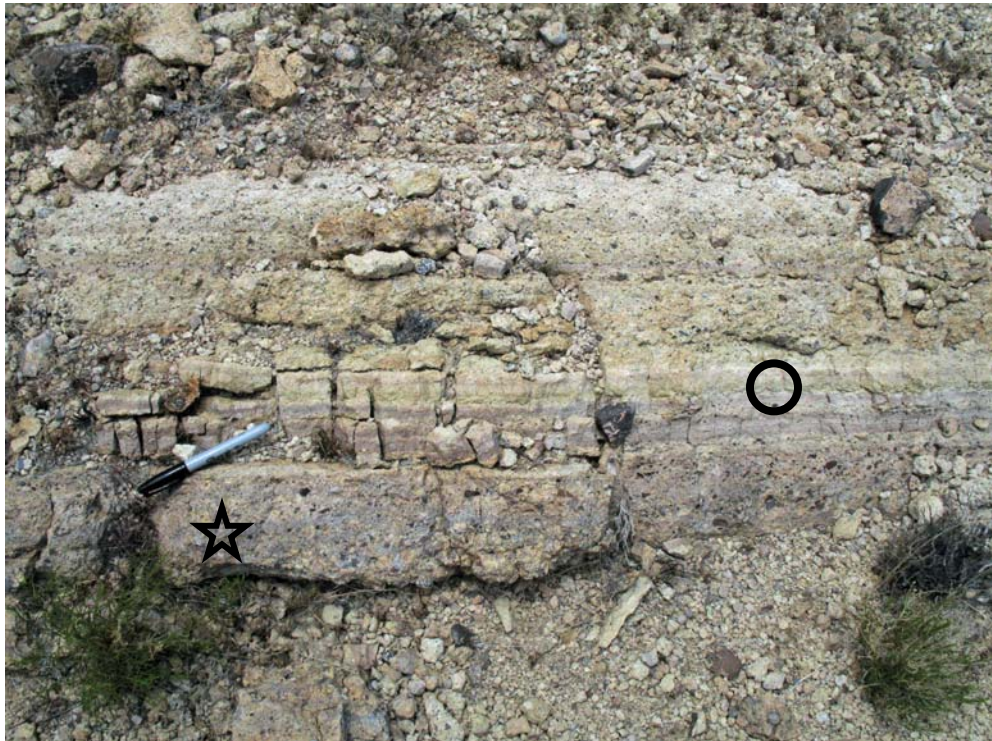


Figure 7, continued

E)



F)



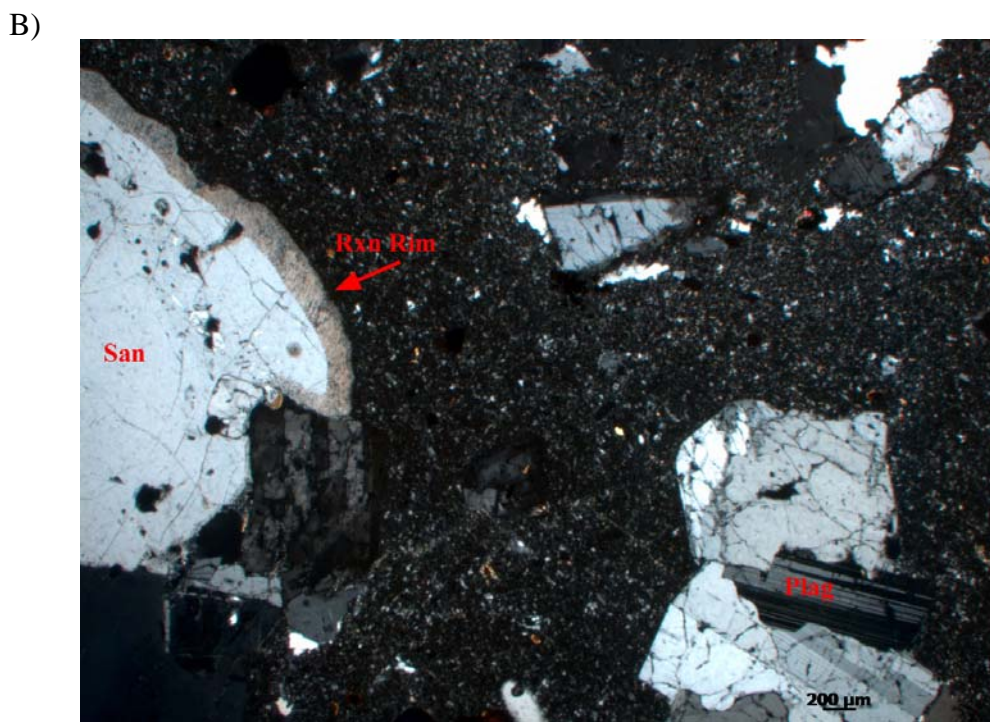


Figure 8. A) Phenocryst growth around a sanidine phenocryst from HRL 14a; B) Reaction rim on sanidine phenocryst from HRL 12a; C) Example phenocryst assemblage from HRL 14a. Note the reaction rim on the sanidine, and the highly altered mineral, possibly olivine, and the clinopyroxene.

Figure 8, continued

C)



Contact Descriptions

Observed visible contacts between the units of the Highland Range silicic sequence are described below (cf. figure 9).

A: Contact between trachyandesite (Thlb) lava and overlying trachydacite (Thr 1) lava:

Thr 1 at its base is glassy, with 2-3 m of porphyritic vitrophyre at the contact. The contact appears to be sharp between Thlb and Thr1, though a direct contact is difficult to see due to local scree.

B: Contact between Thr 1 (trachydacite lava) and overlying Tht 1 (lower rhyolite tuff):

The lava is altered, pale green to cream/white in color and grades upward into a

lava breccia (figure 5B) with 30 cm devitrified blocks. The blocks are flow banded. The matrix of the breccia appears to be ash. The breccia appears to grade into the overlying tuff, starting with a gravel to boulder-sized lithic-rich layer that grades into a massive (~5-7 m thick) pumice-rich tuff, which is then overlain by the more typical Tht 1 tuff described above.

C: Contact between Tht 1 and overlying lower rhyolite lava (Thr 2): The tuff grades into a lava breccia that contains several different types of clasts, including pumice, mafic enclaves, glassy lava blocks (some of which contain mafic enclaves), and pumice which can also contain mafic enclaves. The lava breccia then grades into a banded rhyolite lava flow.

D: Contact between Thr 2 and overlying Tht 2 (upper rhyolite tuff): Silicified at contact, the lava changes from being flow banded and filled with mafic enclaves, to a breccia with boulder-shaped lava blocks that are flow banded. There are small mafic enclaves mixed in with and within the lava blocks. The breccia grades into a pumice-rich tuff.

E: Contact between Tht 2 and base of overlying rhyolite lava (Thr 3): There are two large lenses of Thr 3, both enclosed within Tht 2. At one exposure of the basal contact of Thr 3, Tht 2 contains abundant gravel lithics and pumices and grades upward into a devitrified lava breccia that changes slowly from being devitrified into grey glassy obsidian.

F: Contact between Thr 3 and overlying tuff (Tht 2): The lava is flow banded and silicified. The lava grades from being obsidian to boulder-size pumice and ash layers to quite abruptly being a thinly laminated tuff.

G: 1) **Contact between Tht 2 and overlying basaltic andesite (Thb):** Faulds *et al.* (2002b and 2002c) shows Thrd to intervene between Tht and Thb throughout the study area, but to the northeast I found that Thrd pinches out. Here, the uppermost part of the Tht section is mostly tuffaceous sandstone. The sandstone grades from white to dark red approaching the contact with Thb, indicating that it was “baked” by the lava. The base of the lava is brecciated but it rapidly grades upward within ~1 m into vesicle-rich lava. The sandstone displays soft sediment deformation where it is in contact with the lava, including load casts and sandstone dikes. A finger-like Thb feature shown on the Faulds *et al.* (2002b) map appears to be an invasive lava flow that cuts down through the uppermost sandstone and tuff of Tht 2 and then forms a partially disaggregated sill with spectacular soft-sediment deformation at both its bottom and top (cf. Duffield *et al.* 1986).

2) **Contact between Tht 2 and overlying rhyodacite lava (Thrd):** Similar to the Tht 2 – Thb contact, the Tht 2 – Thrd contact places brecciated lava over red, baked sandstone and tuff. The Thrd breccia contains vesicle-rich black vitrophyre and magenta mafic lava enclaves. As at the Tht 2 – Thb contact but at smaller scale, soft sediment deformation is evident here (figure 10).

H: **Contact between Thrd and overlying basaltic andesite (Thb):** The capping lava changes abruptly from a lava flow with abundant magenta and black clasts, to a breccia of the basaltic andesite that slowly grades to a massive lava flow.

I: Contact between rhyodacite plug (Trdi) and Tht 2: The edges of the intrusion form a quenched vitrophyre that is black and glassy. The tuff is dark red/black in color and has a baked appearance.

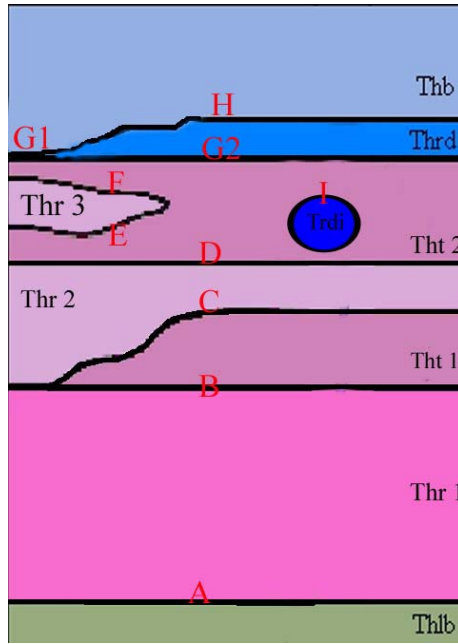


Figure 9. Stratigraphic section of Highland Range silicic sequence. Red letters, A, B, C, D, E, F, G, H1, and H2, represent different contacts.

Ages

The zircon U-Pb and feldspar Ar-Ar ages for the Highland Range silicic sequence are shown in table 1, with complete Ar-Ar and U-Pb data in appendices F and C, respectively.

With one exception, the new ages are consistent with the stratigraphy and with previous ages reported by Faulds *et al.* (2002b and 2002a). They indicate that the

A)



B)



Figure 10. A) Contact of Thrd with Tht 2. Note soft sediment deformation. B) Same contact at a distance.

trachyandesite immediately underlying the studied section (Thlb, sample HRL 26: 16.69 ± 0.11 Ma, Ar-Ar) has an age that is within error of the age of both the base and the upper part of the overlying trachydacite unit (Thr 1, samples HRL 27 and HRL 31: 16.55 ± 0.10 and 16.64 ± 0.13 Ma, Ar-Ar, respectively). The lava that overlies the upper tuff and a small intrusion into the upper part of the tuff (Thrd and Thrdi are essentially identical in age by both U-Pb and Ar-Ar at 16.0 Ma, and within error of the adjusted, previously reported Ar-Ar age of the base of the overlying basaltic andesite (Thb: 16.08 ± 0.05 Ma).

The 15.5 ± 0.3 Ma U-Pb zircon age for sample HRL 27 (base of Thr 1) is inconsistent with the rest of the zircon and Ar-Ar ages. It is about 1 Ma younger than the 16.55 Ma Ar-Ar age for the same sample, and 0.5 Ma younger than Ar-Ar and U-Pb ages for the youngest rocks of the rhyolite section. We accept the Ar-Ar because it is consistent stratigraphically with the other zircon and Ar-Ar ages.

Geochemistry

Figure 11 shows variation in the oxides, TiO_2 , CaO , Fe_2O_3 , and K_2O , to SiO_2 , as well as the trace elements Ba, Sr, and Gd, plotted against SiO_2 , for the silicic sequence. Compositions of samples from the Searchlight pluton are shown for comparison. In general, the Harker diagrams display trends typical of evolving magmas, with major and trace elements concentrated in liquidus (phenocryst) phases decreasing with declining SiO_2 . K_2O does not increase as steeply as in many volcanic and plutonic sequences, probably because biotite and/or sanidine is abundant as a phenocryst phase. The significance of the rapid decline in Gd at high SiO_2 is discussed in chapter VI.

Table 1. Ar-Ar and zircon ages for the Highland Range silicic sequence. Ages from Faulds *et al.* 2002c are from biotites. Numbers in parenthesis are adjusted for the new calibration of the standard (0.6% older).

Highland Range Units	Sample	Age (Ma)	Sample	Age Faulds <i>et al.</i> 2002c
Thb			JF-94-63	16.08 ± 0.05 Ma
Thrd	HRL 14A	16.04 ± 0.03 (Ar-Ar) 15.9 ± 0.2 (Zircon)		
Trdi	HRL 12A	16.07± 0.03 (Ar-Ar) 16.0 ± 0.2 (Zircon)		
Tht 2	HRL 10B			
Thr 3	HRL 21			
Thr 2	HRL 23A			
Tht 1	HRL 7B HRL 8E			
Thr 1 (top)	HRL 31 HRL 29 HRL 28	16.64 ± 0.13 (Ar-Ar)	JF-94-62	16.21 ± 0.17 (16.31)
(bottom)	HRL 27	16.55 ± 0.10 (Ar-Ar) 15.5 ± 0.3 (zircon)	JF-94-61	16.26 ± 0.15 (16.36)
Thlb	HRL 26	16.69 ± 0.11 (Ar-Ar)		

There are a few samples for which data appear to reflect mobility of Na, Ca, and Sr, and in some cases, Mg. The three most obvious samples are HRL 8E, HRL 7B, and HRL 22A, which have low Na₂O values, high CaO values, low totals and a high LOI (loss on ignition). These data for these samples are usable for less mobile elements, but with caution. Representative geochemical data are found in table 2 and a more detailed data table can be found in appendices B, C & F.

Table 2. Major and trace element abundances from whole rock analysis of lavas and pumices, separated by unit. Analyses of enclaves are not included. For a complete table see appendix B. Note that the wt.% of silica increase throughout the sequence. * normalized to 100

Highland Range Units	Thrd	Trdi	Tht 2	Thr 3													(bottom)	Thlb
Sample	HRL 14A	HRL 12A	HRL 10B	HRL 21	HRL 41A	HRL 45	HRL 22A	HRL 23A	HRL 7B	HRL 8C	HRL 8E	HRL 42	HRL 31	HRL 29	HRL 28	HRL 27	HRL 26	
SiO₂*	66	73	75	77	77	77	71	73	74	72	69	71	67	69	68	68	62	
Al₂O₃*	15	14	14	12	12	12	14	14	14	14	15	15	16	15	16	16	15	
Fe₂O₃*	4.51	2.13	0.78	0.69	0.89	0.88	2.18	2.07	0.70	2.74	3.00	2.05	3.30	2.78	2.94	3.11	4.98	
MnO*	0.08	0.05	0.03	0.04	0.04	0.04	0.06	0.04	0.04	0.06	0.07	0.09	0.08	0.06	0.08	0.08	0.05	
MgO*	2.76	0.76	0.67	0.10	0.22	0.27	1.94	0.86	1.10	0.74	2.86	0.43	1.06	0.70	0.84	0.89	3.11	
CaO*	4.21	1.47	2.21	0.64	1.42	1.08	3.79	1.75	4.17	2.13	4.60	1.22	2.78	2.02	2.60	2.21	4.83	
Na₂O*	3.41	3.28	2.78	2.64	3.24	2.57	1.55	2.83	0.88	3.11	1.20	4.09	4.17	4.23	4.28	4.96	3.39	
K₂O*	3.88	5.69	4.06	5.92	5.31	5.30	4.15	5.21	4.45	4.23	3.40	5.67	4.56	4.85	4.89	4.18	4.98	
TiO₂*	0.79	0.40	0.12	0.12	0.11	0.12	0.40	0.40	0.11	0.49	0.53	0.40	0.65	0.58	0.62	0.64	0.95	
P₂O₅*	0.30	0.12	0.02	0.01	0.01	0.02	0.14	0.15	0.02	0.18	0.23	0.05	0.24	0.17	0.19	0.18	0.53	
La	56	59	35	36	44	40	56	56	19	56	54	103	72	72	72	72	83	
Ce	110	104	45	60	71	70	103	97	37	97	103	201	140	140	139	138	160	
Pr	13	10	4	5	5	5	9	9	2	9	10	19	16	16	16	16	17	
Nd	40	31	10	13	15	14	28	27	5	28	29	70	47	48	46	46	55	
Sm	7.24	5.78	1.50	2.08	2.16	2.28	4.97	4.86	0.63	4.95	5.22	10.80	7.90	7.90	7.80	8.06	10.20	
Eu	1.54	0.94	0.19	0.20	0.21	0.21	0.91	0.91	0.08	1.02	1.08	2.21	1.83	1.83	1.83	2.01	2.40	
Gd	5.25	4.03	0.89	1.41	1.56	1.74	3.34	3.20	0.33	3.29	3.47	7.79	5.61	5.65	5.59	5.61	6.60	
Tb	0.74	0.62	0.13	0.27	0.26	0.27	0.49	0.47	0.07	0.46	0.49	0.98	0.80	0.81	0.79	0.81		
Dy	4.11	3.62	0.67	1.81	1.72	1.80	2.75	2.65	0.46	2.54	2.69	5.61	4.27	4.34	4.33	4.36	3.90	
Ho	0.83	0.73	0.14	0.42	0.41	0.42	0.57	0.55	0.11	0.52	0.55	1.15	0.83	0.85	0.87	0.84	0.72	
Er	2.39	2.20	0.51	1.47	1.41	1.52	1.77	1.66	0.44	1.60	1.66	3.40	2.43	2.53	2.57	2.47	1.95	
Tm	0.35	0.36	0.09	0.26	0.24	0.26	0.29	0.28	0.09	0.25	0.28	0.48	0.36	0.38	0.38	0.38	0.28	
Yb	2.16	2.25	0.76	1.77	1.74	1.79	1.84	1.80	0.78	1.66	1.78	2.96	2.28	2.38	2.39	2.36	1.68	
Lu	0.33	0.31	0.12	0.25	0.28	0.29	0.28	0.25	0.14	0.25	0.26	0.44	0.33	0.34	0.33	0.35	0.23	
Ba	797	525	23	33	28	26	391	751	23	1448	613	1418	1589	1578	1561	1488	1610	
Rb	119	155	152	202	209	220	114	138	151	141	109	245	112	127	120	146	106	
Sr	584	173	106	19	20	84	445	540	107	432	716	137	554	455	460	486	1083	
Cr	59	25	30	18	18	7	61.4	58	19	74	68	8	30	11	13 < 0.5	101		
Ni	46	15	3	1	< 1	2	35	27	3	40	61	3	17	5	5	5	85	
Hf	7	6	4	4	4	4	5	5	4	5	6	11	9	9	9	10		
Nb	20	21	20	23	25	22	22	21	21	22	22	29	22	23	23	23	18	
Y	21	21	4	12	11	13	16	15	4	15	15	28	20	20	23	19	19	
Zr	260	210	84	91	122	103	174	163	82	181	196	503	377	389	396	405	382	

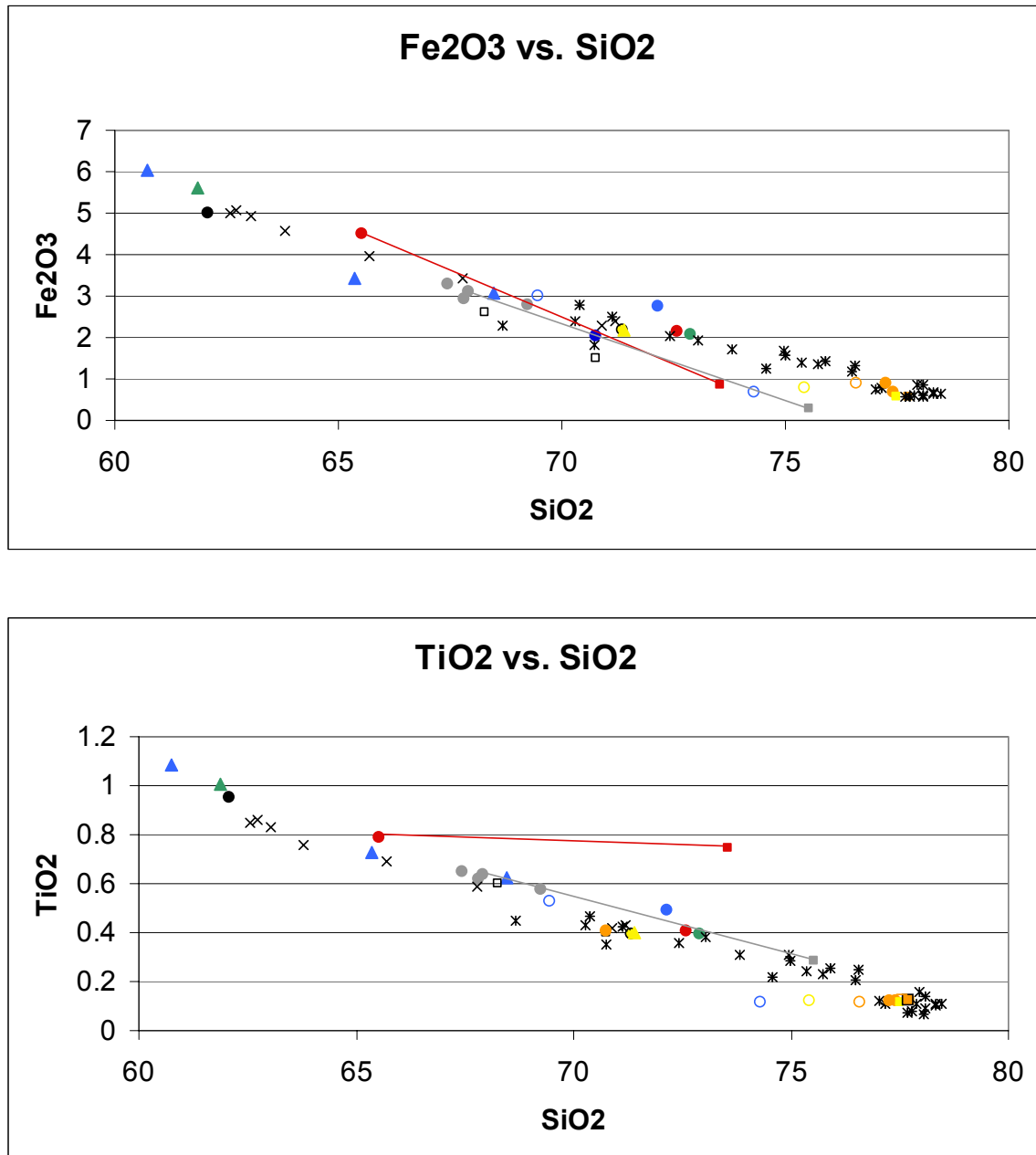


Figure 11. Diagrams comparing TiO₂, K₂O, and Fe₂O₃ (wt%), and Ba, Sr, and Gd (ppm) to SiO₂ wt% (appendix B). The symbols are color coded to match the unit they represent in the Highland Range silicic sequence (legend after last diagram). Included for comparison are data from Faulds *et al.* (2002b and 2002c) and data from Searchlight pluton (Miller & Miller, unpublished data). For the oxides, microprobe glass data is also included (appendix G).

Figure 11, continued

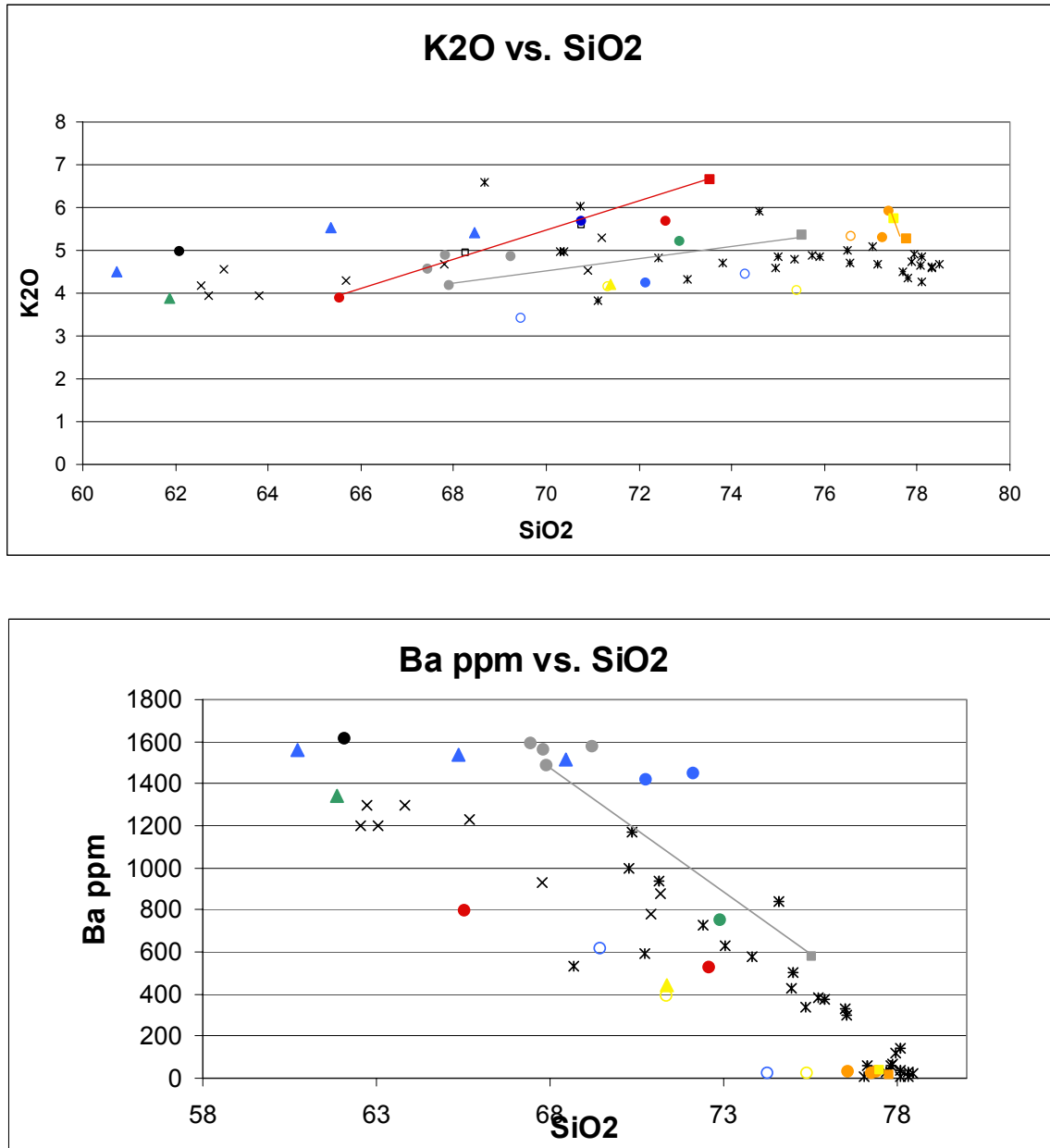


Figure 11, continued

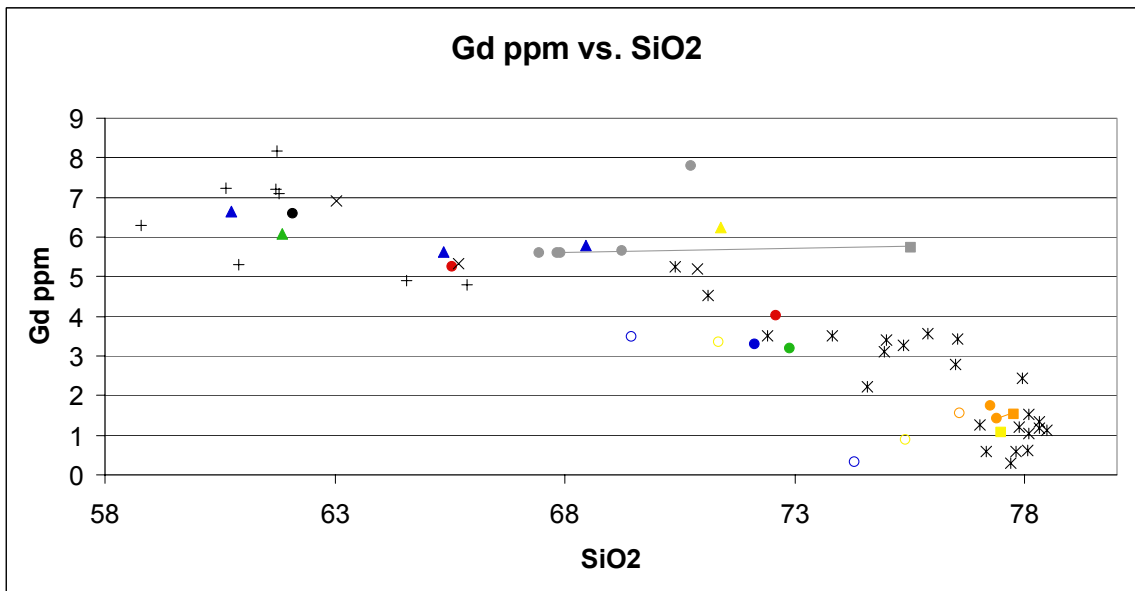
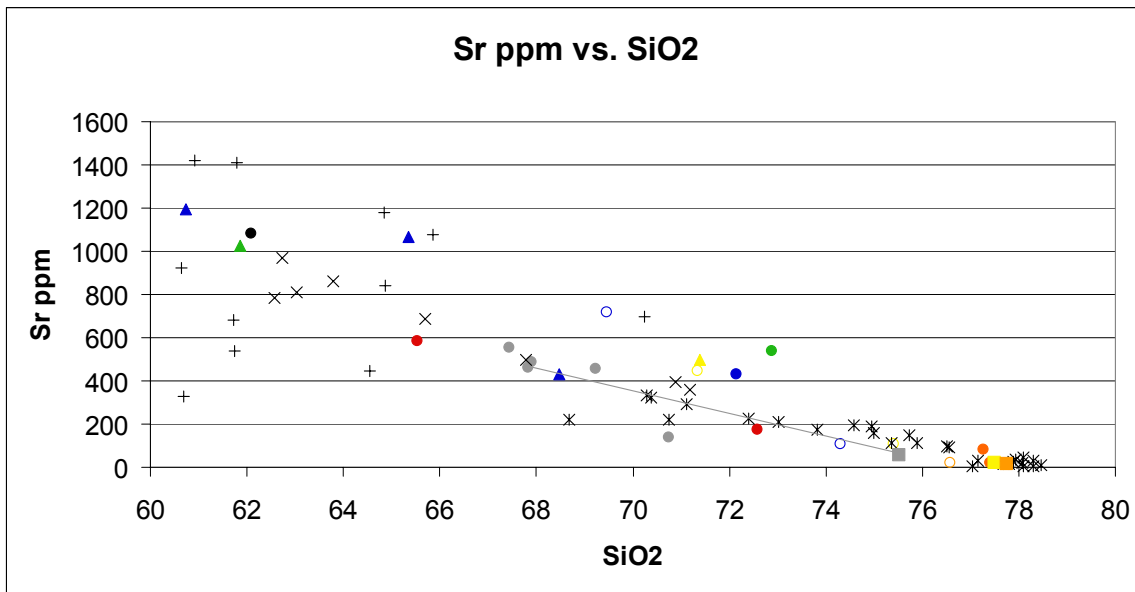
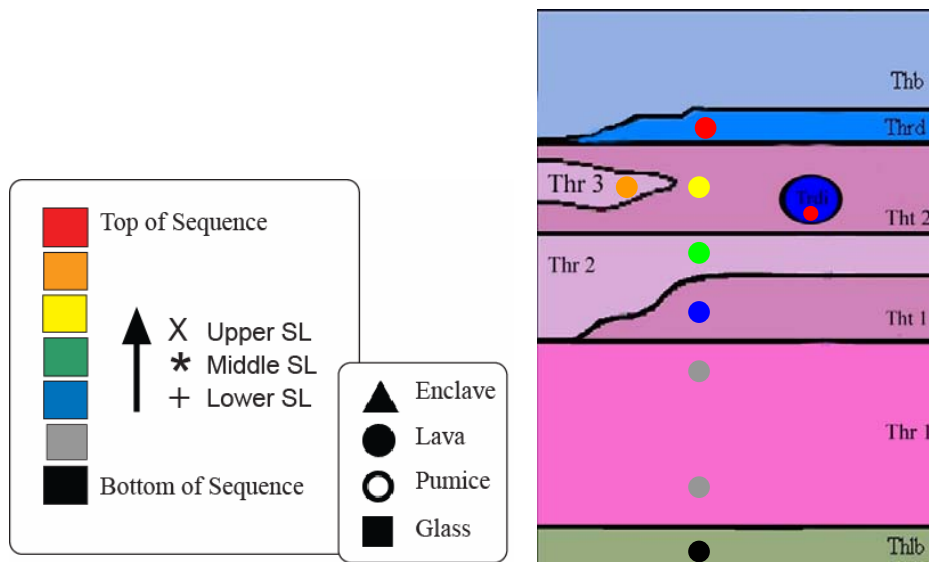


Figure 11 continued



CHAPTER V

ERUPTION OF THE HIGHLAND RANGE SILICIC SEQUENCE

Unit Deposition

The Highland Range silicic sequence lava flows were emplaced effusively. They exhibit flow banding and autobrecciation (figure 5). The flow banding is most prevalent in the top portions of Thr 1, and in the north eastern part of Thr 3. At Thr 3, a dense pumice or frothy lava fills the space between the narrow flow bands. As the lava slowly moved over the landscape the tops of the flows cooled and broke apart, forming a brecciated top surface. These blocks also exhibit dense pumice and flow banding.

Above the flow banded lavas of the north eastern Thr 3 is a monolithologic breccia flow. The lithics in the flow are all poorly vesiculated pumices, while matrix is ash of the same composition as the pumice, as seen in figure 6, making it a block and ash flow. I interpret the block and ash flow to have formed by dome collapse.

Both Tht 1 and Tht 2 contain massive tuff layers but unlike Tht 2, Tht 1 contains thinly bedded layers in-between the massive layers (figure 7). Tht 1 is also different from Tht 2 in that it lacks abundant pumice. Pumice in Tht 1 is on average sparse and small (2-4 cm), while pumice in Tht 2 is more abundant, increasingly so at the top of the section, and much larger (2-15 cm). It is clear that different processes were involved in depositing these two units.

This study has two main hypotheses as to how the massive and thin layers of Tht 1 were deposited. The first one is that the layers are the product of lahars and fluvial

reworking. The thin layers have several characteristics (Fisher 1984) of fluvial reworking, including moderate sorting, a lack of large boulders, clasts are generally subrounded (figure 7), and lack a substantial amount of pumice. They layers do lack cross bedding and evidence of thin channels, which are indicative of fluvial reworking. The massive beds are poorly sorted, containing large boulders (up to 1 m in size), contain abundant clay size materials, and have vague internal bedding (figure 7B). The larger clasts found in the layers are also subangular. All of these characteristics are typical of lahars (Fisher 1984).

The second hypothesis considers pyroclastic flows and surge deposits as the cause of the alternating thinly bedded and massive layers. Pyroclastic flows form a poorly inflated, particle rich, non-turbulent flow that is full of hot air and moves at high velocities for long distances (Cas and Wright 1987). The deposits are poorly sorted and massive (Fisher 1984). Figure 7B shows a massive layer deposit in Tht 1 that is particle-rich and poorly sorted, and if this hypothesis is correct, could possibly be a pyroclastic flow deposit.

Pyroclastic surges are highly inflated (lofting ash into the air), turbulent, particle-poor flows that are generally smaller but more violent than pyroclastic flows. The deposits can be ash-rich or lapilli-rich, exhibit massive, planar-bedded, reverse-graded and cross-bedded textures depending on the turbulence in the system (Cas and Wright 1987). The possible pyroclastic surges of Tht 1 show both thin, massive, lapilli-rich layers as well as planar-bedded ash-fall layers (figure 7C & D). The thin massive lapilli layers would be the ‘body’ of the surge deposit while the finally bedded ash layers would be the fallout from the lofted particles. The lack of cross-bedding in the layers does not

support this hypothesis, though it is possible to get planar-bedded features in surge deposits.

Tht 2 tuff deposits do not show evidence of water interaction during deposition, but do show signs of increasing explosiveness in eruption. The thick (1-5 m) massive deposits are most likely formed from pyroclastic flows, possibly during one or two very large eruptions. The tuffs of Tht 2 exhibit poor sorting, thick layers, and vague bedding forms indicating deposition through pyroclastic flow (figure 7). The increase in pumice abundance and size indicates an increase in explosive activity. Rapid deposition of Tht 2 (through one or two eruptions) would be consistent with absence of evidence for reworking.

The sequences of tuffs were emplaced explosively as a possible result of sub-plinian to plinian eruptions. Evidence for plinian eruption includes the explosivity of the eruption inferred from the presence of large tuff deposits, the large sheets of tuff, the lack of fumarolic pipes, and general lack of welding, and the large pumice rich, massively layered, cliff forming upper tuff deposits (samples HRL 15 & HRL 16) (Fisher 1984). Dome collapse is another possible cause leading to smaller explosive eruptions. Vulcanian eruptive activity may have occurred, sporadically during and/or in-between plinian eruption. This would lead to the large (up to 1 m) boulders and boulder trains found in the tuff deposits.

Eruptive Transition

The Highland Range silicic sequence has a distinctive eruptive history. It transitions from erupting effusively forming lava flows into erupting explosively forming tuff deposits. There is a ~0.5 Ma difference between the deposition of Thr 1, the start of

the system, and Thrd, the end of the system (table 1). We have no ages for units Tht 1, Tht 2, or Thr 3 (the middle units), and therefore cannot estimate whether this is a fast transition or just a change in the magmatic system.

An interesting question is why did such a change in eruptive style take place? At the transition from effusive to explosive eruptions in the Highland Range, there are two other changes within the magma, a change in composition and a change in enclave abundance. During effusive eruption, the erupted magma contained less than 0.01% enclaves (figure 4A) and once the system starts to erupt explosively, the erupted magma increases in abundance (up to at least 10%) of enclaves (figure 4B). Figure 11 shows how the composition changes from being more mafic (below 70 wt.% SiO₂) to having a rhyolitic composition (above 70 wt.% SiO₂) at the same time as it transitions from erupting effusively to erupting explosively.

This study has two main hypotheses as to why there is a change in the eruption style of the Highland Range rhyolitic system. The first hypothesis is that crystallization of the observed relatively volatile-poor assemblage enriched the remaining melt in volatiles, eventually leading to volatile saturation, bubble formation, and finally fragmentation. The increase of silica from the bottom to the top of the sequence indicates that fractionation may have occurred (Platz *et al.* 2007, Harper *et al.* 2004; figure 11; table 1)

Evidence for fractionation is given by elemental chemistry, especially the REE patterns. As discussed in chapter VI, the strong depletion of the REE, especially the MREE, of the glass of the high silica rhyolites (Thr 3) found within the explosive tuff sections (Tht) suggests fractionation of sphene out of the system (see chapter VI).

Sphene fractionation presumably was accompanied by fractionation of other minerals as well, driving up the volatile content in the system.

The second hypothesis is that recharging the magma chamber replenished the volatile content. An injection of hot mafic magma will quench when reaching the cooler magma within the chamber, causing the solidifying mafic magma to release gasses (figure 12) (Bachmann and Bergantz 2003). Pallister *et al.* (1992) gives an example of this happening in the 1991 eruption of Pinatubo volcano where an injection of basalt into the shallow dacitic magma chamber added enough volatiles to cause an explosive eruption. The increase in enclave size and abundance from Thr 1 to Thr 2 indicates that there may have been an injection of magma into the system, possibly bringing fresh volatiles with it. The enclaves in Thr 2 have crenulate edges, implying that a warm, more mafic magma was mingling into the erupted rhyolite magma (figure 4B and 13).

Evidence for possible magma injection is also found in Searchlight pluton. The mafic pods found at the base of the MSL unit are most likely caused by an injection of mafic magma (Bachl *et al.* 2001). Furthermore, rhyolite dikes that are thought to have been derived from MSL are also enclave-rich (Hodge *et al.* 2006).

Both hypotheses describe ways to increase the amount of volatiles to saturation, and drive an explosive eruption. It is possible that both fractionation and a recharging event, together, led to a change in eruption style. This is especially likely since there is evidence for both fractionation and an injection of mafic magma.

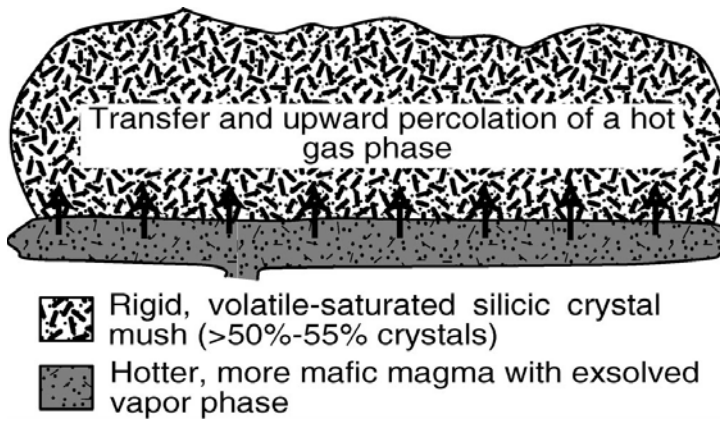


Figure 12. Diagram of volatile release from injected warmer mafic magma into the cooler siliceous magma. Figure from Bachman and Bergantz 2003.

Possible Modern Analogue

It is interesting to compare the Highland Range rhyolitic sequence to the Vulcano or Lipari volcanoes of the Aeolian Islands in southern Italy, using them as a modern analogue. These volcanoes have erupted both effusively and explosively, and transitioned from being dacitic to rhyolitic in composition (Lucchi *et al.* 2008; Dolfi *et al.* 2007). Gioncada *et al.* (2005) state that fractionation is the cause the compositional change and that there are also injections of mafic magma into the source chamber. It is important to point out that the Aeolian island volcanoes have a cyclic eruptive behavior due to water-magma interaction creating phreatomagmatic eruptions.

Phreatomagmatic eruptions occur when water comes into contact with magma. The heat energy in the magma is converted into kinetic energy by thermodynamic properties of water which causes the magma and anything around it to explode (Buttner

et al. 1999). The magma can come into contact with water in several ways, a few examples being (1) eruption into shallow oceans or lakes, (2) magma rising into ground water, (3) water flowing into a partially empty magma chamber or vent, (4) eruption beneath a glacier, and (5) a lava or hot pyroclastic flow flowing over or into wet ground (Fisher 1984; McPhie *et al.* 1993). According to Fisher (1984), phreatomagmatic deposits lack fumarolic alteration or pipes (gas escape), and welding, and can exhibit base surge transport of the clasts, all of which may apply to the Highland Range rhyolite sequence.

Glass shards (ash) that are blocky, contain few vesicles, and can have perlitic or “mosaic” fractures indicating rapid cooling, are formed during phreatomagmatic eruptions. In an eruption that is explosive due to bubble growth and magma fragmentation, the glass shards exhibit cuspatate shapes, or are the broken walls of vesicles, the deposits also contain highly vesiculated pumice fragments (McPhie *et al.* 1993; Cas and Wright 1987; Fisher 1985; Buttner *et al.* 1999). Figure 13 shows examples of glass shards from both phreatomagmatic and bubble fragmentation eruptions, and compares these to two thin section pictures from the Highland Range silicic sequence (samples HRL 18, and HRL 16 from units Tht 1 and Tht 2, respectively).

It is difficult to say whether or not the Highland Range rhyolitic was emplaced due to phreatomagmatic eruptions, with one sample implying that it is (HRL 18) and one sample implying that it isn’t (HRL 16). It is possible that there were multiple vents erupting, where one intersected with water, possibly erupting into a lake, while one vent missed the water. It is also possible that the magma-water interaction did not occur until the magma became vesiculated and was about to erupt explosively due to bubble

fragmentation when it hit a water source. This would account for the vesicularity within the glass shards of the rhyolite tuff. A third possibility is that the volcano changed with time and that Tht 1 experienced different eruption mechanisms than Tht 2. These eruption mechanisms could have also changed with time from the eruption of Tht 1 and Tht 2. If it is indeed phreatomagmatic eruptions, this would account for the repeated explosive eruptions in the Highland Range silicic sequence, similar to the Aeolian Island volcanoes.

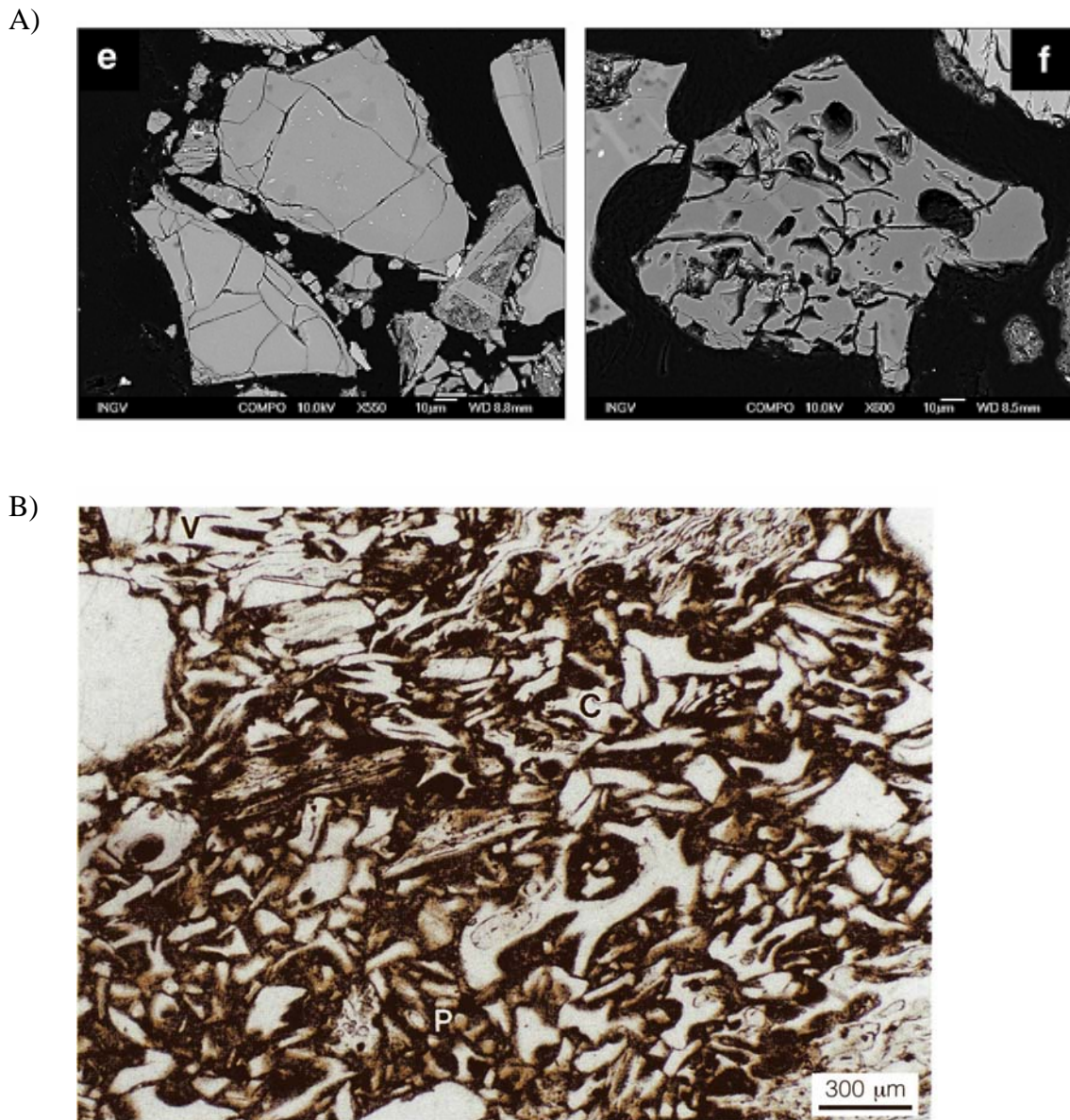
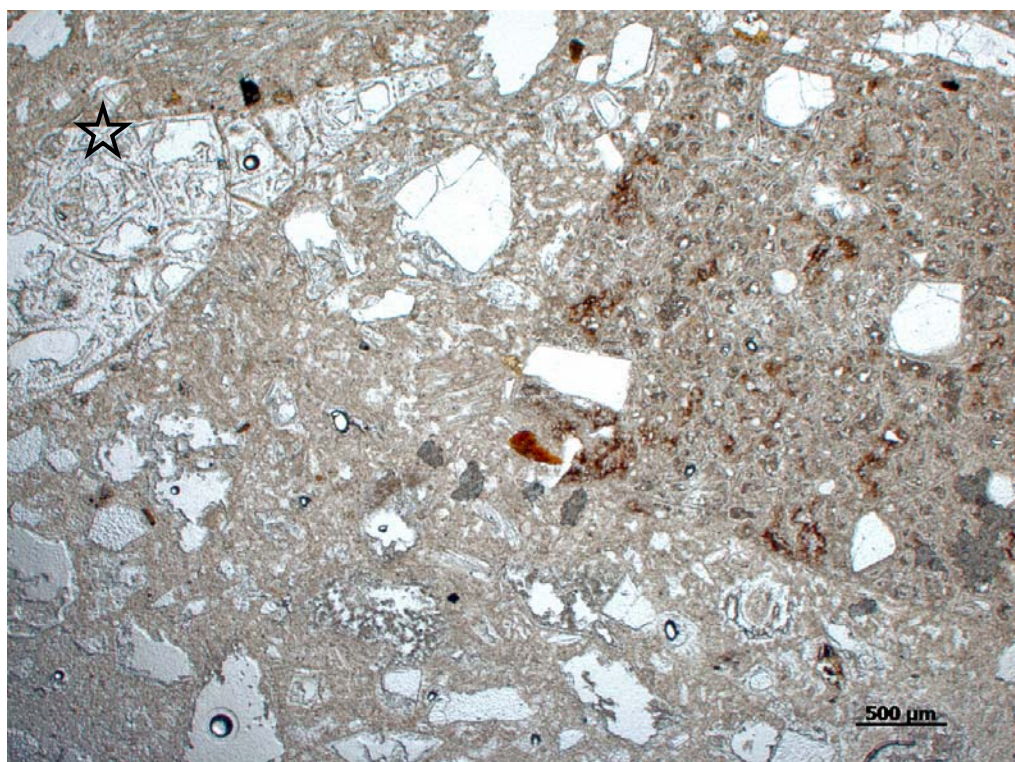


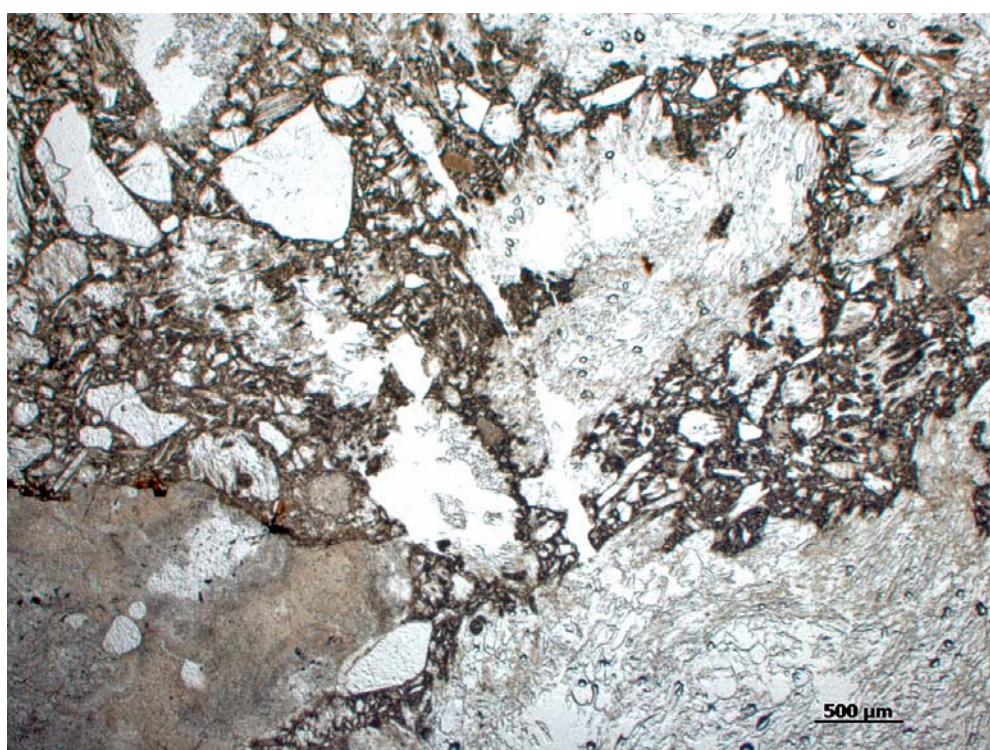
Figure 13. A) Examples of phreatomagmatic ash from Lipari (Lucchi *et al.* 2008). B) Ash fragments from a bubble/fragmentation explosive eruption from the Bishop Tuff (McPhie *et al.* 1993) The letters V, C, and P, represent the cuspatate shapes. The shapes being V-shaped, C-shaped or P-shaped. C) Possible phreatomagmatic fractured shard (star) from sample HRL 18, unit Th1. D) Cuspatate glass shards and vesiculated pumice fragments from HRL 16, unit Th2.

Figure 13, Continued

C)



D)



CHAPTER VI

COMPOSITION OF HIGHLAND RANGE SPHENE AND ZIRCON: ZONING, ELEMENT PARTITIONING, ESTIMATED TEMPERATURES OF GROWTH, AND IMPLICATIONS FOR MELT EVOLUTION

Zircon

The separated zircon phenocrysts range in size from ~ 70 – 500 μm and are generally euhedral in shape. Cathodoluminescence images of the grains reveal common inclusions and well-defined patterns of compositional zoning within grains (appendix C). Crystals are concentrically zoned, and some also have rounded edges of internal zones that I interpret to be the results of resorption. The cores of most grains are dark in CL with a bright interior (area between the core and rim) and medium-gray rim (figure 14).

The analysis spots on the zircon grains are designated as representing edge (rim), interior, and core zones, and also dark, medium or light, based on the CL brightness of that section of the grain (figure 14, appendix C). The REE analyses are presented in appendix D. The REE patterns in the zircon grains are plotted in figure 15 with concentrations normalized to both chondrite and typical “primitive” zircon values (high T_{TiZ} , low Hf) (Claiborne *et al.*, in review). Chondrite-normalized REE patterns display positive cerium anomalies and generally negative europium anomalies, and like almost all zircons are highly enriched in heavy REE relative to light REE (figure 15A). The edges of the grains are generally more depleted in REE than the cores (figure 14B). In sample HRL 12a, the medium brightness zones are less enriched in REE than the dark zones, while in sample HRL 27 the lighter zones are more depleted.

Sphene

The sphene phenocrysts are about 200 – 1000 µm in size and are generally euhedral. Backscattered electron (BSE) images reveal both regular concentrical zoning and brighter zones that transect the concentric zones, usually running through the center of the grains. They may be either sector zones, formed during magmatic growth, or secondary veins running through the phenocrysts. For this thesis I refer to them as sector zones, but am careful not to include them in my major interpretations concerning magmatic processes.

Inclusions, including probably melt inclusions, are abundant within the sphene phenocrysts. Sample HRL 14a shows reactions rims, with ilmenite growing around the edges of the grains (figure 14).

The sphene analysis locations are labeled as edge, interior, core, and sector zones, and also as dark, light, or sector, based on the BSE image (figure 14, appendix E). The edge zones generally are dark while the interior and core zones are generally light for all samples except sample HRL 14a, which has dark interior and light edge zones. For all samples, the sector zones are light. The concentrations of the REEs in sphene are normalized to chondrite and to sample spot HRL 12a-6.2MODZ (figure 16), which is near the median of all analyses in REE concentrations. The chondrite-normalized plots demonstrate extreme enrichment in all of the REEs, with the middle rare earth elements (MREE) the most enriched. When comparing the zones, the edges are less enriched in REEs than the core and sector zones for samples HRL 12a, HRL 21, and HRL 19a. Sample HRL 14a shows the opposite with the cores more depleted than the edge and

sector zones. Generally the light and sector brightness zones are more enriched in REEs than the dark zones.

Rare earth element partition coefficients ($C_s / C_l = K$) are estimated for sphene in sample HRL 21, a glassy flow. The C_s values for each REE are the average of the analyses of the grain edges of sample HRL 21 (3.1ED, 5.1ED, 6.4ED, 7.1ED, and 8.1ED) (table 3). The C_l values are the average of glass analyses from the same sample (table 3, appendix H). Figure 17 compares the calculated K values for sphene in HRL 21, together with other estimates for sphene K in silicic magmas estimated by Bachmann *et al.* (2005), Rollinson (1993) and Simmons and Hedge (1978). All of the K values reflect compatibility (values $>>1$) and plot on convex-upward (middle REE-enriched) curves that are generally compatible with the lattice strain model of Blundy and Wood (1994). However, the values differ from study to study by two orders of magnitude, with the Highland Range values being the highest of all (up to >1000 for middle REE). They are closest to those of Bachmann *et al.* (2005), who used similar methods (LA-ICPMS spot analyses) on coexisting sphene and high silica rhyolite glass from the dacitic Fish Canyon Tuff. Simmons and Hedge (1978) analyzed sphene and whole plutonic rock, and Rollinson (1993) cites an experimental study by Green and Pearson (1987) using synthetic trachyte glass with sphene. Prowatke and Klemme (2006) demonstrate the extreme dependence of K values for sphene on melt composition: far higher for more typical melts (toward the metaluminous-peraluminous boundary). Thus my method and that of Bachmann *et al.* (2005), using natural materials, probably yield more generally applicable values than the other studies. Also, note that I have data for all naturally

occurring REE, in contrast to the other studies, and that my patterns are smoother, presumably reflecting higher accuracy.

REE data from the four glasses that I analyzed are shown in table 3 and figure 18. Sample HRL 27 has a pattern typical of a moderately felsic igneous rock. Samples HRL 21, HRL 16, and HRL 10b are depleted in the REE compared to HRL 27, and especially strongly depleted in the MREEs.

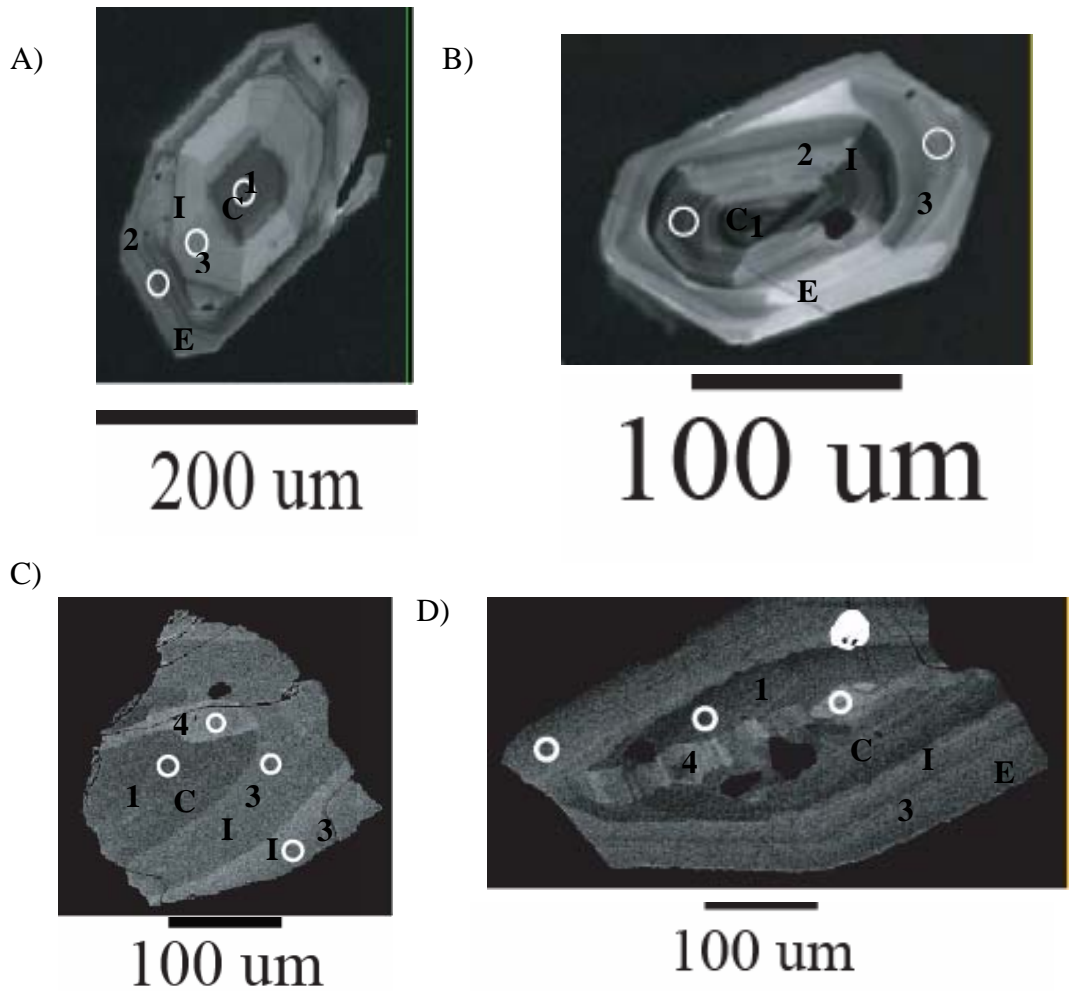
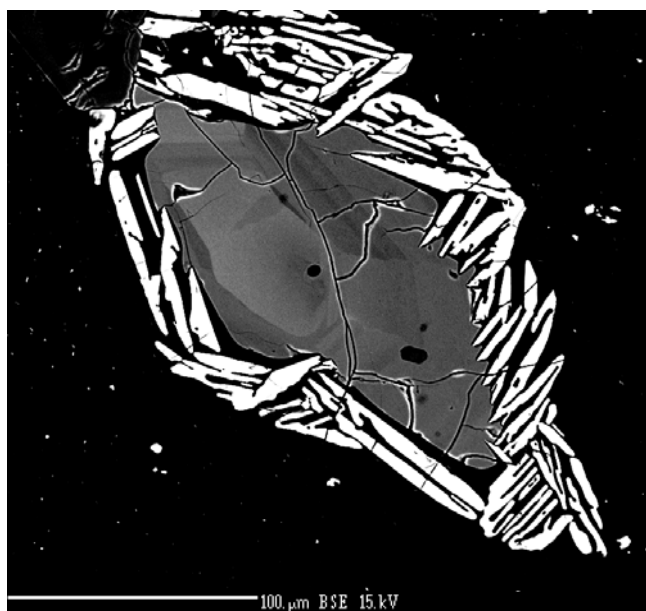


Figure 14. A through D are representative images zircon and sphene. E and F show ilmenite reacting with sphene. Notice the dark (1), medium (2), and light zones (3) on the zircons, and the dark (1), light (3), and sector zones (4) on the sphene. Both the zircons and the sphenes are labeled core (C), interior (I), and edge (E). Note that the first sphene grain does not have an edge. A) zircon from HRL 12a; B) zircon from HRL 14a: note rounding (resorption?) of core; C) sphene from HRL 14a; D) sphene from HRL 12a; E) BSE image of *in situ* sphene phenocryst in HRL 14a; F) BSE image of separate sphene phenocryst fro HRL 14a.

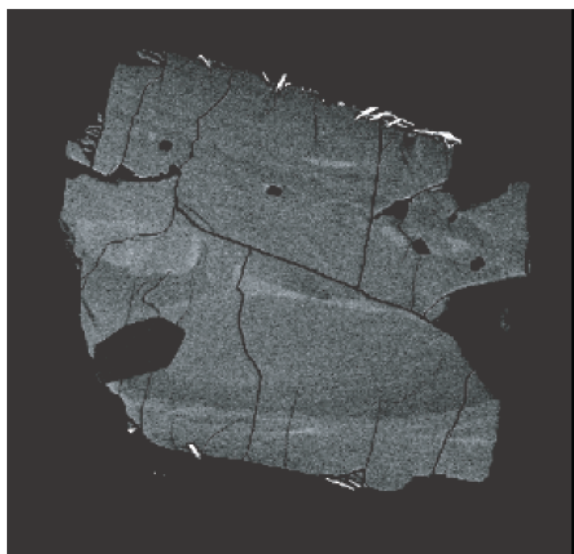
Figure 14, continued

E)



100 μm BSE 15 kV

F)



100 μm

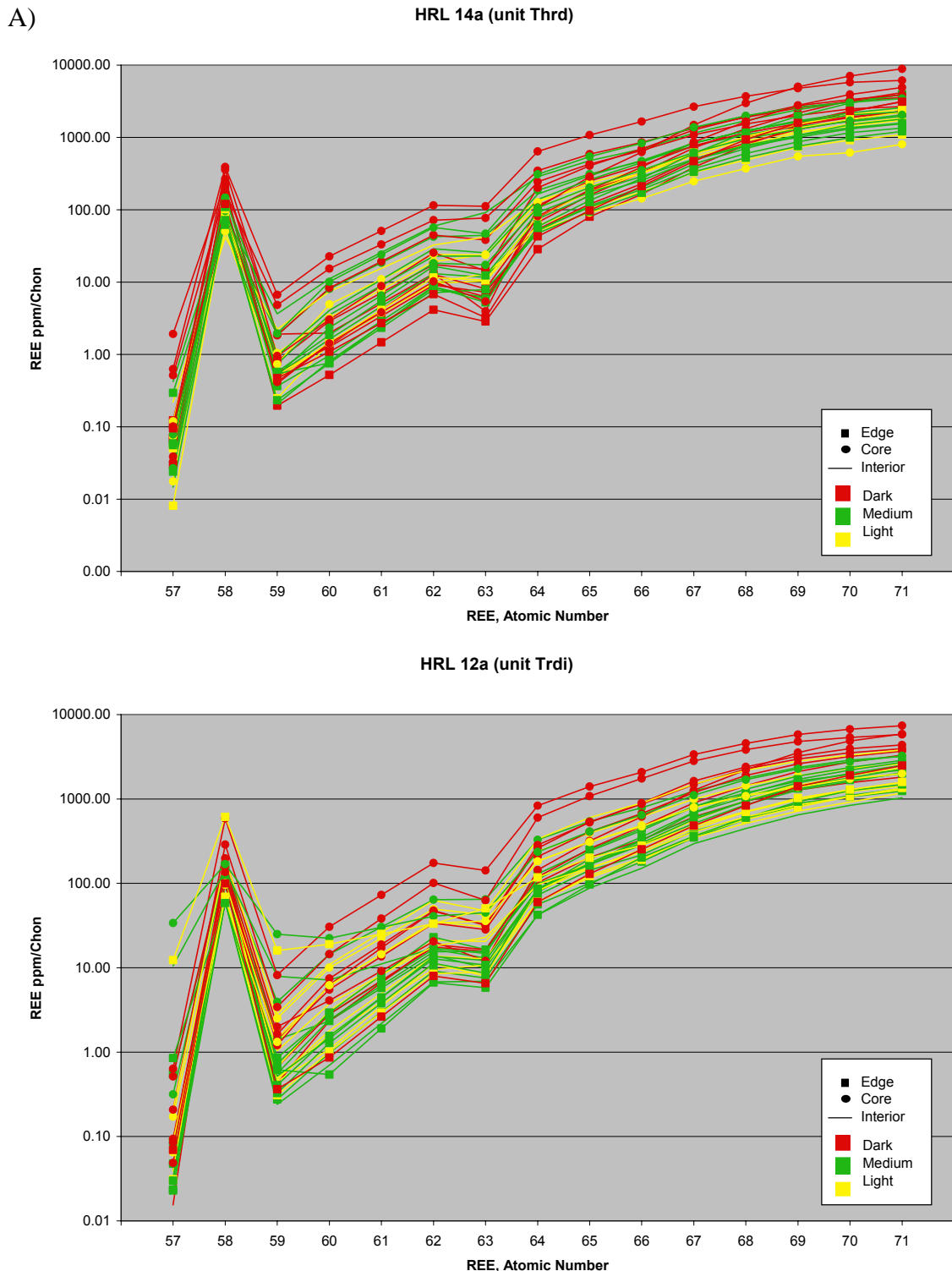
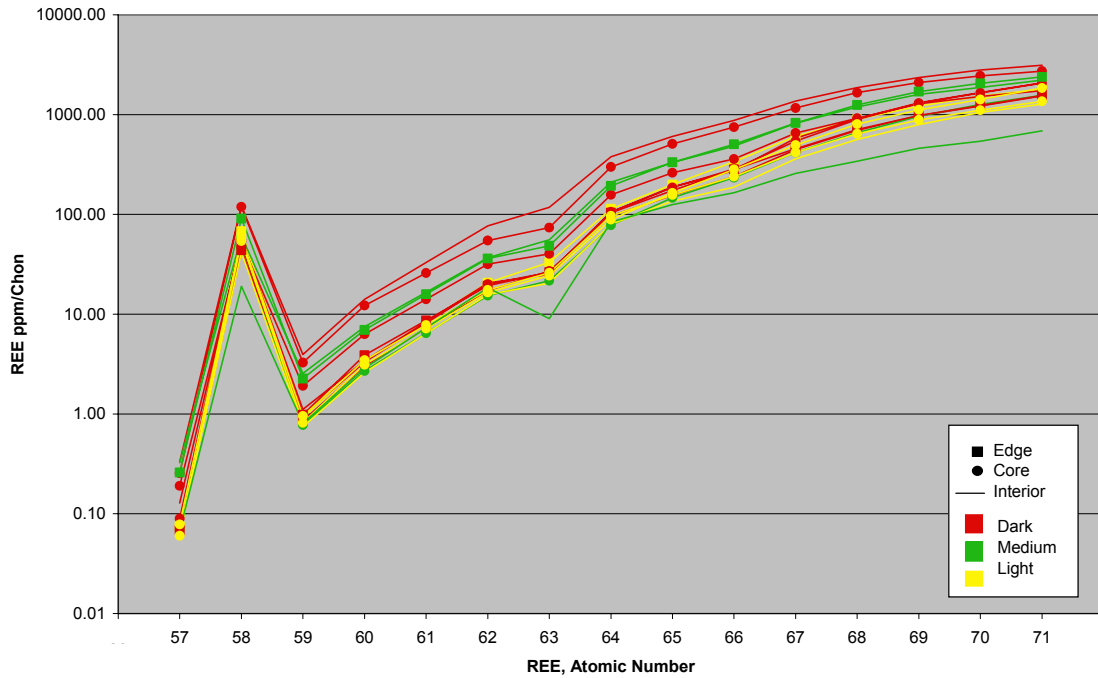


Figure 15. REE diagrams from zircon analysis. A) REE ppm normalized to chondrite. B) REE ppm normalized to a representative, primitive, zircon (Claiborne, in review).

Figure 15, continued

HRL 27 (unit Thr 1)



B)

HRL 14a (unit Thrd)

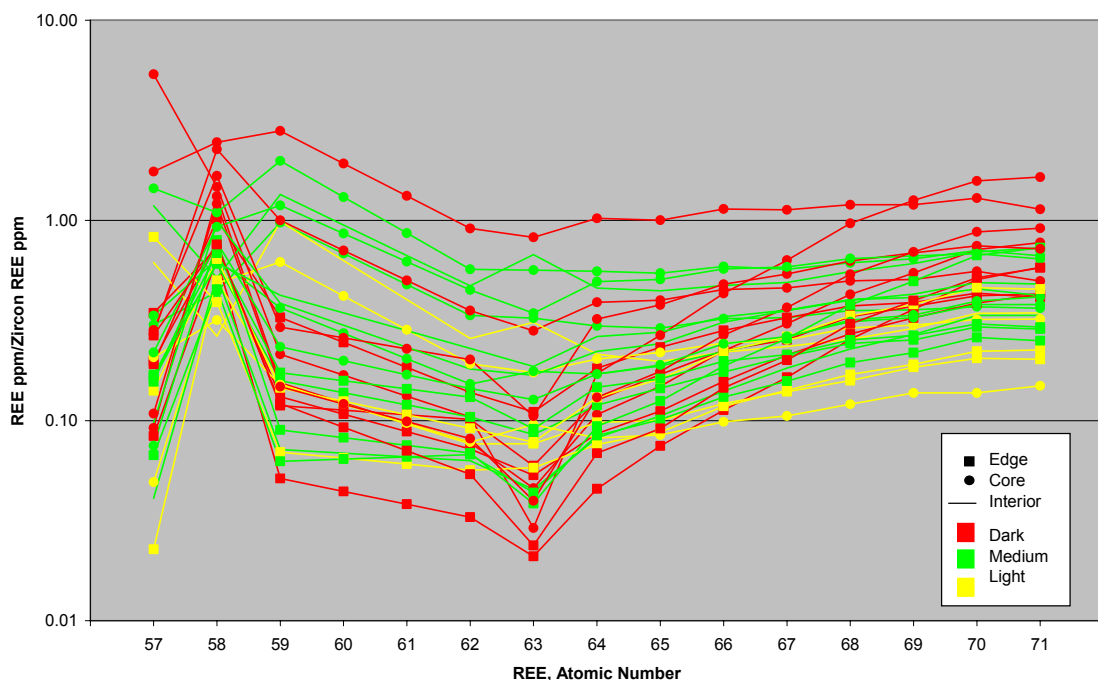
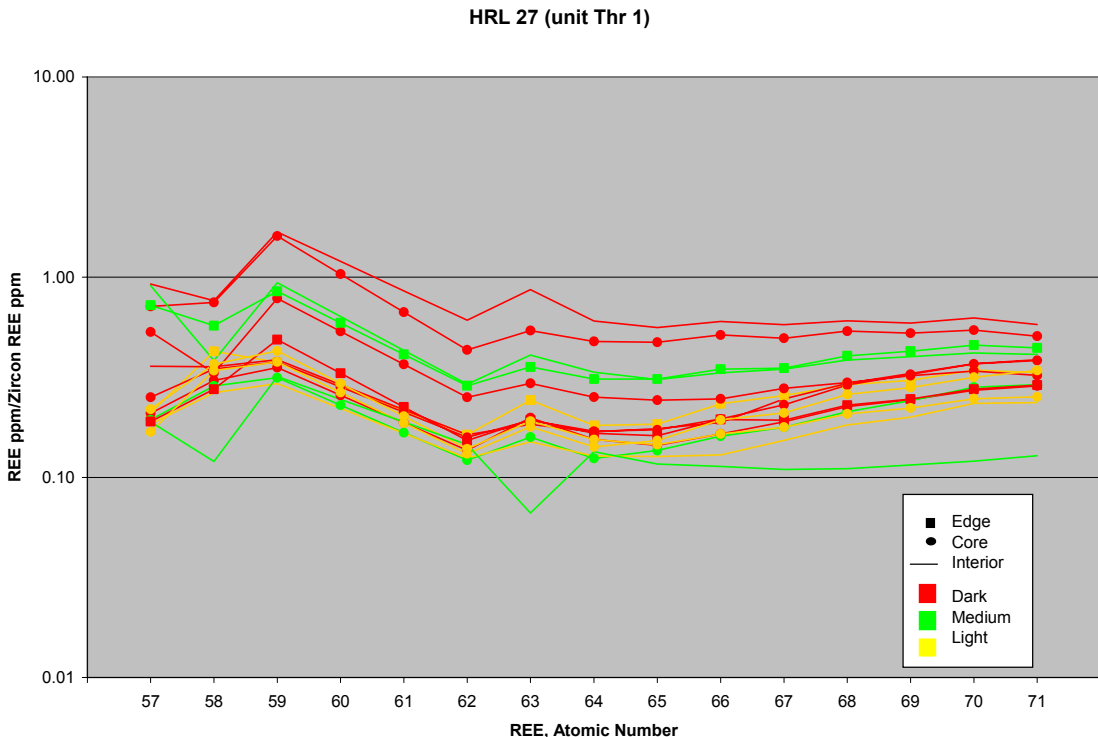
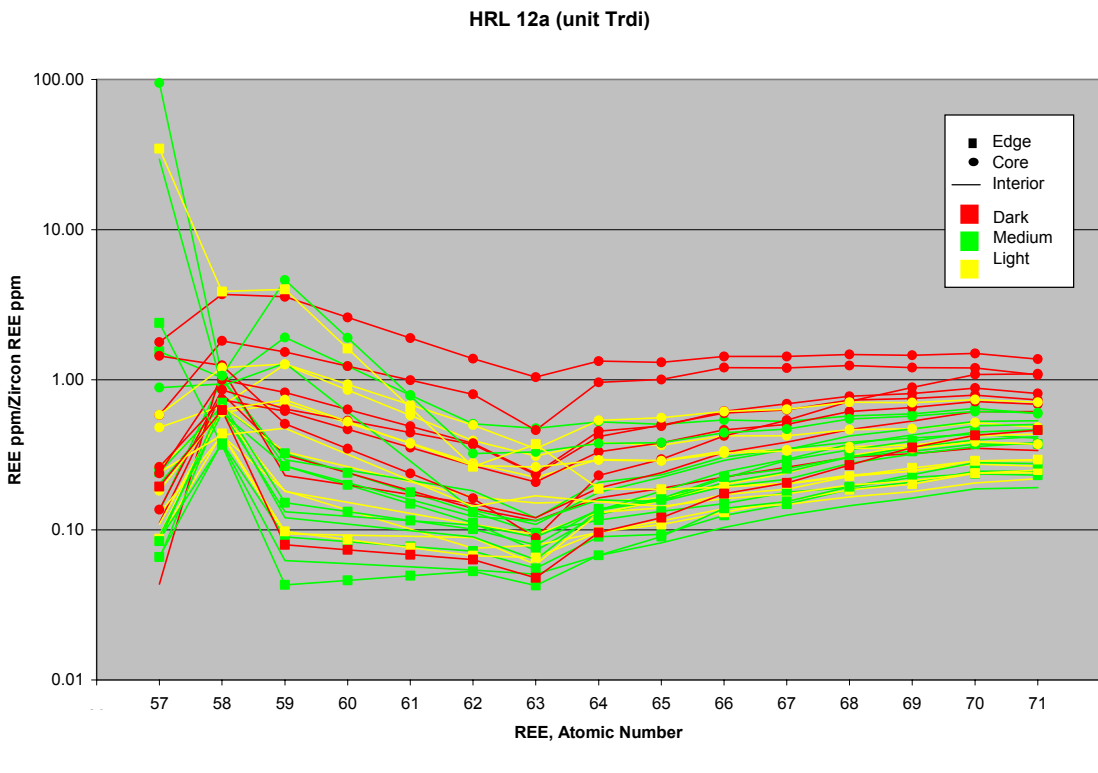
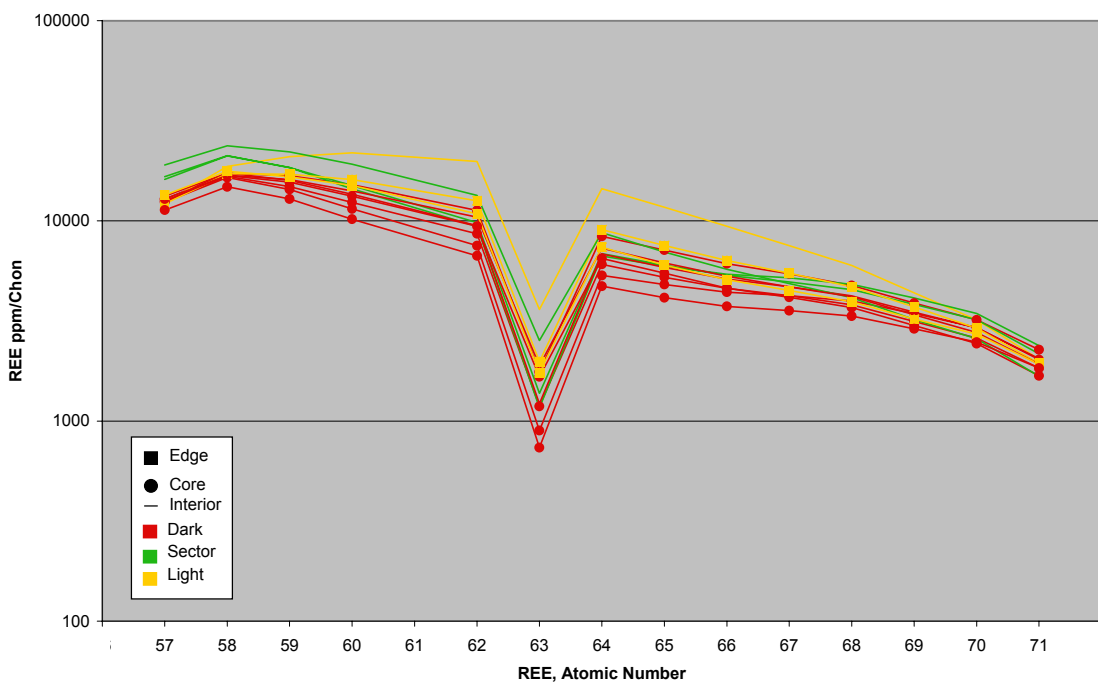


Figure 15, continued



A)

HRL 14a (unit Thrd)



HRL 12a (unit Trdi)

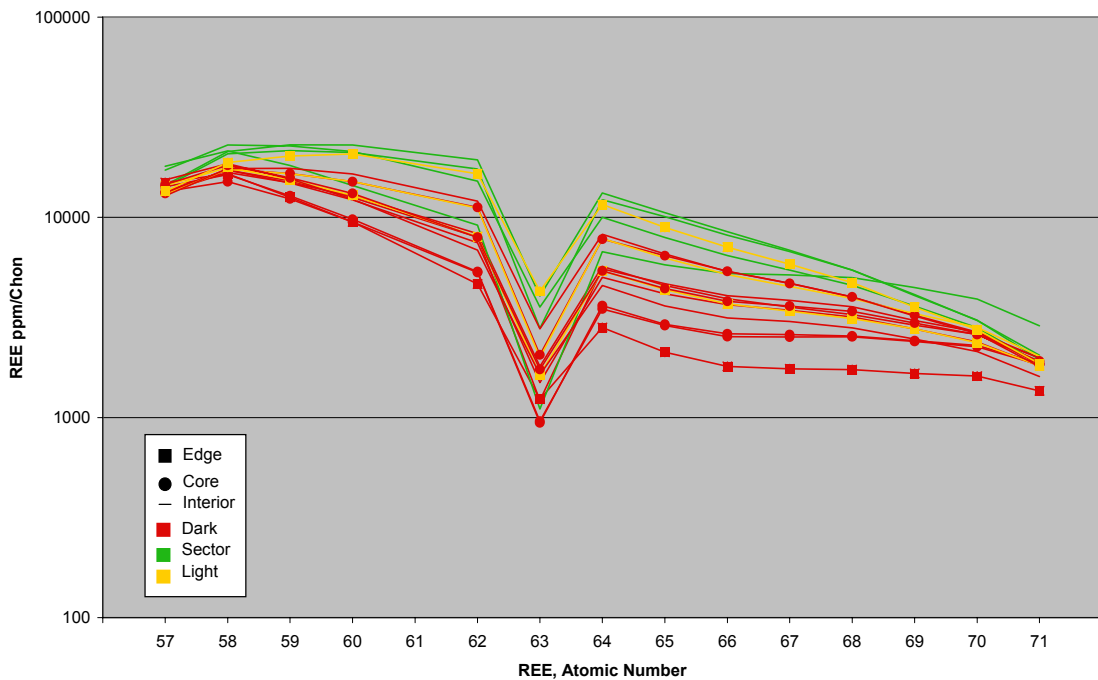


Figure 16. REE diagrams from sphene analysis. A) REE ppm normalized to chondrite. B) REE ppm normalized to a representative sphene sample spot (HRL 12a-6.2MODZ).

Figure 16, continued

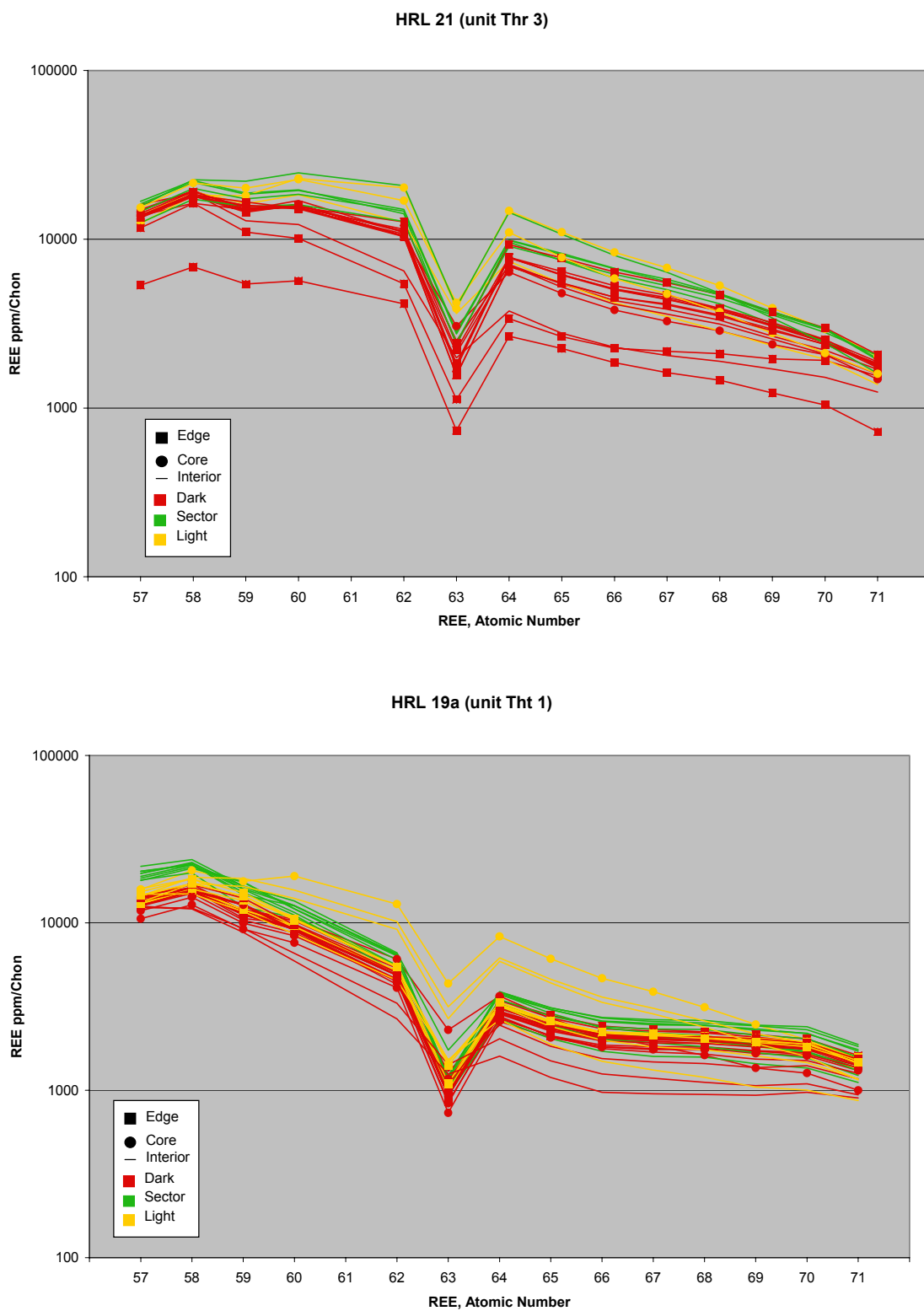


Figure 16, continued

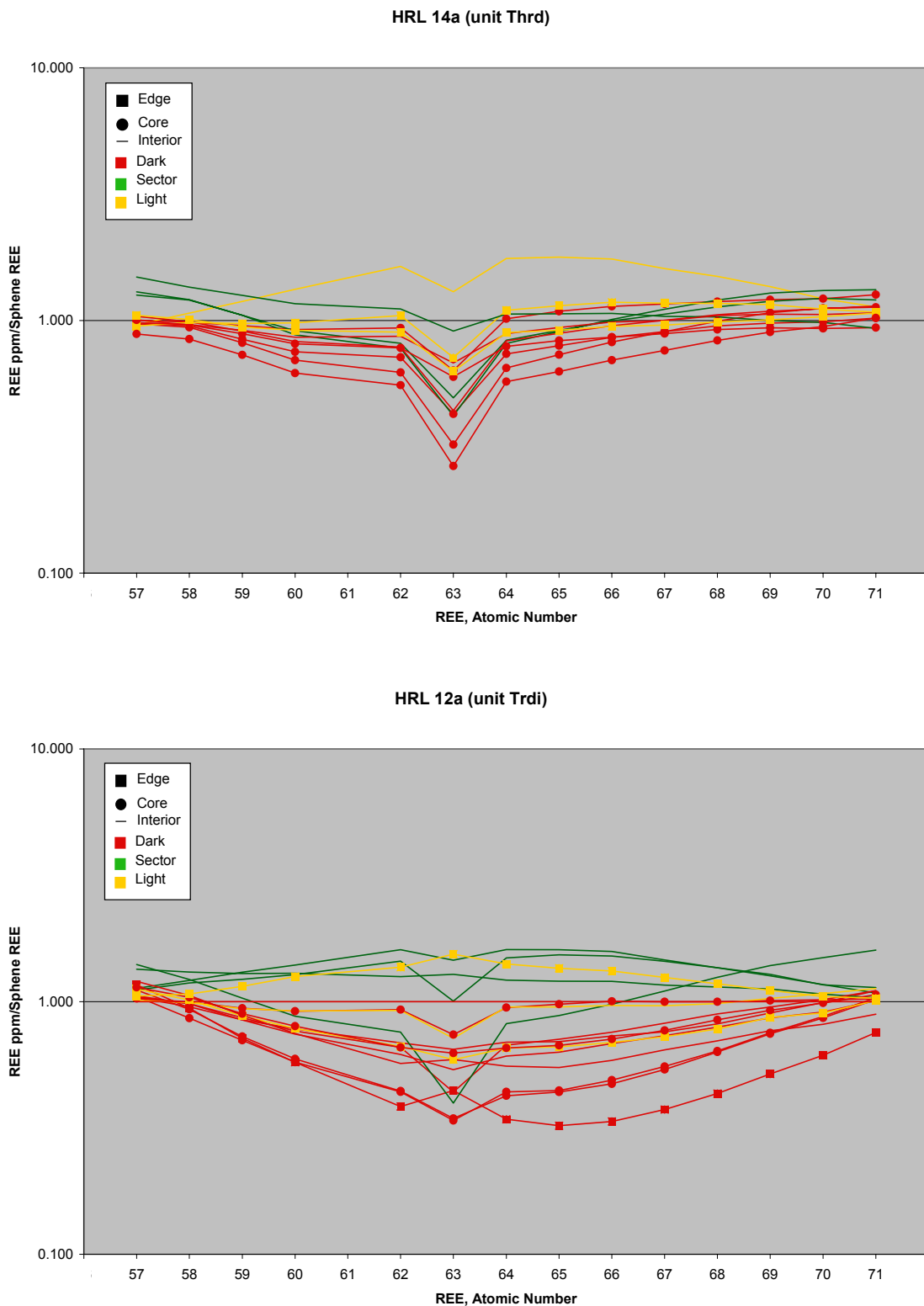


Figure 16, continued

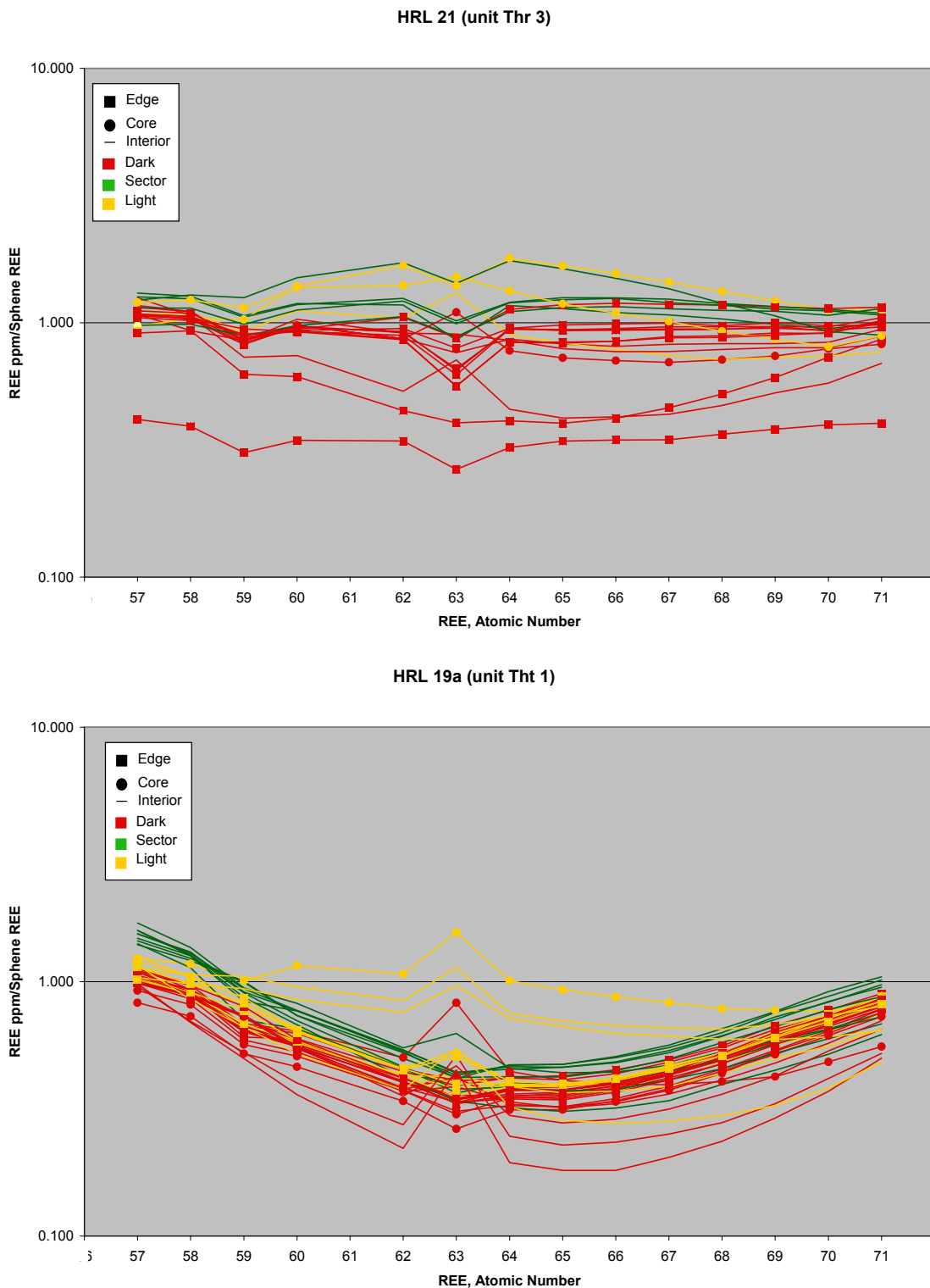


Table 3. Calculation of estimated partition coefficients (K) for REE in sphene. REE concentrations from the edges of sphene grains from sample HRL 21 (unit Thr 3) are averaged to give C_s. This average is divided by the concentration of REEs from the glass (melt) of sample HRL 21 (C_l) to give the partition coefficients (K).

Sample	Concentration of Solids (Cs) ppm						Average Concentration of Solid (Cs)	Concentration of Liquid (Cl)	Cs/Cl
		HRL21- 5.1ED	HLR21- 6.4ED	HRL21- 7.1ED	HRL21- 8.1ED				
La	4231	3618	4157	4220	4416	4129	34	123	
Ce	14778	13172	14456	14771	15436	14523	54	267	
Pr	1790	1832	1933	2026	1883	1893	4.5	419	
Nd	9464	9310	9226	9131	9193	9264	12	750	
Sm	2175	2475	2231	2097	2029	2202	1.8	1208	
Eu	133	179	163	128	116	144	0.22	647	
Gd	2027	2404	2024	2015	1787	2051	1.5	1332	
Tb	288	364	303	291	257	301	0.24	1231	
Dy	1613	2062	1708	1624	1460	1694	1.6	1048	
Ho	316	398	335	318	297	333	0.38	884	
Er	792	986	818	794	748	828	1.2	678	
Tm	99	119	103	98	94	102	0.22	456	
Yb	509	623	533	511	497	535	1.7	316	
Lu	59	66	56	55	58	59	0.25	237	

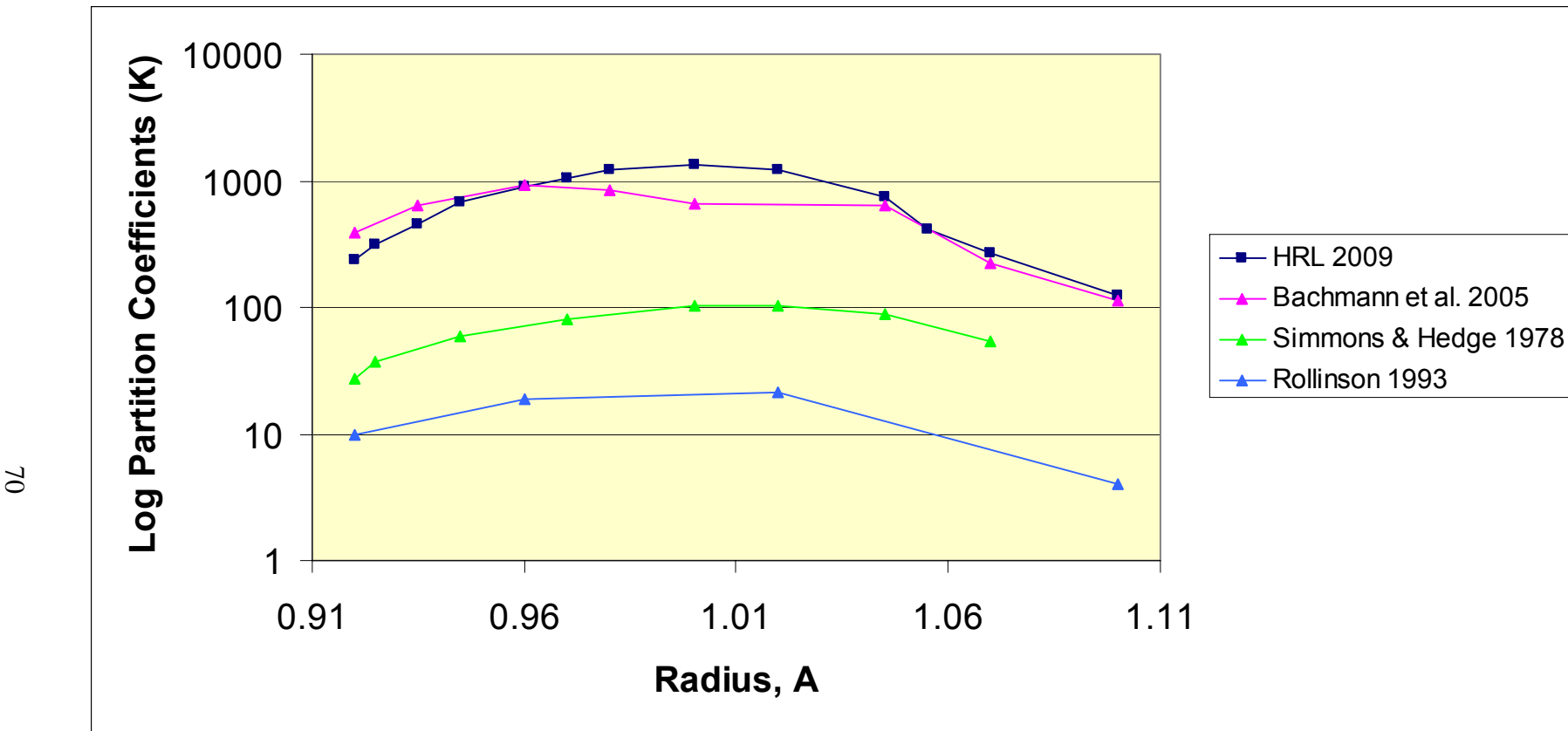


Figure 17. Partition coefficients for sphene REE.

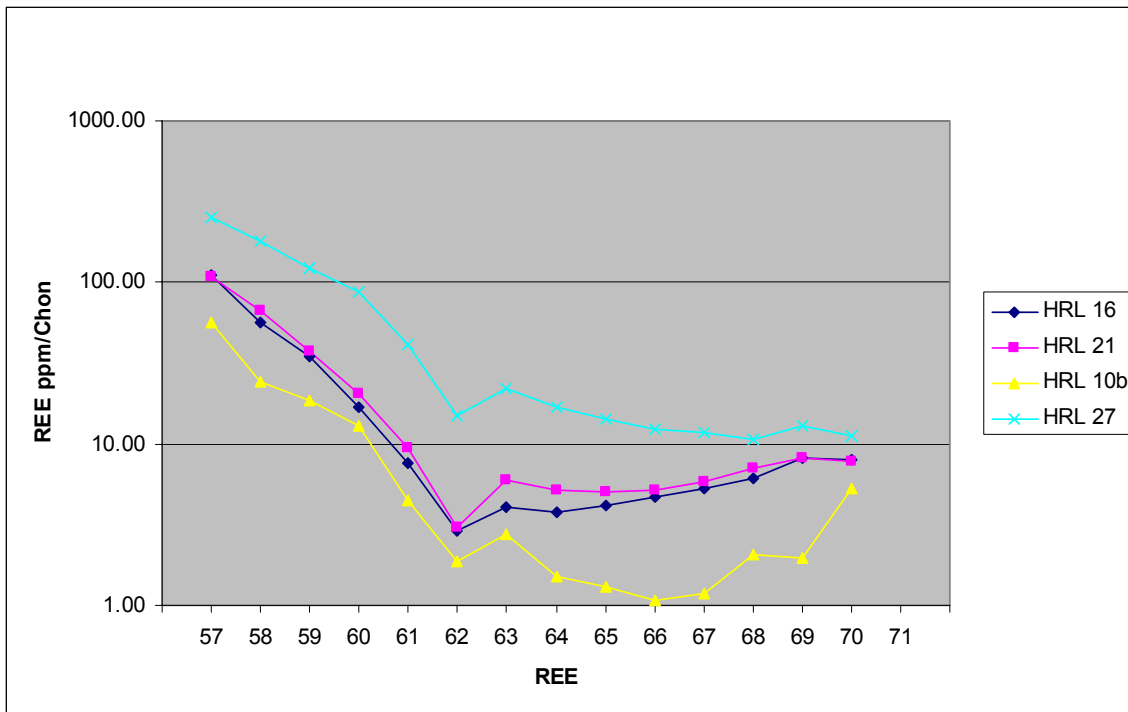


Figure 18. Average REE concentrations from glass analyses. Appendix H shows the values the averages were calculated from.

Estimating Temperatures from Zircon and Sphene Thermometry

The equation for Ti-in-zircon temperatures:

$$\log(\text{ppm Ti-in-zircon}) = (5.711 \pm 0.072) - (4800 \pm 86) / T(\text{K}) - \log a_{\text{SiO}_2} + \log a_{\text{TiO}_2}$$

is based on experiments done by Watson *et al.* (2006) and thermodynamic analysis by Ferry and Watson (2007). When the zircon is growing, Ti substitutes for Zr. The extent of this substitution is dependent on the activities of silica and TiO_2 and on temperature (Watson *et al.* 2006). Therefore if the activity of SiO_2 and the activity of TiO_2 can be estimated, then Ti-in-zircon equation can be used to estimate temperature.

Experiments done by Hayden *et al.* (2008) show that the equation:

$$T(\text{°C}) = [7708 + 960P] / [10.52 - \log(a_{\text{TiO}_2}) - \log(a_{\text{SiO}_2}) - \log(\text{ppm Zr, sphene})] - 273$$

can be used to estimate the temperature of the magma during sphene growth. When the sphene is growing, Zr^{+4} substitutes for Ti^{+4} in the crystal lattice and this substitution is dependent on the activities of TiO_2 and silica, pressure, and temperature.

Table 4 gives the estimated parameters we used in the temperature equations for zircon and sphene. All samples for which I carried out sphene or zircon analyses except HRL 27 contain quartz phenocrysts (appendix A) and therefore became saturated in silica, indicating an activity of one. Sample HRL 27 lacks quartz phenocrysts (appendix A) and is therefore not saturated in silica ($a < 1$). I assigned a silica activity of 0.7 to HRL 27. The assigned value of 0.7 is rather arbitrary, but it is intended to be consistent with the moderate SiO_2 68 wt% of the whole rock and high SiO_2 of the glass (75 wt%). The difference between $a_{SiO_2} = 0.7$ and 1.0 makes about 30-40 degrees difference in estimated temperature of growth. All three samples were undersaturated in TiO_2 (they lack rutile) (appendix A). I used an estimate of 0.7, consistent with the presence of the Ti phase sphene and with previous estimates for magmas in this region (Claiborne *et al.* 2006; Hayden and Watson 2007). A change in activity in either silica or titanium by ± 0.1 will change the temperature by $\sim 15\text{-}18$ degrees in calculated Ti-in-zircon temperature.

Table 4. Activities of SiO_2 and TiO_2 and pressure values used to estimate the temperatures from the analysis of zircon and sphene.

	<u>Sample</u>	<u>$aSiO_2$</u>	<u>$aTiO_2$</u>	<u>Pressure (Kbar)</u>
Zircon	HRL 12a	1	0.7	-----
	HRL 14a	1	0.7	-----
	HRL 27	0.7	0.7	-----
Sphene	HRL 12a	1	0.7	0.15
	HRL 14a	1	0.7	0.15
	HRL 19a	1	0.7	0.15
	HRL 21	1	0.7	0.15

We chose an activity of 1 for silica for the sphene temperature estimates because all four samples contain quartz phenocrysts (appendix A), and therefore were saturated in silica. We also note that this applies to other samples as well: sphene appears to be limited to high-silica rhyolitic melts that were saturated in quartz, so I infer that sphene growth occurs entirely, or almost entirely, with $a_{\text{SiO}_2} = 1$. An activity of TiO_2 of 0.7 was used in this study (see reasoning above for zircon). This study supports the idea that the Highland Range silicic sequence erupted from the middle portion of the Searchlight pluton (chapter VII). If this is indeed true, the pressure at which the analyzed sphene grains grew is determined by the depth of the active Searchlight magma chamber where sphene grew. The depth of middle Searchlight pluton has been estimated at ~5-6 km (Bachl *et al.* 2001), which yields a pressure of ~1.5 kbar. A change in pressure by ± 0.5 kbar will only change the temperature results by ~5 degrees. A change in silica activity by 0.1 will change the temperature by ~5 degrees; if the activity change is from 1.0 to 0.7, the temperature will change by ~20 degrees. A change in TiO_2 activity by ± 0.1 will change the temperature by ~8 degrees.

The estimated temperatures (appendix I) of sphene and zircon indicate that the zircon phenocrysts grew over a wide range of temperatures, about 210°C, while the sphene phenocrysts grew over a much narrower range of temperatures, about 75°C (figure 19). I separated the estimated sphene temperatures by sample and by zone and brightness (figure 20). Sector zones and bright CL zones apparently grew at somewhat higher temperatures than darker zones (figure 20A), except for sample HRL 19a. In sample HRL 19a, the sectors are still “hotter,” but the light and the dark areas generally are within the same temperature ranges. The edge zones generally are cooler than

interior, core, and sector zones (figure 20B). Sample HRL 14a does not follow this pattern, having cooler core and interior zones and warmer edge and sector zones. This is consistent with reaction rims of ilmenite around sphene grains in HRL 14a that are evident in figure 14a.

The equation, determined by Watson and Harrison (1983):

$$T_{\text{Zr}} = 12\ 000 / (2.95 + 0.85 * M + \ln (496\ 000 / Zr_{\text{melt}}))$$

is used to calculate the temperature at which melt of a given composition would be saturated in zircon. T_{Zr} is the saturation temperature, M is a factor dependent on the concentration of major elements in melt, and Zr_{melt} is the concentration of zirconium in the melt. We used the averages of the major oxides of the melt (appendix G) to calculate M , and the average Zr ppm from appendix H to calculate T_{Zr} . Zircon is evident in many thin sections and is present in all samples for which minerals have been separated, and Ti-in-zircon thermometry documents early saturation. Thus, it can be assumed that the melts represented by the glasses were zircon-saturated. The results for samples HRL 16, HRL 21, and HRL 27 are listed in table 5. The high silica rhyolite samples (HRL 16 and HRL 21) have an average T_{Zr} of $\sim 720^{\circ}\text{C}$, which is consistent with the estimated Zr-in-sphene temperatures. This consistency supports the accuracy of both the zircon saturation and Zr-in-sphene temperature equations. The estimated zircon saturation temperature for HRL 27 is $\sim 125^{\circ}\text{C}$ higher than the other two samples. This is consistent with the estimated Ti-in-zircon temperatures (figure 19B) for the same sample (sphene was absent in HRL 27).

Table 5. Zircon saturation temperatures, calculated from glass compositions and equation of Watson and Harrison (1983).

Sample	T (°C)
HRL 16	715
HRL 21	737
HRL 27	846

Implications of estimated temperatures

The wide range of temperatures shown by the Highland Range silicic sequence zircons (figure 19) suggests that the zircon phenocryst growth ranges over a wider span of time than growth of sphenes in the same magmas. The magmas apparently became saturated in zircon at a relatively high temperature and zircon started growing early, continuing while the magma cooled. The narrow temperature range of the sphenes suggests that they represent one specific time period of their host magma's history, while their cooler temperatures suggest that this time period probably occurs at the end stages of this magma's history. The consistency of the estimated zircon saturation temperature and the average Zr-in-sphene temperatures as stated above implies that the eruption temperature was probably close to ~720°C, the average of these temperature estimates.

In the case of sample HRL 14a, there is evidence of a reheating event. The edges of sphene phenocrysts grew at temperatures generally warmer than the core (figure 20B). Evidence for this event also includes the cores of HRL 14a being more depleted in REEs than the edges (figure 16), suggesting that a warmer injection of magma replenished the system. This event is also indicated by the reaction textures in various minerals and the unusual phenocryst assemblage (appendix A). Reheating would also cause the resorption and ilmenite growth around the sphene grains as shown in figure 14.

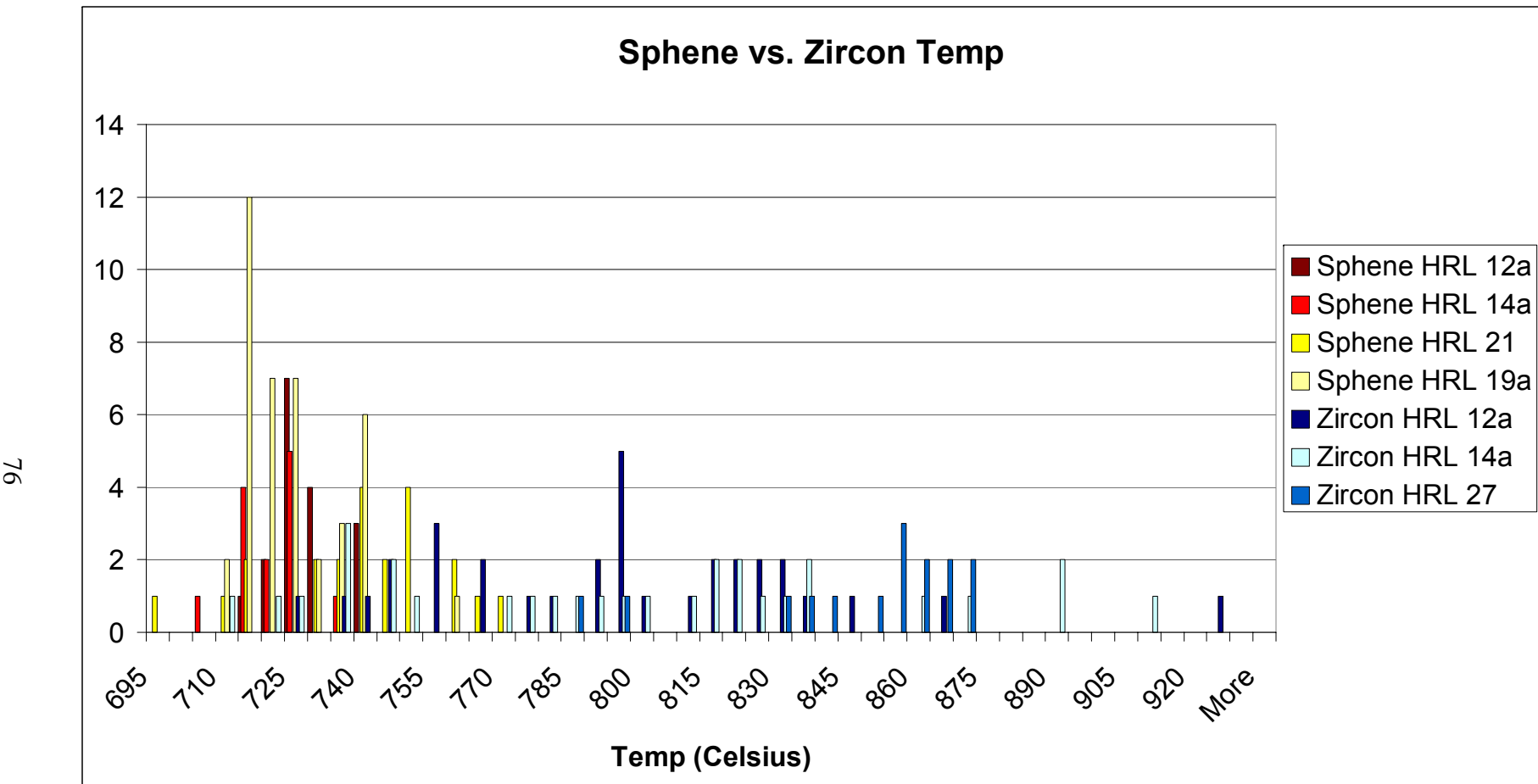
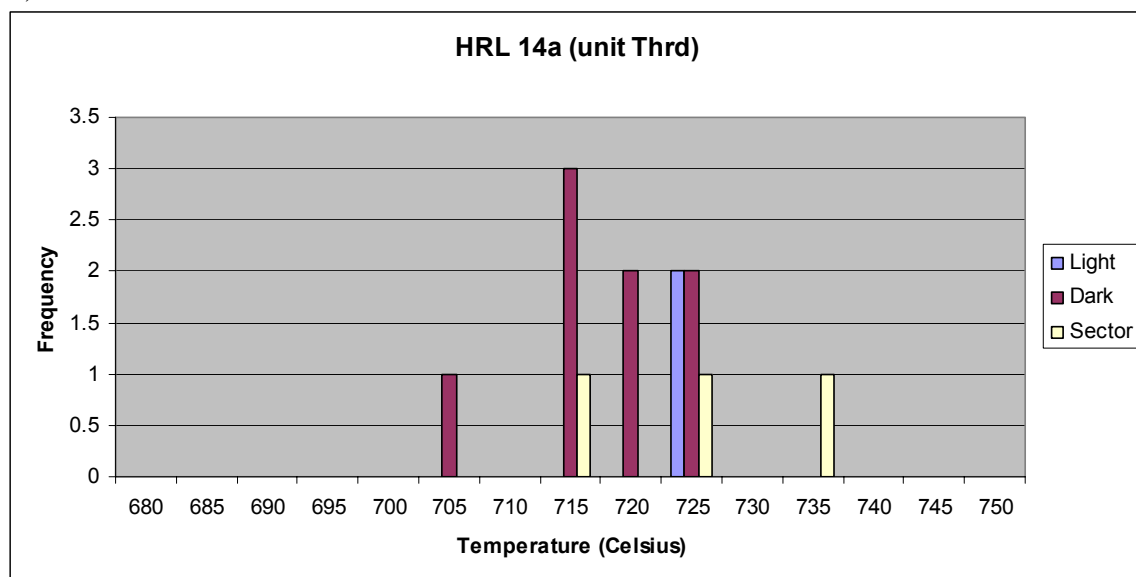


Figure 19. Temperature histogram comparing sphene temperature estimates (red and yellow) to zircon temperature estimates (blue).

A)



HRL 12a (unit Trdi)

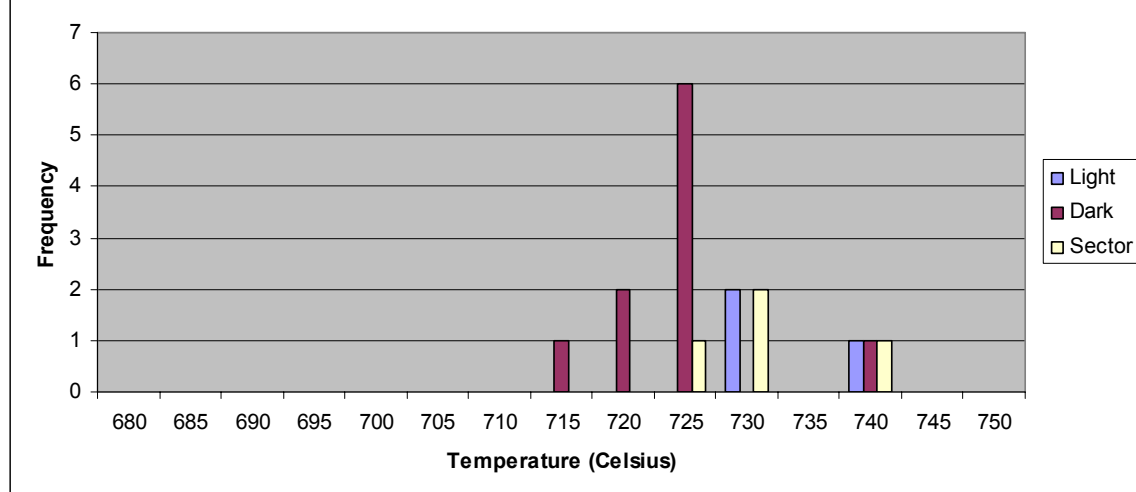


Figure 20. Histograms of temperature estimates of sphene sorted by sample. A) Histograms compare brightness temperatures within samples. B) Histograms compare zone temperatures within samples.

Figure 20, continued

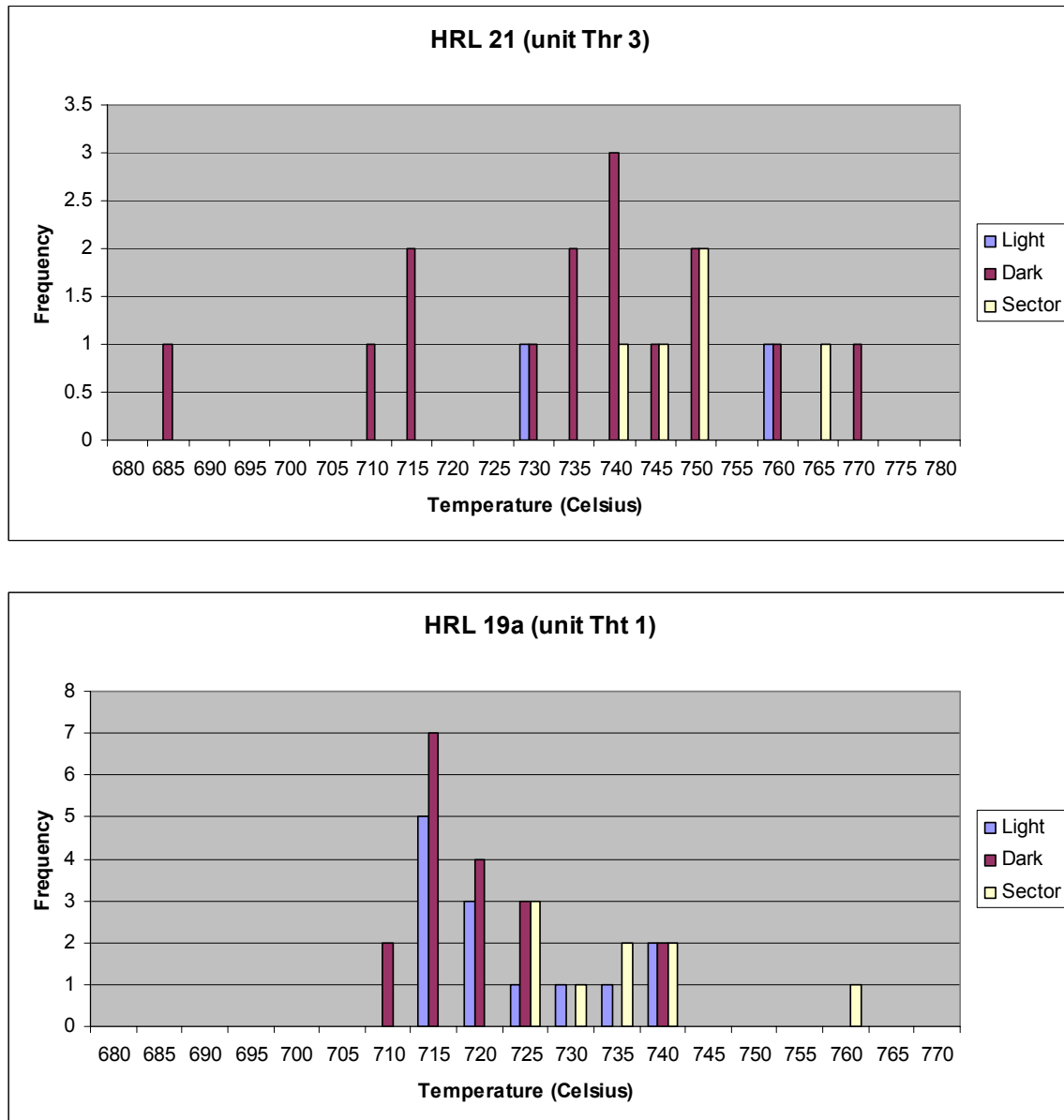


Figure 20, continued

B)

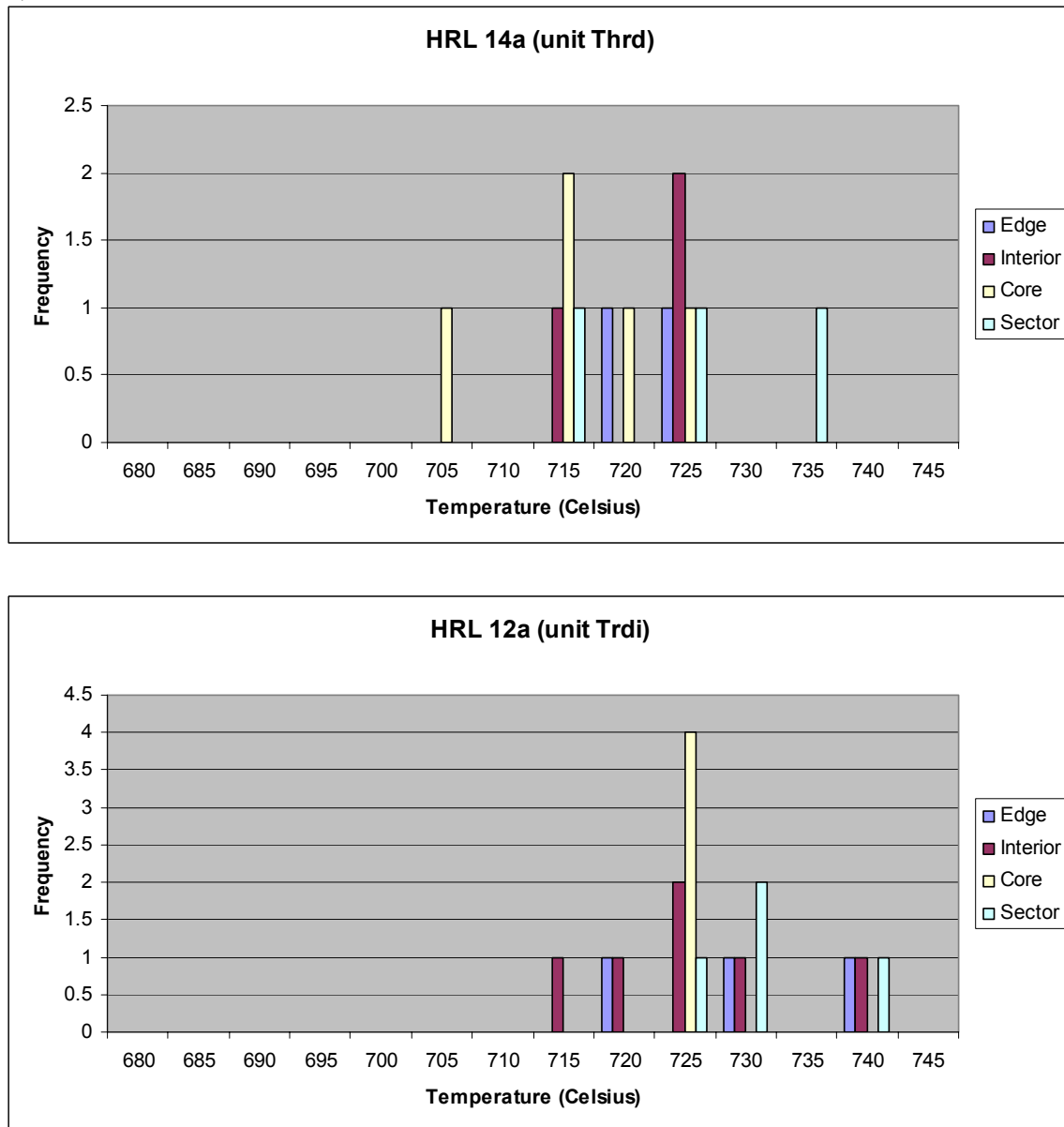
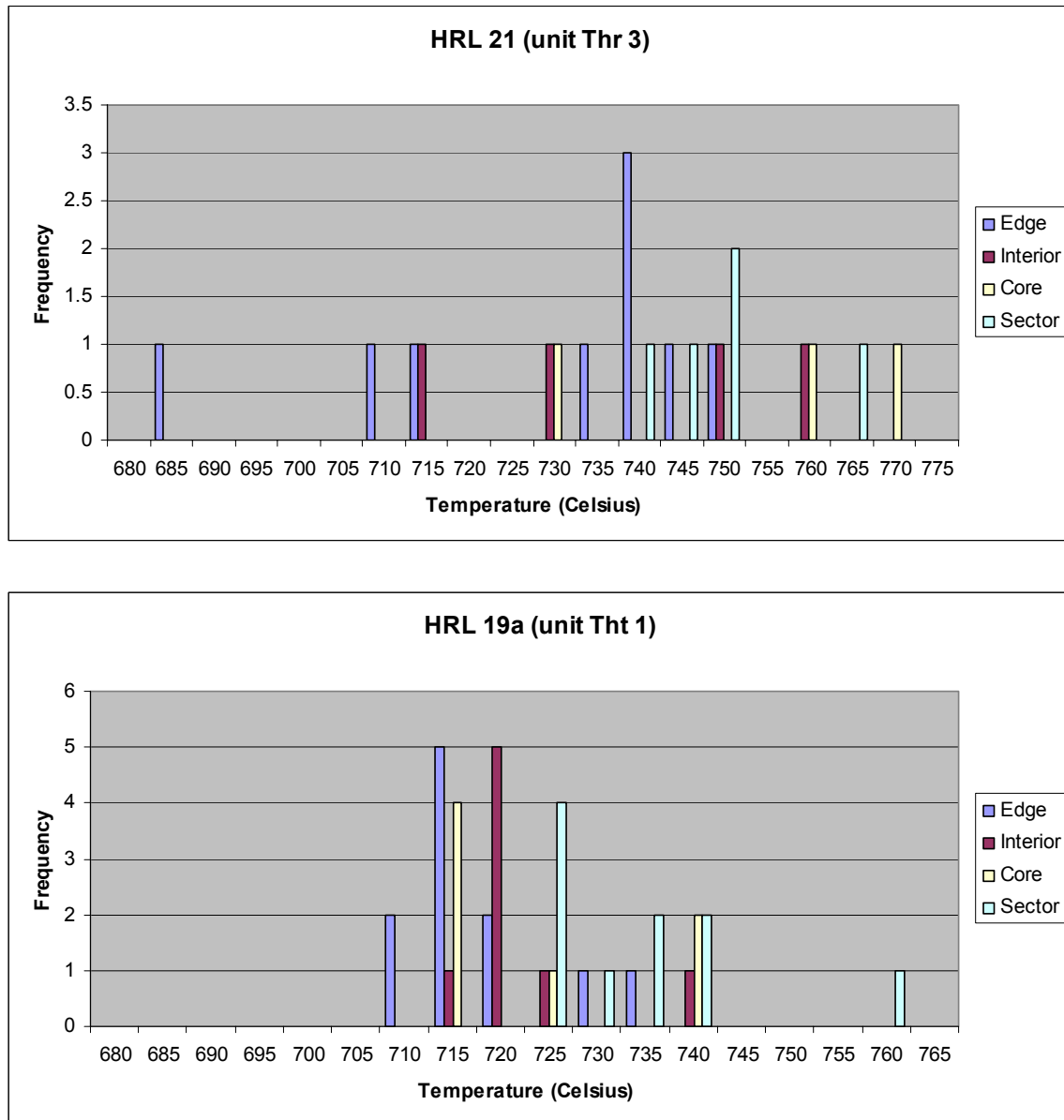


Figure 20, continued



Sphene Effects on Magmatic Processes

According to Glazner *et al.* (2008) high silica rhyolites erupt from a different source than leucogranites (highly siliceous granites) and aplite dikes, as indicated by differences in their REE patterns (figure 21). Aplite dikes in the Sierra Nevada batholith that they studied show a depleted U-shaped REE pattern with a minimal Eu anomaly, while high silica rhyolites from the Western North American Volcanic and Intrusive Rock Database (NAVDAT) that they used for comparison show an elevated REE pattern with a deep Eu anomaly. Glazner *et al.* (2008) account for this difference by suggesting that high silica rhyolites come from a different source and/or reflect different processes than the leucogranites.

The depleted U-shaped pattern is thought to be due to the fractionation of sphene out of the melt. As is clear from this thesis and other studies (figure 16; appendix E), sphene is extremely enriched in the REEs, and especially the MREEs. By fractionating out sphene, the MREEs are depleted from the melt, causing the MREE to drop dramatically in concentration, creating a U-shape pattern. The Eu depletion caused by fractionation of feldspar crystallization is in part, obscured by the fact that Eu is much less compatible with sphene than MREE (MREE can be depleted as much as or more than Eu as fractionation progresses, and thus the Eu anomaly does not grow as in sphene-free magmas).

The Highland Range silicic sequence indeed shows the effects fractionation of sphene out of the system. The core-to-rim change in abundance of REE in sphene phenocrysts provides evidence for the strong effect. When the core zones started growing the melt was not strongly depleted in the MREEs, but as the sphene continued to

grow it removed them from the melt. Lower concentrations of REEs were then available to be partitioned into the edges of the phenocrysts, causing the edges to be depleted, especially in middle REE.

The REE patterns of the glass, or melt, analyses (figure 18) have a distinctive U-shaped pattern for the sphene-bearing high silica rhyolite samples (HRL 10b, HRL 16 and HRL 21). In contrast, the less evolved sample HRL 27, which does not contain sphene and is not a high silica rhyolite, lacks the distinctive U-shape (figure 18). When we compare REE patterns of rhyolites with greater than 70 wt.% silica from the Highland range silicic sequence to the granites with similar compositions from the middle Searchlight Unit we see that both rock types plot almost the same, and the more siliceous samples of both granites and rhyolites have similar U-shaped curves (figure 22A). Middle REE depletion follows an essentially identical path with increasing SiO₂ in both granites and rhyolites (figure 22B).

The conclusions of Glazner *et al.* (2008) that high silica rhyolites come from a different source than leucogranites based REE patterns are inconsistent with the data for the Highland Range silicic sequence. The high silica rhyolites from the Highland Range silicic sequence have a U-shaped REE pattern due to sphene fractionation that matches the patterns of their strongly suspected source (chapter VII), the middle Searchlight pluton. Glazner *et al.* (2008) uses the difference between high silica rhyolites and leucogranites to imply that plutons are not the remains of large eruptive systems, but are instead magmatic systems that erupted very little if at all. In my case study of the Highland Range silicic system, I show that those conclusions are not always the case (cf.

Bachmann and Bergantz 2008a, who reach general conclusions consistent with my study).

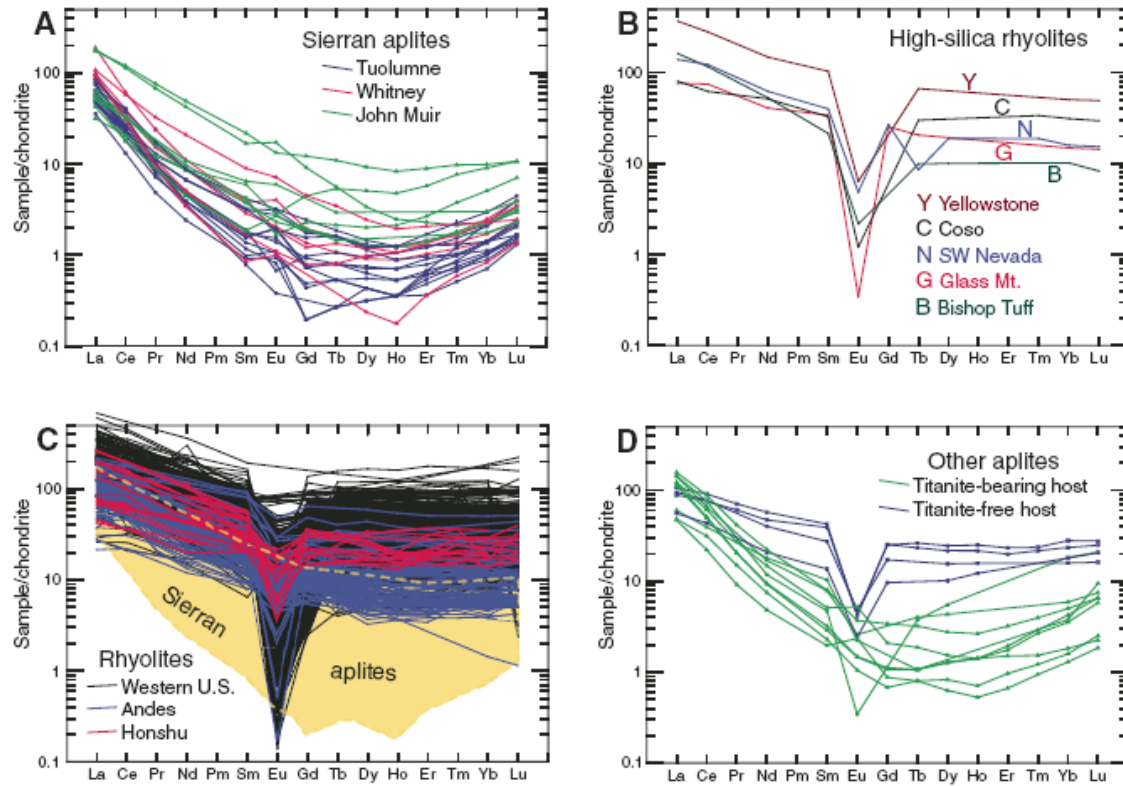


Figure 21. REE diagrams from figure 1, Glazner *et al.* 2008. A: Chondrite-normalized REE patterns of aplites from three large intrusive suites in Sierra Nevada; note consistent U-shaped patterns with depleted MREE. B: REE patterns from representative high-silica rhyolites from western U.S.; note elevated REE and deep Eu anomalies. C: REE patterns of high-silica rhyolites. D: REE patterns for other aplites that cut metaluminous plutons whose trace mineralogy are known. Titanite-bearing plutons host U-shaped aplite patterns, and titanite-free plutons do not. Data sources can be found in Glazner *et al.* 2008.

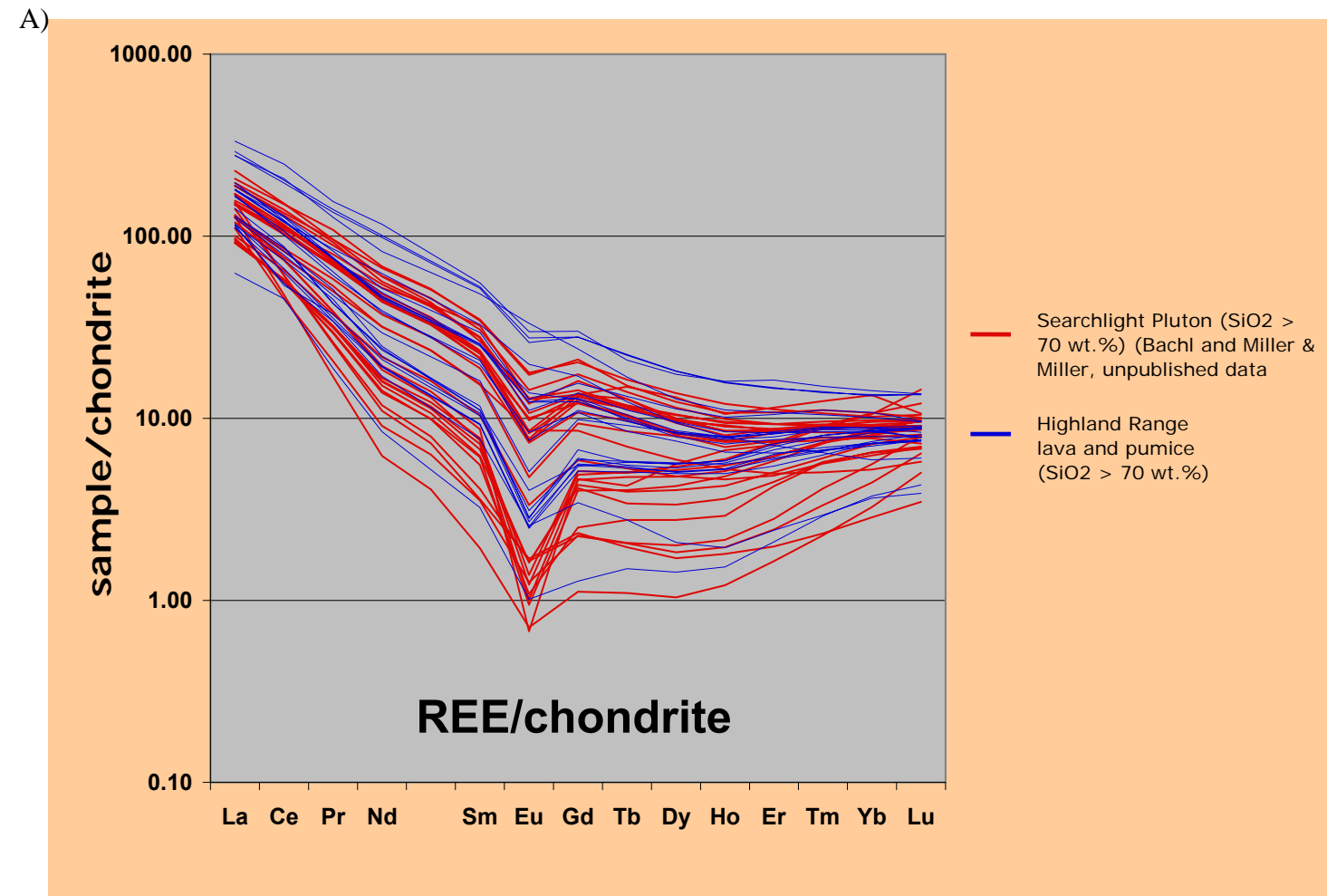
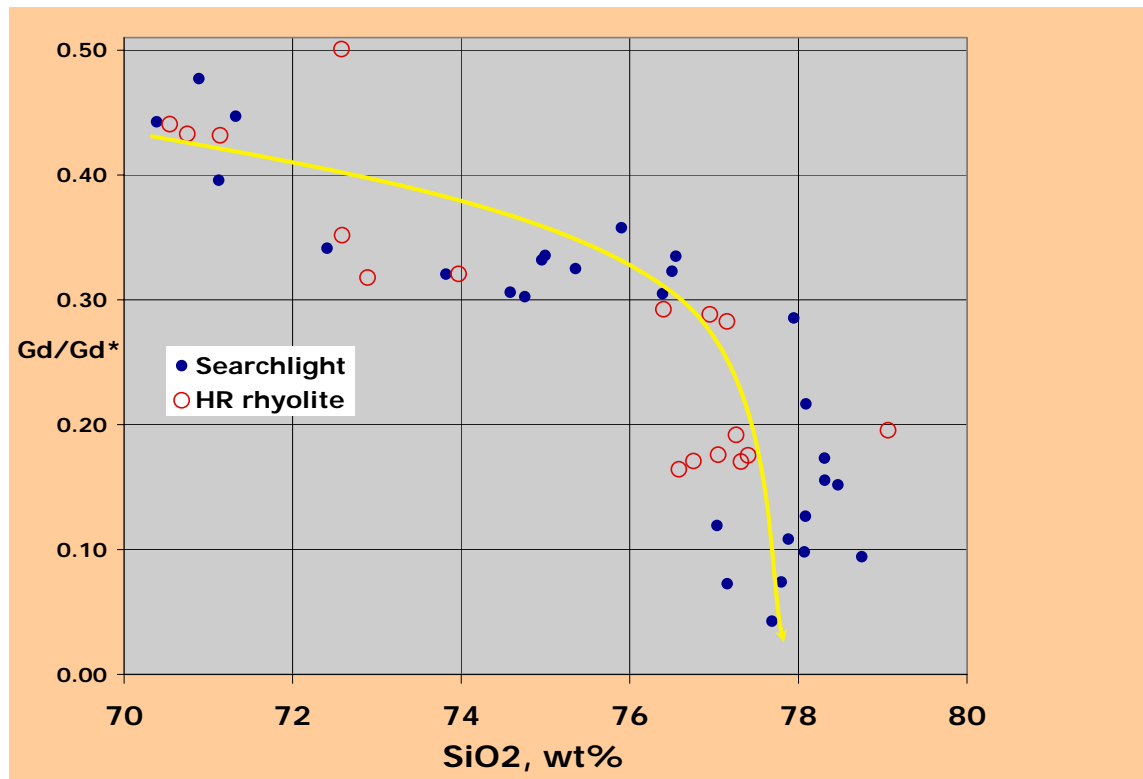


Figure 22. A) Comparison of leucogranite REE concentrations from Searchlight pluton to the high silica rhyolite REE concentrations from the Highland Range silicic sequence. B) Gd anomaly vs. SiO_2 .

Figure 22, continued

B)



CHAPTER VII

VOLCANO – PLUTON CONNECTION: RELATION BETWEEN SEARCHLIGHT PLUTON AND THE HIGHLAND RANGE SILICIC SEQUENCE

Searchlight Pluton

Searchlight pluton is tilted west about 90 degrees, exposing a 10 km section from a shallow roof, at ~4 km depth at the time of emplacement, to its floor (Bachl *et al.* 2001; Miller & Miller 2002). The roof-to-floor exposure can be split into three stratified units (figure 23): (1) the Upper Searchlight (USL) unit, a 2 km thick quartz monzonite that coarsens from a fine-grained equigranular rock at the roof to a medium-grained equigranular rock at the base; (2) the Middle Searchlight (MSL) unit, a 2 km thick medium-grained, moderate to high-silica granite that contains mafic pods, up to km-scale in size, at the base; and (3) the Lower Searchlight (LSL) unit, a 6 km thick coarse-grained quartz monzonite, containing a higher abundance of hornblende and sphene than the USL. The LSL also contains relatively large mafic pods both at its base and at its top (as does the overlying base of the MSL), and small mafic enclaves throughout (Bachl *et al.* 2001; Miller & Miller 2002). The USL intrudes into volcanic rocks of the Highland Range and southern Eldorado and northern Newberry Mountains that span the same compositional range and time interval as the Searchlight pluton, which has led to the interpretation that it is the source of the mid-Miocene volcanic center (e.g., Bachl *et al.* 2001; Faulds *et al.* 2001, 2002a; Dodge *et al.* 2005; Miller *et al.* 2007).

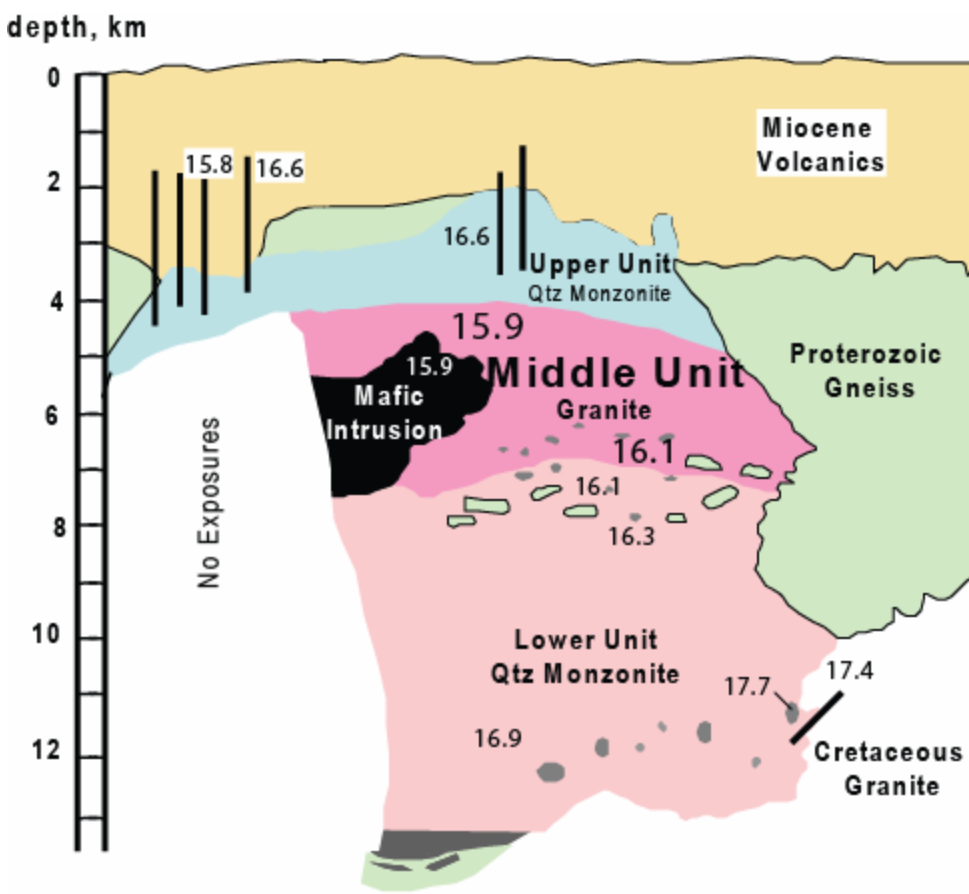


Figure 23. Reconstructed cross section of the Searchlight pluton divided into its three units, the Upper, Middle, and Lower Searchlight. Host rocks: Ireteba granite, Proterozoic gneiss, and Miocene volcanic rocks. Block horizons are visible in the upper LSL and base of the MSL, which are thought to be the products of stoping (Bachl 2001; Perrault, in review). Mafic pods are visible in the lower LSL and lower MSL.

Searchlight pluton – Highland Range Connection

Searchlight pluton intrudes the volcanic section that includes the Highland Range silicic sequence. Most of this section, including the rocks described in this thesis, is thought to be the erupted products of the pluton (Leslie *et al.* 2007; Dodge *et al.* 2005). It has been thought by workers in this area that the base of the Highland Range silicic sequence (contact between Thlb and Thr 1) might correlate with the base of the granite section of the Middle Searchlight unit (C.F. Miller, personal communication, 2008).

(figure 24). Geochemical analysis and geochronological data from this study call this interpretation into question. The zircon ages of rocks immediately above and below the Middle – Lower Searchlight pluton contact have ages of about 16.1 Ma at the contact (Perrault, in review; figure 24), while the lavas at the Thlb – Thr 1 contact have ages of about 16.6 – 16.7 Ma (table 1; figure 24). There is a compositional difference as well. The Middle Searchlight pluton is almost entirely granite with > 70 wt.% SiO₂, whereas all analyses of Thr 1 indicate trachydacitic compositions (65-70 wt.% SiO₂).

Figure 24 indicates a more likely correlation between Searchlight pluton and the Highland Range silicic sequence. Here, the Lower to Middle Searchlight transition, from a quartz monzonite to granite, is represented in the Highland Range silicic sequence by the transition from trachydacite to rhyolite at the Thr 1 – Tht 1 contact. The 16.1 Ma age of the base of Middle Searchlight is consistent with the new U-Pb and Ar-Ar ages in this study that demonstrate that the top of the rhyolite section is 16.0 Ma. The base of Thr 1 is tentatively suggested to correlate with a newly identified contact within the Lower Searchlight pluton, between more mafic quartz monzonite below (correlates with trachyandesite of Thlb) and less mafic quartz monzonite above (correlates with trachydacite of Thr 1) (N. Hinz, personal communication, 2008) and the top-most and youngest part of the rhyolite being just under 16.1 Ma.

Figure 11 shows that at 70 wt.% SiO₂ and higher, both the rhyolite unit from the Highland Range and the Middle Searchlight unit plot closely on Harker diagrams. At lower than 70 wt.% SiO₂, the Highland Range trachydacite and trachyandesite plot with the Searchlight Upper and Lower units. This is consistent with the rhyolite unit having been derived from the Middle Searchlight unit, while the Lower Searchlight unit was

likely the source of the trachyandesite and trachydacite units. A particularly compelling line of evidence supporting the connection between the silicic sequence of the Highland Range and the Middle Searchlight granite is the identical REE fractionation evident in both, strongly indicating that sphene saturation and fractionation played the same role in magma evolution in both cases (figure 22A, B).

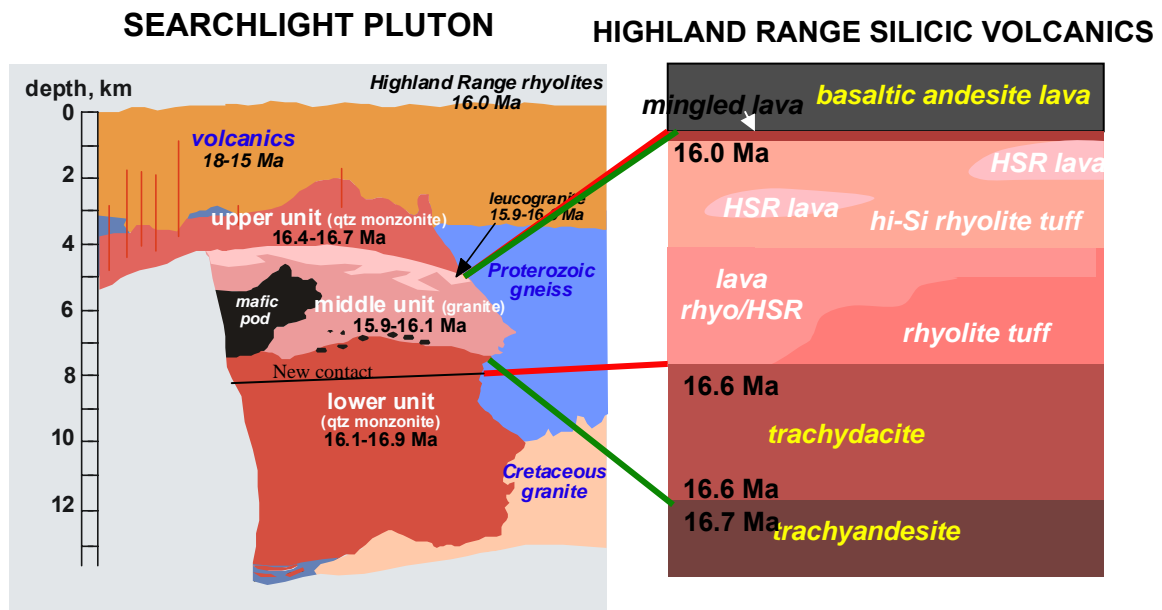


Figure 24. Previously suggested correlation between contacts in the Searchlight pluton and those in the Highland Range silicic sequence are designated by green lines. Suggested revisions of the correlation are designated by red lines.

CHAPTER VIII

CONCLUSIONS

The source of the Highland Range silicic sequence of southern Nevada is most likely from a magma chamber that formed the nearby Searchlight pluton. The rocks of the pluton and the silicic sequence are very similar in both composition and age. More research still needs to be done to unravel where each unit of the Highland Range silicic sequence came from within the Searchlight pluton units. Sphene dramatically changes the REE composition of the high-silica melt by fractionating out the middle REEs, which is apparent in both the Highland Range high-silica rhyolites and the in the leucogranites of Searchlight pluton.

. The results of this study are inconsistent with the broad conclusions Glazner *et al.* (2008) regarding the sources of high-silica rhyolites and leucogranites. Glazner *et al.* (2008) suggest that REE patterns in rhyolites show distinctly different trends from those of highly evolved granites, suggesting that they form by different processes. We demonstrate that evolution of REE in silicic rocks of the pluton and the volcanic sequence is essentially identical and that the dominant factor in both is sphene fractionation.

The Highland Range silicic sequence transitioned in eruptive style, from effusive to explosive, at the same time as it changed in composition (trachydacite to rhyolite), and in enclave abundance (enclave poor to enclave rich). These changes are hypothesized to have happened due to magma fractional crystallization, leading to more evolved, volatile

rich magma, magma rejuvenation by mafic recharge, adding volatiles and expelling melt from resident crystal mush, or both.

APPENDIX A:
Petrography and Photomicrographs of the
Highland Range Silicic Sequence

Table A1. Key to analysis processes in table A2.

Key
ρ = Thin Section
π = Geochemistry
δ = SHRIMP
ω = Ar-Ar

Table A2. Petrography of the Highland Range silicic sequence.

Sample # Analysis Processes Location Coordinates	Lithology	Descriptive Location/ Unit	Thin Section Description				Inclusions			
			Major Phenocrysts	Accessory Minerals	Groundmass			Type	Phenocrysts	
					%	Texture	Comments			
Thlb										
HRL 26 ρ π ω N35°32.037' W114°57.147'	Trachyandesite Lava	Thlb	Plag 50%; Cpx 20%; Bt 15%; San 5%	Opaques, Apatite, Zircon	70	Partial devitrification	Phenocrysts are oriented in the direction of flow	Mafic	Olv, plag, cpx, bt	Has a crenulated margin; plags are rounded and lack crystal form and twinning
Thr 1										
HRL 1 ρ N35°32.245' W114°56.976'	Trachydacite Lava	Thr 1	Plag 74%; San 20%; Bt 5%; Cpx 1%; Qtz <1%	Opaques, Apatite, Zircon	55	Devitrified glass	Possible flow banding	Clumps of Phenocrysts	Plag, bt, cpx	The larger phenocrysts of plag tend to clump together
HRL 2 ρ N35°32.189' W114°57.038'	Trachydacite Lava	Thr 1	Plag 60%; San 30%; Bt 8%; Cpx 2%	Opaques, Apatite, Zircon	60	Glassy	Flow banding with microlites	Mafic	Cpx, bt, opaques	Phenocrysts are highly altered, possible the inclusion is in the process of separating
HRL 3 ρ N35°32.631' W114°57.029'	Trachydacite Lava	Thr 1	Plag 65%; San 15%; Cpx 10%; Bt 5%	Apatite, Zircon, Opaques	40-30	Crystalline		Clumps	Cpx Plag	_____
HRL 4 ρ N35°32.850' W114°57.205'	Trachydacite Lava	Thr 1	Plag 70%; San 15%; Bt 10%; Cpx 5%	Apatite, Zircon, Opaques	40-30	Glassy	Partly devitrified; perlitic fracturing	1. Clumps 2. Clumps	1. Plag, bt 2. Plag, cpx, bt	1. The large phenocrysts of plag and bt clump together; 2. Large and small plag and cpx phenocrysts. Some of the Cpx have been altered. The bt are large phenocrysts.
HRL 11 ρ N35°32.690' W114°57.182'	Trachydacite Lava	Thr 1	Plag 70%; San 15%; Bt 10%; Cpx 5%	Opaques, Apatite, Zircon	30-40	Devitrified glass		Clumps	Plag, cpx, bt	Can be clumped or found in close proximity to each other
HRL 27 ρ δ N35°32.035' W114°57.157'	Trachydacite	Bottom of Thr 1	Plag 70%; San 15%; Bt 10%; Cpx 5%	Opaques, Apatite, Zircon	80	Glassy	Partial devitrification; microlites oriented in flow direction	—	—	_____

Table A2, continued

Sample #	Lithology	Descriptive Location/ Unit	Thin Section Description					Inclusions		
			Major Phenocrysts	Accessory Minerals	Groundmass			Type	Phenocrysts	Comments
					%	Texture	Comments			
Thr 1, cont.										
HRL 28 ρ π ω N35°32.051' W114°57.164'	Trachydacite	Thr 1	Plag 92%; Bt 6%; Cpx 2%; San =1%	Opaques, Apatite, Zircon, Sphene	80	Devitrified glass		—	—	_____
HRL 29 ρ π N35°32.448' W114°57.393'	Trachydacite	Thr 1	Plag 90%; San 5%; Bt 3%; Cpx 2%	Opaques, Apatite, Zircon	85	Crystallized	Contains microlites	—	—	_____
HRL 30 ρ N35°32.526' W114°57.497'	Trachydacite	Thr 1	Plag 90%; Bt 7%; San 2%; Cpx 1%	Opaques, Apatite, Zircon	60	Devitrified glass		Clumps	Plag, bt	Clumps are not strongly formed
HRL 31 ρ π ω N35°32.606' W114°57.595'	Trachydacite	Topmost part of Thr 1	Plag 78%; Bt 10%; Cpx 7%; San 5%	Opaques, Apatite, Zircon	50	Part devitrified, part crystallized	The microphenocrysts are oriented slightly in flow direction in the devitrified areas	Clumps	Cpx, plag	The cpx are highly altered, and the plag has little alteration
HRL 37 N35°32.664' W114°57.550'	Trachydacite lava	Top of Thr 1 at contact								

Table A2, continued

96

Analysis Processes Location Coordinates	Sample #	Lithology	Descriptive Location/ Unit	Thin Section Description					Inclusions			
				Major Phenocrysts	Accessory Minerals	Groundmass			Type	Phenocrysts	Comments	
						%	Texture	Comments				
Thr 2												
HRL 9 N35°32.618' W114°57.677'	Rhyolite Lava	Thr 2	Thr 2	—	—	—	—	—	—	—	—	—
HRL 23a p π N35°32.773' W114°57.714'	Rhyolite Lava	Thr 2	Plag 54%; Cpx 20%; San 12%; Qtz 10%; Bt 3%; Sphene 1%	Opaques	70	Recrystallized	Crystallized by secondary qtz	Mafic	Cpx, orange altered mystery mineral, plag			
HRL 23b p π N35°32.773' W114°57.714'	Mafic enclave	Collected from HRL 23a	Plag 75%; Cpx 15%; Orange mystery mineral 5%; San 4%; Qtz 1%	Opaques, Apatite	60	Devitrified glass		Clumps	Prx, plag, altered mystery mineral	Some clumps are missing pieces, as if they were plucked out		
HRL 24 p N35°32.791' W114°57.650'	Rhyolite lava	Thr 2	San 90%; Plag 6%; Bt 4%	Opaques, Zircon, Sphene	85	Crystallized	Crystallized by secondary qtz	—	—	—	—	—
HRL 25 p N35°32.771' W114°57.619'	Mafic enclave	Thr 2	San 50%; Plag 20%; Qtz 20%; Cpx 7%; Bt 3%	Sphene	90	Crystallized	Crystallized by secondary qtz	Mafic	Plag, san, cpx, bt, opaques	Groundmass (40%) is devitrified with abundant microphenocrysts; almost all prx have rims, melt inclusion cores and zones abundant in fspars; possibly highly altered olv		

Table A2, continued

Sample # Analysis Processes Location Coordinates	Lithology	Descriptive Location/ Unit	Thin Section Description				Inclusions		
			Major Phenocrysts	Accessory Minerals	Groundmass			Type	Phenocrysts
					%	Texture	Comments		
Th 1									
HRL 5 p π N35°32.861' W114°57.214'	Large lithic in rhyolite tuff	Tht 1	Plag 55%; San 35%; Bt7%; Cpx 3%	Opaques, Apatite, Zircon	40	Devitrified glass		—	—
HRL 6a N35°32.861' W114°57.214'	Rhyolite tuff	Tht 1					1. Rhy lava ? 2. Clumps 3. Mafic lava ?	1. Plag, san, bt, cpx mystery mineral 2. Cpx, plag 3. Microlites, plag microphenocrysts, mystery mineral	1. Most minerals are recrystallized or partially recrystallized, except bt; some have opaque rims 2. Not much alteration; appears as a bunch of laths jumbled together. 3. Oriented in the same direction
HRL 6b p N35°32.861' W114°57.214'	Rhyolite tuff	Tht 1	Qtz 49%; San 40%; Plag 10%; Bt 1%		10-20	Glassy	1. Mafic lava 2. Unknown lava 3. Unknown lava	1. Plag, san, bt, cpx mystery mineral 2. Plag, cpx, bt 3. Plag microlites and micro phenocrysts, cpx	1. Has a crystalline matrix; most minerals appear recrystallized (except few bt); crenulate edge; opaque rims on most phenocrysts 2. Plag laths are jumbled close together; little alteration 3. Microphenocrysts oriented in same direction

Table A2, continued

Analysis Processes	Sample #	Lithology	Descriptive Location/ Unit	Thin Section Description					Inclusions		
				Major Phenocrysts	Accessory Minerals	Groundmass			Type	Phenocrysts	Comments
						%	Texture	Comments			
	Tht 1, cont.										
HRL 7a	N35°32.814' W114°57.497'	Pumice	Tht 1								
HRL 7b	N35°32.814' W114°57.497'	Pumice	Tht 1								
HRL 7c	N35°32.814' W114°57.497'	Pumice	Tht 1								
HRL 7d	N35°32.814' W114°57.497'	Pumice	Tht 1	Qtz 70%; San 23%; Plag 7%	Sphene (inclusion in plag)	95	Glassy	Contains microlites; possible partial devitrification	—	—	—
HRL 8a	N35°32.747' W114°57.593'	Rhyolite tuff	Tht 1	Plag 55%; San 22%; Qtz 15%; Cpx 5%; Bt 3%		43	Glassy	Partial devitrification	1. Pumice 2. Rhy lava ? 3. Rhy Lava?	1. Qtz, san, plag, cpx 2. Plag, cpx, bt 3. Plag, cpx, bt	1. Qtz grows in the voids 2. Many small laths of bt between grains 3. Similar to inclusion 2, but has a glassier matrix and more plag microphenocrysts
HRL 8b	N35°32.747' W114°57.593'	Mafic inclusion	Collected from HRL 8a	Plag 65%; Cpx 30%; San 5%	Opaques	50	Devitrified glass	Contains microlites	Clumps	Cpx, plag	Large grain size

Table A2, continued

Sample # Analysis Processes Location Coordinates	Lithology	Descriptive Location/ Unit	Thin Section Description					Inclusions		
			Major Phenocrysts	Accessory Minerals	Groundmass			Type	Phenocrysts	Comments
					%	Texture	Comments			
Tht 1, cont.										
HRL 8c p π N35°32.747' W114°57.593'	Glass inclusion	Collected from HRL 8a	Plag 69%; Qtz 15%; San 10%; Bt 1%	Apatite, sphene, opaques	70-80	Glassy	Perlitic fracturing; moderate amount of microlites; microlites and microphenocrysts are foliated in flow direction	Mafic	Plag, san, cpx, olv, bt	It is either a lava clump with a possibly quenched margin
HRL 8d p π N35°32.747' W114°57.593'	Mafic inclusion in glass inclusion	Collected from HRL 8a	Plag 57%; Cpx 40%; San 3%	Opaques	30	Devitrified glass	Prevalent plag microphenocrysts	—	—	—
HRL 8e p π N35°32.747' W114°57.593'	Pumice clasts	Collected from HRL 8a	Plag 65%; Cpx 20%; San 10%; Qtz 3%; Bt 2%	Zircon and Apatite in plag	95	Glassy	Possible partial devitrification	Clumps	Plag, cpx	Sometimes an old boundary is apparent around the clumps, sometimes not
HRL 17 p N35°33.082' W114°58.737'	Rhyolite	Tht 1	Plat 40%; Cpx 40%; San 20%		50	Crystallized		—	—	—
HRL 18 p N35°32.858' W114°57.298'	Rhyolite tuff	Tht 1	Qtz 65%; Plag 25%; San 5%; Bt 5%	Sphene, opaques	30	Glassy	Partial devitrification	1. Mafic 2. Grey blobs 3. Glass fragment	1. Plag, cpx, micro-phenocrysts 2. Plag 3. Abundant plag microphenocrysts	1. Crenulated margin; 2. Crystallized grey and white 3. Abundant plag microphenocrysts

Table A2, continued

Sample # Analysis Processes Location Coordinates	Lithology	Descriptive Location/ Unit	Thin Section Description					Inclusions		
			Major Phenocrysts	Accessory Minerals	Groundmass			Type	Phenocrysts	Comments
					%	Texture	Comments			
Tht 1, cont.										
HRL 19a ρ N35°32.850' W114°57.235'	Rhyolite tuff	Tht 1	Plag 80%; San 15%; Qtz 5% Bt <1%; Cpx <1%	Sphene, opaques	20	Glassy		1. Mafic 2. Silver 3. Red	1. Plag, olv 2. Plag, cpx, olv 3. plag	1. Crystallized matrix; abundant plag microphenocrysts; olivine is altered 2. Crystallized groundmass, contains few phenocrysts, abundant opaques 3. Matrix is oxidized red, abundant plag microphenocrysts, large plag phenocrysts have absorption centers, rims, and are rounded
HRL 19b ρ N35°32.850' W114°57.235'	Rhyolite tuff	Tht 1	Qtz 55%; Plag 30%; San 13% Bt 1%; Orange mystery mineral 1%	Sphene	40	Devitrified glass		1. Silver lithic 2. Grey blobs 3. Red lithic	1. Cpx, olv, plag, bt, opaques 2. No phenocrysts 3. plag, opaques, cpx	1. Crystallized matrix; bt form small laths 2. Crystallized matrix; voids present 3. Red devitrified glass groundmass
HRL 20 ρ N35°32.850' W114°57.235'	Rhyolite tuff	Tht 1	Qtz 40%; Plag 32%; San 25%; Bt 3%		40	Devitrified glass		1. Large silver lithics 2. Mafic 3. Small silver lithics	1. Plag, cpx, opaques 2. Bt, plag, olv, cpx 3. No phenocrysts	1. Slightly devitrified groundmass; large plag phenocrysts 2. Devitrified glass groundmass; plag microphenocrysts 3. Just crystallized groundmass
HRL 38 N35°32.664' W114°57.550'	Pumice from tuff	Bottom of Tht 1 at contact with HRL 37								

Table A2, continued

Sample # Analysis Processes Location Coordinates	Lithology	Descriptive Location/ Unit	Thin Section Description				Inclusions		
			Major Phenocrysts	Accessory Minerals	Groundmass			Type	Phenocrysts
					%	Texture	Comments		
Thr 3									
HRL 21 P TT N35°32.668' W114°57.903'	High silica rhyolite lava	Thr 3	Qtz 65%; San 22%; Plag 10%; Bt 3%	Sphene, opaques	95	Glassy	Perlitic fracturing; contains sparse microlites	—	—
HRL 35 P N35°33.529' W114°57.283'	Block and Ash Flow	Thr 3	Plag 38%; San 30%; Qtz 30%; Bt 2%	Sphene; Opaques	96	Pumice	The matrix groundmass is composed of smaller pumice, glass shards and broken phenocrysts	—	—
HRL 36-1 P N35°33.659' W114°57.263'	Rhyolite lava	Dome breccia (Thr 3)	Qtz 75%; San 20%; Plag 4%; Bt 1%	Sphene	85	Glass	Perlitic fractures abundant	-----	-----
HRL 36-2 P N35°33.659' W114°57.263'	Rhyolite Lava	Dome Breccia (Thr 3)	Qtz 75%; San 20%; Plag 4%; Bt 1%	Sphene	86	Glass	Perlitic fractures abundant		
HRL 40 P N35°33.555' W114°57.188'	Rhyolite lava	Dome breccia (Thr 3)	San 55%; Qtz 33%; Plag 10%; Bt 2%		85	Glassy	Partial devitrification; perlitic fracturing	Clump	Plag
HRL 41a P TT N35°33.555' W114°57.188'	Pumice	Dome breccia (Thr 3)	San 55%; Qtz 33%; Plag 10%; Bt 2%	Epidote; sphene; Magnetite	90	Glassy			Large phenocrysts

Table A2, continued

Sample # Analysis Processes Location Coordinates	Lithology	Descriptive Location/ Unit	Thin Section Description					Inclusions		
			Major Phenocrysts	Accessory Minerals	Groundmass			Type	Phenocrysts	Comments
					%	Texture	Comments			
Thr 3, cont.										
HRL 41b p N35°33.555' W114°57.188'	Mafic enclave in flow band	Dome breccia (Thr 3)	Qtz 50%; San 39%; Plag 10%; Bt 1%	—	90	Devitrified glass		Mafic	Plag, cpx, olv	The olv is altered, the large enclave contains abundant plag microphenocrysts; the enclaves are abundant
HRL 42 p _{TT} N35°31.832' W114°58.125'	Trachydacite lava	Top of Thr 3	Plag 80%; San 10%; Bt 5%; Cpx 3%; Qtz 2%	-----	10	Glassy	It is almost crystallized do to the abundance of plag microphenocrysts	Clump	Plag, Cpx	The plag are large and euhedral
HRL 45 p _{TT} N35°33.565' W114°57.596'	Rhyolite lava	Dome breccia (Thr 3)	San 49%; Qtz 30%; Plag 20%; Bt 1%		90	Glassy	Contains elongated bubbles, like a dense pumice	Clump	Plag	Sparce
Tht 2										
HRL 10a p N35°32.583' W114°57.774'	Rhyolite tuff	Tht 2	Qtz 74%; Plag 20%; San 5%; Bt 1%	Opaques	40-50			1. Mafic 2. Grey blobs	1. Bt, plag, san, cpx 2. Glass, qtz?	1. Plags have "rotten" cores; possible crenulated margin 2. Crystallized glass, not many if any phenocrysts in them
HRL 10b p _{TT} N35°32.583' W114°57.774'	Pumice clasts	Collected from HRL 10a	Plag 49%; San 30%; Qtz 20%; Bt 1%		95	Glassy	Contains microlites, possibly biotite in composition	—	—	—

Table A2, continued

Sample # Analysis Processes Location Coordinates	Lithology	Descriptive Location/ Unit	Thin Section Description					Inclusions		
			Major Phenocrysts	Accessory Minerals	Groundmass			Type	Phenocrysts	Comments
					%	Texture	Comments			
Tht 2 cont.										
HRL 10c N35°32.583' W114°57.774'	Pumice clasts	Collected from HRL 10a	Plag 55%; San 25%; Qtz 20%		95	Glassy	Contains microlites	—	—	—
HRL 15 P N35°32.543' W114°58.062'	Pumice rich rhyolite tuff	Tht 2	Qtz 65%; Plag 33%; San 2%	Apatite, sphene	20	Glassy	Possible partial devitrification	1. Rhyolite lithics 2. Silver 3. Mafic	1. Qtz, plag, prx 2. Qtz 3. Plag, cpx	1. Has a devitrified glass groundmass with plag microphenocrysts; possible crenulate edges 2. Possibly secondary crystallized quartz 3. Small size, possible melt inclusion in cpx
HRL 16 P N35°32.640' W114°57.970'	Pumice rich rhyolite tuff	Tht 2	Qtz 60%; Plag 35%; San 5%	Apatite, Zircon, Sphene	15	Glassy		1. Rhyolite 2. Mafic	1. San, qtz, plag 2. Cpx, plag, san, apatite, olv	1. Grey crystallized, possible crenulate edges 2.
HRL 22a P II N35°32.743' W114°57.751'	Pumice	Tht 2	Plag 55%; Cpx 25%; Qtz 15%; Bt 5%	Opaques	85	Devitrified glass		Mafic	Plag, bt, cpx	Large phenocrysts of plag and cpx; tiny laths of bt; highly altered
HRL 22b P II N35°32.743' W114°57.751'	Mafic enclave	Collected from HRL 22a	Plag 75%; Cpx 25%	Apatite, Zircon, Opaques	50	Devitrified glass		Clumps	Olv, cpx, san, plag	Plag are cleaner laths in the inclusions than the plag in the groundmass

Table A2, continued

Sample # Analysis Processes Location Coordinates	Lithology	Descriptive Location/ Unit	Thin Section Description					Inclusions		
			Major Phenocrysts	Accessory Minerals	Groundmass			Type	Phenocrysts	Comments
					%	Texture	Comments			
Tht 2 cont.										
HRL 22c N35°32.743' W114°57.751'	Rhyolite tuff matrix	Collected from HRL 22a	Plag 66%; Cpx 20%; Qtz 10%; San 3%; Bt 1%	Opaques, Apatite	65	Devitrified glass		Mafic	Cpx, plag	Large grain size, with a darker groundmass than surrounding rock
HRL 32 N35°33.241' W114°57.651'	Tuffaceous sandstone	Top of Tht 2	Qtz 35%; San 25%; Cpx 25%; Plag 15%	----- --	65	Slightly Devitrified Glass	Contains fragments of pumice, glass, and lithics	1. Silver lithic 2. Lava	1. Bt, san 2. Plag, cpx	1. Has been recrystallized or altered by silica 2. Devitrified groundmass; phenocrysts are oriented in direction of flow; contains small and large plag phenocrysts
HRL 39 N35°33.273' W114°57.533'	Mafic dike	Mafic dike running through Tht 2								
HRL 43 N35°32.170' W114°58.159'	Welded tuff	SW sections of map (Tht 2)								
HRL 43a N35°32.170' W114°58.159'	Welded tuff	SW sections of map (Tht 2)	Plag 45%; San 45%; Qtz 5%; Bt 5%	Magnetite	80	Fiamme, with devitrified glass inbetween	The devitrified glass is about 15%	1. Lithic 2. Mafic	1. No minerals 2. Plag, olv, cpx	1. Brown with black speckles, brittle fractures on edges

Table A2, continued

Sample # Analysis Processes Location Coordinates	Lithology	Descriptive Location/ Unit	Thin Section Description					Inclusions		
			Major Phenocrysts	Accessory Minerals	Groundmass			Type	Phenocrysts	Comments
					%	Texture	Comments			
Thrd										
HRL 14a ρ π δ ω N35°32.543' W114°58.061'	Vitrophyre	Thrd	Plag 60%; Cpx 20%; San 15%; Bt 5%	Opaques, Apatite	80	Slightly Devitrified	Contains microlites	1. Mafic 2. Large mafic enclave	1. Plag, san, cpx 2. Plag, olv, cpx, san	1. Crystallized groundmass filled with plag microphenocrysts; the phenocrysts are larger than the ones in the large enclave 2. Contains about 75% crystallized groundmass
HRL 14b ρ N35°32.543' W114°58.061'		Enclave from HRL 14b	Plag 60%; San 25%; Qtz 5%; Cpx 5%; Olv 2%	Apatite, Zircon	30	Glassy	Contains microlites and plag microphenocrysts	1. Mafic 2. Jack Straw clump	1. Cpx, plag, olv 2. Plag, san, cpx	1. Olv, cpx, and plag phenocrysts are grouped together with abundant melt inclusions in the large plag and cpx grains 2. Abundant small opaques; jack straw texture of the san
HRL 14c ρ N35°32.543' W114°58.061'		Enclave from HRL 14b	Plag 60%; San 26%; Qtz 6%; Cpx 6%; Bt 1%; Orange mystery mineral 1%	Opaques, Apatite, Zircon, Sphene	40	Devitrified glass	Abundant microphenocrysts; very few microlites	1. Clumps 2. Mafic	1. Plag, san 2. Opaques, plag, cpx, olv	1. Very large plag phenocrysts stuck together; one clump has feathery growths along its' edges; on clump has a alteration rim all the way around it 2. Groundmass is crystallized around it
HRL 33 ρ N35°33.040' W114°57.745'	Lava breccia	Thrd	Qtz 39%; San 37%; Plag 23%; Cpx 9%; Bt 3%	Opaques	65	Devitrified glass		Lava	Plag, cpx, possible sphene	Groundmass is devitrified glass; Sphene phenocrysts may be altered Cpx

Table A2, continued

Sample # Analysis Processes Location Coordinates	Lithology	Descriptive Location/ Unit	Thin Section Description					Inclusions		
			Major Phenocrysts	Accessory Minerals	Groundmass			Type	Phenocrysts	Comments
					%	Texture	Comments			
Trdi										
HRL 12a ρ π δ ω N35°32.530' W114°57.967'	Rhyolite Porphyry	Trdi	San 60%; Plag 15%; Bt 12%; Qtz 7%; Cpx 5%	Opaques, Apatite, Zircon, Sphene	75	Devitrified glass	Groundmass contains abundant secondary quartz	Clumps	Plag, bt, san	Sparse, some bts are "bent"
HRL 12b ρ N35°32.530' W114°57.967'	Mafic inclusion	Found within intrusion (Trdi)	Plag 83%; Qtz 6%; Bt 5%; San 4%; Sphene 1%	Apatite, Zircon	30	Glass and crystalline mix		Mafic	Plag, cpx, olv, san	Many of the phenocrysts are large, especially the cpx; can see where the rust colored alteration flow lines were; Plag is the most abundant phenocrysts and contains melt inclusions and zoning; possible crenulation around edge
HRL 13 ρ N35°32.526' W114°58.037'	Vitrophyre	Collected from edge of the intrusion (Trdi)	Qtz 60%; Plag 36%; San 3%; Bt 1%		85	Glassy	Contains microlites that are foliated in places; perlitic fracturing present	—	—	—
Thb										
HRL 34 ρ	Basaltic andesite lava	Thb	Plag 85%; Cpx 10%; Orange Mystery Mineral 5%	—	5	Devitrified glass	Partly crystallized	—	—	—
Thta										
HRL 44 ρ N35°32.308' W114°58.431'	That, welded tuff	SW sections of map (Thta; see Faulds <i>et al.</i> 2002c)	Plag 45%; San 40%; Qtz 8%; Bt 2%; Cpx 1%		80	Glassy	Some alteration, perlitic fracturing	1. Lithic 2. Mafic	1. One contains no minerals, one contains foliated plag 2. Plag, cpx, devitrified groundmass	

Table A2, continued

Sample #	Evidence of Disequilibrium	Outcrop Description	Hand Sample Description	General Comments
Analysis Processes				
Location Coordinates				
Thib				
HRL 26 ρ π ω N35°32.037' W114°57.147'	Phenocrysts trend in direction of flow; few bts are altered to a higher order color; plags contain step zoning, melt inclusions, melt inclusion margins, and some are small and rounded	Forms a sharp contact with the above trachydacite lava	Maroon in color; devitrified glass; bt: euhedral, 1-2mm, altered; fspars: sub to euhedral, 0.7 - 1cm; prx: sub to euhedral, 2mm-1cm, altered, has a green center with a dark rim	
Thr 1				
HRL 1 ρ N35°32.245' W114°56.976'	San reaction rims on some plag, plags also contain melt inclusions, step zoning, and exsolution rims	_____	Red color; devitrified; fspars: sub to euhedral, 1-2mm; bt: euhedral, 2mm, altered	
HRL 2 ρ N35°32.189' W114°57.038'	Fspars exhibit melt inclusions, step zoning; possible replacement of cpx with bt	Outcrop ran as a strata, along the boundary	Black color; glassy; fspars: sub to euhedral, 1-4mm; Red/orange mineral: subhedral, 2mm; bt: euhedral, 1-2mm	
HRL 3 ρ N35°32.631' W114°57.029'	Fspars exhibit melt inclusions, step zoning; one melt inclusion in a plage contains bt and cpx	The groundmass is softer, and different than typical HR trachydacite lava groundmass; it is has a tuffaceous affect, possibly it is highly altered	White color; devitrified; bt: euhedral, 1-2mm; prx: sub to euhedral, 1-2mm; fspars: altered to a white color	There is possible secondary crystallization
HRL 4 ρ N35°32.850' W114°57.205'	Fspars contain melt inclusions, step zoning; San overgrowths are apparent; Cpx is found as inclusions in plag	Lava grades from darker color to a light white/green color, from the top of a hill to the bottom through alteration;	White color; devitrified; bt: euhedral, 2mm; prx: euhedral, 1-2mm; fspars: sub to euhedral, 2-4mm; voids: 2-3mm, some are filled completely; this sample is not as altered as HRL 3	Contains filled and unfilled spherulites
HRL 11 ρ N35°32.690' W114°57.182'	Secondary Ca and Qtz; Qtz exhibits undulatory extinction; fspars contain melt inclusions and step zoning; oxidation alteration of bt	Outcrop exhibits 2cm flow banding that has a strike of 40° N	Medium grey color; bt: subhedral, 1mm, altered; fspars: subhedral, 2-3mm, 5-6 mm; the sample is mostly devitrified glass but not completely	
HRL 27 ρ δ N35°32.035' W114°57.157'	Plag contain step zoning, melt inclusions, melt inclusion margins, san rims	The contact with HRL 26 is a black/red glassy lava	Black color; glassy; bt: euhedral, 1-2mm; fspars: reddish color, sub to euhedral, 2-4mm, abundant	Microphenocrysts are mainly plag

Table A2, continued

Sample #	Evidence of Disequilibrium	Outcrop Description	Hand Sample Description	General Comments
Analysis Processes				
Location Coordinates				
Thr 1, cont.				
HRL 28 ρ π ω N35°32.051' W114°57.164'	Plag phenocrysts are stepped zoned and contain resorption rims and cores, melt inclusions.	This is the most representative of all the trachydacite lava	Maroon red color; devitrified glass; fspat: sub to euhedral, 2-7mm; bt: euhedral, 1mm, altered; contains sparse voids, <1 -2 mm	Abundant microphenocrysts that trend in similar direction. Plag twinning more clear in this sample than majority
HRL 29 ρ π N35°32.448' W114°57.393'	Plag phenocrysts contain cores, rims, melt inclusions, step zoning	Outcrop is flow banded with a strike and dip of 335,50W	Lavender/cream color; bt: subhedral, 2-5mm, abundant; fspat: subhedral, 3-4mm, altered; prx: euhedral, 1mm, sparse	Zircon is found in the groundmass
HRL 30 ρ N35°32.526' W114°57.497'	Plag contain thin rims, slight cores, step zoning, melt inclusions	Trachydacite lava without flow banding found below the contact with the lava with flow banding; contains one mafic enclave, 10cm long, and one 3cm long. The flow banded lava has a strike and dip of 20,70NW	Light grey color; devitrified glass; fspat: euhedral, 1-5mm; bt: subhedral, 1-2mm, altered; qtz: secondary found in 1-2mm voids	Plag phenocrysts come in two sizes: Large and micro
HRL 31 ρ π ω N35°32.606' W114°57.595'	Plag contain melt inclusions in the cores and rims.	Representative outcrop of trachydacite lava, with a strike and dip of 30,35NW	Lavender/cream color; devitrified glass; fspat: subhedral, =5mm; bt: sub to euhedral, 1-2mm, altered; qtz: secondary found in =7mm voids	
HRL 37 N35°32.664' W114°57.550'		Contact grades from a tuff to a lava breccia where the boulder sized blocks contain flow banding, to a lava		

Table A2, continued

Sample #	Evidence of Disequilibrium	Outcrop Description	Hand Sample Description	General Comments
Analysis Processes				
Location Coordinates				
Thr 2				
HRL 9 N35°32.618' W114°57.677'		The elevation is at 1150m	Green color; devitrified glass; fspars: euhedral, 1mm-1cm; bt: euhedral, 1-2mm; prx: euhedral, 1mm; qtz: secondary; voids: 1mm-1cm	
HRL 23a ρ π N35°32.773' W114°57.714'	San is fractured, contains melt inclusions and absorption cores; apatite and zircon found in an altered mineral; bt has a plag inclusion;	Outcrop contains large, 15-30cm, to small, 2-4cm, mafic enclaves with crenulate margins that were then fractured	Light pink/cream color; qtz: anhedral, 1-2mm; fspars: subhedral, 1-2mm; altered red mineral: 1-3mm; lithics, sub angular, 4mm, dark grey/red color, sparse	Sometimes it seems that the dark mineral is missing/plucked out;
HRL 23b ρ π N35°32.773' W114°57.714'	Fspars have melt inclusions, resorption cores; few plags show no sign of disequilibrium	Same as HRL 23a	Dark pink color; altered rust red mineral: 1-2mm; fspars: subhedral, =1mm; prx: subhedral, 1-4mm	
HRL 24 ρ N35°32.791' W114°57.650'	Few san phenocrysts contain melt inclusions; few plag phenocrysts contain cores and zoned rims	—	Partially devitrified glass; sparse vugs filled with qtz, =1cm; contains spherolite; bt: subhedral, =1mm, sparse; fspars: sub to euhedral, 1mm	
HRL 25 ρ N35°32.771' W114°57.619'	Fspars have melt inclusions; some plag phenocrysts have san rims; few cpx phenocrysts are zoned	Contains fewer mafic enclaves than previous samples (HRL 22, HRL 23)	Rhyolite: light pink color; sparse voids, 1-4mm, filled with qtz; fspars: euhedral, 1mm and 5mm; bt: euhedral, 1mm, altered; altered red mineral =1-2mm; enclaves are 0.5 mm with larger ones, 7 X 10 cm; Enclave: Mafic; dark red color; has a chilled margin and crenulated edges; prx: =1mm; altered red mineral: =1-2mm	

Table A2, continued

Sample #	Evidence of Disequilibrium	Outcrop Description	Hand Sample Description	General Comments
Analysis Processes				
Location Coordinates				
Tht 1				
HRL 5 ρ π N35°32.861' W114°57.214'	Fspars contain undulose extinction, step zoning, inclusion rims, and melt inclusions; Bt has an oxidation altered rim	Found in a lithic rich tuff, lithics are 2mm to cobble size, with few boulders. The larger mafic lithics form horizons in the tuff. Strike and dip: NNE20, 50	Red/brown color; devitrified; fspars: subhedral, 1-5mm, altered; prx: euhedral, 1-2mm, thin laths; bt: sub to euhedral, 1mm, sparse; voids: <1-2 mm with partial filling	A bright colored mineral replaced a bt or plag grain completely, keeping the shape.
HRL 6a N35°32.861' W114°57.214'		Same outcrop as HRL 5; more abundant cobble sized lithics, both mafic and rhyolite	Cream color; pumices: 0.5-1cm; sparse lithics, = 1cm, rounded, dark red in color; bt: 1-2mm, altered	
HRL 6b ρ N35°32.861' W114°57.214'	Granophyre texture present; few melt inclusions in qtz and san; zircon found in inclusion;	Same outcrop as HRL 5; more abundant cobble sized lithics, both mafic and rhyolite	Cream color; pumices: 0.5-1cm; lithics: sub-rounded, 1mm-1cm, red, grey, tan in color; fspars: euhedral, =1mm; bt: euhedral, =1mm	Many phenocrysts are fractured through the center

Table A2, continued

Sample #	Evidence of Disequilibrium	Outcrop Description	Hand Sample Description	General Comments
Analysis Processes				
Location Coordinates				
Tht 1, cont.				
HRL 7a N35°32.814' W114°57.497'		Found in a tuff	Cream colored, large sample, solid, weathered	
HRL 7b π N35°32.814' W114°57.497'		Found in a tuff	Cream colored, large sample, solid, weathered	
HRL 7c N35°32.814' W114°57.497'		Found in a tuff	Cream colored, small sample; bt: euhedral, =1mm	
HRL 7d ρ N35°32.814' W114°57.497'	Calcite alteration	Found in a tuff	Cream colored, small sample	Qtz phenocrysts are rounded
HRL 8a ρ N35°32.747' W114°57.593'	Melt inclusions and melt inclusion rims in fspars; most inclusions show signs of alteration; secondary qtz inbetween phenocryst fragments	This outcrop is a tuff that contains large, angular, boulder sized, glassy blocks that are flow banded. It also contains cobble sized mafic blobs. The glassy blocks also contain the inclusions of the mafic blobs. The tuff contains large pumice as well.	Green color; pumice: 1-2 cm, sparse; lithics: 1- 2 mm, few are larger than 3 cm, mafic; the small lithics are rounded and the larger ones are sub angular	
HRL 8b ρ π N35°32.747' W114°57.593'	Cpx oxidation rims; San has undulose extinction, inclusion rims; plagioclase contains melt inclusion rich cores; some cpx heavily altered containing secondary quartz cores, some cpx not altered	Same as HRL 8a	Red color; prx: subhedral, 1-2mm; olv: anhedral, =1mm, altered	

III

Table A2, continued

Sample #	Evidence of Disequilibrium	Outcrop Description	Hand Sample Description	General Comments
Analysis Processes				
Location Coordinates				
Tht 1, cont.				
HRL 8c ρ _{TT} N35°32.747' W114°57.593'	Oxidation rims of cpx, cpx rimmed san, fspars contain melt inclusions; qtz and san are rounded	Same as HRL 8a	Glassy, partial devitrification; flow banded; lithics: red color, mafic, rounded, 1-2.5cm; fspars: rounded, 1-3mm; bt: euhedral, 1mm	Contains spherulites
HRL 8d ρ _{TT} N35°32.747' W114°57.593'	Fspars contain melt inclusions, rims, slight zoning	Same as HRL 8a	Tan color; prx: subhedral, 1-2 mm; bt: euhedral, 1mm; olv: anhedral, 1-3mm, altered	
HRL 8e ρ _{TT} N35°32.747' W114°57.593'	Fspars contain melt inclusions and melt inclusion rims; growth rims on san phenocrysts; san phenocrysts are rounded	Same as HRL 8a	Light tan color; bt: euhedral, 1mm, altered; fspars: subhedral, 1mm, rounded; prx: anhedral, 1-2mm, rounded	
HRL 17 ρ N35°33.082' W114°58.737'	Fspars exhibit melt inclusions, growth and resorption rims, and resorption centers; some Plag centers are altered; oxidation alteration has occurred over large areas of the slide	A brecciated lava top that contains dark tan/brown, angular 24 cm blocks within a rhyolite tuff. The tuff was squeezed into the cracks between the blocks.	Red/grey color; possible foliation; voids: elongated and flattened; prx: subhedral, 1mm; fspars: subhedral, 1mm, altered; contains an oxidized rusty colored altered unknown mineral that is anhedral and about 1mm in size	Few large vesicles; abundant fractured grains with secondary mineral growth within the fractures.
HRL 18 ρ N35°32.858' W114°57.298'	Minor oxidation of bt; fspars contain melt inclusions; Qtz is rounded and fragmented, some phenocrysts are subhedral; same san phenocrysts are euhedral	Outcrop is a large rhyolite tuff with a strike and dip of 25,50W; it contains bedded lithics that alternates from fine grain layers to coarse grain layers to a wide massive layer, until eventually forming a 20m thick massive layer.	Cream colored; pumice: 1-5mm; lithics: sub-rounded, red/brown color, 1-3mm; fspars: sub to euhedral, =1mm; qtz: anhedral, =1mm; bt: =1mm, sparse	

Table A2, continued

Sample #	Evidence of Disequilibrium	Outcrop Description	Hand Sample Description	General Comments
Analysis Processes				
Location Coordinates				
Tht 1, cont.				
HRL 19a P N35°32.850' W114°57.235'	Fspars have step zoning and resorption centers; many phenocrysts are broken	Thin 1-3cm thick course grained layer in HRL 18 rhyolitic tuff. Contains large angular clasts from 2mm to 2 cm.	Yellow/cream color; pumice: 1-4mm; lithics: subangular to sub-rounded, 1mm-1cm, orange, red, and grey colors; the smaller and large clasts form slight layers in the rock	Contains apprx. 50% pumice fragments; several broken inclusions looked like the shape or space inbetween bubbles
HRL 19b P N35°32.850' W114°57.235'	Qtz are rounded and then fractured, some are subhedral	HRL 19a alternates with this thin, coarse sand sized particle, layer, that is about 0.5 -10cm thick. This layer contains fewer clasts, 1-2mm, and similar sized pumices.	Peach cream color; pumice: 2-3 mm, sparse; lithics: =1mm, abundant, large lithics, 2-4mm, are sub-rounded and red or grey colored; there is a slight layering of the lithics, where some layers contain less lithics than others, but there is no grading between them	Phenocrysts trend in a general direction; contains spherulites, flame; generally the lithics are rounded
HRL 20 P N35°32.850' W114°57.235'	Lithics and crystals vary in size from small to large; lithics and glass are subangular to sub rounded; many phenocrysts are broken	This is a fine grained layer similar to HRL 19b but does not alternate with the coarse layer. It is possible that these layers (coarse and fine) are water lain.	Orange cream color; pumice: 2-3mm, abundant; lithics: =1mm; bt:<1mm	The phenocrysts and lithics show slight layer formation
HRL 38 N35°32.664' W114°57.550'		There is a 7m pumice section in the tuff right before it grades into the lava		

Table A2, continued

Sample #	Evidence of Disequilibrium	Outcrop Description	Hand Sample Description	General Comments
Analysis Processes				
Location Coordinates				
Thr 3				
HRL 21 ρ π N35°32.668' W114°57.903'	San contains melt inclusions that are not completely closed in; Qtz are euhedral to subhedral	This outcrop is flow banded	Blue/grey color; glassy with some flow bands; mafic inclusions are elongated and stretched in the direction of flow; fspars: euhedral, 1mm	
HRL 35 ρ N35°33.529' W114°57.283'	Pumice slightly squished; calcite alteration; melt inclusions in qtz and fspars	Clast supported, large cobble to boulder sized clasts, poorly sorted, outcrop may have been altered by silica rich hot fluids; Grades upwards from small to larger clasts and from polylithologic to monolithologic.	Pumice clast surrounded by matrix composed of smaller bits of pumice.	Phenocrysts are either large and whole OR small and broken
HRL 36-1 ρ N35°33.659' W114°57.263'	Melt inclusions in plag, san, and qtz; few microlites	Flow banded rhyolite with red nodules (chert?) running through it. The rock is a dark blue grey glass		Bts are long and thin
HRL 36-2 ρ N35°33.659' W114°57.263'	Melt inclusions in plag, san, and qtz; few microlites	Flow banded rhyolite with red nodules (chert?) running through it. The rock is a dark blue grey glass		Bts are long and thin
HRL 40 ρ N35°33.555' W114°57.188'	Spherolites, silica alteration, brittle fracturing of phenocrysts, melt inclusions in san, rounded qtz	Flow banded lava located inbetween a block and ash flow	Contains lava flow bands and the matrix	
HRL 41a ρπ N35°33.555' W114°57.188'	Some secondary calcite, Bt inclusion in san, san rimmed plag	Continuing up section from HRL 40, the flow banding decreases, while the lava becomes more pumice like		Dense pumice with flowing smooshed bubbles;

Table A2, continued

Sample #	Evidence of Disequilibrium	Outcrop Description	Hand Sample Description	General Comments
Analysis Processes				
Location Coordinates				
Thr 3, cont.				
HRL 41b ρ N35°33.555' W114°57.188'	Secondary silica and calcite alteration; san has some melt inclusions	Continuing up section from HRL 40, the flow banding decreases, while the lava becomes more pumice like		There is a fine grained rim around the large enclave implying quenching of the magma, though the enclave looks to be slightly crenulated
HRL 42 ρπ N35°31.832' W114°58.125'	Contains large plagioclase phenocrysts that have edges that are "step-like"	Contact of bottom lava to overlying tuff, the lava is very glassy and grey, the contact itself is unclear	Glassy, few spherulites, light grey in color	
HRL 45 ρπ N35°33.565' W114°57.596'	Secondary calcite filling bubbles		Lava is white in color, but not altered	
Thr 2				
HRL 10a ρ N35°32.583' W114°57.774'	Qtz contain melt inclusions and exhibit undulose extinction	A light tan colored tuff containing abundant 1cm pumice clasts with sparse pumices that are up to 3cm. Also contains 1cm lithic clasts that are less abundant than the pumice	Cream color; pumice: 1mm-1cm; lithics: red and grey colors are sub-rounded, white ones are angular, 1mm-3cm	Qtz are rounded and fractured
HRL 10b ρ π N35°32.583' W114°57.774'	Qtz is subhedral, contains melt inclusions; fspars have step zoned rims	The same as HRL 10a	Cream color; bt: euhedral, = 1mm; fspars: subhedral, 2mm	Contains partially filled spherulites; phenocrysts and microlites oriented in flow direction in some areas; perlitic fracturing of glass

Table A2, continued

Sample #	Evidence of Disequilibrium	Outcrop Description	Hand Sample Description	General Comments
Analysis Processes				
Location Coordinates				
Tht 2 cont.				
HRL 10c N35°32.583' W114°57.774'	Melt inclusions in plag cores and rims; plag also contain step zoning and undulose extinction	The same as HRL 10a	Cream color; bt: euhedral, = 1mm; fspars: subhedral, 2mm	
HRL 15 p N35°32.543' W114°58.062'		A cream rhyolite tuff containing abundant 1-4cm sized pumice, and less abundant similar sized lithics.	Cream colored; pumice filled; pumice: 0.5 mm to 2 cm; lithics: sub-rounded, 2mm - 1.5 cm, red and dark grey colored; qtz: anhedral, 1-3mm, sparse	Several grains are fractured; some pumice fragments have a bright yellow secondary growth in their vesicles
HRL 16 p N35°32.640' W114°57.970'		A cream rhyolite tuff containing abundant 1-4cm sized pumice, and less abundant 1cm lithics.	Cream colored; abundant pumice: 0.5-4cm; lithics: angular to rounded, dark grey color; qtz: possibly secondary, filling voids	Contains spherulites
HRL 22a p II N35°32.743' W114°57.751'	Two sizes of plag, small laths and large ones with melt inclusions, step zoning and resorption centers; Qtz rounded, contain melt inclusions, fractured; Cpx altered with opaque centers;	Contains sub-rounded to sub angular white enclaves, possibly pumice, as a breccia in a rhyolite matrix. The enclaves are 14-20cm in size, with 2-8cm mafic enclaves found within both the enclaves and the matrix.	Green/cream color; fspars: =1mm; bt: 1mm; prx: 1mm; altered orange mineral: 2mm; voids and phenocrysts show foliation	
HRL 22b p II N35°32.743' W114°57.751'	Two sizes of plag, microphenocrysts and large phenocrysts which contain resorption centers and melt inclusion rich rims	Same as HRL 22a	Red color; olv: anhedral, 1-3mm; fspars: subhedral, =1mm; voids: <1mm	

Table A2, continued

Sample #	Evidence of Disequilibrium	Outcrop Description	Hand Sample Description	General Comments
Analysis Processes				
Location Coordinates				
Tht 2 cont.				
HRL 22c N35°32.743' W114°57.751'	Fspars contain melt inclusion rich rims and step zoning; Qtz grains are large, rounded and contain unenclosed melt inclusions; a euhedral cpx is found in the center of a plagioclase grain	Same as HRL 22a	Red color; olv: anhedral, 1-2mm; bt: euhedral, 1mm; voids: <1 to 2 mm; possible pumice present, 2-6mm	It's possible the opaques are altered bt or possibly prx
HRL 32 N35°33.241' W114°57.651'	Secondary Ca, some alteration of phenocrysts;	Contains small 2-3 mm pumice clasts; Exhibits no layering; Lithics are 2-4 mm in size with ~10-15% lithics		Subrounded to angular fragments comprise the rock; contains pumice shards; looks similar to a sandstone; phenocrysts and enclaves much larger than size of rounded grains
HRL 39 N35°33.273' W114°57.533'		Shows quenching and backing at the contact	Vesicle rich, similar (same) as the bt. Rich basalt on top	
HRL 43 N35°32.170' W114°58.159'	Contact of top tuff to capping lava. The contact transitions from a welded tuff to a red baked layer with an undulating contact line, similar to other capping lava contacts	Contains fiamme (1cm), but welded tuff is a thin layer, about 4m wide		
HRL 43a N35°32.170' W114°58.159'	Contact of top tuff to capping lava. The contact transitions from a welded tuff to a red baked layer with an undulating contact line, similar to other capping lava contacts	Contains fiamme (1cm), but welded tuff is a thin layer, about 4m wide	Contains half a spherulite and a possible granophyre or mermikite.	

Table A2, continued

Sample #	Evidence of Disequilibrium	Outcrop Description	Hand Sample Description	General Comments
Analysis Processes				
Location Coordinates				
Thrd				
HRL 14a ρ π δ ω N35°32.543' W114°58.061'	Fspars contain step zoning, melt inclusions, sparse alteration along rims; cpx contains melt inclusions	A black lava breccia that contains abundant lithics, including heavily vesiculated lithics, and enclaves similar to the ones visible in the intrusion (HRL 12a,b & HRL 13). The contact between the black lava and the tuff beneath it transitions from pink to orange to cream, it is possible that this colored area is due to being "baked" by the incoming lava or because it is a paleosol.	Dark grey color; devitrified; qtz: anhedral, 1-5mm; bt: <1mm; fspars: sub to euhedral, 1-2mm; voids: 1mm; red alteration rims around some of the spars	Microlites and microphenocrysts trend in direction of flow; check sheet for sketches and interesting info relating one grain to one in the enclave.
HRL 14b ρ N35°32.543' W114°58.061'	Fspars contain melt inclusions, undulose extinction, melt inclusion rims	Same as HRL 14a	Red color; devitrified glass; bt: 1mm; fspars: <1mm; voids present	Several cpx phenocrysts have a black alteration rim
HRL 14c ρ N35°32.543' W114°58.061'	Fspars contain melt inclusions, growth rims, undulose extinction; small bright rims around altered cpx	Same as HRL 14a	Contains fragments of both HRL 14a and HRL 14b	
HRL 33 ρ N35°33.040' W114°57.745'	Calcite alteration ~3%	Black lava layer has a crenulate margin with the red/pink layer; black lava is brecciated but becomes more solid up section		Grains are oriented in direction of flow; 3 layers comprising a change from small to larger phenocrysts; contains lithics

Table A2, continued

Sample #	Evidence of Disequilibrium	Outcrop Description	Hand Sample Description	General Comments
Analysis Processes				
Location Coordinates				
Trdi				
HRL 12a ρ π δ ω N35°32.530' W114°57.967'	Large fspars are rounded, contain melt inclusions; bt not altered but has a higher order color	A felsic hypabyssal intrusion that intrudes into the top of above tuff layer indicating the ending time of the rhyolite activity. Contains mafic blobs that were molten, 1-15cm, they are visible all the way up to the contact.	Lavender color; bt: euhedral, 1mm; fspars: sub to euhedral, =0.5 - 1cm; sphene: euhedral, <1mm; qtz: anhedral, 1-3mm	
HRL 12b ρ N35°32.530' W114°57.967'	Fspars (mostly san) contain melt inclusions and a secondary "eating" into the mineral; abundant secondary qtz	Same as HRL 12a	Dark red color; bt: <1mm; fspars: <1mm; an unknown altered mineral is present; possible crenulated edges of enclave with rhyolite	
HRL 13 ρ N35°32.526' W114°58.037'	Fspars are fractured with possible secondary growth within the fractures	There is a black vitrophyre rind at the contact, surrounding tuff appearing orange and "baked".	Dark grey color; glassy, partial devitrification; flow banded; fspars: subhedral, some rounding	Contains spherulites
Tnb				
HRL 34 ρ	Three sizes of plagioclase, microphenocryst, medium and large; Fluid inclusions in plagioclase; orange mineral seems to be replacing or is the altered state of another mineral, maybe cpx			
Thta				
HRL 44 ρ N35°32.308' W114°58.431'		Contact between tuff and welded tuff is weakly defined, red in color, hard, solid, possible fiamme.		Possible granophyre or mermikite

Figure A1: HRL 1, overview texture, XPL.

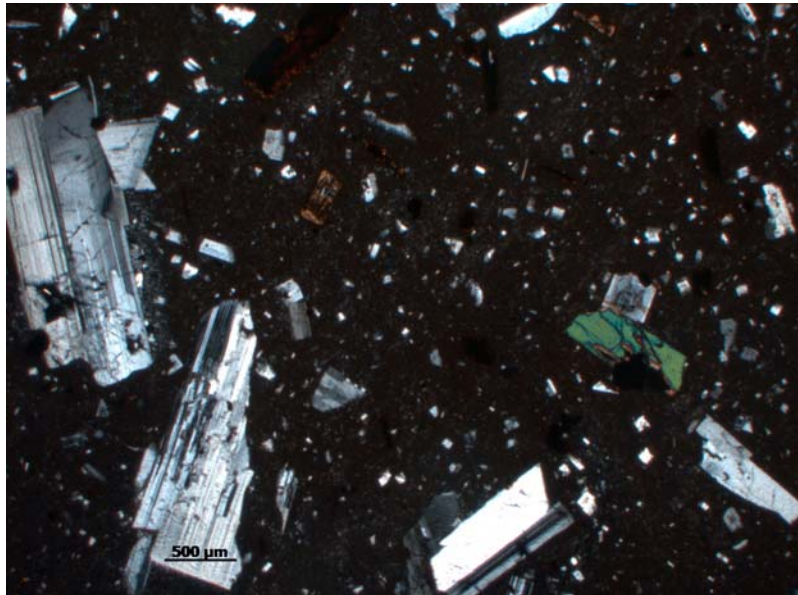


Figure A2: HRL 2, overview texture, XPL.

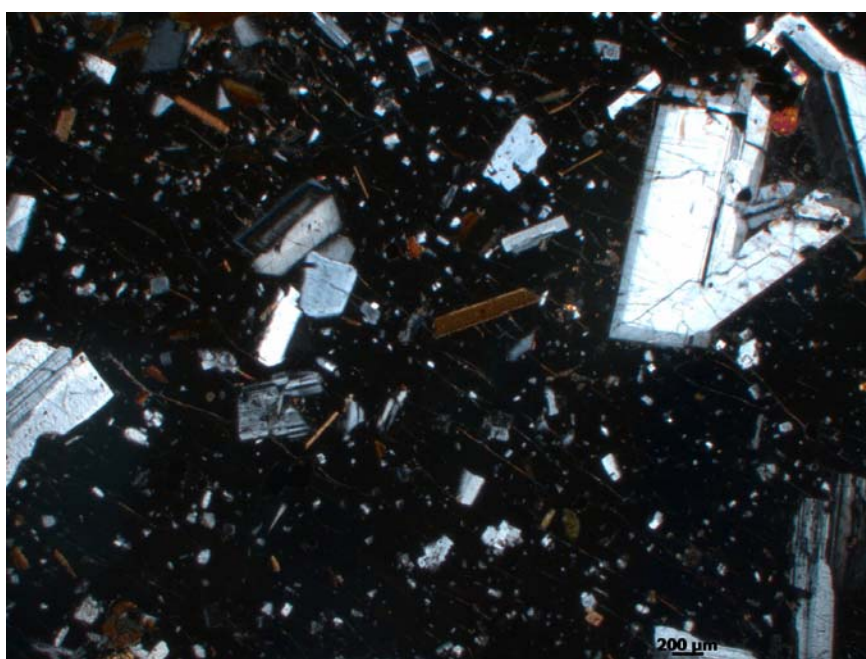


Figure A3: HRL 3, overview texture, XPL.

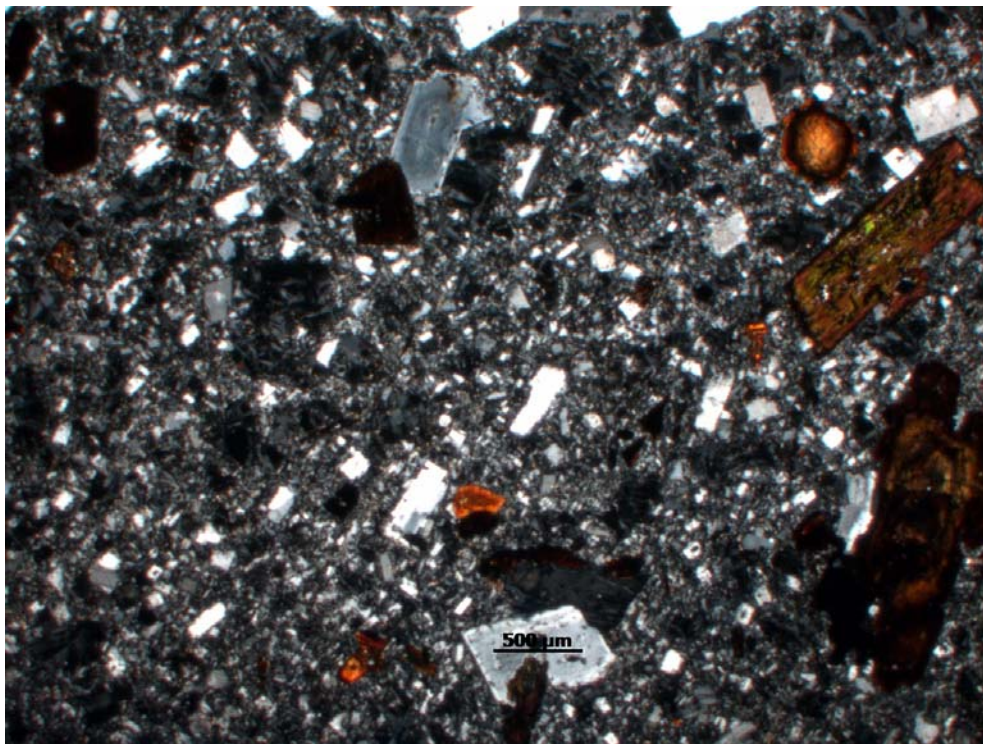


Figure A4: HRL 3, plagioclase rimmed by sanidine.

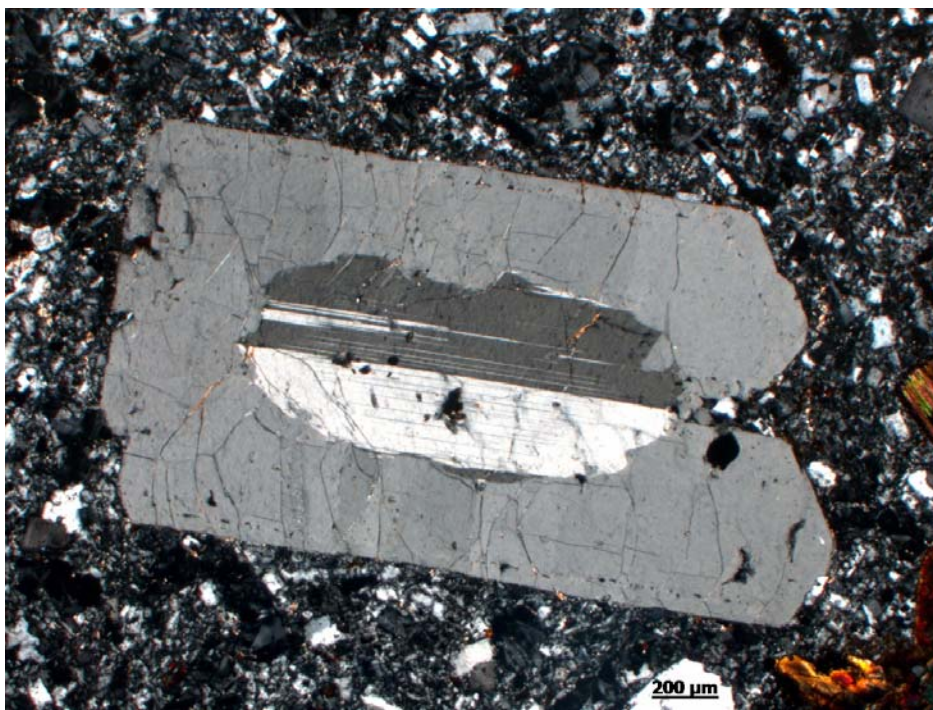


Figure A5: HRL 4, overview texture, XPL2.

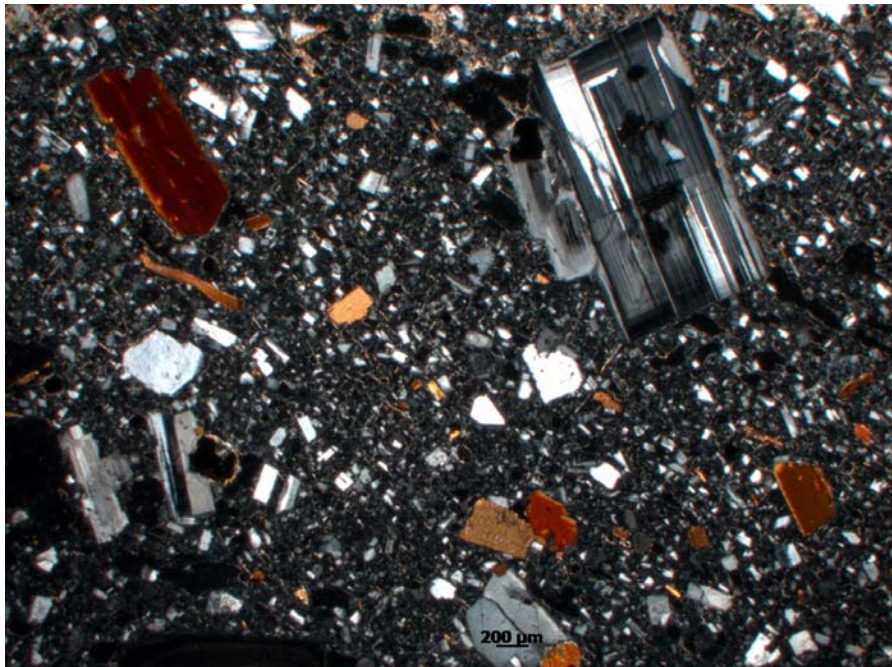


Figure A6: HRL 4, phenocryst clump inclusion.

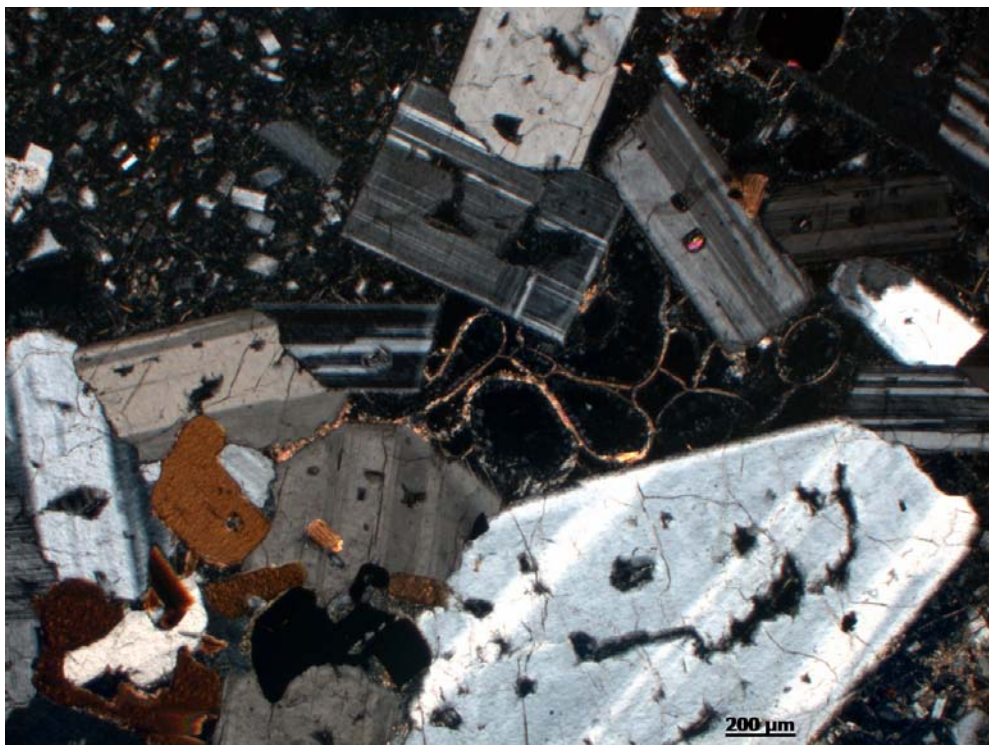


Figure A7: HRL 5, grungy yellow mystery mineral, XPL.

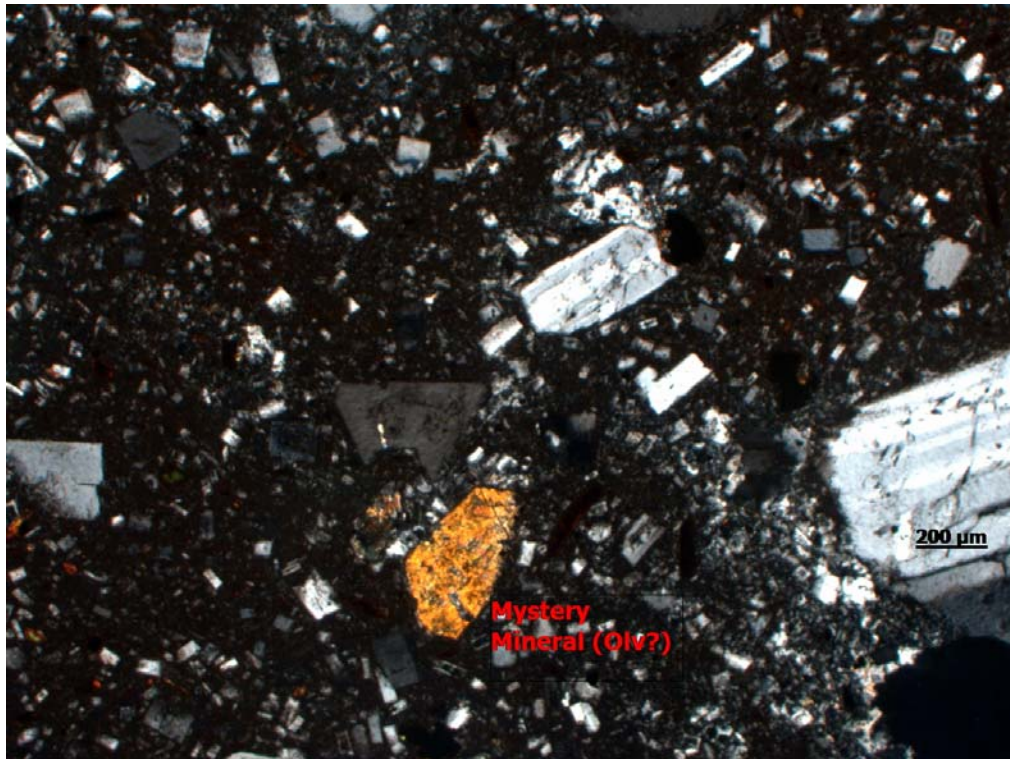


Figure A7: HRL 5, overview texture, PPL.

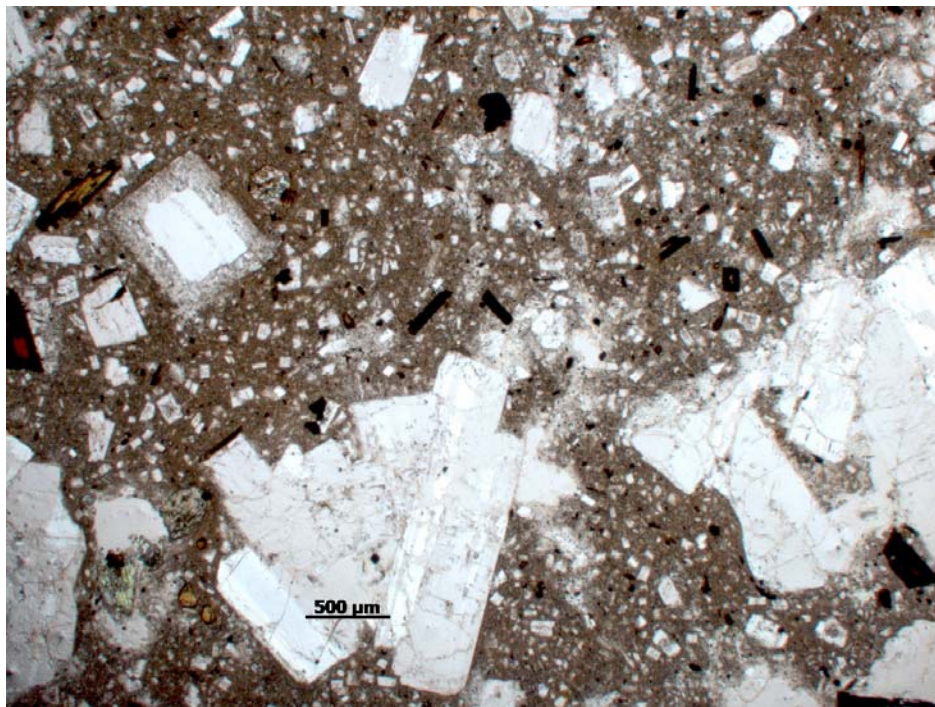


Figure A8: HRL 5, overview texture, XPL.



Figure A9: HRL 6b, inclusion.

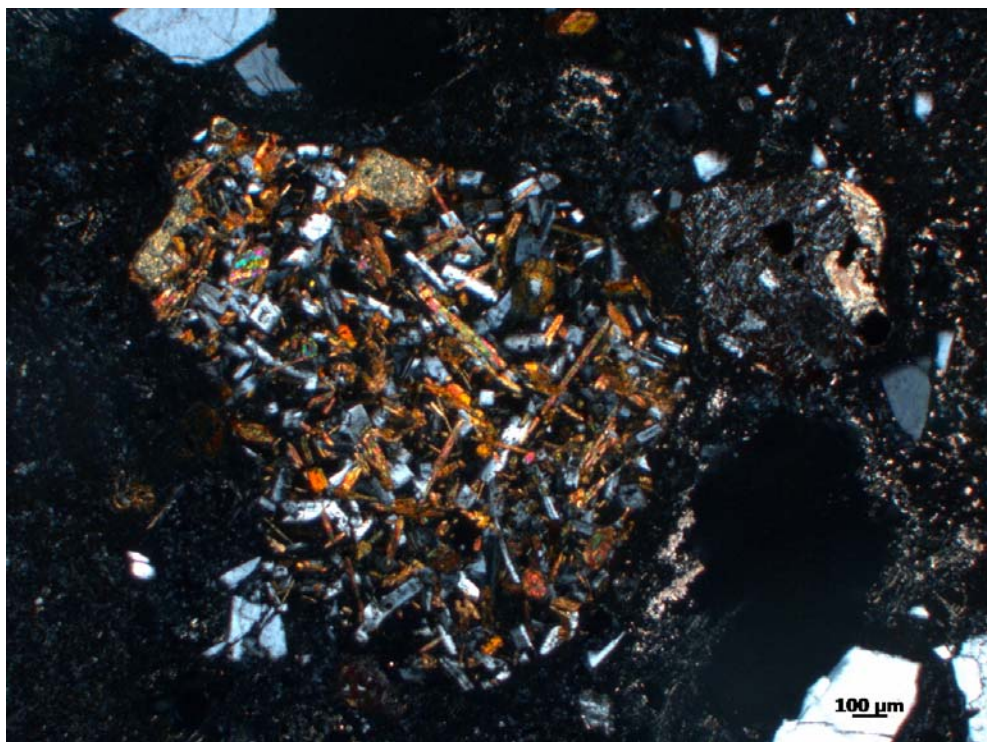


Figure A10: HRL 6b, inclusion.

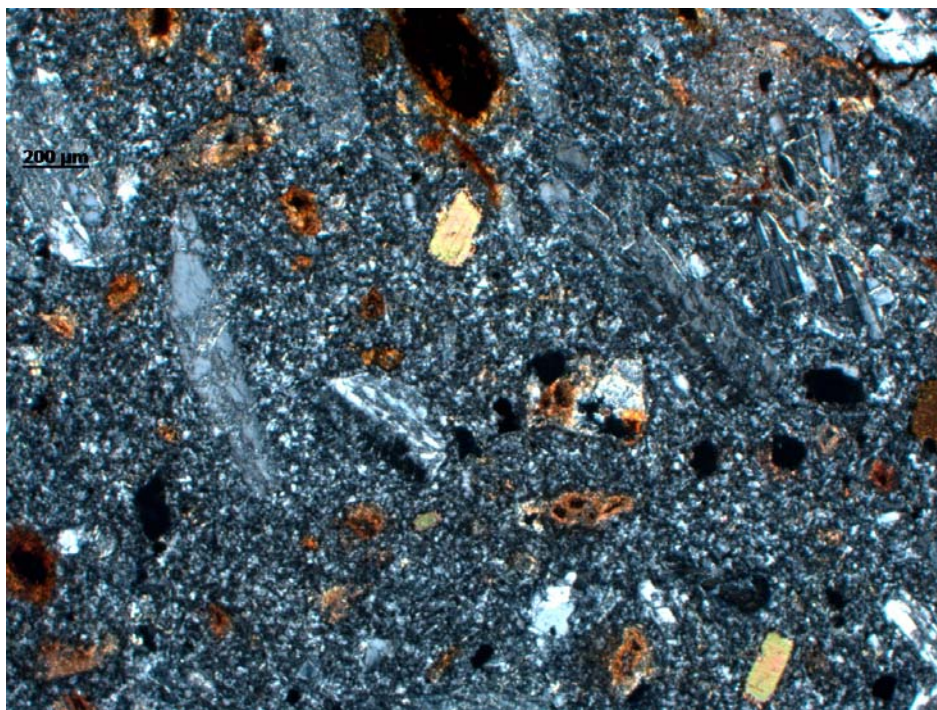


Figure A11: HRL 6b, inclusion.

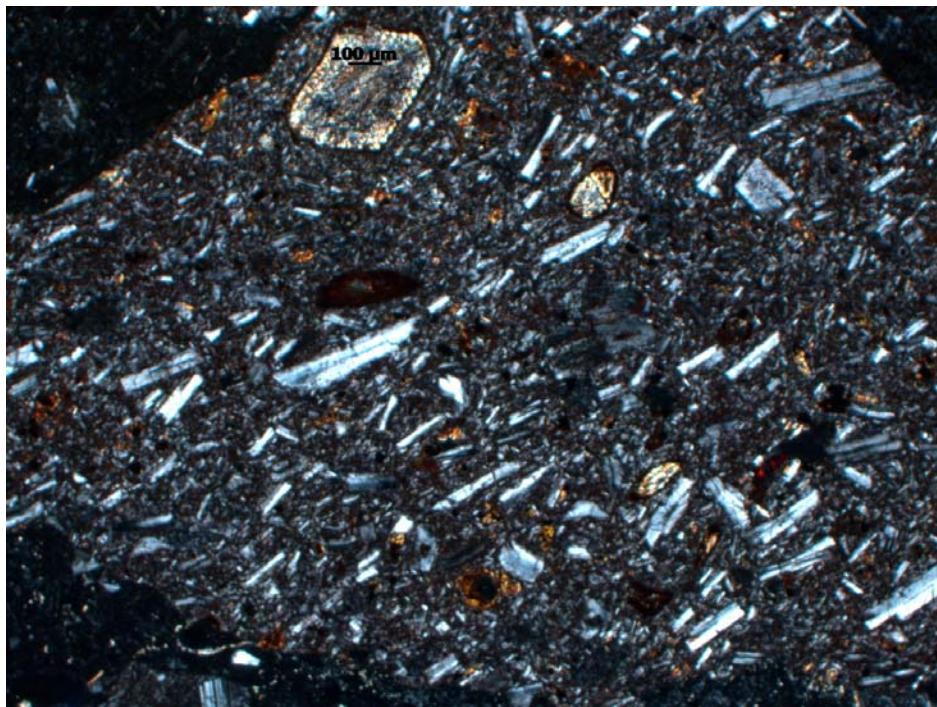


Figure A12: HRL 6b, overview texture, PPL.

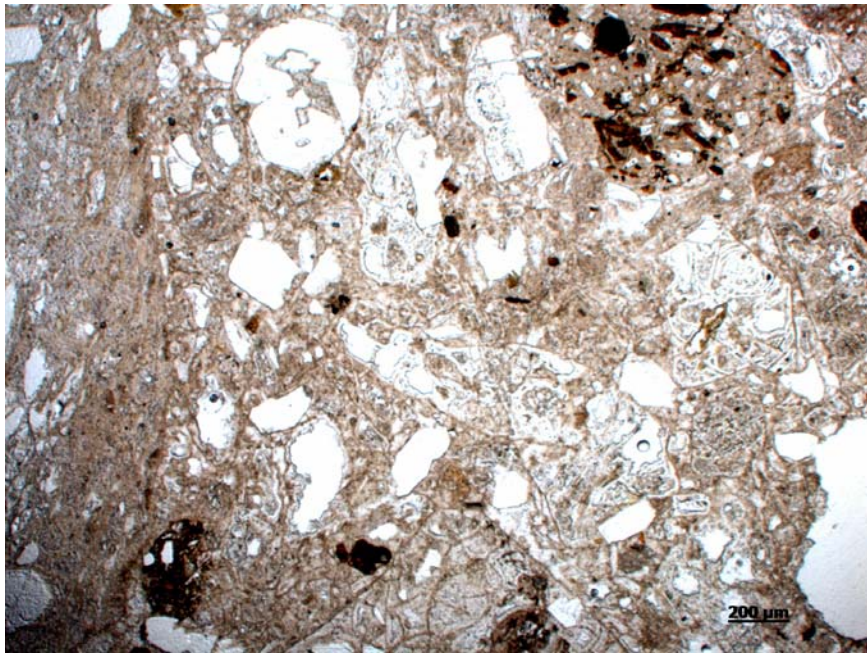


Figure A13: HRL 6b, overview texture, XPL.

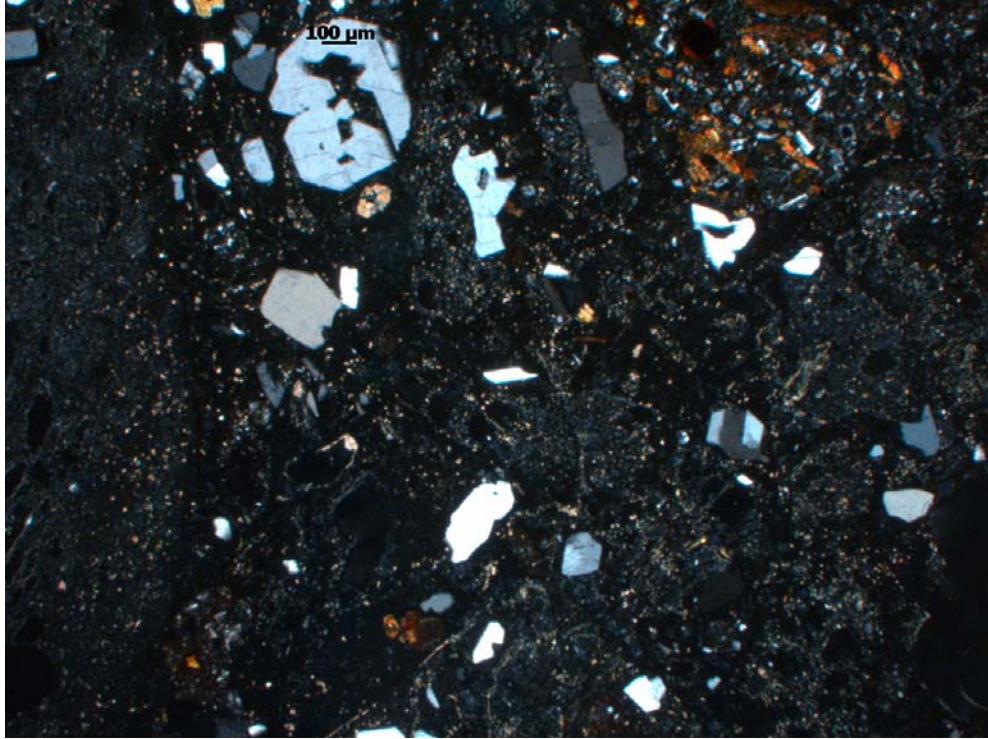


Figure A14: HRL 7d, overview texture, PPL.

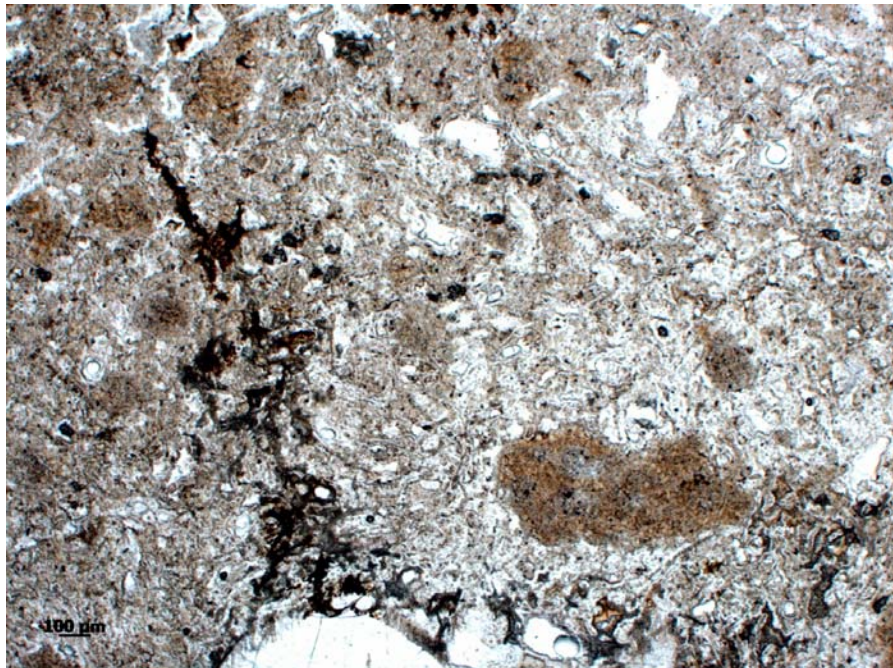


Figure A15: HRL 7d, overview texture, XPL.

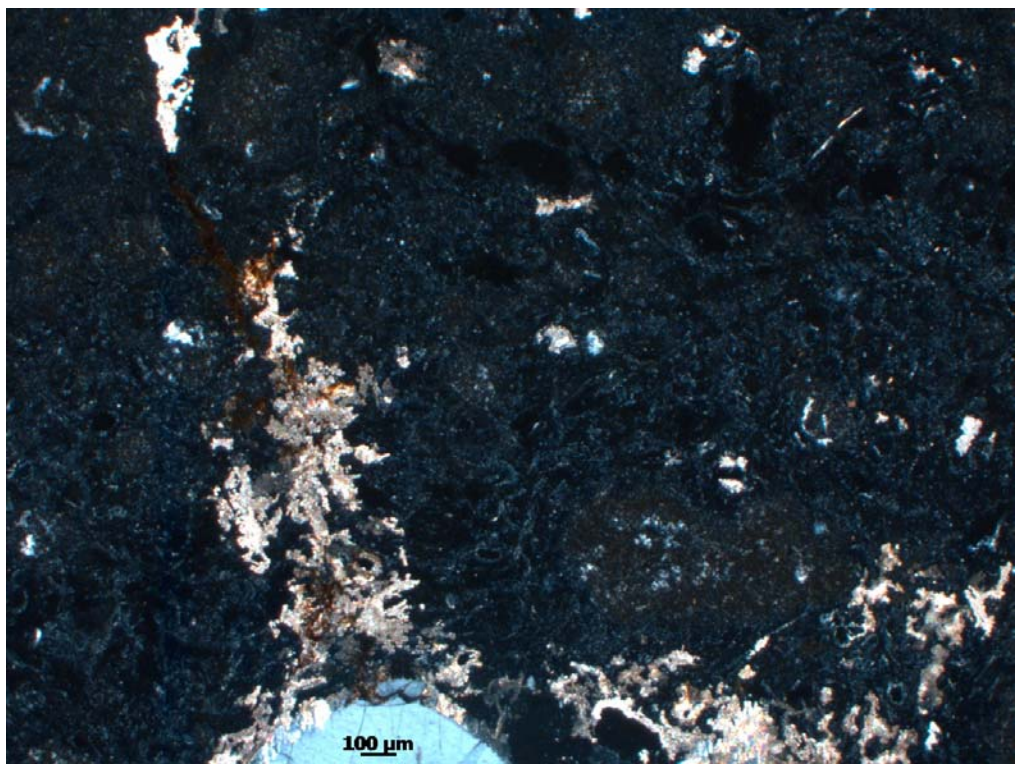


Figure A16: HRL 8a, inclusion, XPL.



Figure A17: HRL 8a, overview texture, PPL.

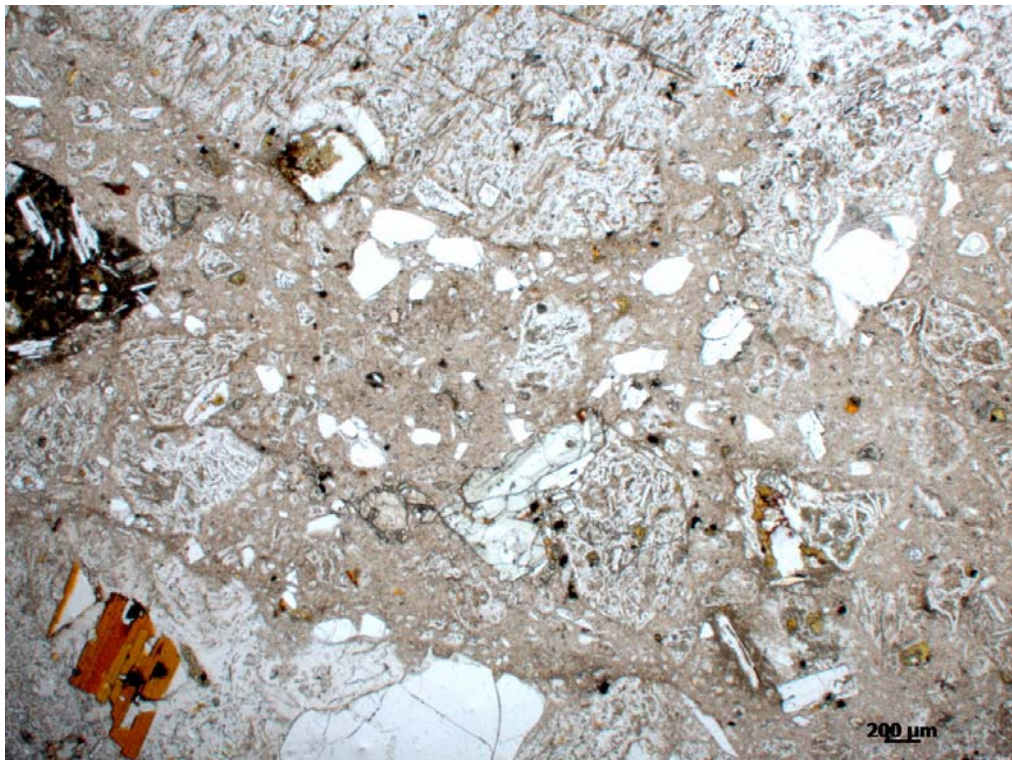


Figure A18: HRL 8b, overview texture, PPL.

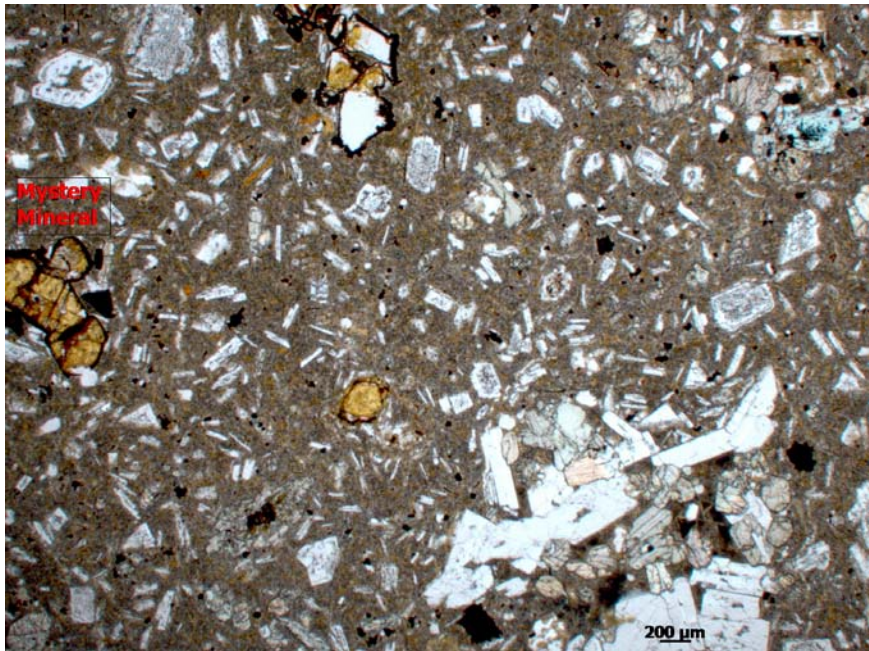


Figure A19: HRL 8b, overview texture, XPL.



Figure A20: HRL 8c, inclusion, XPL.

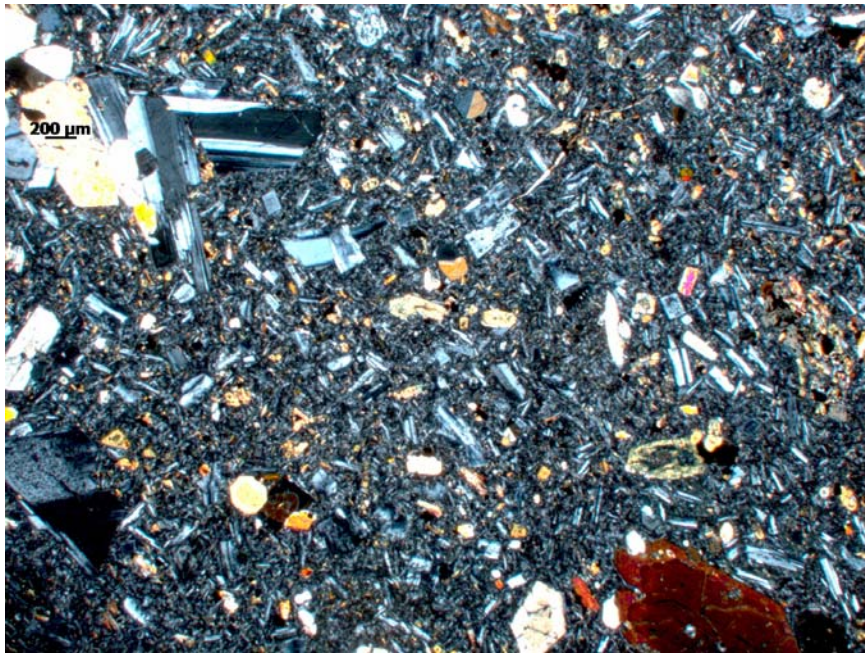


Figure A21: HRL 8c, overview texture, PPL.

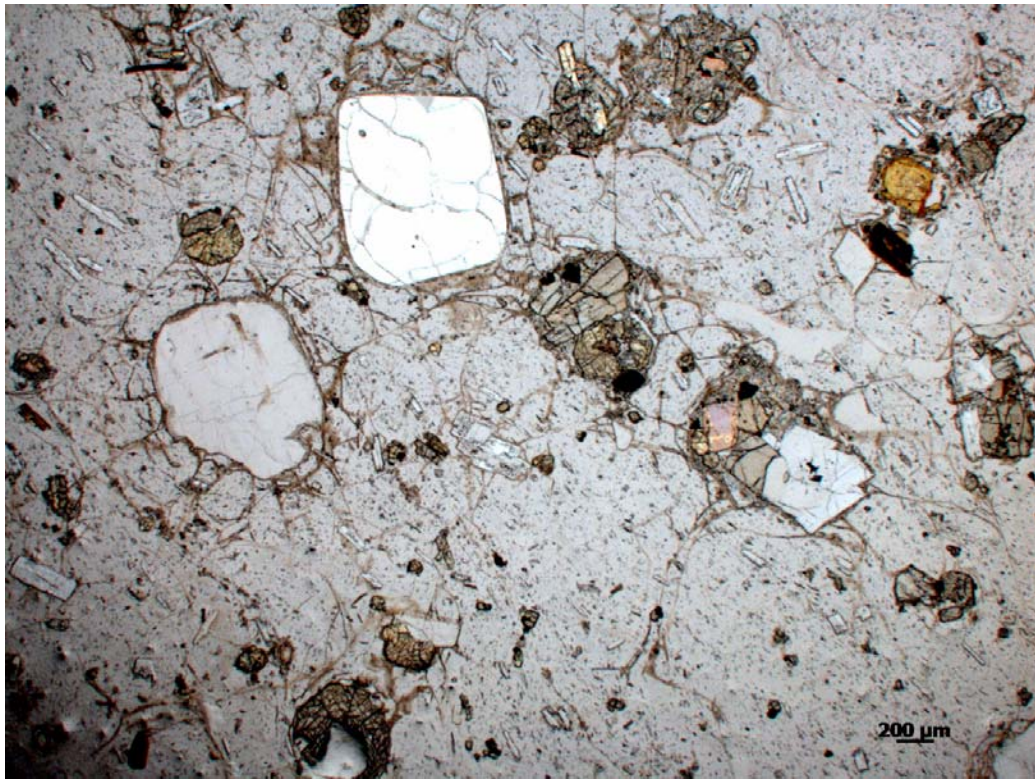


Figure A22: HRL 8c, overview texture, XPL.

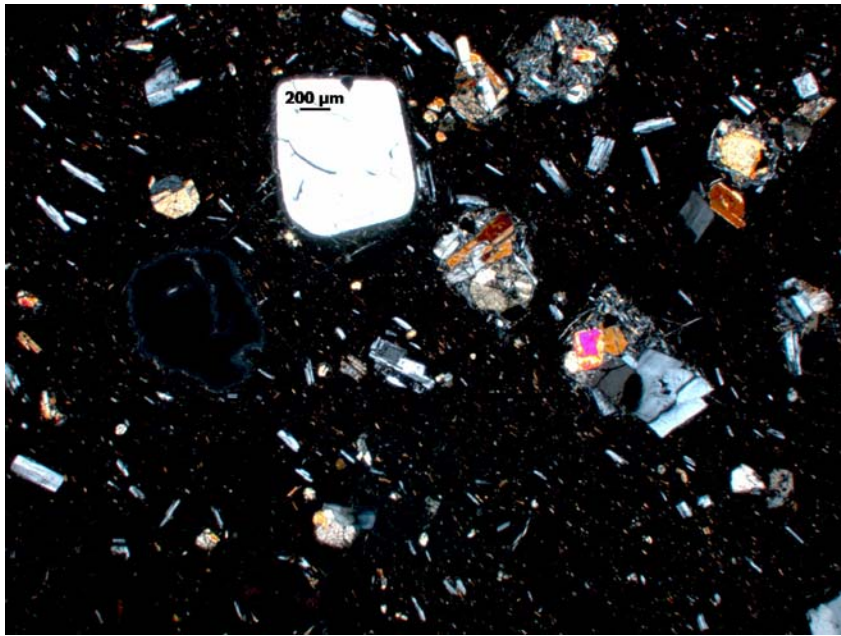


Figure A23: HRL 8d, overview texture, PPL.

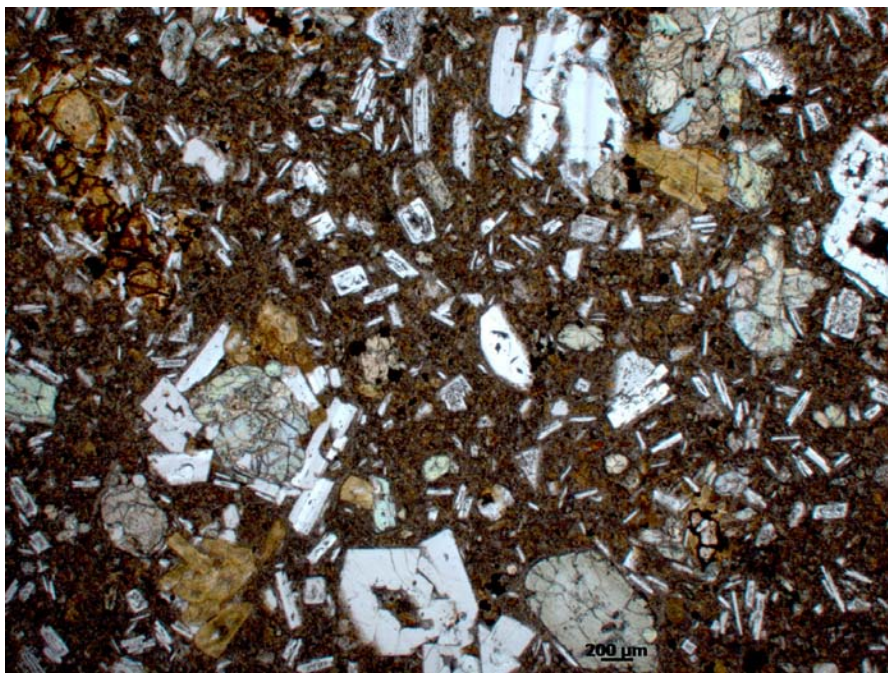


Figure A24: HRL 8d, overview texture, XPL.



Figure A25: HRL 8e, overview texture, PPL.

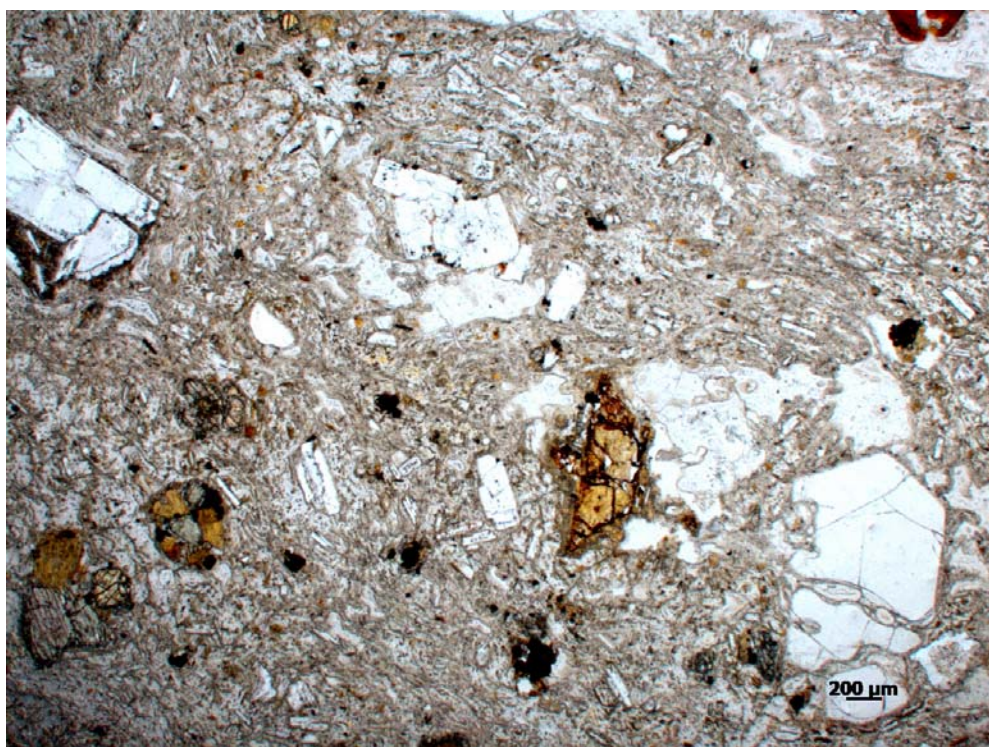


Figure A26: HRL 10a, overview texture, PPL.

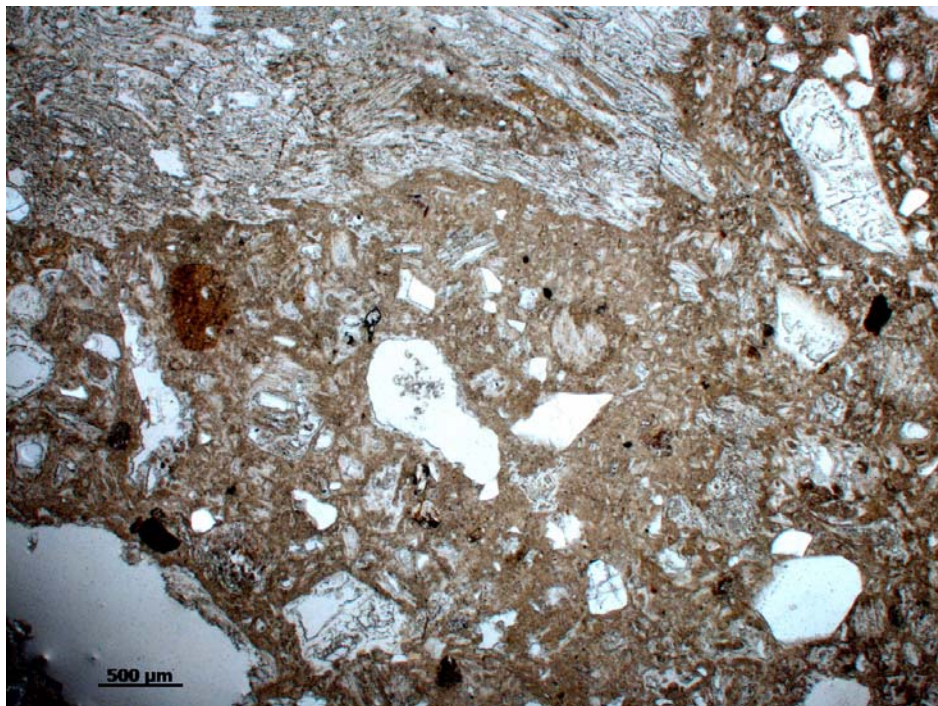


Figure A 27: HRL 10b, overview texture, PPL.



Figure A28: HRL 10c, overview texture, PPL.



Figure A29: HRL 11, overview texture, PPL.



Figure A30: HRL 11, overview texture, XPL.



Figure A31: HRL 12a, overview texture, XPL.

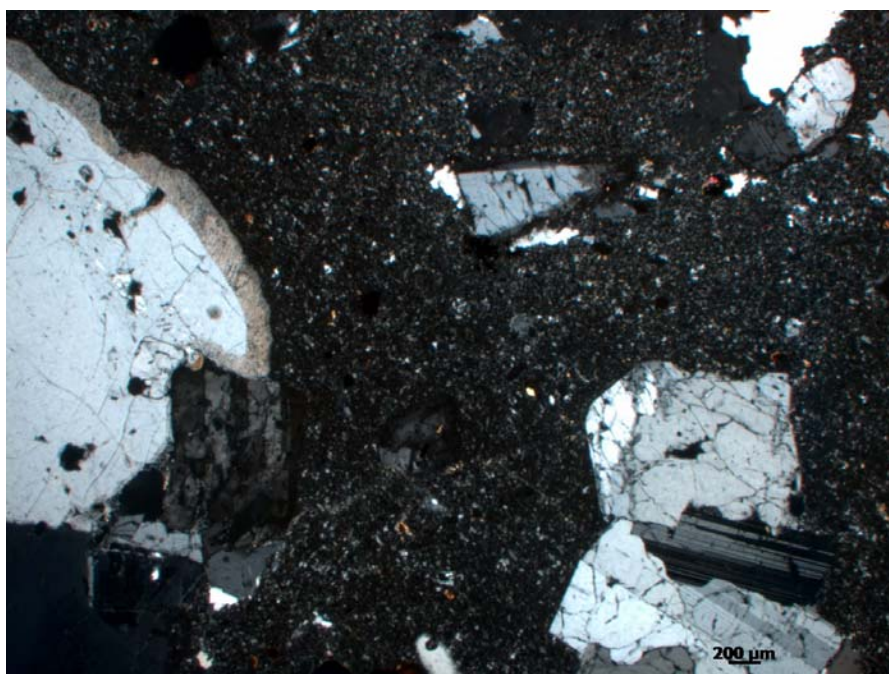


Figure A32: HRL 12b, overview texture of inclusion, PPL.



Figure A33: HRL 12b, overview texture, PPL.

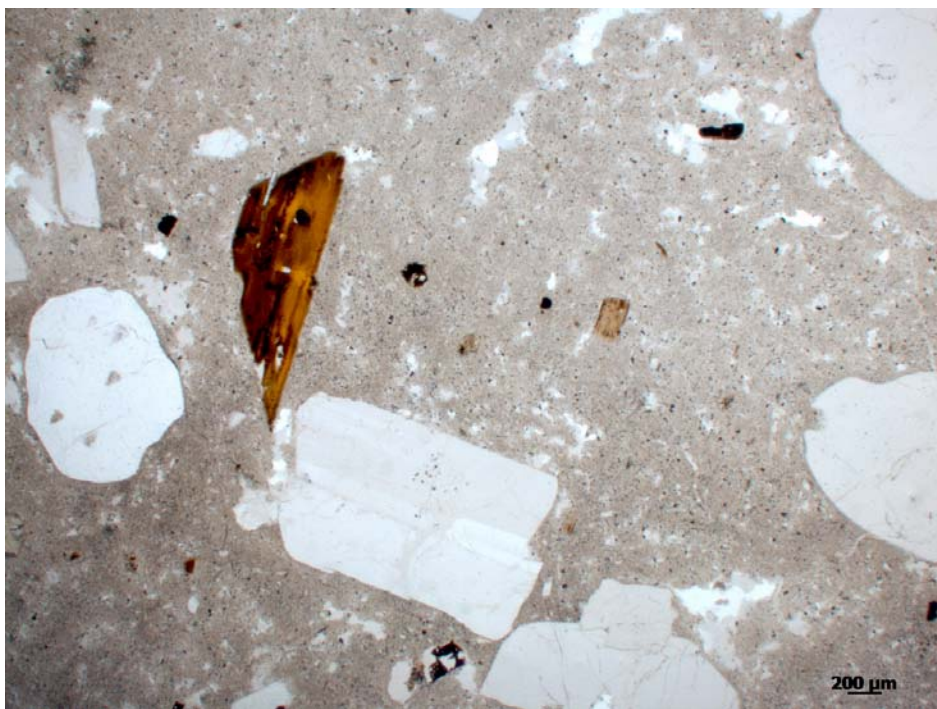


Figure A34: HRL 12b, overview texture, XPL.



Figure A35: HRL 13, overview texture, PPL.

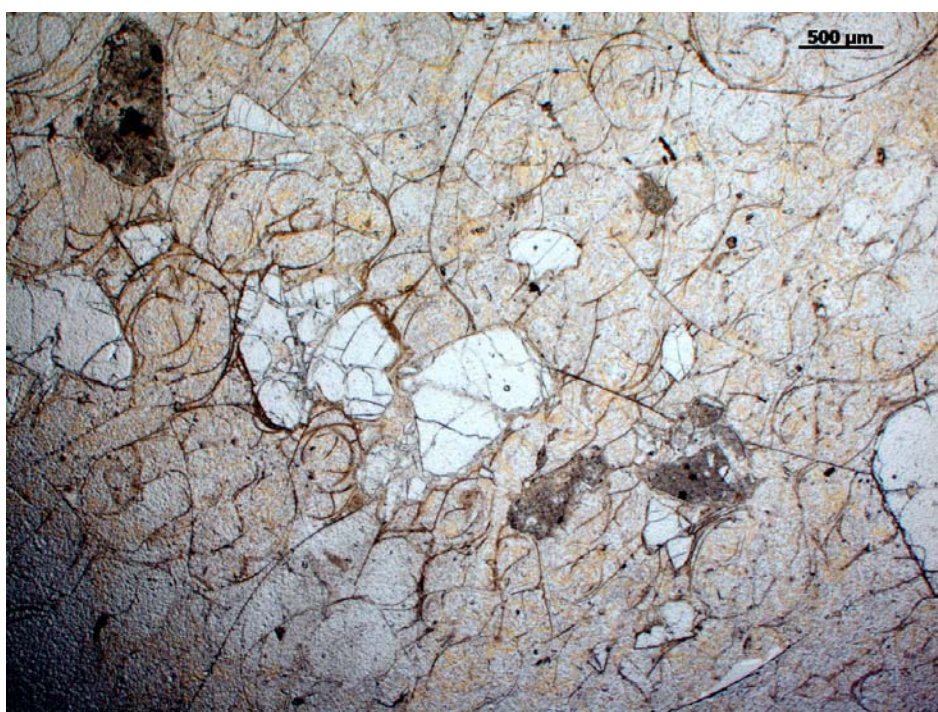


Figure A36: HRL 13, overview texture, XPL.

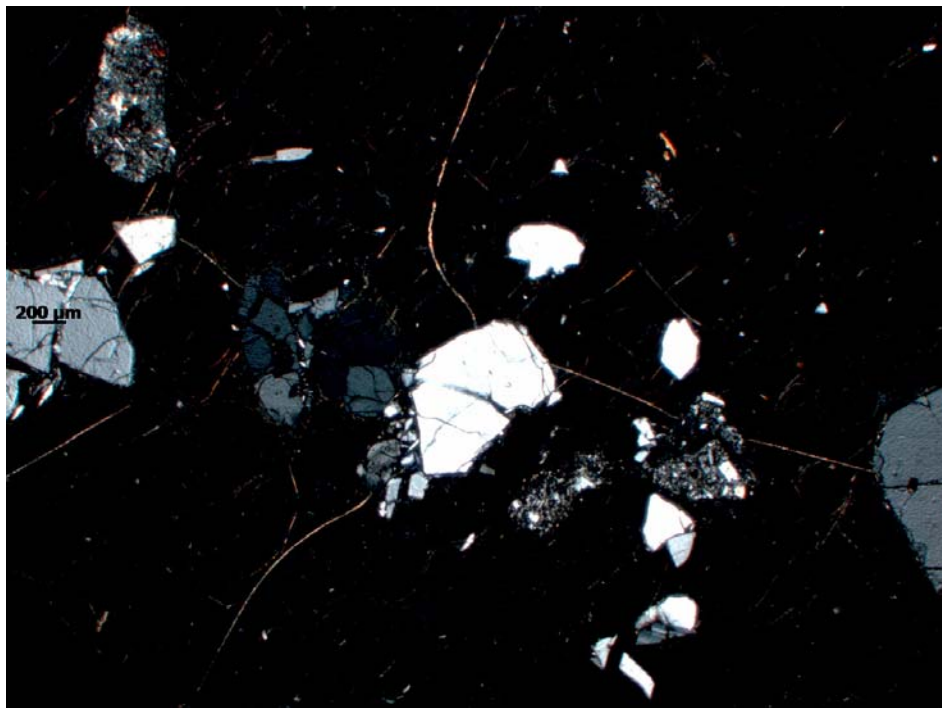


Figure A37: HRL 14a, contact between enclave and lava, XPL.

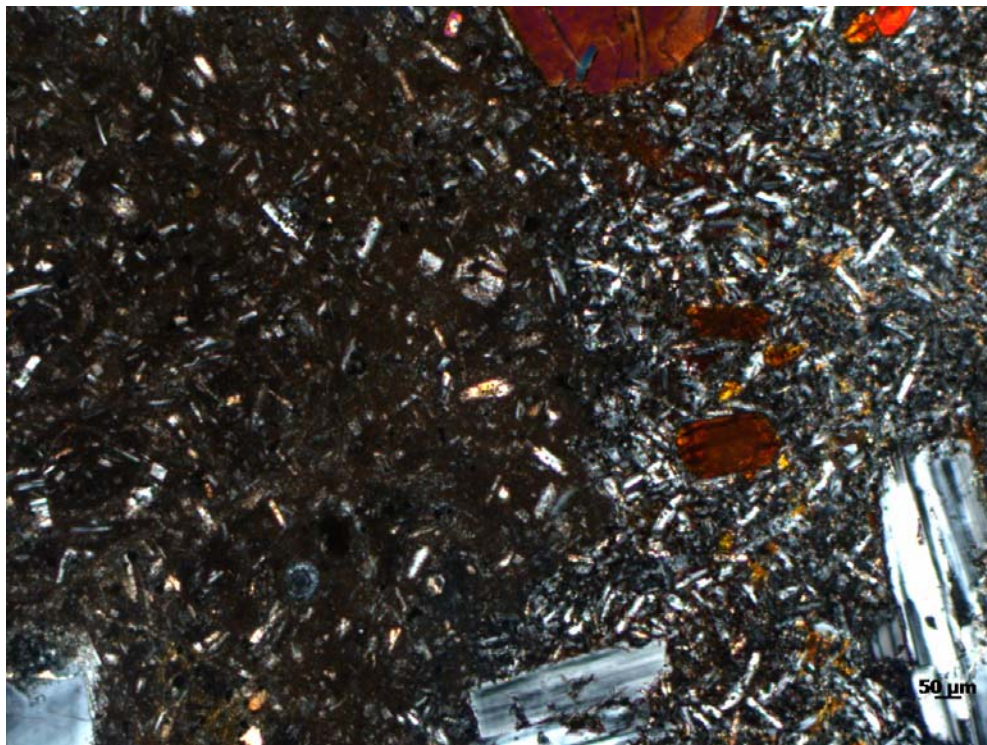


Figure A38: HRL 14a, phenocryst growth around quartz.

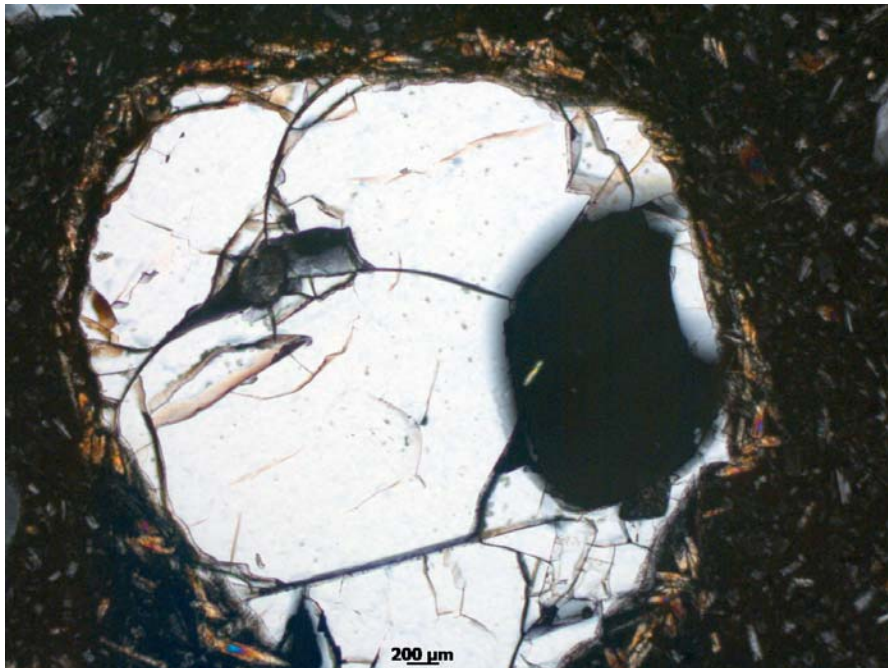


Figure A39: HRL 14a, phenocryst found in enclave.

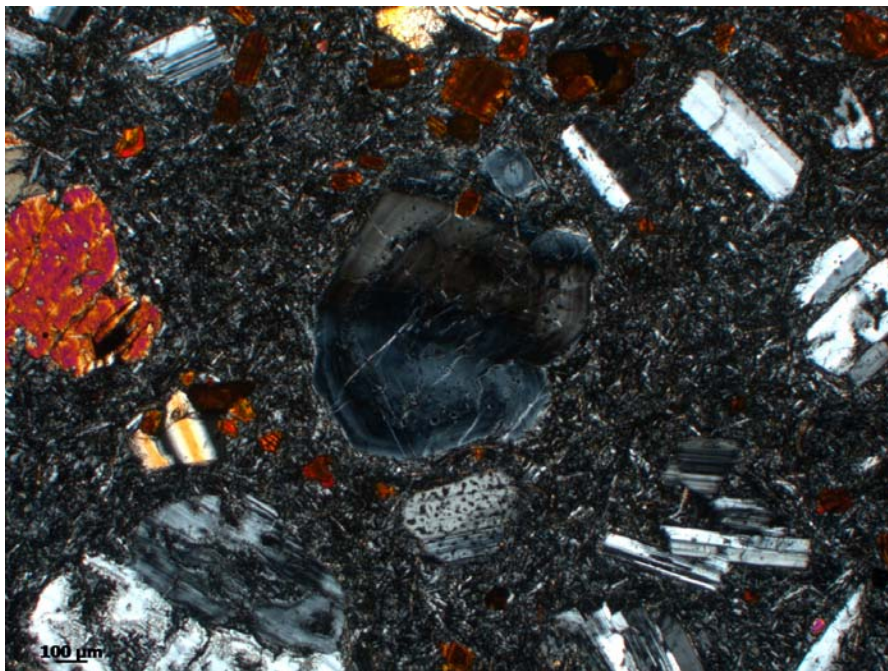


Figure A40: HRL 14a, phenocryst found in lava.

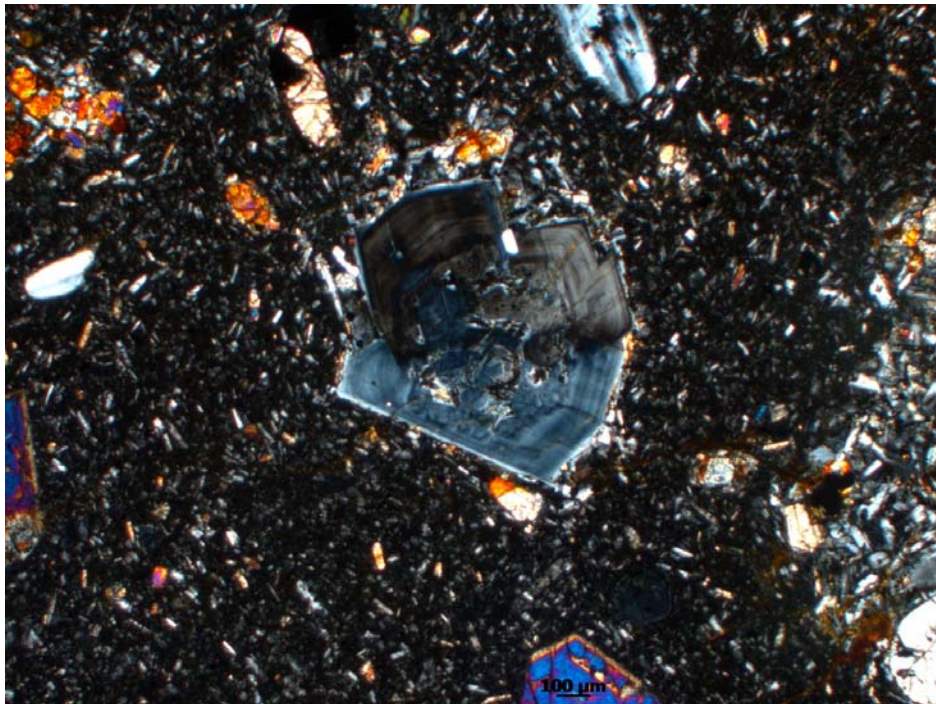


Figure A41: HRL 14b, overview texture, PPL.

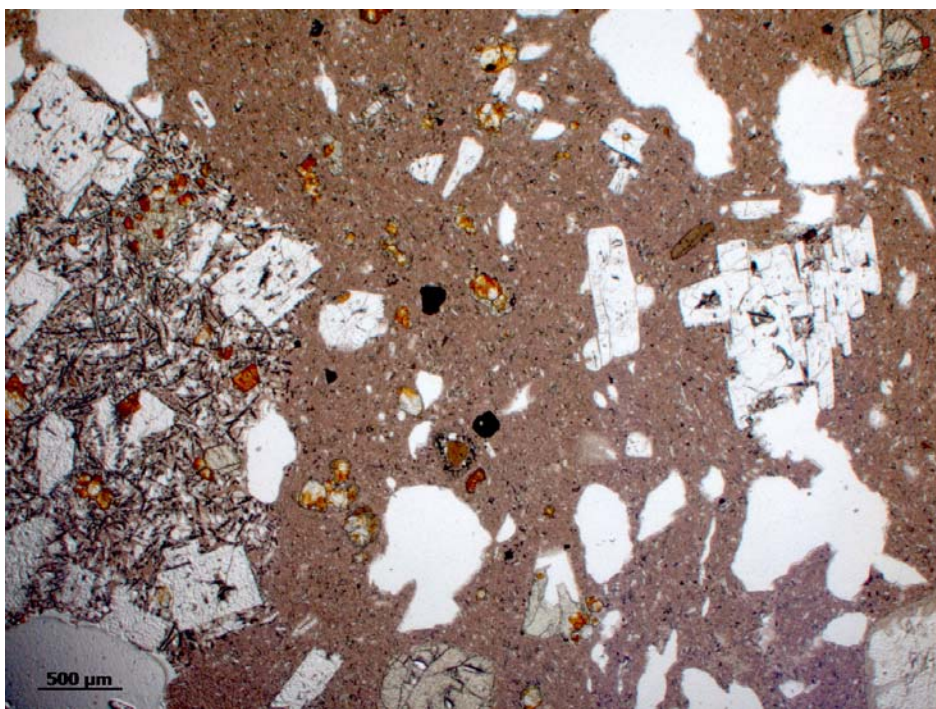


Figure A42: HRL 14c, overview texture, PPL.

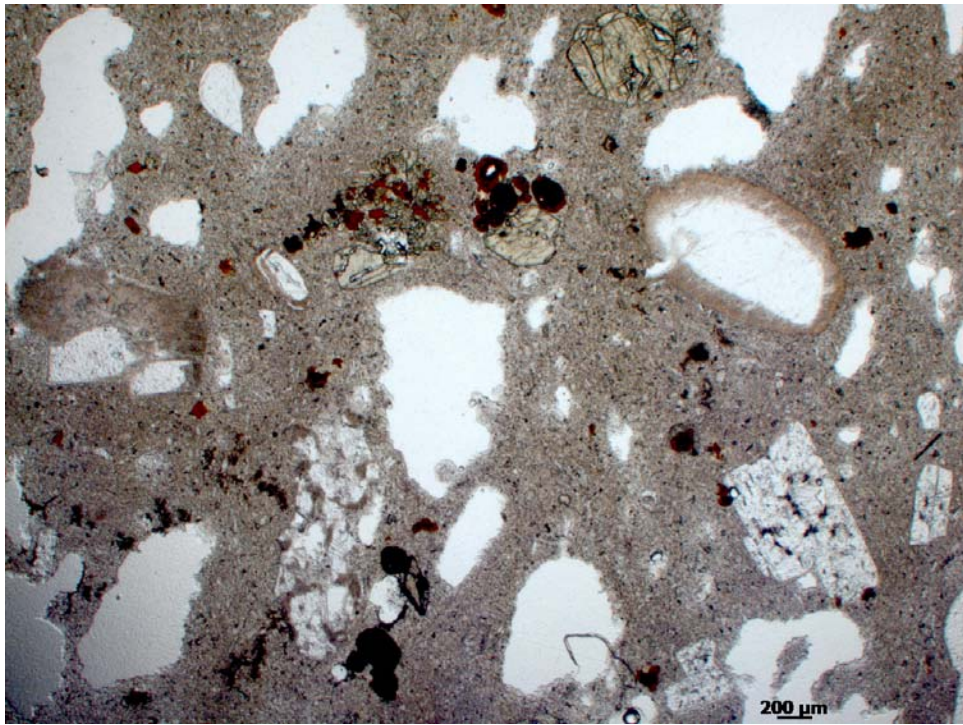


Figure A43: HRL 14c, overview texture, XPL.



Figure A44: HRL 15, overview texture, PPL.

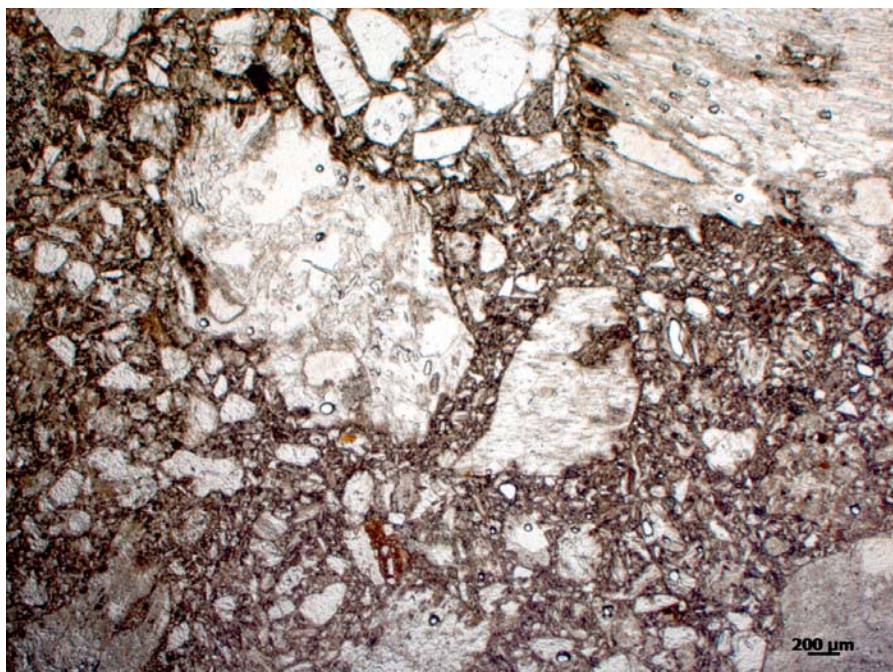


Figure A45: HRL 16, overview texture, PPL.

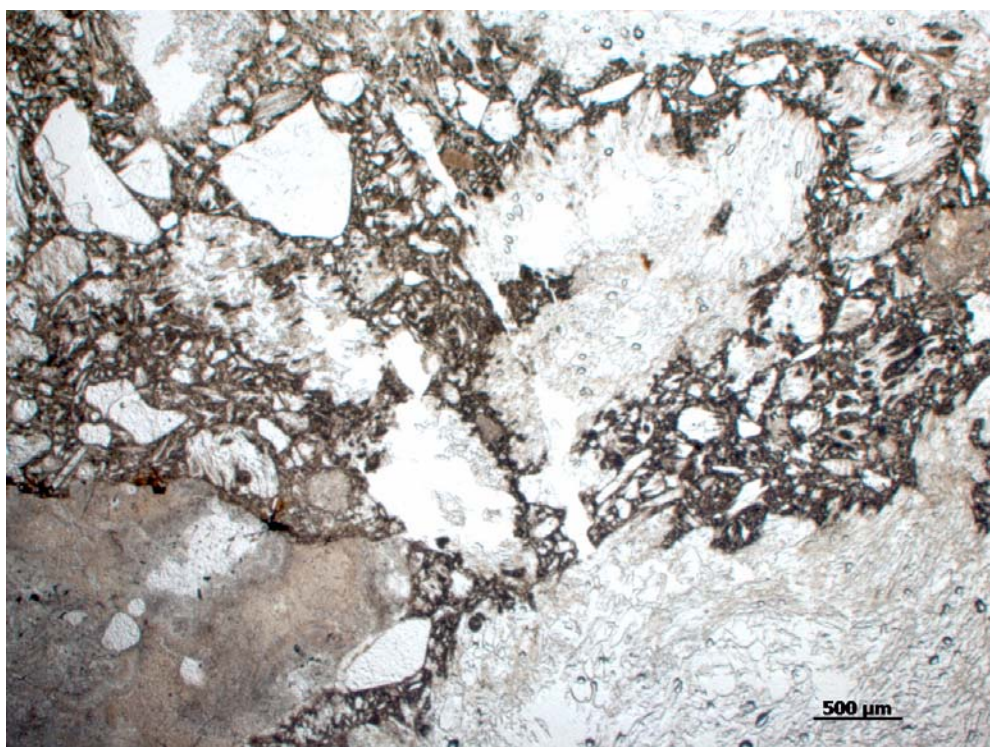


Figure A46: HRL 17, overview texture, PPL.

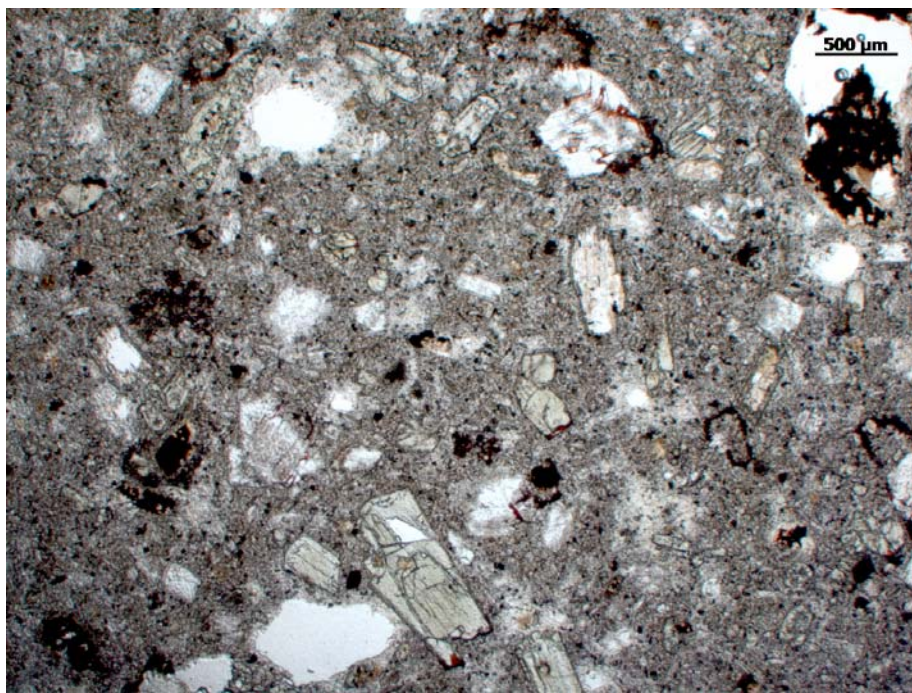


Figure A47: HRL 18, overview texture, PPL.

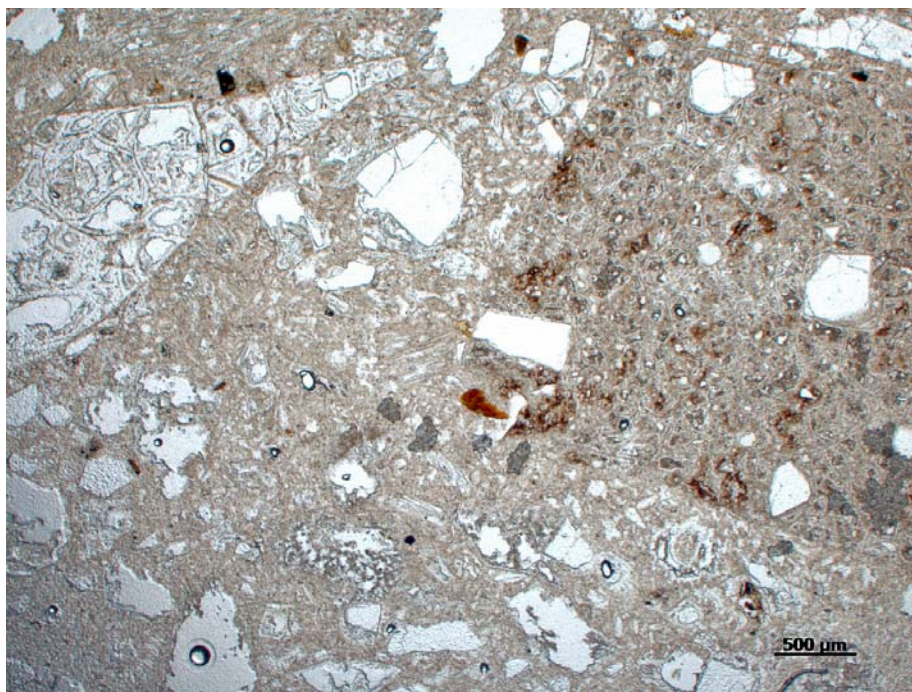


Figure A48: HRL 19a, overview texture, PPL.

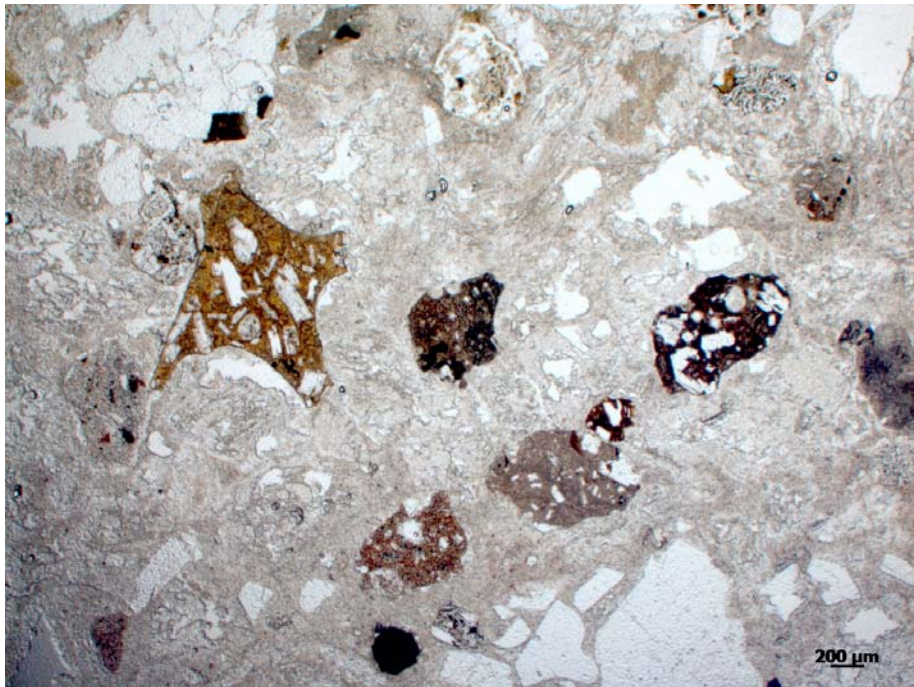


Figure A49: HRL 19a, overview texture, XPL.

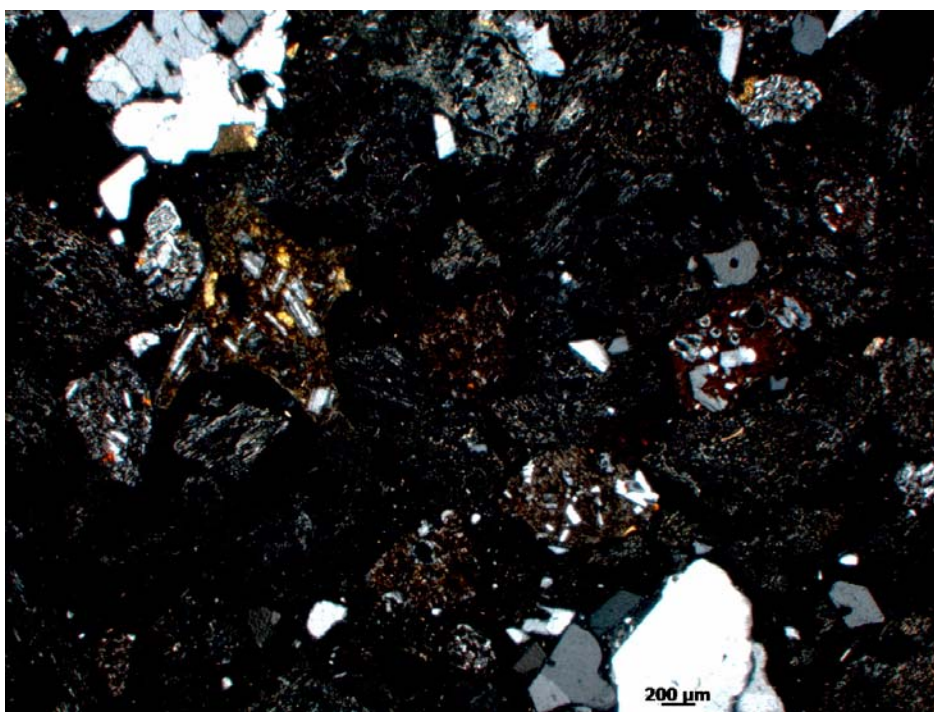


Figure A50: HRL 19b, large silver lithic, XPL.

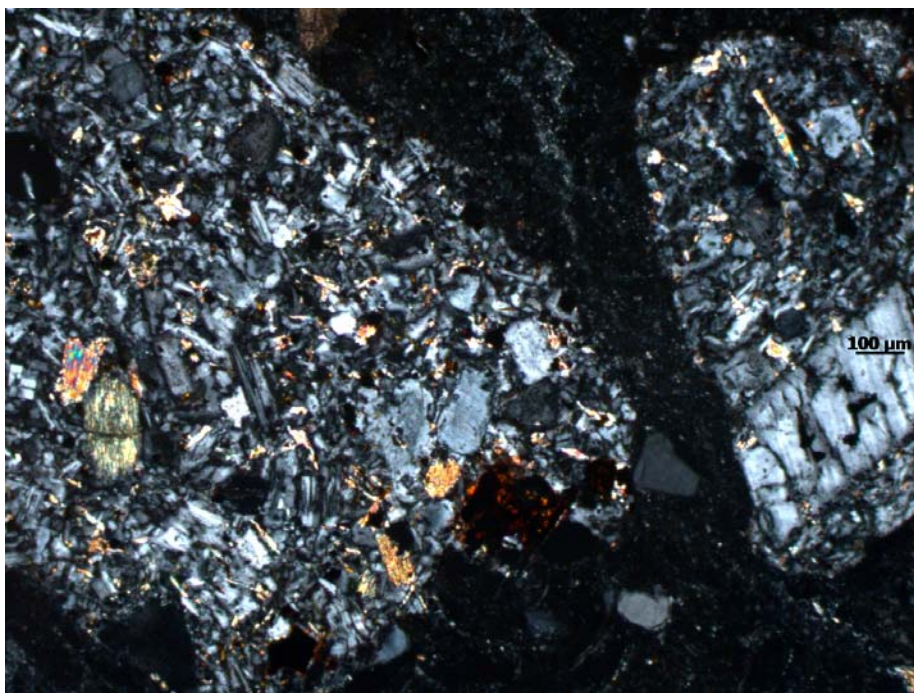


Figure A51: HRL 19b, overview texture, PPL.

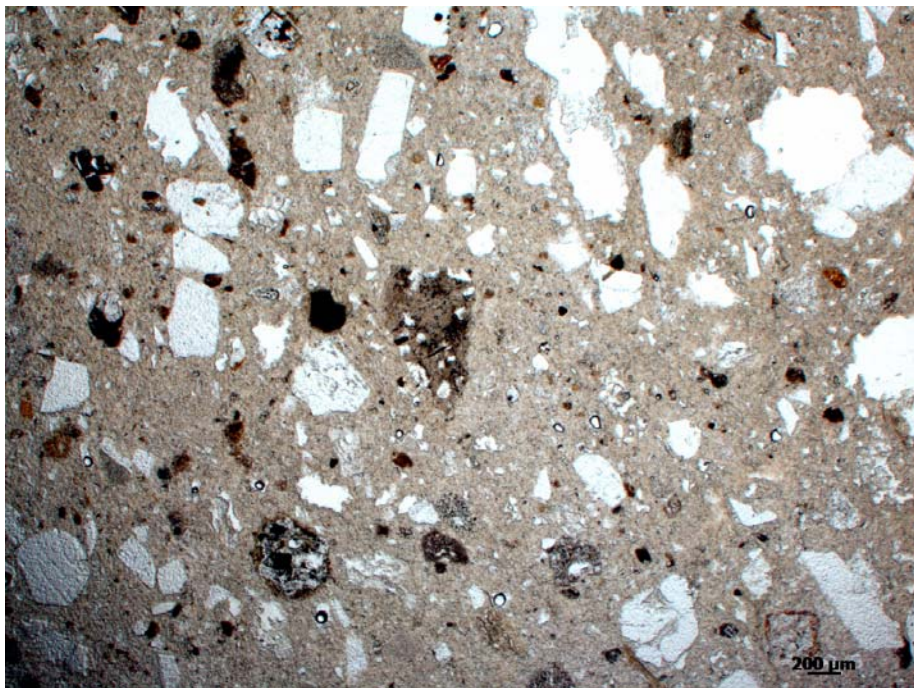


Figure A52: HRL 19b, lithic.

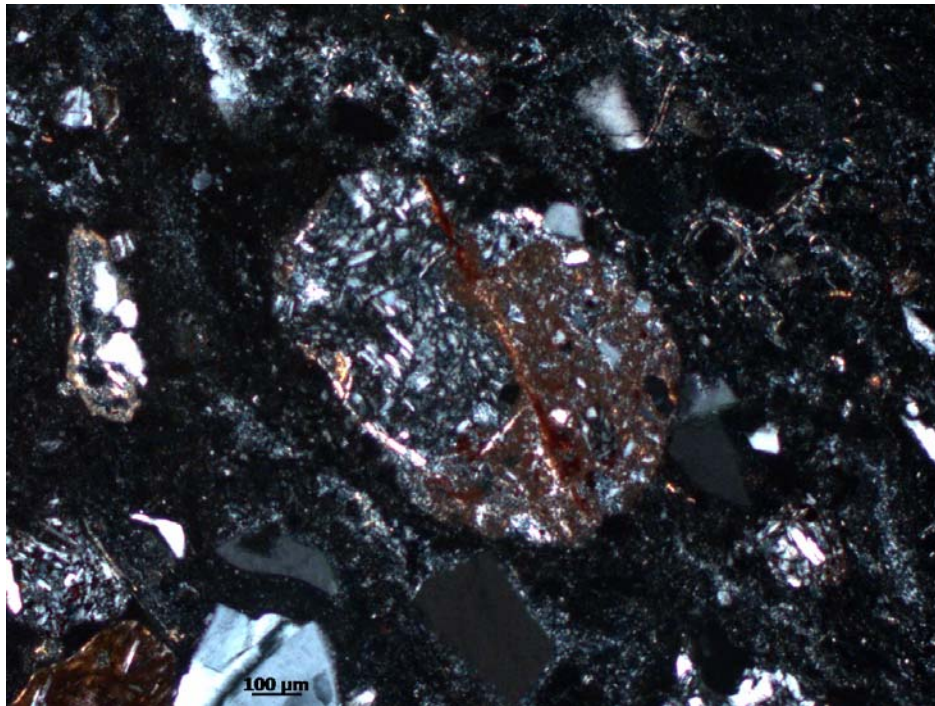


Figure A53: HRL 20, overview texture, PPL.

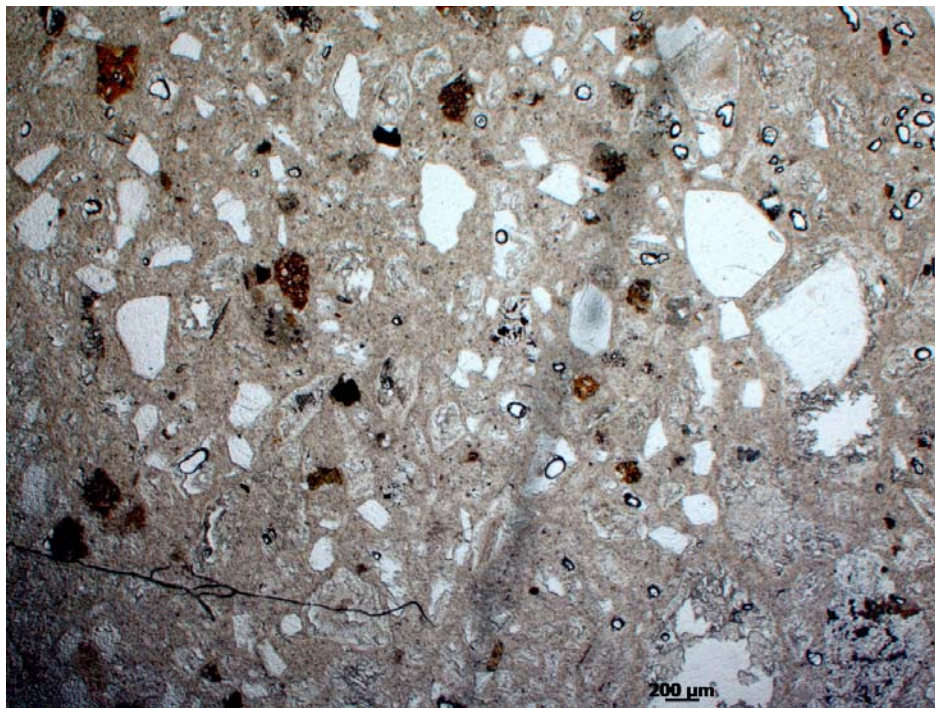


Figure A54: HRL 20, red and small silver lithic, XPL.



Figure A55: HRL 21, microlites, PPL.

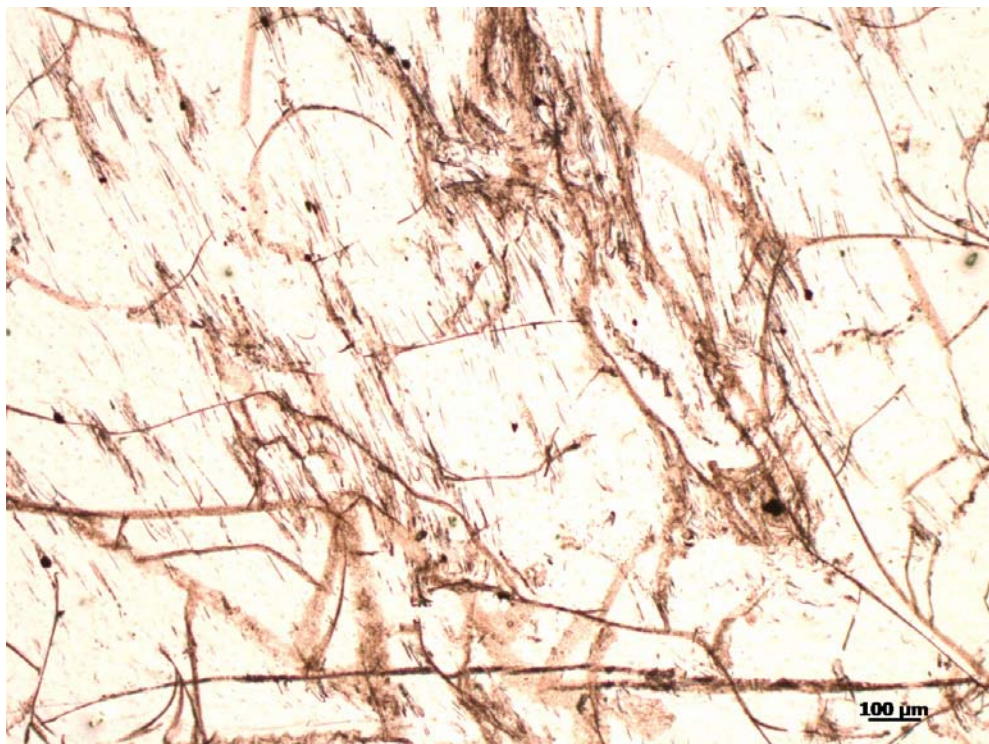


Figure A56: HRL 21, microlites, XPL.

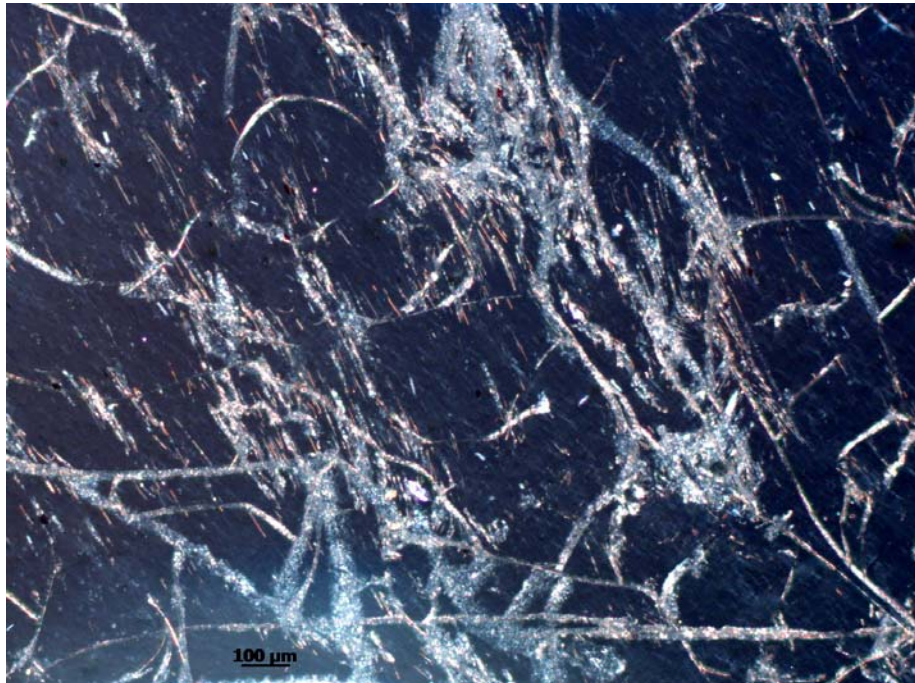


Figure A57: HRL 21, perlitic fractures, XPL.

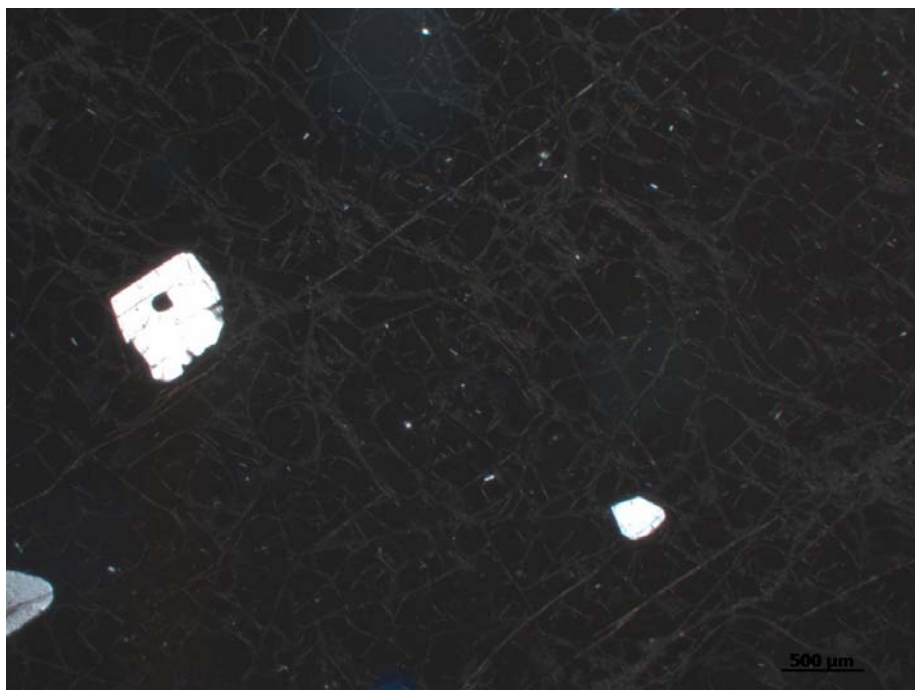


Figure A58: HRL 21, sphene, quartz, sanidine.



Figure A59: HRL 22a, clinopyroxene, PPL.

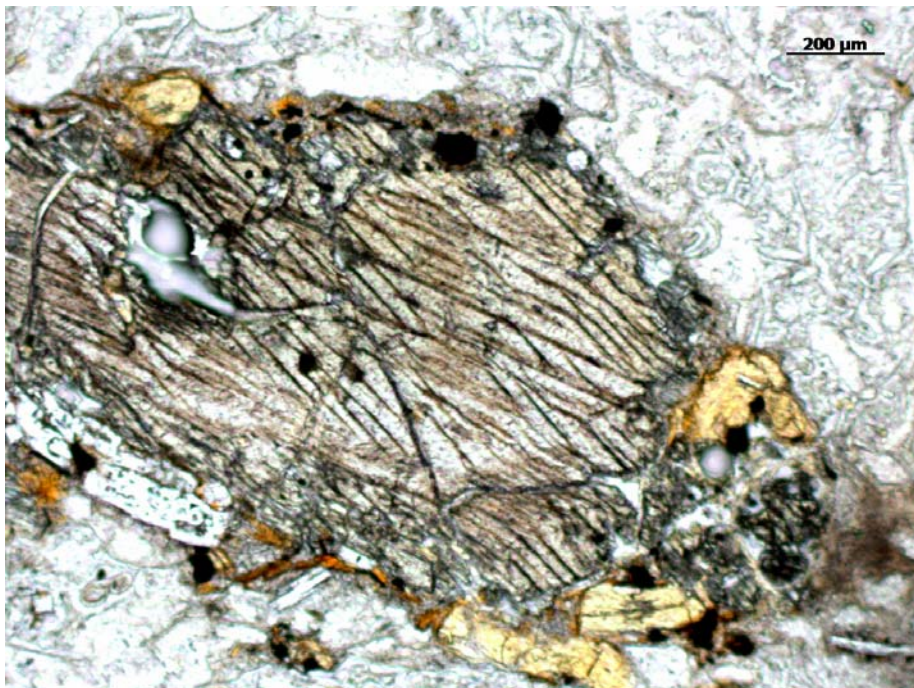


Figure A60: HRL 22a, inclusion, XPL.

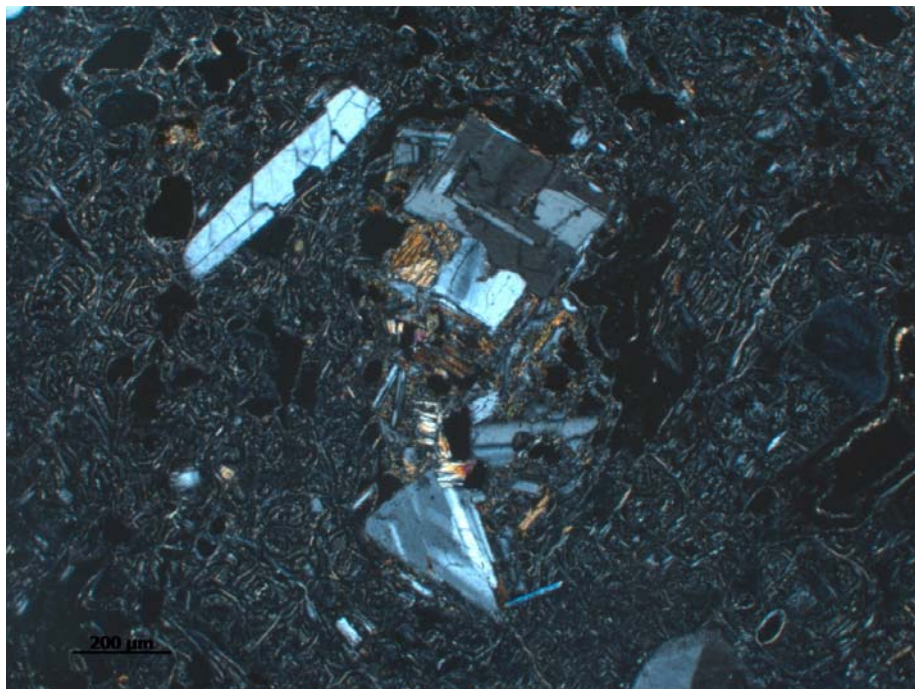


Figure A61: HRL 22a, overview texture, PPL.

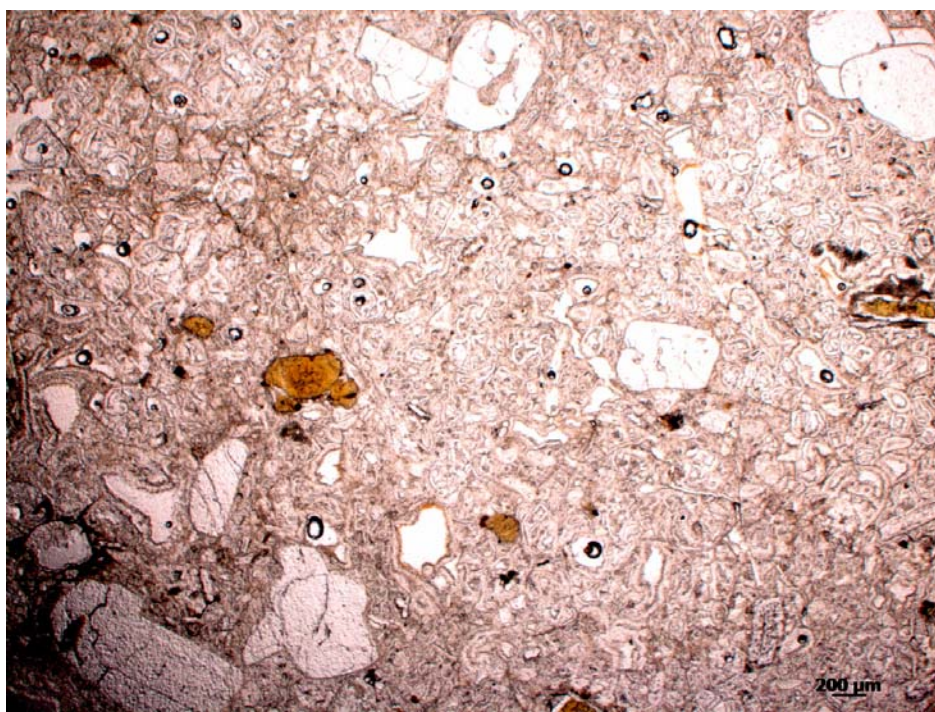


Figure A62: HRL 22a, overview texture, XPL.



Figure A63: HRL 22b, inclusion, XPL.

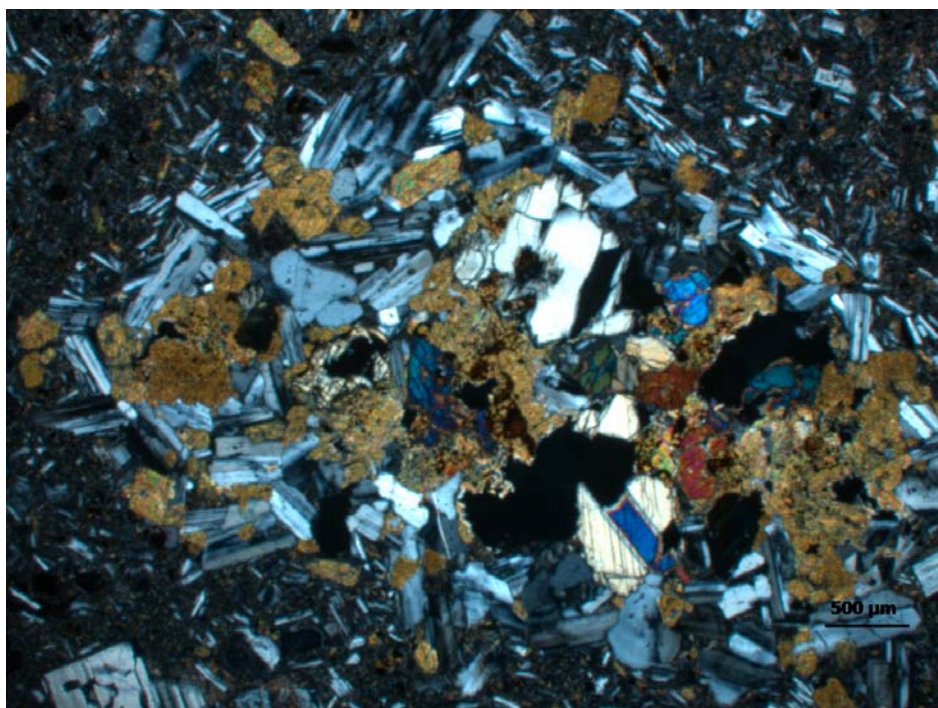


Figure A64: HRL 22b, overview texture, PPL.



Figure A65: HRL 22b, overview texture, XPL.

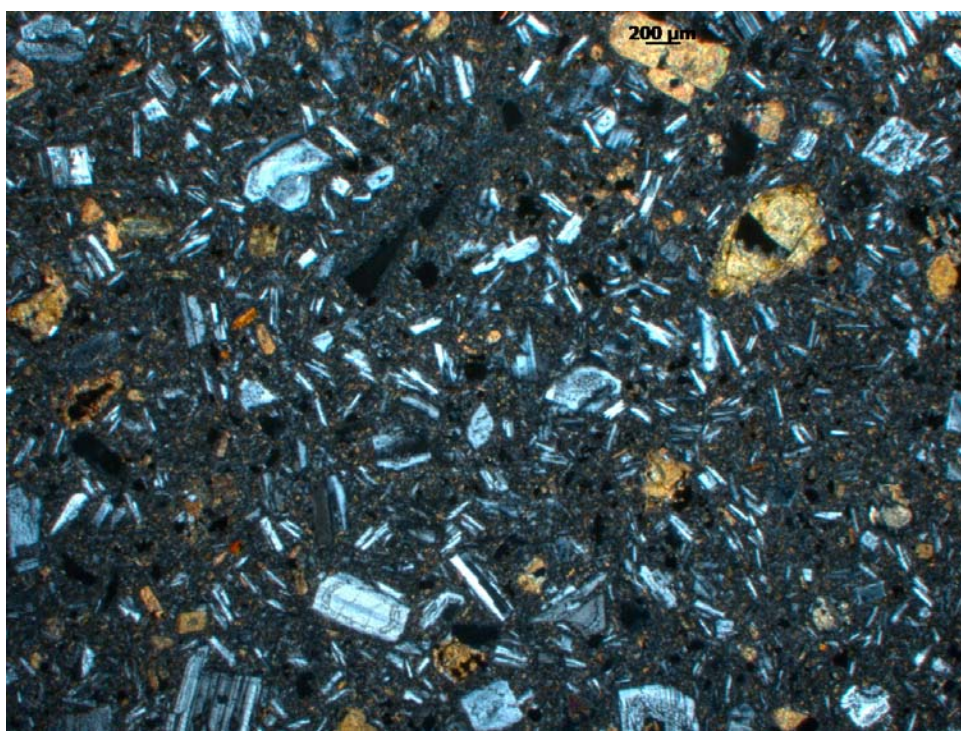


Figure A66: HRL 22c, overview texture, PPL.

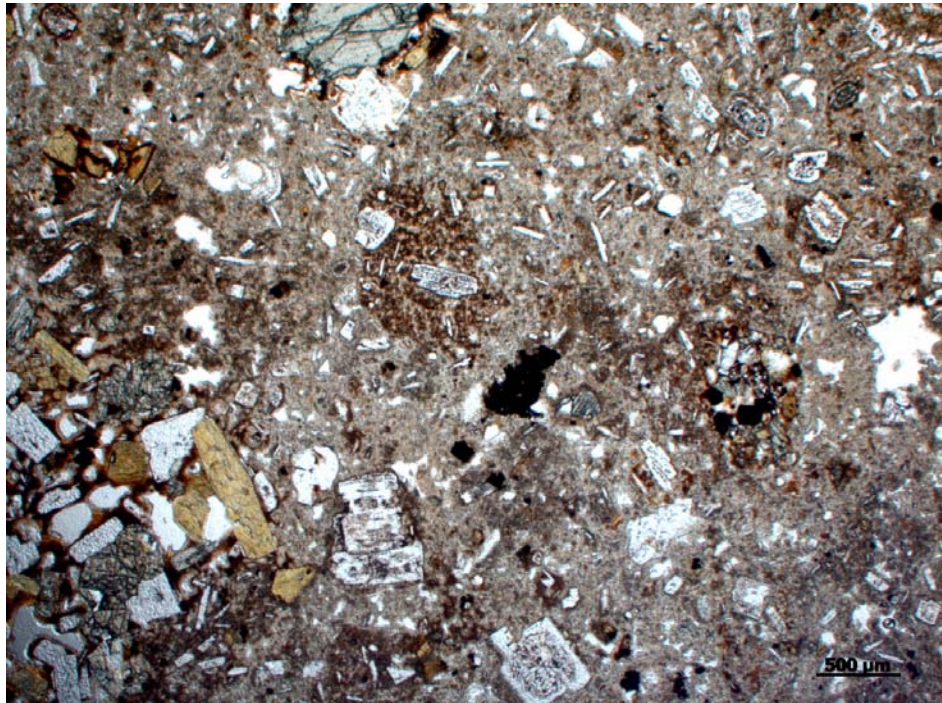


Figure A67: HRL 22c, overview texture, XPL.



Figure A68: HRL 23b, general texture, PPL.

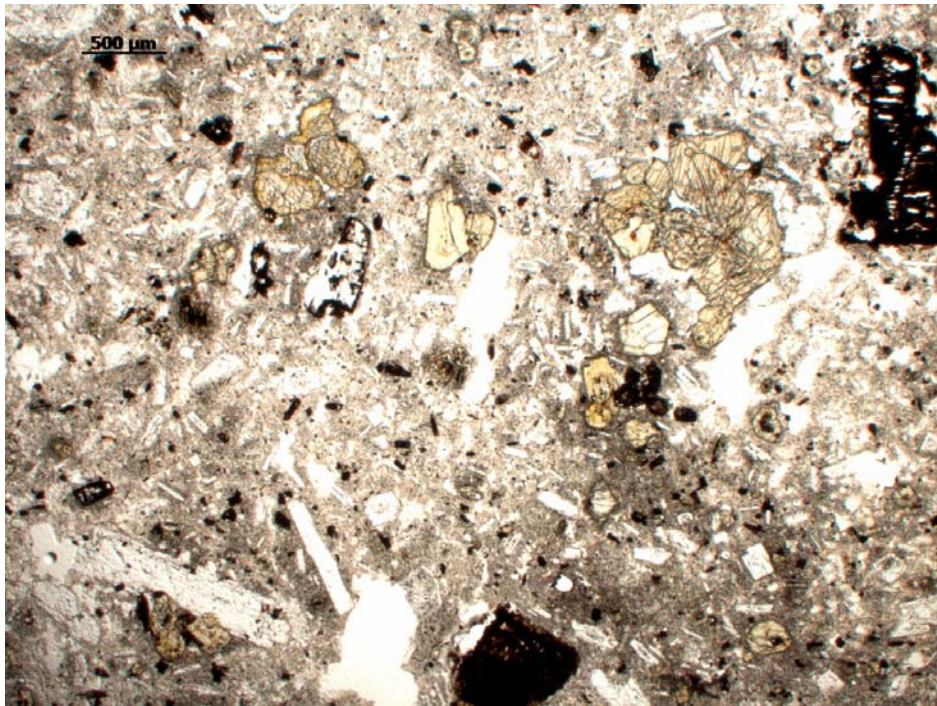


Figure A69: HRL 23b, general texture, XPL.

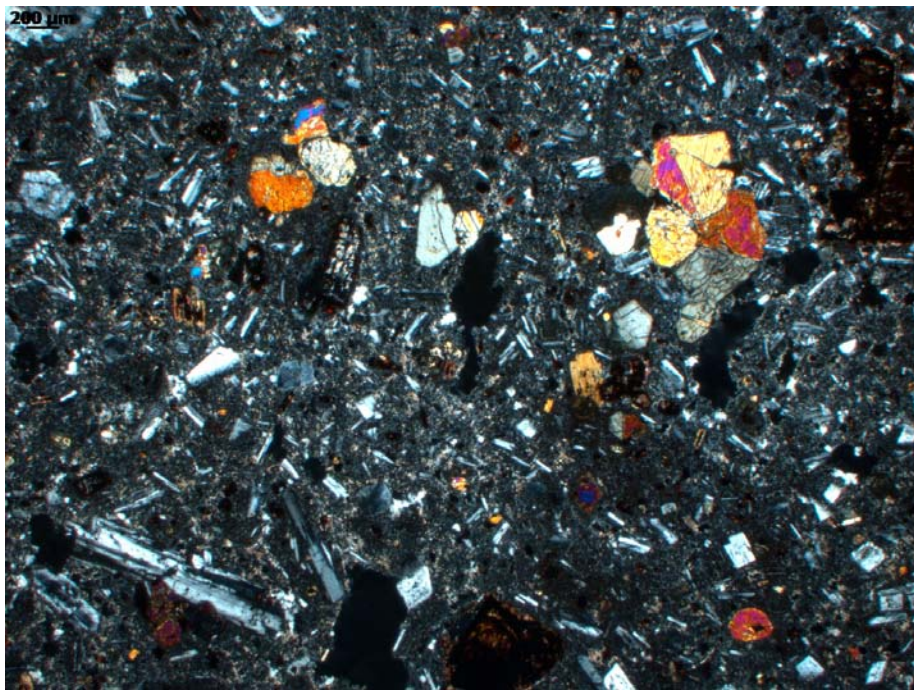


Figure A70: HRL 24, general texture, XPL.

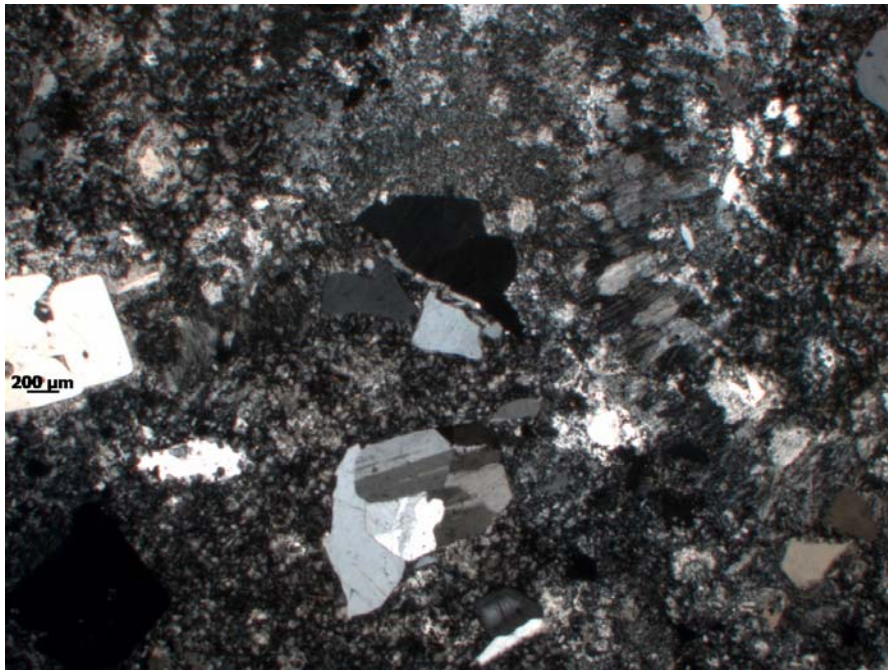


Figure A71: HRL 25, lava overview, XPL.

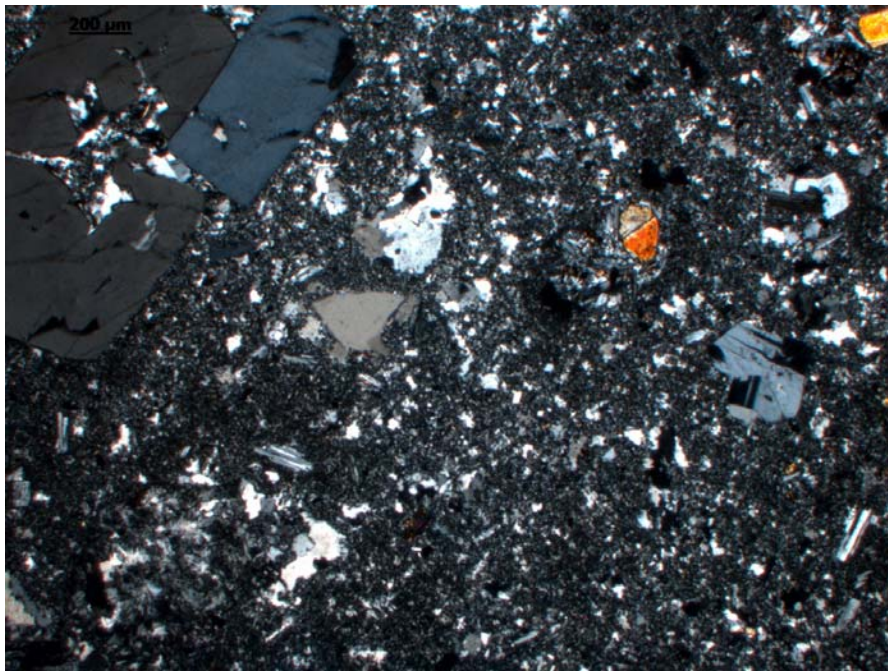


Figure A72: HRL 25, plucked olivine, XPL.



Figure A73: HRL 26, inclusion, XPL,

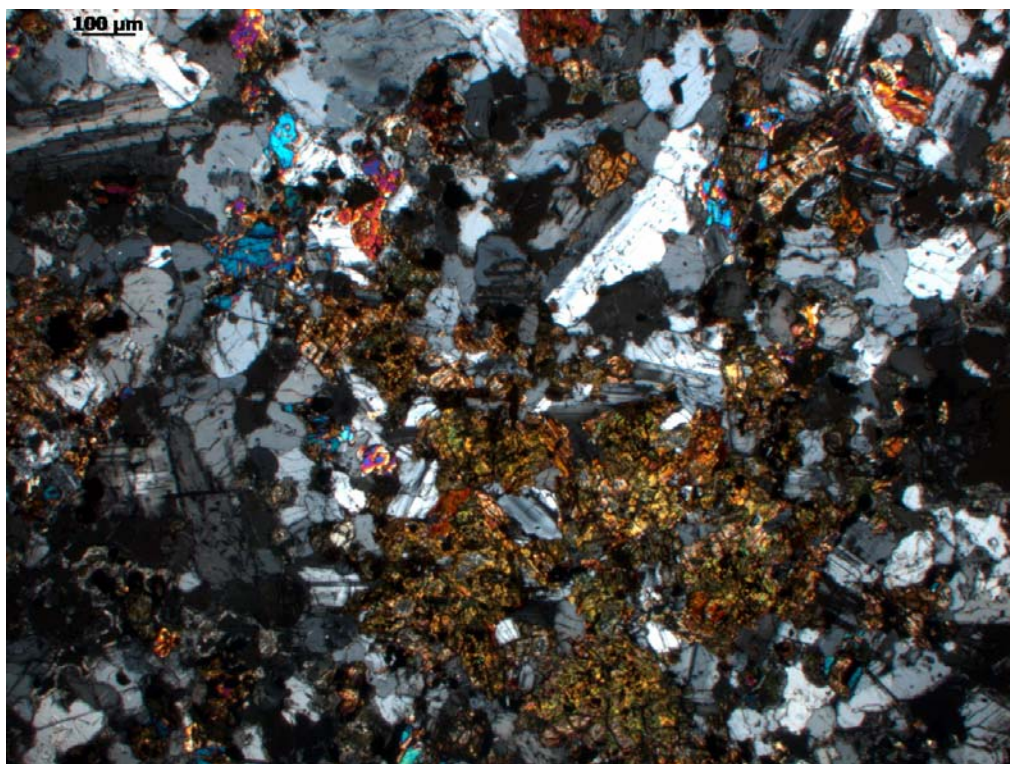


Figure A74: HRL 26, overview texture, XPL.



Figure A75: HRL 27, microlite flows, PPL.

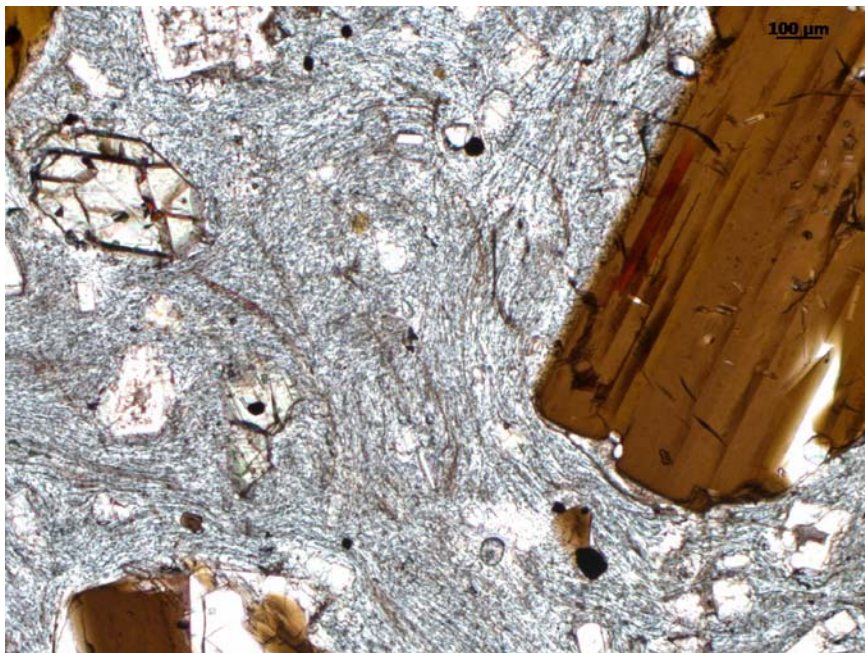


Figure A76: HRL 27, overview texture, XPL.

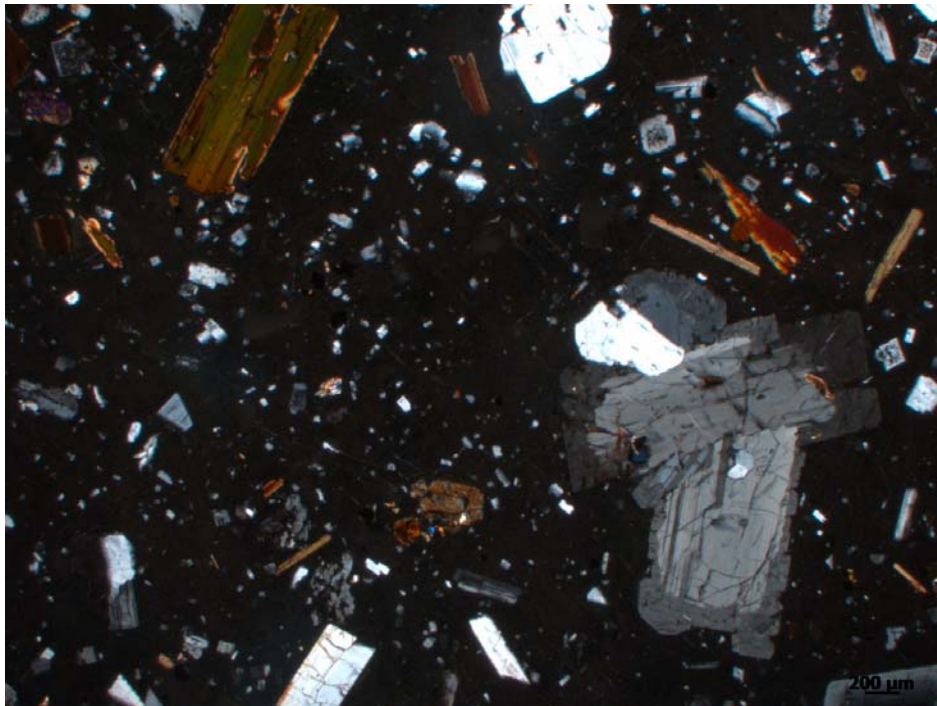


Figure A77: HRL 28, overview textures, PPL.

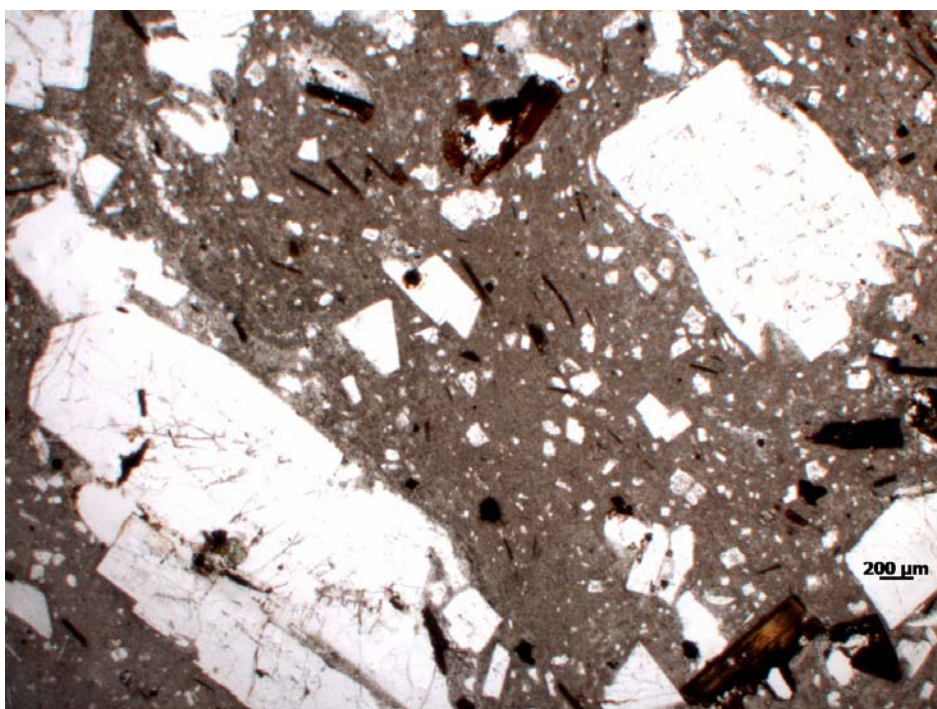


Figure A78: HRL 28, overview textures, XPL.

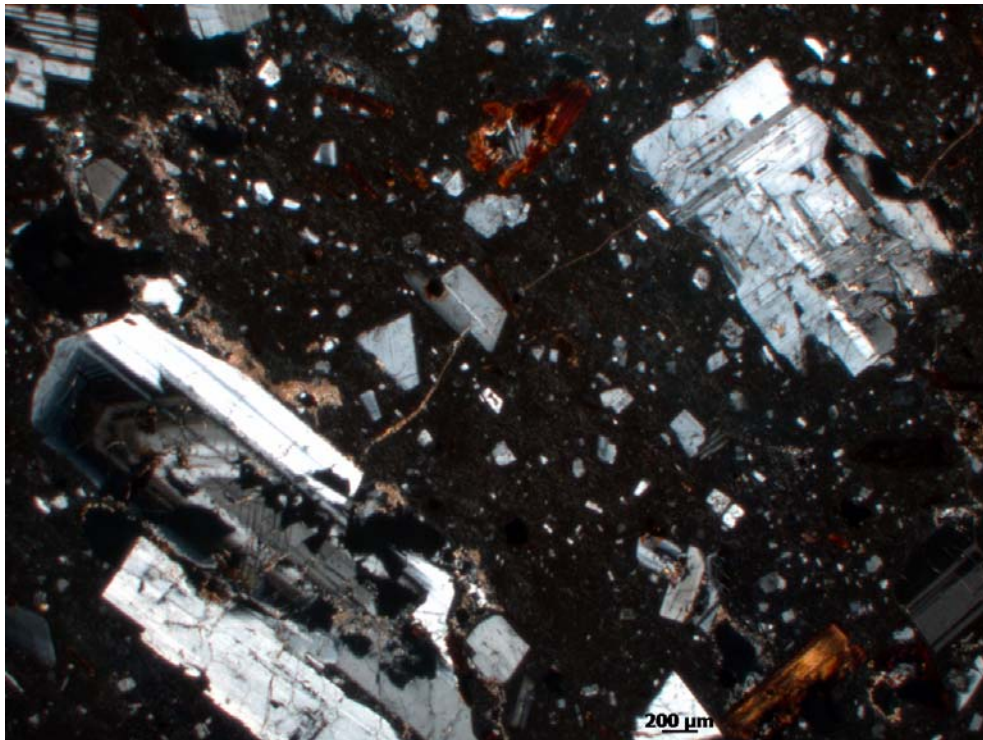


Figure A79: HRL 29, overview texture, XPL.

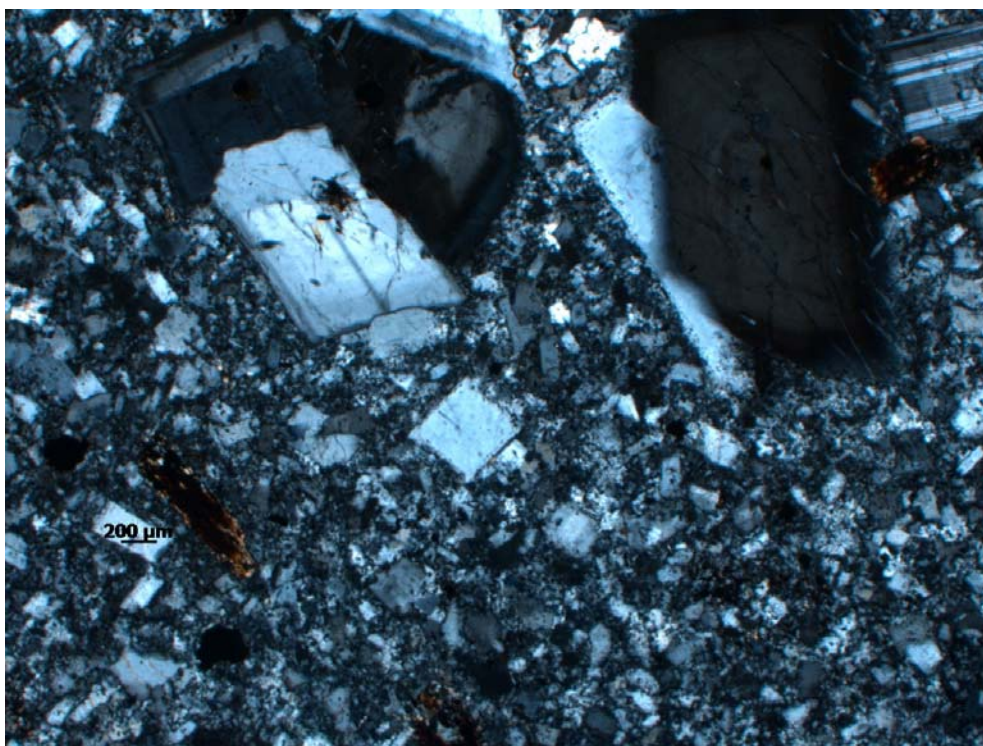


Figure A80: HRL 29, zircon in groundmass, PPL.

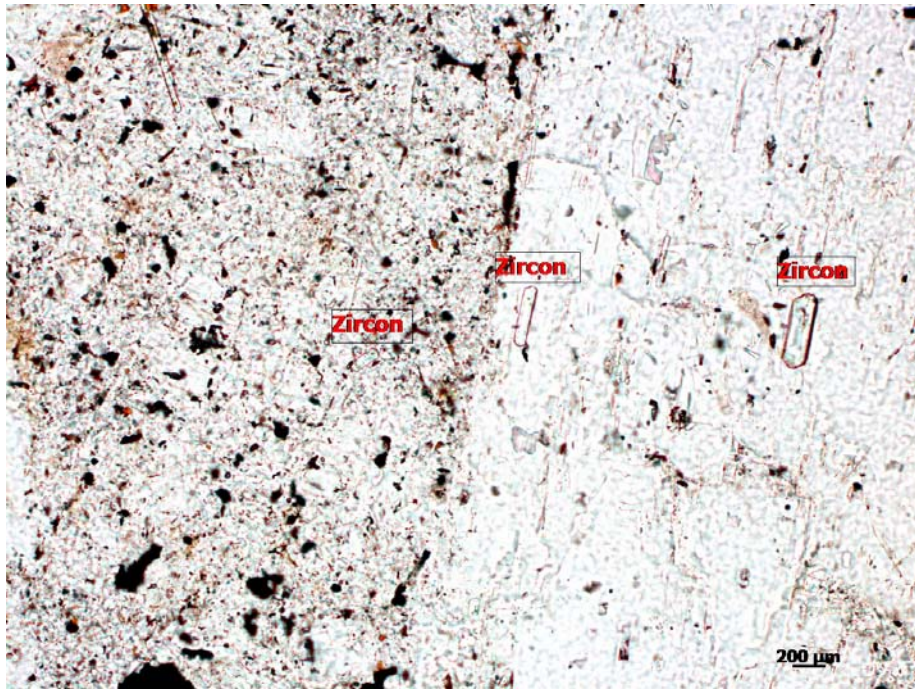


Figure A81: HRL 30, overview texture, PPL.

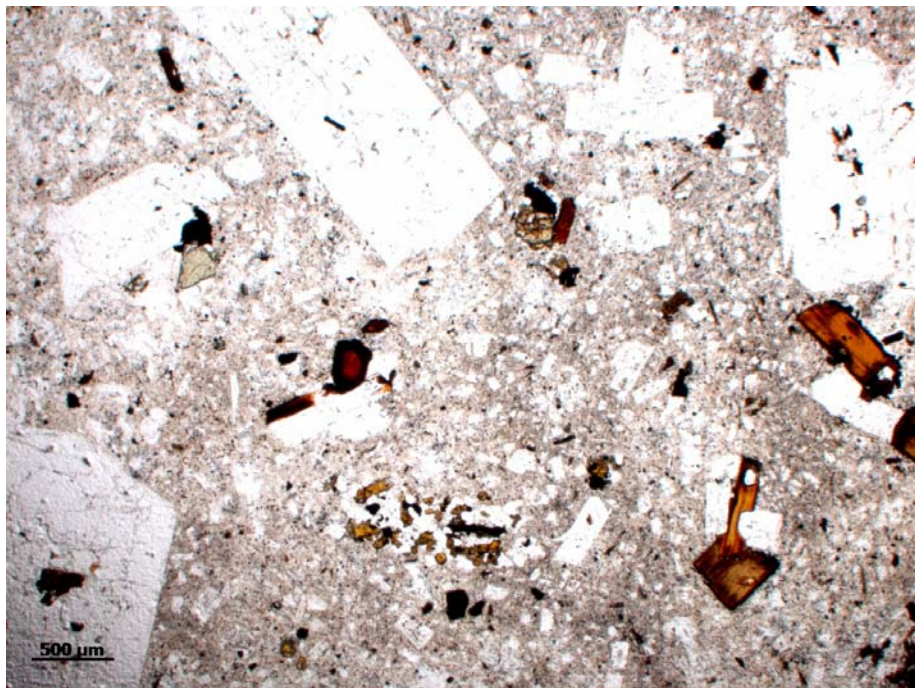


Figure A82: HRL 30, overview texture, XPL.



Figure A83: HRL 31, oriented microphenocrysts, PPL.

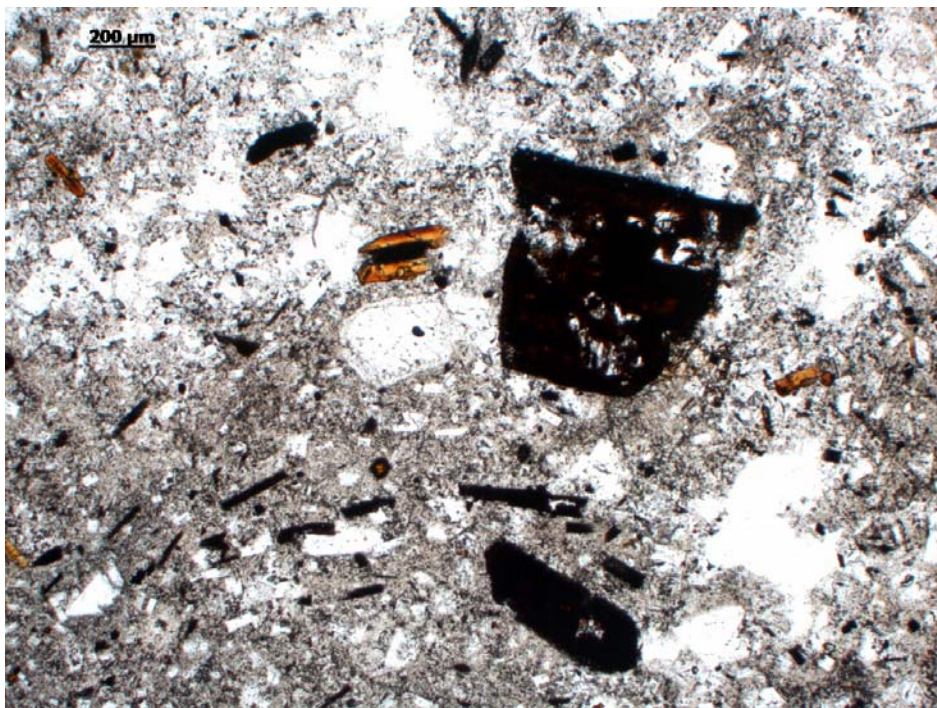


Figure A84: HRL 32, overview texture, PPL.

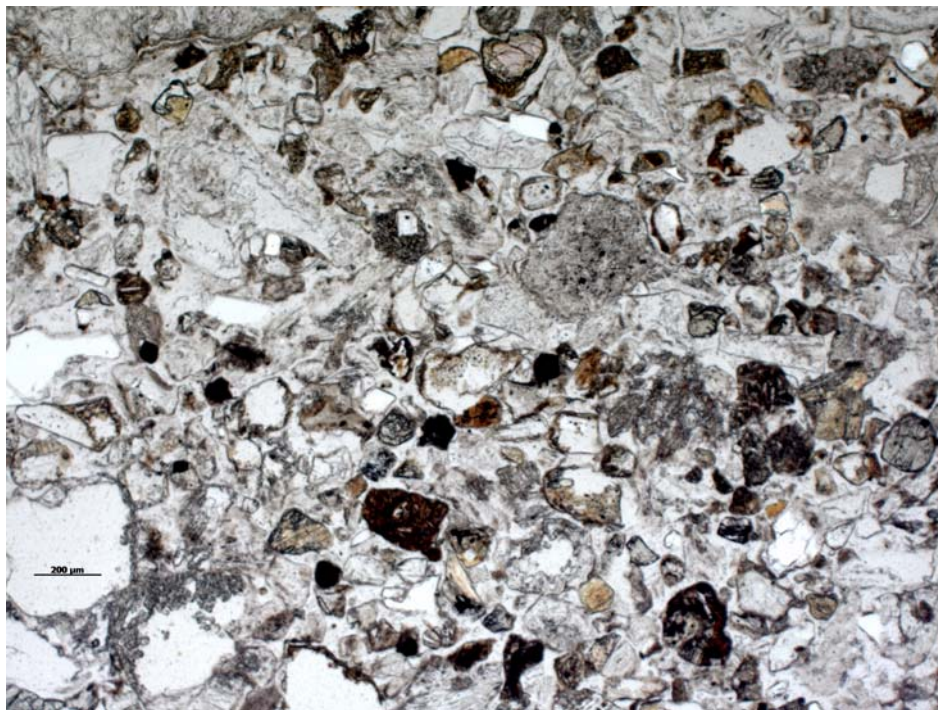


Figure A85: HRL 32, overview texture, XPL.



Figure A86: HRL 33, overview texture, PPL.

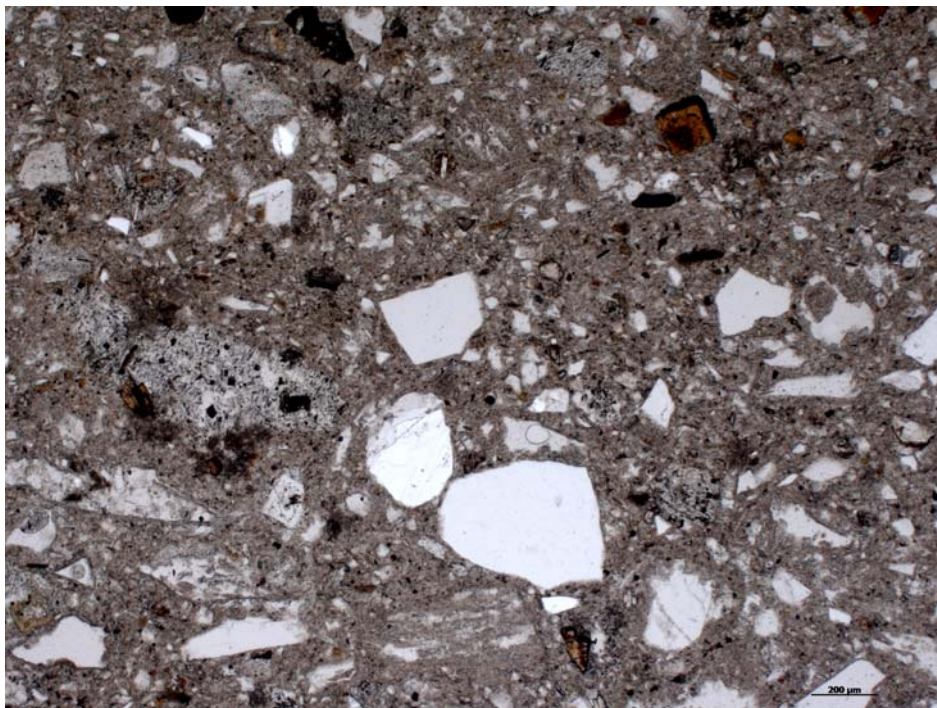


Figure A87: HRL 33, overview texture, XPL.

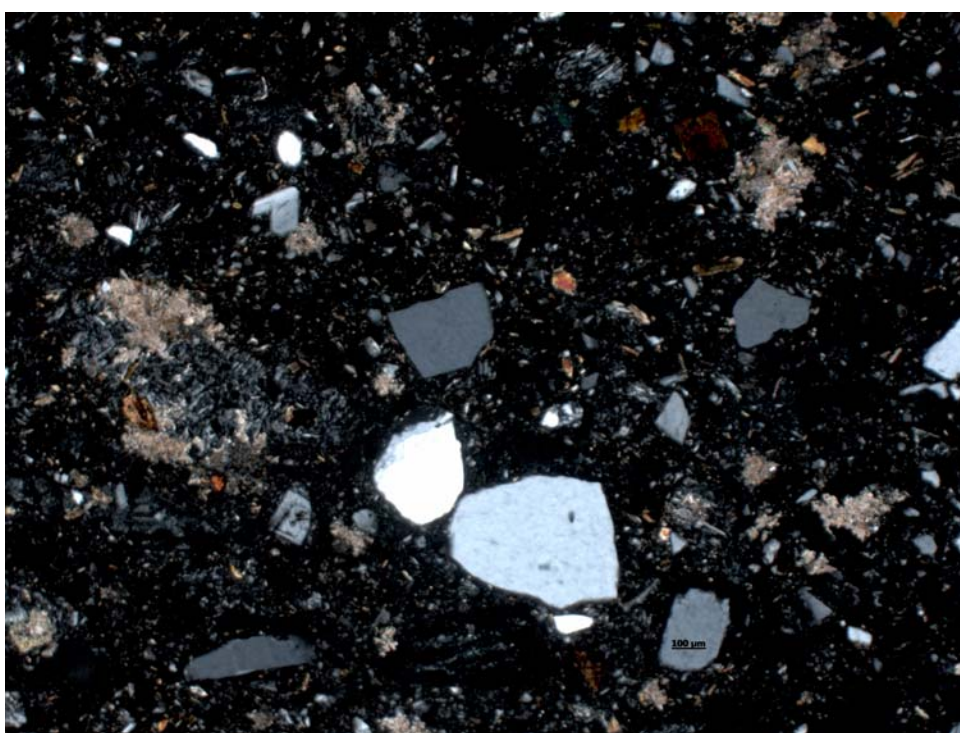


Figure A88: HRL 34, overview texture, PPL.

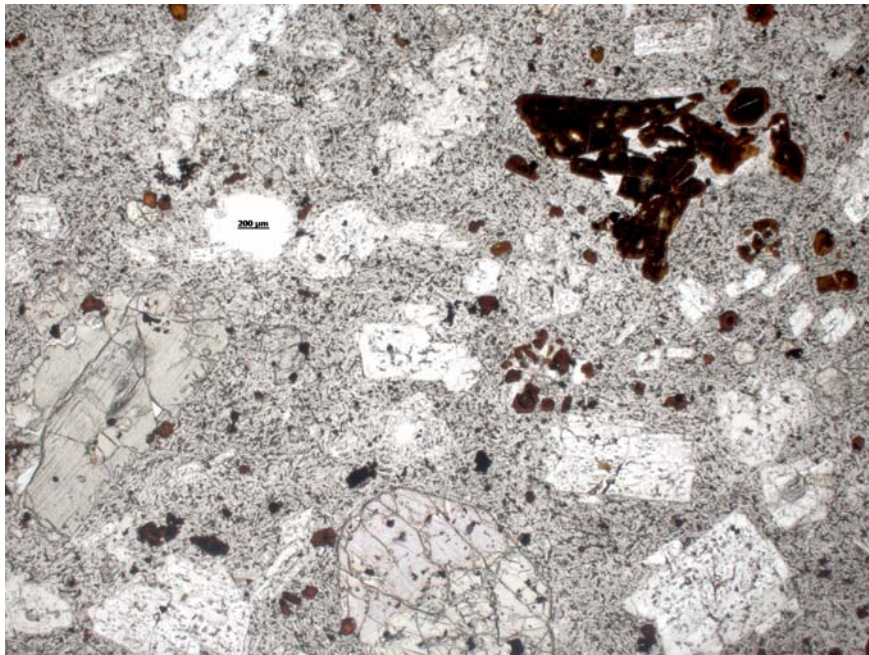


Figure A89: HRL 34, overview texture, XPL.

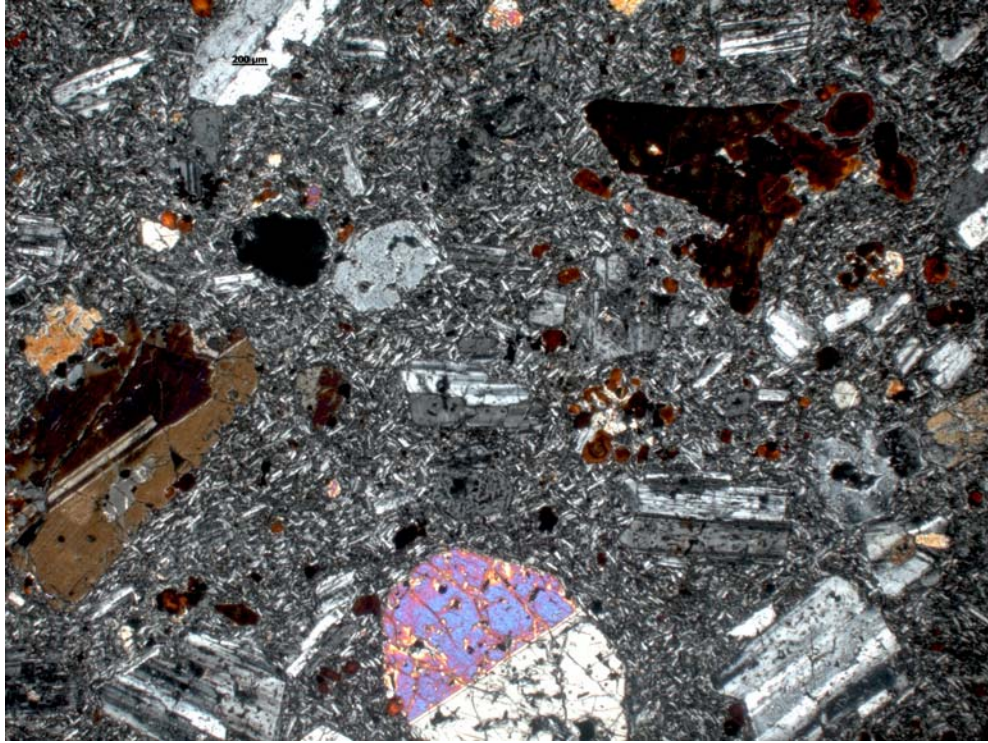


Figure A90: HRL 34, mystery mineral replacing another mineral XPL.



Figure A91: HRL 35, contact, PPL.

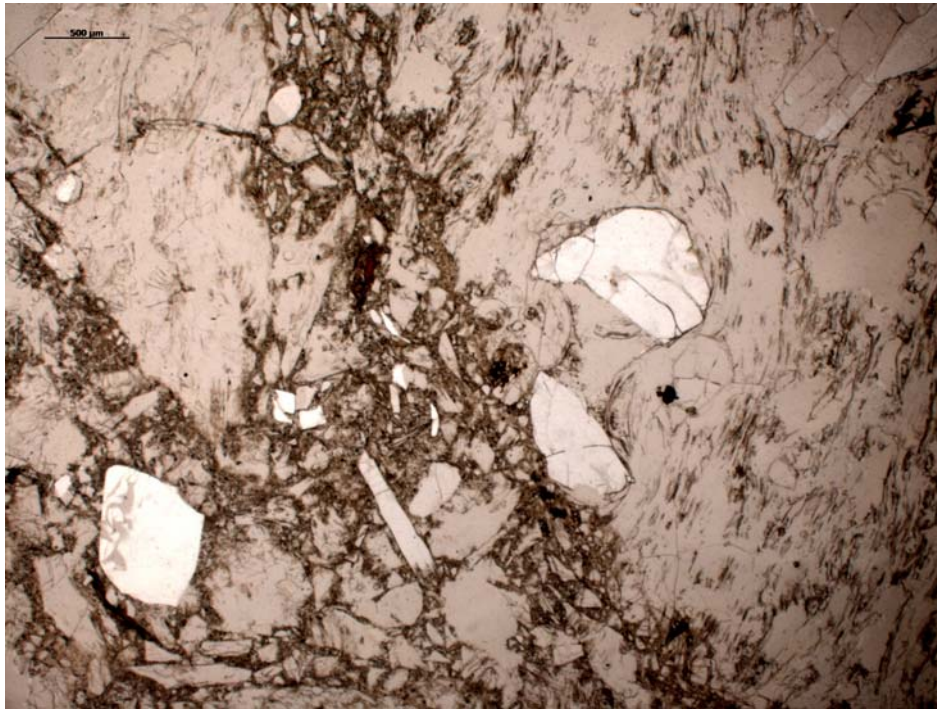


Figure A92: HRL 35, overview texture, PPL.



Figure A93: HRL 36, overview texture, PPL.

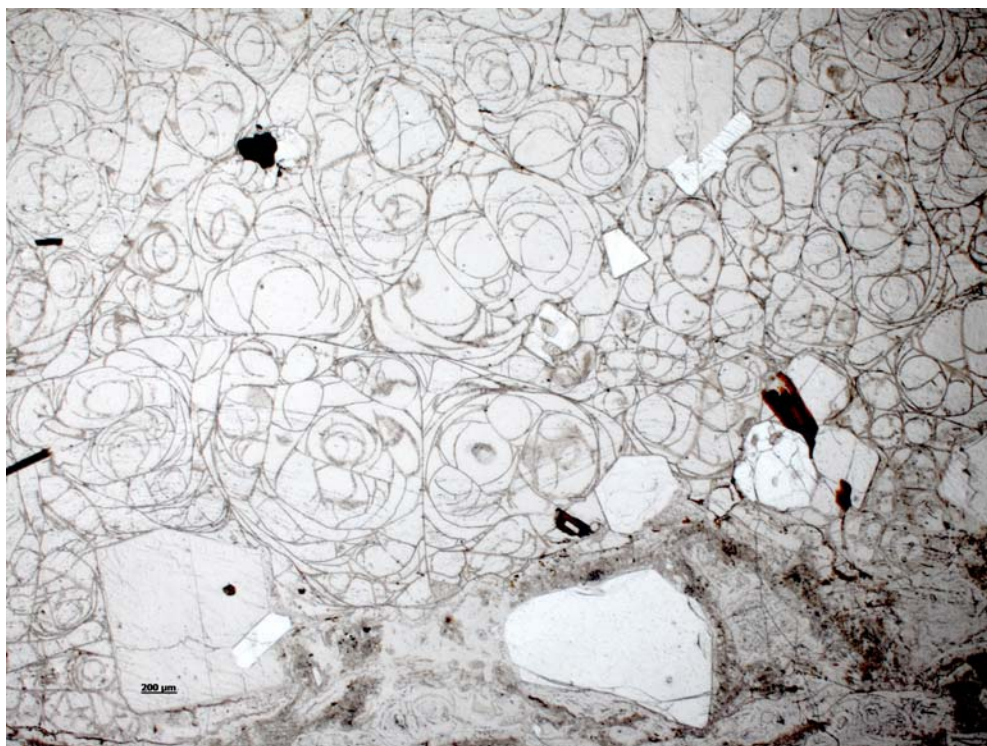


Figure A94: HRL 36, overview texture, XPL.



APPENDIX B:
Whole Rock Geochemistry of the
Highland Range Rhyolite Sequence

Table B1: Raw whole-rock major element oxide geochemistry of the Highland Range silicic sequence. Concentrations listed in wt%.

Analyte Symbol	SiO ₂	Al ₂ O ₃	Fe ₂ O ₃ (T)	MnO	MgO	CaO	Na ₂ O	K ₂ O	TiO ₂	P ₂ O ₅	LOI	Total
Detection Limit	0.01	0.01	0.01	0.001	0.01	0.01	0.01	0.01	0.001	0.01		
Analysis Method	FUS-ICP	FUS-ICP	FUS-ICP	FUS-ICP	FUS-ICP	FUS-ICP	FUS-ICP	FUS-ICP	FUS-ICP	FUS-ICP	FUS-ICP	
HRL 5	67.3	15.2	3.02	0.067	0.7	1.91	4.04	5.31	0.612	0.14	0.87	99.17
HRL 7B	63.1	12.09	0.59	0.036	0.93	3.54	0.75	3.78	0.096	0.02	15.56	100.49
HRL 8B	54.94	14.81	2.89	0.075	0.77	2.39	2.75	4.65	0.612	0.18	1.74	85.81
HRL 8C	64.92	12.75	2.47	0.051	0.67	1.92	2.8	3.81	0.442	0.16	5.14	95.13
HRL 8D	59.86	14.63	5.94	0.085	3.13	5.62	3.14	4.44	1.069	0.63	2.06	100.60
HRL 8E	60.44	12.76	2.61	0.059	2.49	4	1.04	2.96	0.461	0.2	11.5	98.52
HRL 10B	65.2	12.03	0.67	0.029	0.58	1.91	2.4	3.51	0.103	0.02	14.01	100.46
HRL 12A	71.6	13.33	2.1	0.051	0.75	1.45	3.23	5.61	0.398	0.12	0.92	99.56
HRL 14A	63.57	14.09	4.37	0.076	2.68	4.08	3.31	3.76	0.767	0.29	1.91	98.90
HRL 21	72.99	11.74	0.65	0.037	0.09	0.6	2.49	5.58	0.112	0.01	5.55	99.85
HRL 22A	61.5	12.45	1.88	0.049	1.67	3.27	1.34	3.58	0.342	0.12	12.36	98.56
HRL 22B	68.47	13.98	2.1	0.056	1.75	3.51	1.51	4.04	0.382	0.12	3.3	99.22
HRL 23A	72.74	13.77	2.07	0.04	0.86	1.75	2.82	5.2	0.394	0.15	1.18	100.97
HRL 23B	60.56	14.2	5.5	0.083	3.36	5.52	3.39	3.81	0.985	0.48	2.58	100.47
HRL 26	60.81	14.77	4.88	0.045	3.05	4.73	3.32	4.88	0.932	0.52	1.55	99.49
HRL 27	66.12	15.44	3.03	0.075	0.87	2.15	4.83	4.07	0.619	0.17	3.13	100.50
HRL 28	66.46	15.43	2.88	0.075	0.82	2.55	4.19	4.79	0.604	0.19	0.77	98.76
HRL 29	68.94	15.3	2.77	0.062	0.7	2.01	4.21	4.83	0.572	0.17	0.93	100.49
HRL 31	66.07	15.4	3.23	0.078	1.04	2.72	4.08	4.47	0.636	0.23	1.08	99.03
HRL 41A	73.22	11.63	0.85	0.04	0.21	1.36	3.1	5.08	0.109	0.01	5.02	100.63
HRL 42	67.64	14.57	1.96	0.087	0.41	1.17	3.91	5.42	0.387	0.05	4.62	100.22
HRL 45	71.05	11.46	0.81	0.04	0.25	0.99	2.36	4.87	0.111	0.02	6.49	98.45

Table B2: Normalized whole-rock major element oxide geochemistry of the Highland Range silicic sequence. Concentrations listed in wt%.

Analyte Symbol	SiO ₂	Al ₂ O ₃	Fe ₂ O ₃ (T)	MnO	MgO	CaO	Na ₂ O	K ₂ O	TiO ₂	P ₂ O ₅
Detection Limit	0.01	0.01	0.01	0.001	0.01	0.01	0.01	0.01	0.001	0.01
Analysis Method	FUS-ICP	FUS-ICP	FUS-ICP	FUS-ICP	FUS-ICP	FUS-ICP	FUS-ICP	FUS-ICP	FUS-ICP	FUS-ICP
HRL 5	68.46	15.46	3.07	0.068	0.71	1.94	4.11	5.40	0.623	0.142
HRL 7B	74.29	14.23	0.69	0.042	1.09	4.17	0.88	4.45	0.113	0.024
HRL 8B	65.35	17.62	3.44	0.089	0.92	2.84	3.27	5.53	0.728	0.214
HRL 8C	72.14	14.17	2.74	0.057	0.74	2.13	3.11	4.23	0.491	0.178
HRL 8D	60.74	14.85	6.03	0.086	3.18	5.70	3.19	4.51	1.085	0.639
HRL 8E	69.46	14.66	3.00	0.068	2.86	4.60	1.20	3.40	0.530	0.230
HRL 10B	75.42	13.92	0.77	0.034	0.67	2.21	2.78	4.06	0.119	0.023
HRL 12A	72.59	13.51	2.13	0.052	0.76	1.47	3.27	5.69	0.403	0.122
HRL 14A	65.54	14.53	4.51	0.078	2.76	4.21	3.41	3.88	0.791	0.299
HRL 21	77.40	12.45	0.69	0.039	0.10	0.64	2.64	5.92	0.119	0.011
HRL 22A	71.34	14.44	2.18	0.057	1.94	3.79	1.55	4.15	0.397	0.139
HRL 22B	71.38	14.57	2.19	0.058	1.82	3.66	1.57	4.21	0.398	0.125
HRL 23A	72.89	13.80	2.07	0.040	0.86	1.75	2.83	5.21	0.395	0.150
HRL 23B	61.87	14.51	5.62	0.085	3.43	5.64	3.46	3.89	1.006	0.490
HRL 26	62.09	15.08	4.98	0.046	3.11	4.83	3.39	4.98	0.952	0.531
HRL 27	67.90	15.86	3.11	0.077	0.89	2.21	4.96	4.18	0.636	0.175
HRL 28	67.82	15.75	2.94	0.077	0.84	2.60	4.28	4.89	0.616	0.194
HRL 29	69.24	15.37	2.78	0.062	0.70	2.02	4.23	4.85	0.575	0.171
HRL 31	67.45	15.72	3.30	0.080	1.06	2.78	4.17	4.56	0.649	0.235
HRL 41A	76.58	12.16	0.89	0.042	0.22	1.42	3.24	5.31	0.114	0.010
HRL 42	70.75	15.24	2.05	0.091	0.43	1.22	4.09	5.67	0.405	0.052
HRL 45	77.26	12.46	0.88	0.043	0.27	1.08	2.57	5.30	0.121	0.022

Table B3: Whole-rock trace element geochemistry of the Highland Range silicic sequence. Concentrations listed in ppm.

Analyte Symbol	Au	Ag	As	Ba	Be	Bi	Br	Cd	Co	Cr	Cs
Detection Limit	1	0.5	1	1	1	0.1	0.5	0.5	0.1	0.5	0.1
Analysis Method	INAA	MULT INAA / TD-ICP	INAA	FUS-ICP	FUS-ICP	FUS-MS	INAA	TD-ICP	INAA	INAA	FUS-MS
HRL 5	< 1	< 0.5	4	1512	3	< 0.1	< 0.5	< 0.5	5.3	23.4	1.4
HRL 7B	< 1	< 0.5	2	23	3	0.3	1	< 0.5	1.6	19.3	5.3
HRL 8B	< 1	0.6	5	1539	3	< 0.1	< 0.5	0.5	20.9	228	1.3
HRL 8C	4	< 0.5	5	1448	3	0.3	1.4	< 0.5	8.7	73.8	3.3
HRL 8D	< 1	< 0.5	4	1560	2	0.1	< 0.5	0.5	20.8	224	2.6
HRL 8E	< 1	< 0.5	2	613	2	0.2	< 0.5	< 0.5	11.8	67.8	4.8
HRL 10B	1	< 0.5	4	23	5	0.3	1.6	< 0.5	2.4	30	5.1
HRL 12A	5	< 0.5	< 1	525	3	< 0.1	< 0.5	< 0.5	6	24.6	1.2
HRL 14A	1	< 0.5	3	797	3	0.2	1	< 0.5	14.6	58.8	1.9
HRL 21	< 1	< 0.5	5	33	3	0.3	1.8	< 0.5	1.7	18	3.1
HRL 22A	< 1	< 0.5	1	391	3	0.6	2.1	< 0.5	7.8	61.4	3.1
HRL 22B	< 1	< 0.5	1	443	3	0.5	< 0.5	< 0.5	19.8	185	1.5
HRL 23A	< 1	< 0.5	3	751	3	< 0.1	< 0.5	0.5	6.4	57.8	1.5
HRL 23B	< 1	< 0.5	6	1342	3	< 0.1	< 0.5	0.5	19.6	178	2
HRL 26	< 1	0.7	4	1610	3	< 0.1	< 0.5	< 0.5	14.6	101	1.2
HRL 27	8	< 0.5	4	1488	3	0.8	< 0.5	0.5	5	< 0.5	2.5
HRL 28	< 1	< 0.5	8	1561	3	< 0.1	< 0.5	< 0.5	4.4	13.3	1.3
HRL 29	< 1	< 0.5	5	1578	3	0.2	< 0.5	< 0.5	4.5	10.9	1.9
HRL 31	< 1	< 0.5	3	1589	3	0.1	< 0.5	< 0.5	7.4	29.6	1.1
HRL 41A	< 1	< 0.5	7	28	4	0.7	2.6	< 0.5	4.4	18.3	4
HRL 42	< 1	< 0.5	3	1418	3	0.3	2.1	< 0.5	1.4	7.9	5
HRL 45	3	< 0.5	3	26	3	0.6	1.8	< 0.5	2.1	6.9	4.5

Table B2, continued

Analyte Symbol	Cu	Ga	Ge	Hf	Hg	In	Ir	Mo	Nb	Ni	Pb	Rb
Detection Limit	1	1	0.5	0.1	1	0.1	1	2	0.2	1	5	2
Analysis Method	TD-ICP	FUS-MS	FUS-MS	FUS-MS	INAA	FUS-MS	INAA	FUS-MS	FUS-MS	TD-ICP	TD-ICP	FUS-MS
HRL 5	8	21	2	8.9	< 1	< 0.1	< 1	< 2	22.9	11	21	138
HRL 7B	4	13	< 0.5	3.7	< 1	< 0.1	< 1	< 2	20.8	3	22	151
HRL 8B	53	22	1.5	9.6	< 1	< 0.1	< 1	2	23.6	97	32	122
HRL 8C	18	17	1.4	5.3	< 1	< 0.1	< 1	2	21.7	40	18	141
HRL 8D	47	22	1.5	7.7	< 1	< 0.1	< 1	< 2	19.8	96	25	86
HRL 8E	24	17	1.2	5.6	< 1	< 0.1	< 1	< 2	21.9	61	25	109
HRL 10B	4	16	0.7	3.7	< 1	< 0.1	< 1	< 2	19.8	3	23	152
HRL 12A	8	17	1.4	5.8	< 1	< 0.1	< 1	< 2	21.3	15	18	155
HRL 14A	28	20	1.3	6.8	< 1	< 0.1	< 1	3	20	46	19	119
HRL 21	2	16	1.4	3.6	< 1	< 0.1	< 1	4	22.7	1	27	202
HRL 22A	13	15	1.1	5.1	< 1	< 0.1	< 1	< 2	21.7	35	24	114
HRL 22B	44	25	2	8.9	< 1	< 0.1	< 1	< 2	23.1	99	23	107
HRL 23A	23	17	1.5	4.9	< 1	< 0.1	< 1	< 2	21.4	27	23	138
HRL 23B	30	21	1.7	7.7	< 1	< 0.1	< 1	< 2	20.1	88	21	98
HRL 26	26	22	1.5	9.6	< 1	< 0.1	< 1	< 2	17.5	85	18	106
HRL 27	5	21	2.1	9.5	< 1	< 0.1	< 1	3	22.5	5	26	146
HRL 28	6	20	2	9	< 1	< 0.1	< 1	< 2	22.6	5	22	120
HRL 29	4	20	2.4	8.9	< 1	< 0.1	< 1	< 2	22.9	5	22	127
HRL 31	10	20	1.9	8.7	< 1	< 0.1	< 1	< 2	21.6	17	17	112
HRL 41A	82	31	1.4	4.3	< 1	< 0.1	< 1	5	24.7	< 1	25	209
HRL 42	7	34	1.3	10.8	< 1	< 0.1	< 1	3	29.3	3	28	245
HRL 45	11	29	1.2	3.6	< 1	< 0.1	< 1	4	22.1	2	22	220

Table B2, continued

Analyte Symbol	S	Sb	Sc	Se	Sn	Sr	Ta	Th	U
Detection Limit	0.001	0.1	0.01	0.5	1	2	0.1	0.05	0.05
Analysis Method	TD-ICP	INAA	INAA	INAA	FUS-MS	FUS-ICP	FUS-MS	FUS-MS	FUS-MS
HRL 5	0.042	1.7	5.42	< 0.5	< 1	430	1.5	13.7	4.12
HRL 7B	0.007	0.3	2.27	< 0.5	< 1	107	2.1	34.3	2.73
HRL 8B	0.022	1.3	13.5	< 0.5	2	1068	1.8	13.1	2.92
HRL 8C	0.023	0.7	5.05	< 0.5	< 1	432	1.7	19.5	3.55
HRL 8D	0.006	1.5	12.6	< 0.5	< 1	1196	1.2	15.1	5
HRL 8E	0.006	1	5.27	< 0.5	< 1	716	1.7	19.5	2.36
HRL 10B	0.008	0.6	2.42	< 0.5	< 1	106	2	33.4	4.01
HRL 12A	0.006	0.5	4.04	< 0.5	< 1	173	1.7	18.6	3.16
HRL 14A	0.004	0.5	8.79	< 0.5	2	584	1.6	15.6	5.53
HRL 21	0.004	0.8	1.48	< 0.5	2	19	2.2	22.8	18.1
HRL 22A	0.007	0.5	4.12	< 0.5	< 1	445	1.8	20.4	2.48
HRL 22B	0.02	1	12.5	< 0.5	< 1	495	1.5	18	6.59
HRL 23A	0.003	0.8	4.17	< 0.5	< 1	540	1.8	19.5	3.68
HRL 23B	0.012	1.1	11.6	< 0.5	2	1026	1.3	15.8	3.84
HRL 26	0.015	0.6	8.79	< 0.5	< 1	1083	1.1	14.7	2.66
HRL 27	0.007	0.5	5.72	< 0.5	2	486	1.5	13.8	3.12
HRL 28	0.007	1.1	4.97	< 0.5	2	460	1.7	12.3	2.7
HRL 29	0.003	0.5	5.07	< 0.5	2	455	1.7	12.2	2.82
HRL 31	0.003	0.5	6.2	< 0.5	2	554	1.6	12	2.33
HRL 41A	0.014	0.9	1.66	< 0.5	4	20	2.48	28.9	6.33
HRL 42	0.006	0.5	5.22	< 0.5	1	137	2.18	16.9	3.24
HRL 45	0.004	0.7	1.44	< 0.5	1	84	2.21	22.5	4.24

Table B2, continued

Analyte Symbol	V	W	Y	Zn	Zr
Detection Limit	5	1	1	1	1
Analysis Method	FUS-ICP	INAA	FUS-ICP	MULT INAA / TD-ICP	FUS-MS
HRL 5	39	2	23	55	359
HRL 7B	13	< 1	4	23	82
HRL 8B	38	< 1	23	66	425
HRL 8C	37	< 1	15	39	181
HRL 8D	91	< 1	24	55	311
HRL 8E	36	< 1	15	43	196
HRL 10B	< 5	< 1	4	24	84
HRL 12A	29	< 1	21	33	210
HRL 14A	84	< 1	21	53	260
HRL 21	< 5	2	12	23	91
HRL 22A	30	< 1	16	29	174
HRL 22B	27	< 1	18	70	357
HRL 23A	29	2	15	28	163
HRL 23B	91	2	19	57	311
HRL 26	140	< 1	19	63	382
HRL 27	46	4	19	64	405
HRL 28	35	2	23	58	396
HRL 29	42	2	20	58	389
HRL 31	35	2	20	53	377
HRL 41A	< 5	< 1	11	24	122
HRL 42	11	< 1	28	66	503
HRL 45	< 5	< 1	13	29	103

Table B3: Whole-rock Rare Earth Element geochemistry of the Highland Range silicic sequence. Concentrations listed in ppm.

Analyte Symbol	La	La	Ce	Ce	Pr	Nd	Nd	Sm	Sm	Eu	Eu	Gd	Tb
Detection Limit	0.05	0.05	0.1	1	0.02	0.05	1	0.01	0.01	0.005	0.05	0.02	0.01
Analysis Method	FUS-MS	INAA	FUS-MS	INAA	FUS-MS	FUS-MS	INAA	FUS-MS	INAA	FUS-MS	INAA	FUS-MS	FUS-MS
HRL 5	76.7	68.6	141	104	14.4	45	46	8.42	6.89	1.97	1.55	5.78	0.8
HRL 7B	19.4	18.5	36.6	29	2.29	5.06	3	0.63	0.59	0.075	0.15	0.33	0.07
HRL 8B	72.9	85.3	142	125	16.2	47.5	65	8.11	9.6	1.84	2.29	5.62	0.78
HRL 8C	56.1	53.4	97.4	77	9.24	28.2	26	4.95	4.43	1.02	0.91	3.29	0.46
HRL 8D	86.4	82.5	149	118	16.3	53.1	52	9.98	9	2.43	2.05	6.65	0.82
HRL 8E	54.3	55.1	103	87	9.65	28.6	33	5.22	4.86	1.08	1	3.47	0.49
HRL 10B	35.1	34.4	44.5	37	4.15	10.2	8	1.5	1.29	0.19	0.18	0.89	0.13
HRL 12A	58.9	56.1	104	87	10.1	31	33	5.78	5.2	0.941	0.88	4.03	0.62
HRL 14A	56	57.7	110	85	13.1	39.8	33	7.24	6.1	1.54	1.29	5.25	0.74
HRL 21	35.7	38.1	59.8	51	5.48	13.2	12	2.08	1.84	0.2	0.35	1.41	0.27
HRL 22A	55.8	54.1	103	84	9.32	27.7	30	4.97	4.57	0.911	0.83	3.34	0.49
HRL 22B	85.9	76.4	167	118	15.5	49.4	45	9.41	7.45	2.46	1.84	6.23	0.79
HRL 23A	56	53.3	97.1	77	9.15	27.2	27	4.86	4.21	0.908	0.8	3.2	0.47
HRL 23B	76.5	72.1	145	112	15.2	49.1	54	9.25	8.1	2.23	1.83	6.07	0.75
HRL 26	83.1	70.4	160	108	17	55.3	47	10.2	8.1	2.4	1.71	6.6	0.81
HRL 27	72.1	72.6	138	113	16.1	45.5	40	8.06	7.78	2.01	2	5.61	0.79
HRL 28	71.6	67.7	139	98	15.8	46.2	40	7.8	6.84	1.83	1.45	5.59	0.81
HRL 29	72.3	70.4	140	109	15.9	47.6	49	7.9	7.2	1.83	1.62	5.65	0.81
HRL 31	72.4	73.2	140	115	16	47	50	7.9	7.62	1.83	1.71	5.61	0.8
HRL 41A	44		70.7		5.21	14.5		2.16		0.211		1.56	0.26
HRL 42	103		201		18.9	69.9		10.8		2.21		7.79	0.98
HRL 45	39.9		69.7		5.22	14.2		2.28		0.208		1.74	0.27

Table B3, continued

Analyte Symbol	Tb	Dy	Ho	Er	Tl	Tm	Yb	Yb	Lu	Lu
Detection Limit	0.1	0.02	0.01	0.01	0.05	0.005	0.01	0.05	0.002	0.01
Analysis Method	INAA	FUS-MS	FUS-MS	FUS-MS	FUS-MS	FUS-MS	FUS-MS	INAA	FUS-MS	INAA
HRL 5	< 0.1	4.26	0.85	2.45	0.88	0.367	2.25	1.9	0.323	0.28
HRL 7B	< 0.1	0.46	0.11	0.44	0.67	0.093	0.78	0.79	0.138	0.12
HRL 8B	0.5	4.31	0.86	2.49	0.13	0.374	2.35	1.86	0.33	0.34
HRL 8C	< 0.1	2.54	0.52	1.6	1.51	0.252	1.66	1.47	0.251	0.23
HRL 8D	0.4	4.02	0.74	2.09	0.73	0.291	1.72	1.47	0.243	0.23
HRL 8E	0.4	2.69	0.55	1.66	1.22	0.281	1.78	1.71	0.256	0.26
HRL 10B	< 0.1	0.67	0.14	0.51	0.29	0.094	0.76	0.7	0.124	0.11
HRL 12A	< 0.1	3.62	0.73	2.2	0.91	0.355	2.25	2.08	0.309	0.31
HRL 14A	< 0.1	4.11	0.83	2.39	0.67	0.348	2.16	1.68	0.327	0.23
HRL 21	< 0.1	1.81	0.42	1.47	1.58	0.258	1.77	1.51	0.251	0.27
HRL 22A	< 0.1	2.75	0.57	1.77	0.64	0.287	1.84	1.66	0.279	0.27
HRL 22B	< 0.1	4.1	0.8	2.26	0.69	0.335	2.11	1.6	0.305	0.23
HRL 23A	< 0.1	2.65	0.55	1.66	1.05	0.277	1.8	1.51	0.251	0.24
HRL 23B	0.4	3.71	0.67	1.88	0.85	0.265	1.66	1.26	0.231	0.19
HRL 26	0.3	3.9	0.72	1.95	0.68	0.278	1.68	1.17	0.233	0.2
HRL 27	0.7	4.36	0.84	2.47	1.02	0.376	2.36	2.34	0.346	0.34
HRL 28	0.4	4.33	0.87	2.57	0.39	0.38	2.39	1.72	0.331	0.29
HRL 29	0.4	4.34	0.85	2.53	0.65	0.376	2.38	1.9	0.342	0.33
HRL 31	0.4	4.27	0.83	2.43	0.14	0.361	2.28	1.95	0.325	0.32
HRL 41A		1.72	0.41	1.41	1.99	0.242	1.74		0.284	
HRL 42		5.61	1.15	3.4	4.17	0.48	2.96		0.436	
HRL 45		1.8	0.42	1.52	3.46	0.258	1.79		0.286	

APPENDIX C:

U-Pb Geochronology, Probability Density Curves and Cathodoluminescence Images
of Zircons from the Highland Range silicic sequence

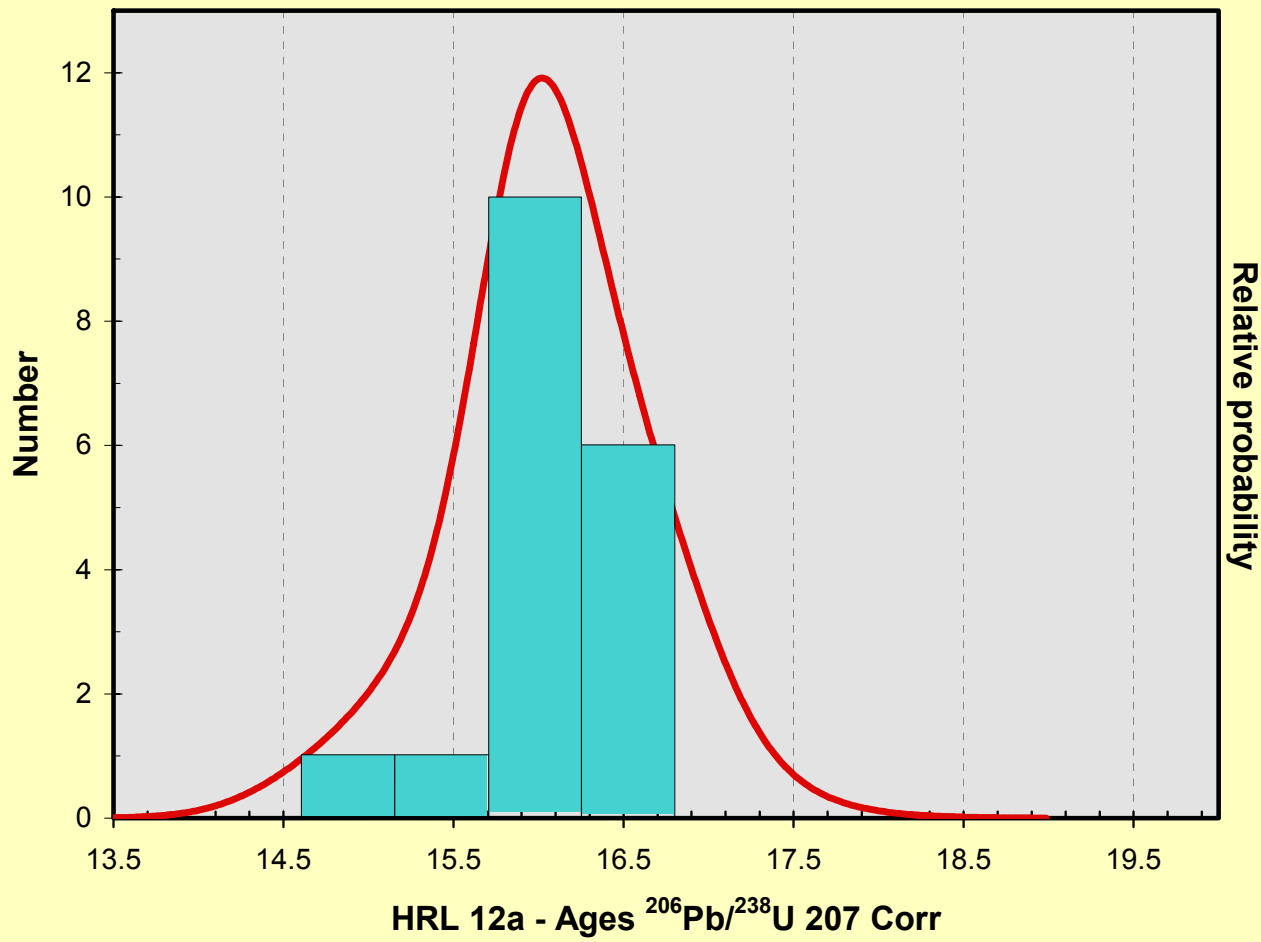
Table C1: Geochronology data from SHRIMP-RG analysis of zircons from the Highland Range silicic system.

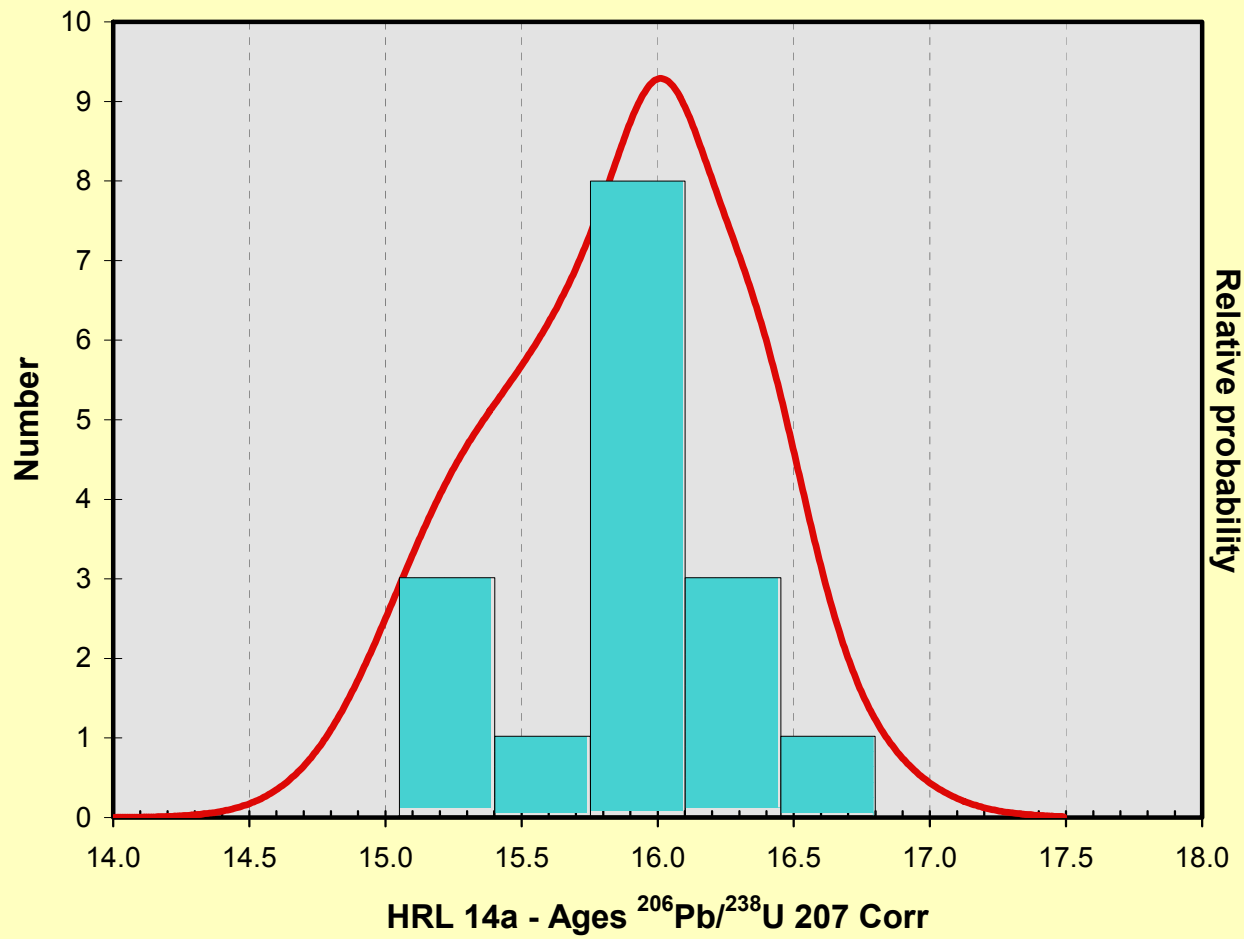
Spot Name	207corr						7corr 206Pbr /238U	1s err	Total 238 /206	Total		
	% comm 206	ppm U	ppm Th	232Th /238U	206Pb /238U Age	1s err				207 /206	% err	
HRL12A-15.1	4.80	218	449	2.13	16.1	0.4	.0022	.0001	395.51	2.4	.0540	12.5
HRL12A-7.1CDK	-7.32	170	280	1.71	14.9	0.4	.0022	.0001	427.40	2.6	.0577	12.0
HRL12A-8.1CDK	2.08	687	961	1.44	18.6	0.3	.0023	.0001	342.74	1.3	.0540	5.6
HRL12A-16.1CM	5.00	167	156	0.97	16.3	0.4	.0023	.0001	397.68	2.7	.0432	12.5
HRL12A-17.1EDK	6.23	267	400	1.55	15.9	0.4	.0024	.0001	400.38	2.1	.0577	9.0
HRL12A-10.2IM	5.77	90	136	1.55	16.6	0.6	.0024	.0001	378.85	3.5	.0644	13.4
HRL12A-18.1	-4.33	248	220	0.92	15.3	0.3	.0025	.0000	418.45	2.2	.0528	10.4
HRL12A-19.1IM	-4.48	167	406	2.52	16.5	0.4	.0025	.0001	389.68	2.5	.0452	12.1
HRL12A-20.1IM	6.15	251	292	1.20	16.2	0.4	.0025	.0001	389.69	2.1	.0633	8.3
HRL12A-11.2i	-9.83	110	127	1.19	14.1	0.6	.0025	.0000	453.09	3.9	.0543	16.2
HRL12A-21.1DKC	2.40	335	704	2.17	16.1	0.3	.0025	.0000	401.28	1.8	.0457	8.4
HRL12A-22.1DKC	5.05	270	547	2.09	16.7	0.3	.0025	.0001	385.09	2.0	.0472	12.1
HRL12A-12.1i	0.00	141	155	1.13	16.6	0.4	.0025	.0001	385.38	2.5	.0534	10.8
HRL12A-13.1C	2.48	144	295	2.11	14.8	0.4	.0025	.0000	422.97	2.7	.0669	11.8
HRL12A-14.3EDK	2.26	166	161	1.00	15.9	0.4	.0025	.0001	407.69	2.5	.0414	13.4
HRL12A-23.1-EDK	6.77	85	132	1.61	14.0	0.5	.0025	.0001	459.73	3.5	.0470	19.1
HRL12A-2.4C	-2.86	405	1253	3.20	17.5	0.3	.0026	.0001	365.08	1.5	.0512	9.2
HRL12A-3.2IDK	1.98	356	514	1.49	16.1	0.3	.0026	.0001	398.27	1.7	.0477	7.9
HRL12A-24.1CM	7.10	216	249	1.19	15.7	0.4	.0026	.0001	407.06	2.2	.0502	9.5
HRL12A-4.1ILT	9.69	73	167	2.38	16.6	0.7	.0026	.0001	381.81	3.9	.0568	16.5
HRL12A-5.1C	4.16	93	222	2.48	16.1	0.5	.0026	.0001	399.40	3.2	.0468	14.9
HRL12A-6.1CDK	1.79	361	585	1.68	15.8	0.3	.0027	.0000	400.28	1.8	.0605	7.1
HRL12A-25.1EDK	2.35	448	513	1.18	15.9	0.3	.0029	.0000	402.86	1.6	.0510	6.8

Table C1 (cont'd): Geochronology data from SHRIMP-RG analysis of zircons from the Highland Range silicic system.

Spot Name	207corr 206Pb												Total		
	% 206 comm	ppm U	ppm Th	232Th /238U	/238U Age	1s err	7corr 206Pbr /238U	1s err	238 /206	% err	207 /206	% err	207 /206	% err	207 /206
HRL14A-1.2EDK	9.07	303	306	1.04	15.9	0.5	.0023	.0001	380.93	1.9	.0958	17.0			
HRL14A-2.1IDK	-0.01	1327	3055	2.38	16.4	0.2	.0023	.0001	392.92	1.0	.0462	4.1			
HRL14A-3.1CDK	1.62	331	1165	3.63	16.7	0.3	.0023	.0001	381.63	1.7	.0530	7.6			
HRL14A-20.1EDK	-1.79	656	942	1.48	16.2	0.2	.0024	.0000	397.19	1.3	.0468	6.3			
HRL14A-5.1I	17.48	99	376	3.92	14.5	0.5	.0024	.0001	431.99	3.3	.0673	15.8			
HRL14A-21.1I	4.04	148	246	1.72	16.0	0.4	.0024	.0000	400.41	2.7	.0500	12.0			
HRL14A-6.1EDK	5.57	250	391	1.62	16.3	0.3	.0024	.0000	390.65	2.0	.0542	8.4			
HRL14A-7.1CDK	3.64	328	918	2.89	16.5	0.3	.0025	.0001	393.25	1.9	.0421	9.1			
HRL14A-7.2EDK	0.00	314	615	2.03	15.2	0.3	.0025	.0000	423.04	1.9	.0474	10.9			
HRL14A-22.1CDK	3.57	496	664	1.38	15.8	0.2	.0025	.0001	403.39	1.5	.0530	6.3			
HRL14A-8.1EDK	5.45	222	315	1.47	15.2	0.3	.0025	.0000	417.97	2.1	.0550	9.5			
HRL14A-23.1CDK	0.58	2039	4222	2.14	17.1	0.1	.0025	.0000	372.39	0.7	.0551	4.2			
HRL14A-9.1CDK	0.79	1428	1831	1.32	16.0	0.1	.0025	.0001	396.98	0.9	.0560	4.4			
HRL14A-11.2EM	5.76	238	240	1.04	14.9	0.3	.0025	.0001	423.69	2.0	.0603	9.6			
HRL14A-10.1IDK	3.08	249	662	2.75	15.8	0.3	.0025	.0000	405.92	2.1	.0507	9.3			
HRL14A-12.3DK	8.63	350	574	1.70	15.5	0.3	.0025	.0000	412.94	1.9	.0494	9.1			
HRL14A-13.1EM	-11.39	102	115	1.17	14.6	0.5	.0025	.0001	440.84	3.3	.0454	19.4			
HRL14A-14.1CDK	0.97	395	574	1.50	15.9	0.3	.0025	.0000	401.50	1.7	.0510	7.6			
HRL14A-15.2EDK	3.84	350	445	1.31	15.9	0.3	.0026	.0001	403.84	1.8	.0485	8.1			
HRL14A-24.1EDK	2.08	423	529	1.29	15.3	0.3	.0026	.0000	420.98	1.7	.0477	7.5			
HRL14A-17.1IDK	0.91	151	246	1.68	16.0	0.4	.0027	.0000	401.89	2.5	.0491	15.2			
HRL27-4IUPb	1.31	76	93	1.26	14.8	0.4	.0023	.0001	430.81	2.3	.0567	9.9			
HRL27-7RUPb	1.46	134	318	2.46	15.2	0.3	.0024	.0000	417.43	1.6	.0579	9.6			
HRL27-8IUPb	0.48	61	105	1.77	15.3	0.4	.0024	.0001	418.40	2.5	.0501	10.9			
HRL27-5CUPb	2.26	47	80	1.77	15.4	0.4	.0024	.0001	409.30	2.7	.0642	11.0			
HRL27-10.2CUPb	0.63	55	55	1.04	15.6	0.4	.0024	.0001	409.32	2.6	.0513	11.6			
HRL27-6CUPb	0.45	81	119	1.51	15.8	0.4	.0024	.0001	406.35	2.2	.0499	9.7			
HRL27-9.1RUPb	0.14	54	77	1.48	16.0	0.4	.0025	.0001	401.13	2.6	.0475	11.7			
HRL27-3CUPb	3.40	42	48	1.17	16.2	0.5	.0025	.0001	384.56	2.9	.0733	11.0			
HRL27-1.2UPb	4.81	33	41	1.28	16.2	0.8	.0025	.0001	378.02	4.4	.0844	17.0			
HRL27-2.1UPb	4.93	49	58	1.22	16.6	0.5	.0026	.0001	368.91	2.9	.0854	10.4			

Figure C1:
Probability density curves for samples HRL 12a, HRL 14a, and HRL 27 of the Highland Range silicic sequence.





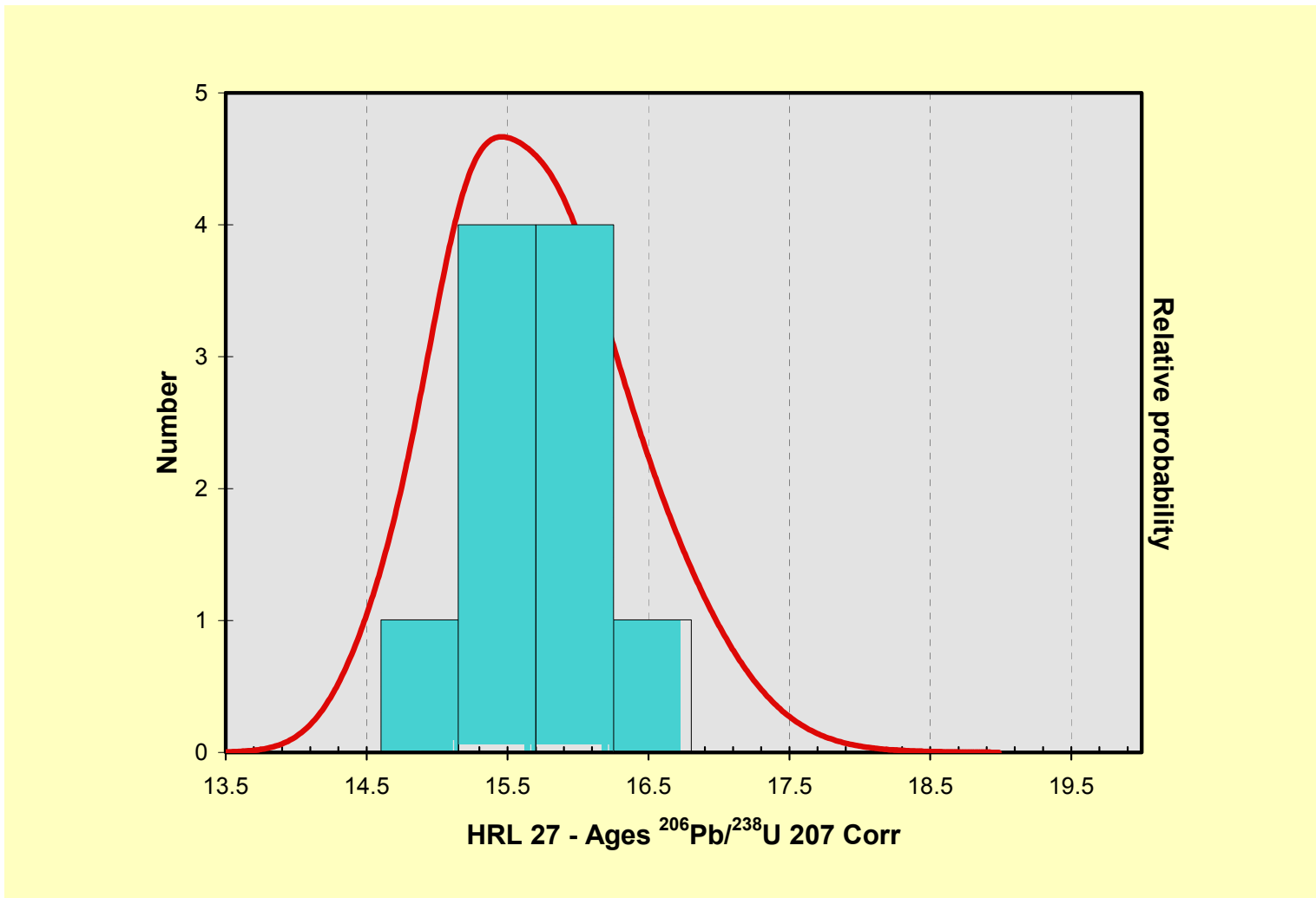
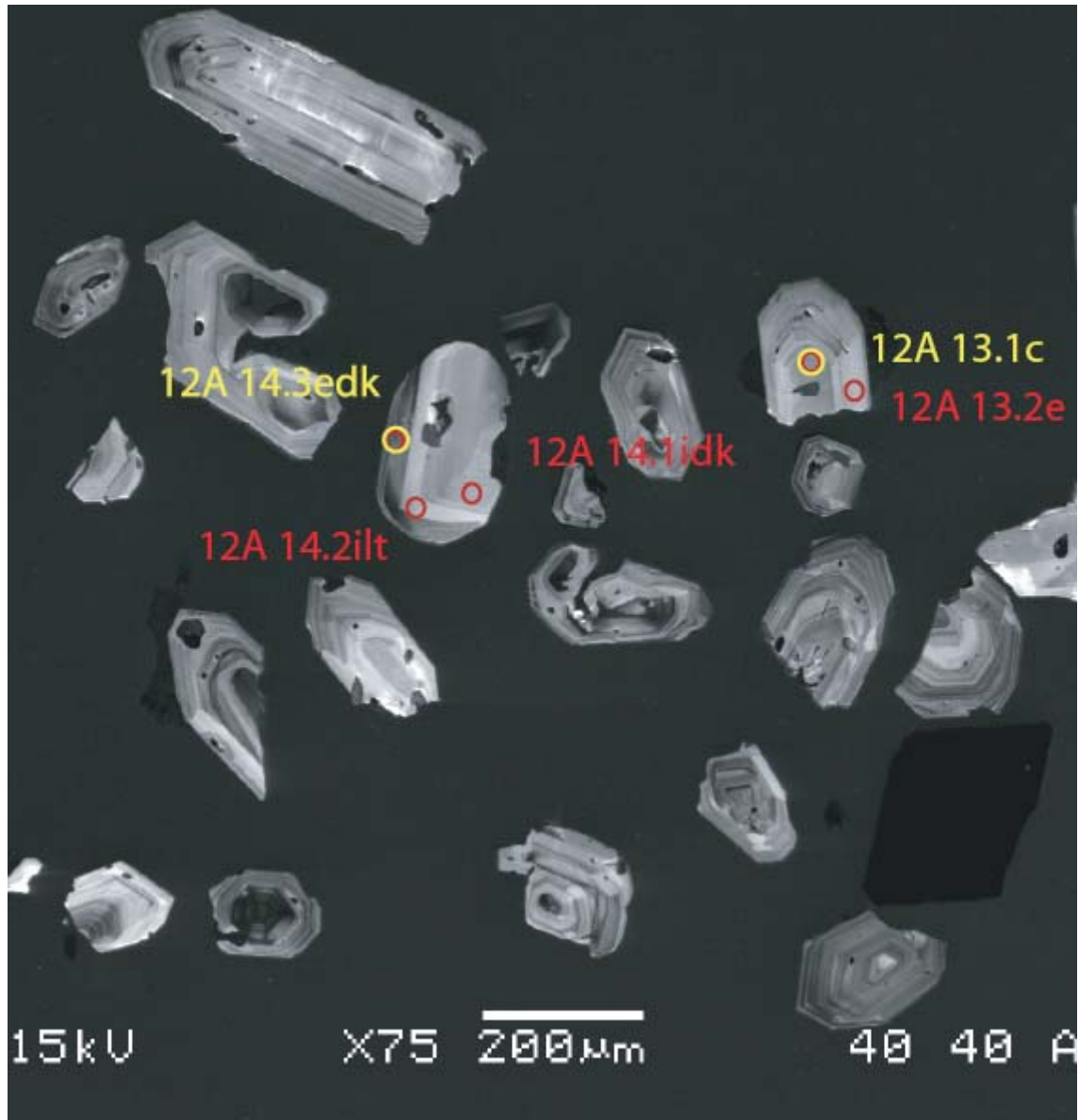
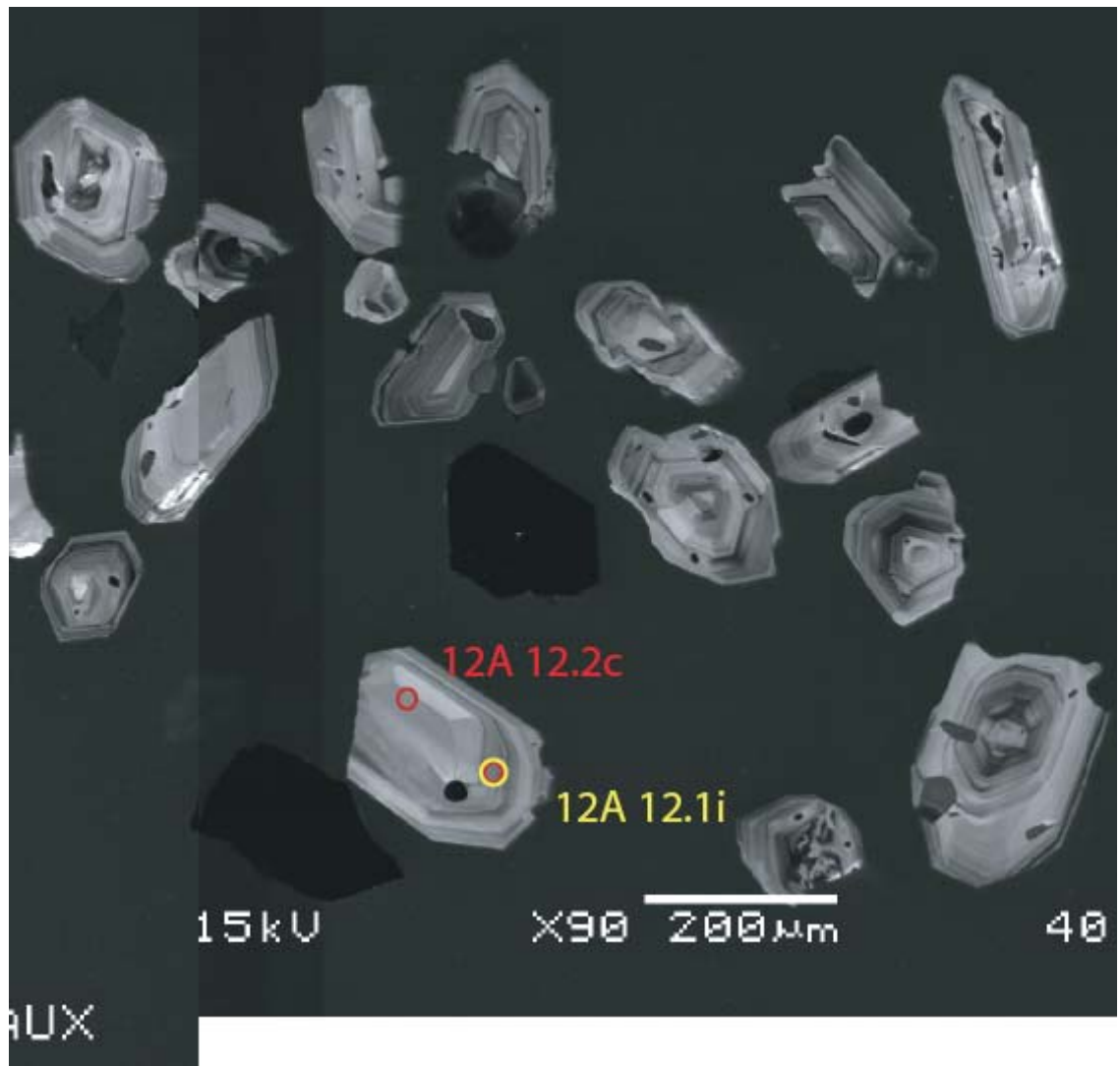
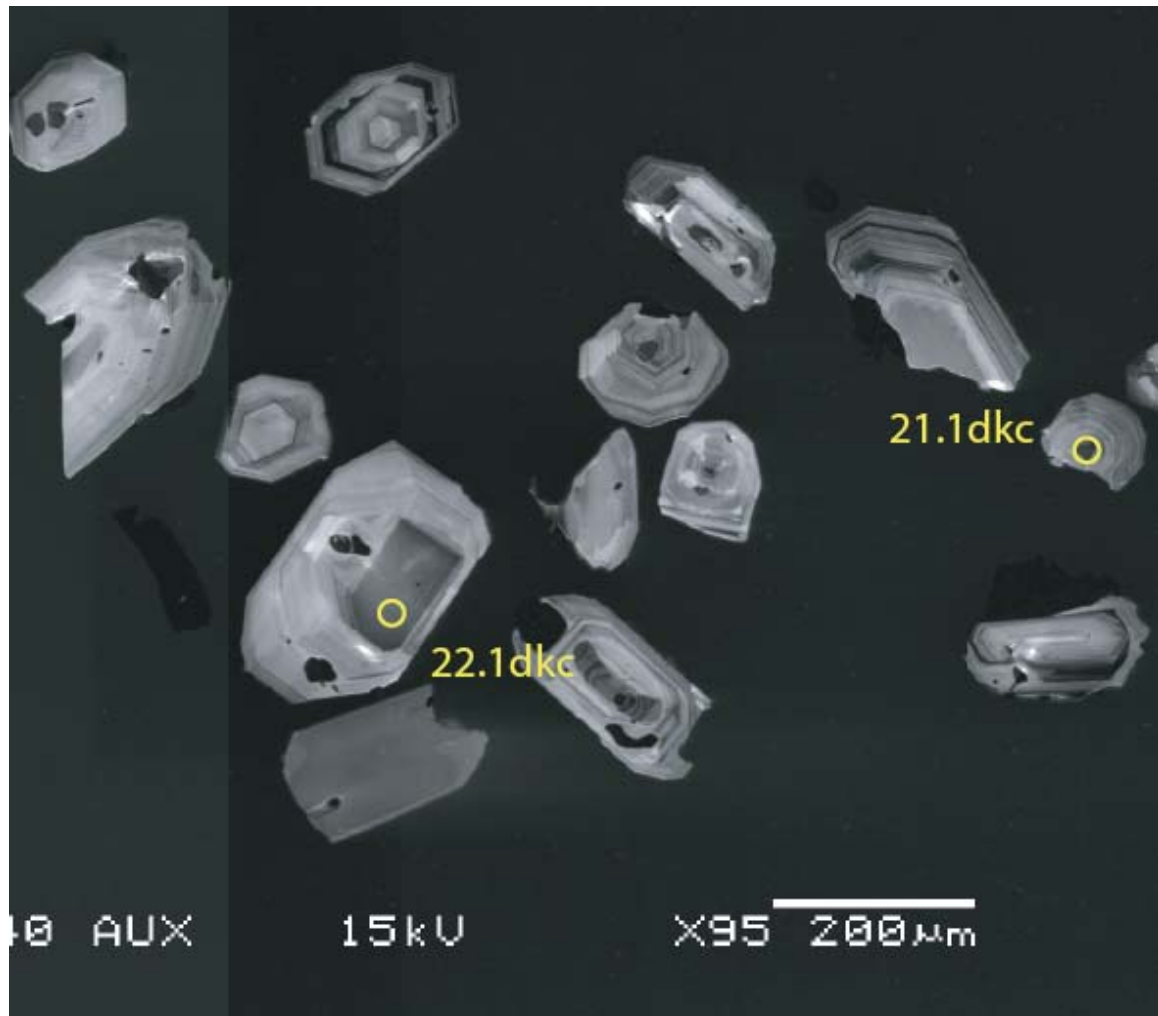


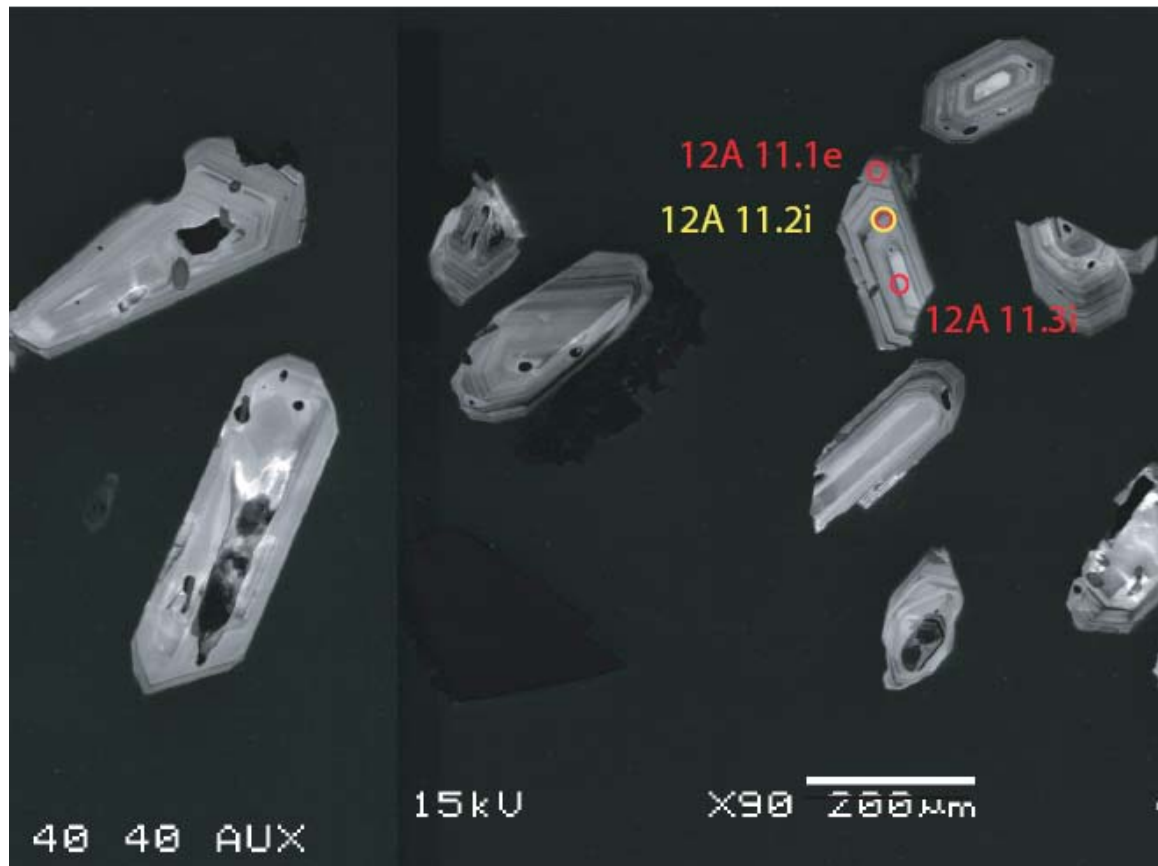
Figure C2:

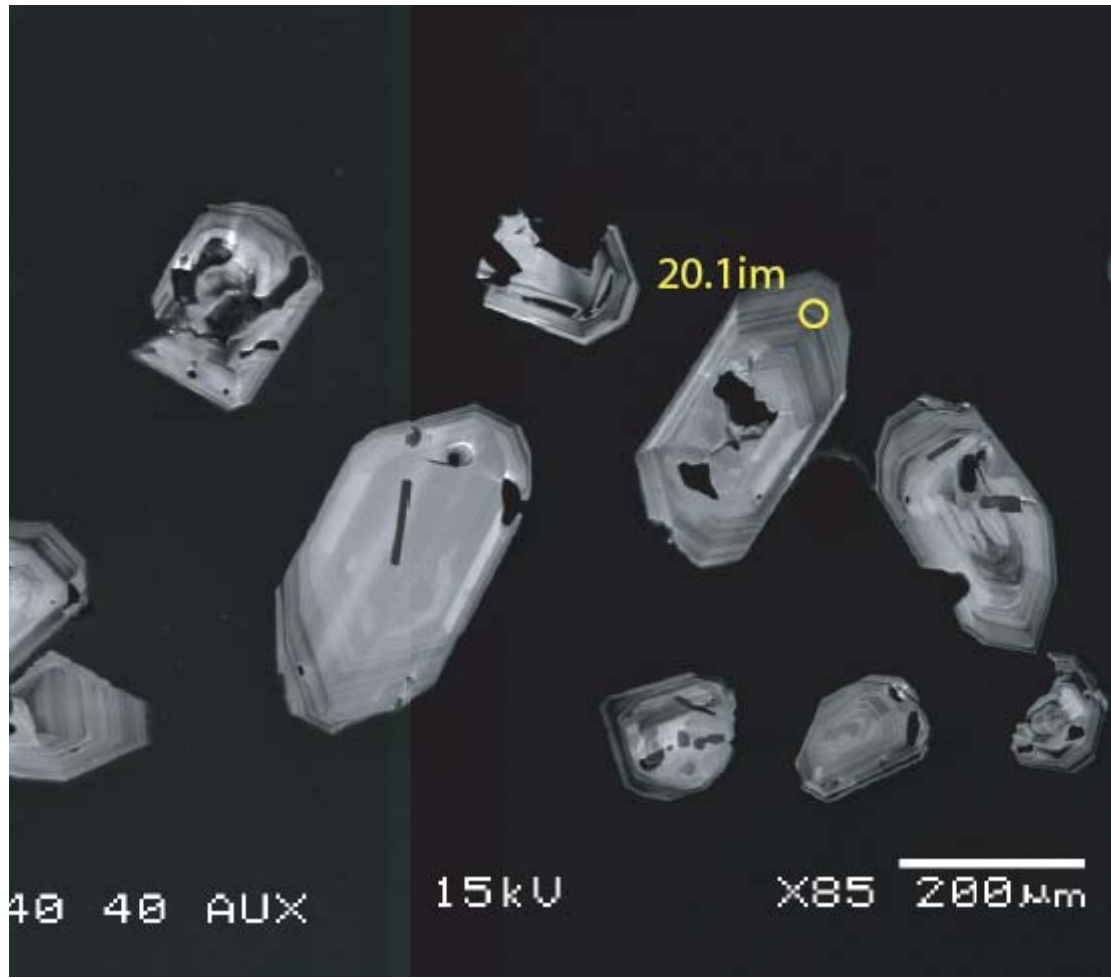
Cathodoluminescence images of zircons from sample HRL 12a with spots from U-Pb (yellow) and trace element (red) SHRIMP-RG analyses marked.

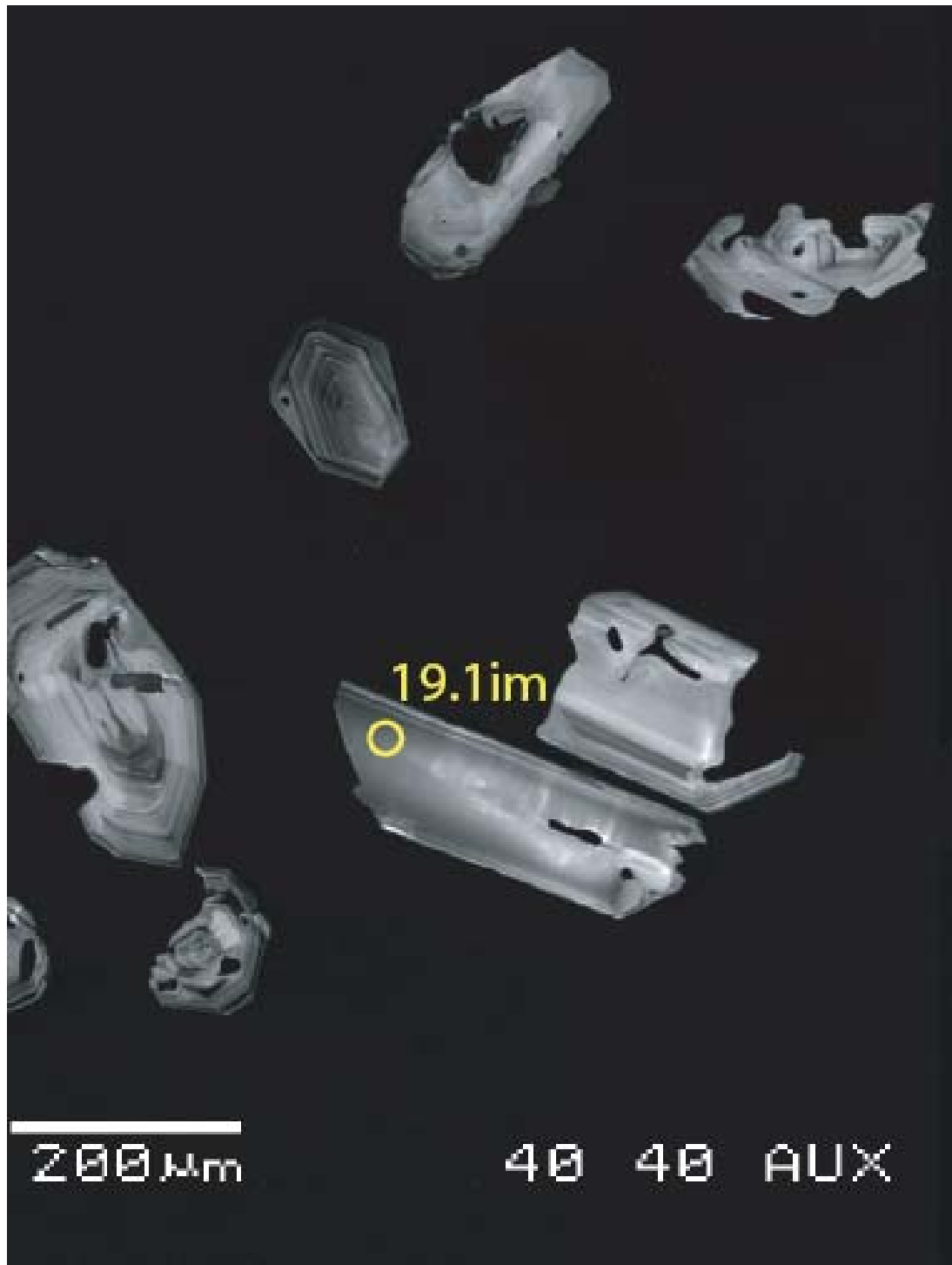


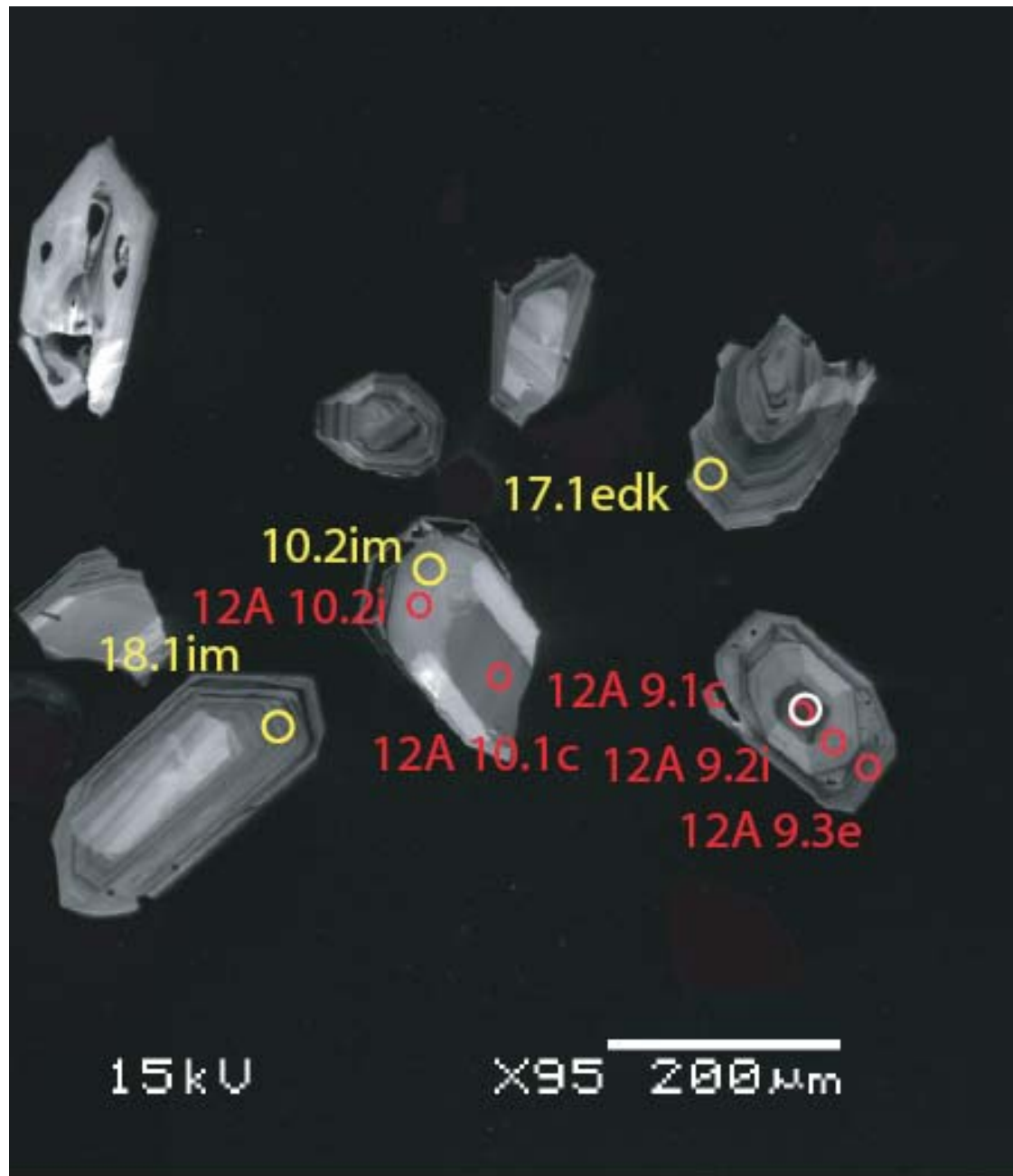


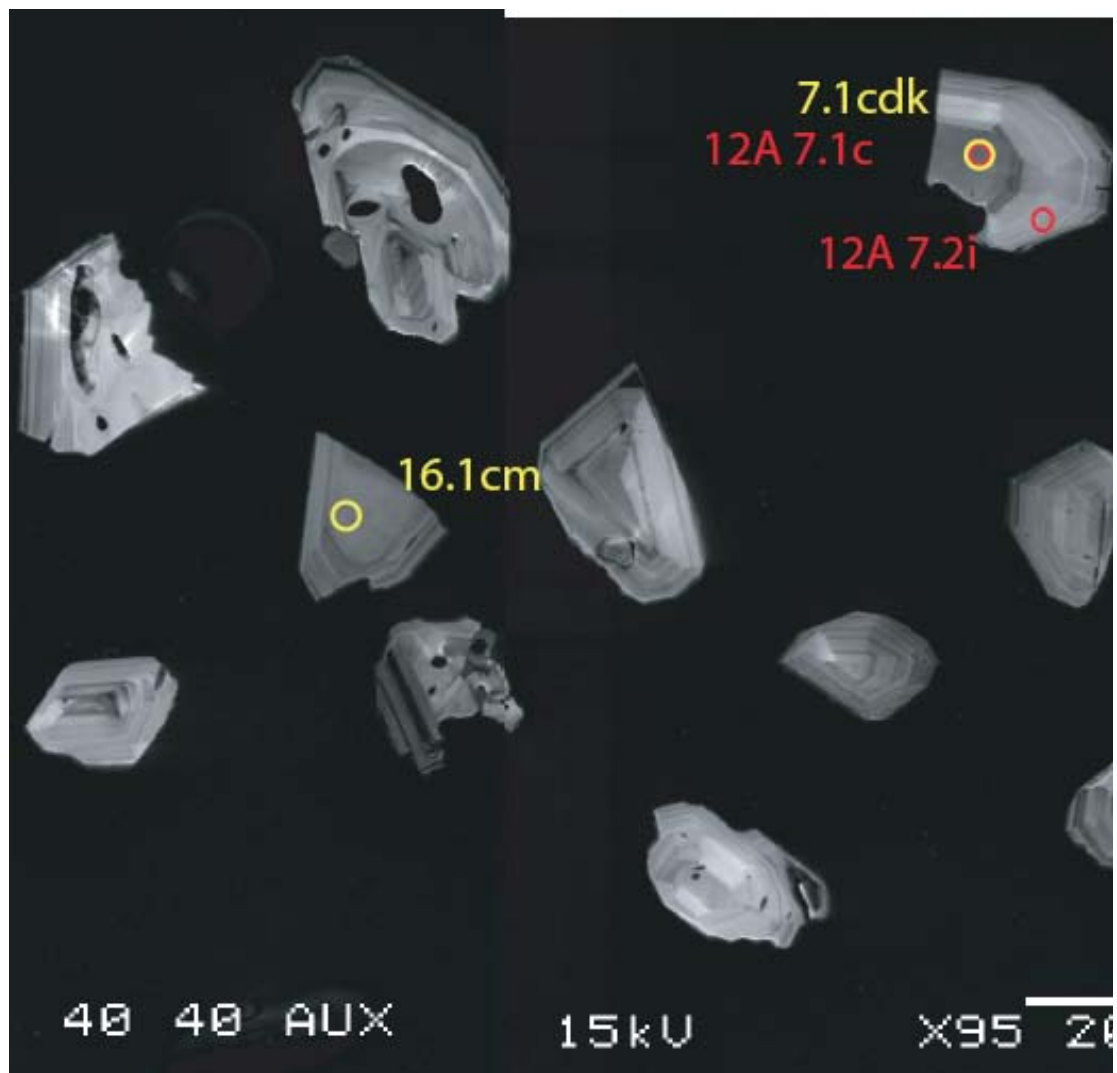


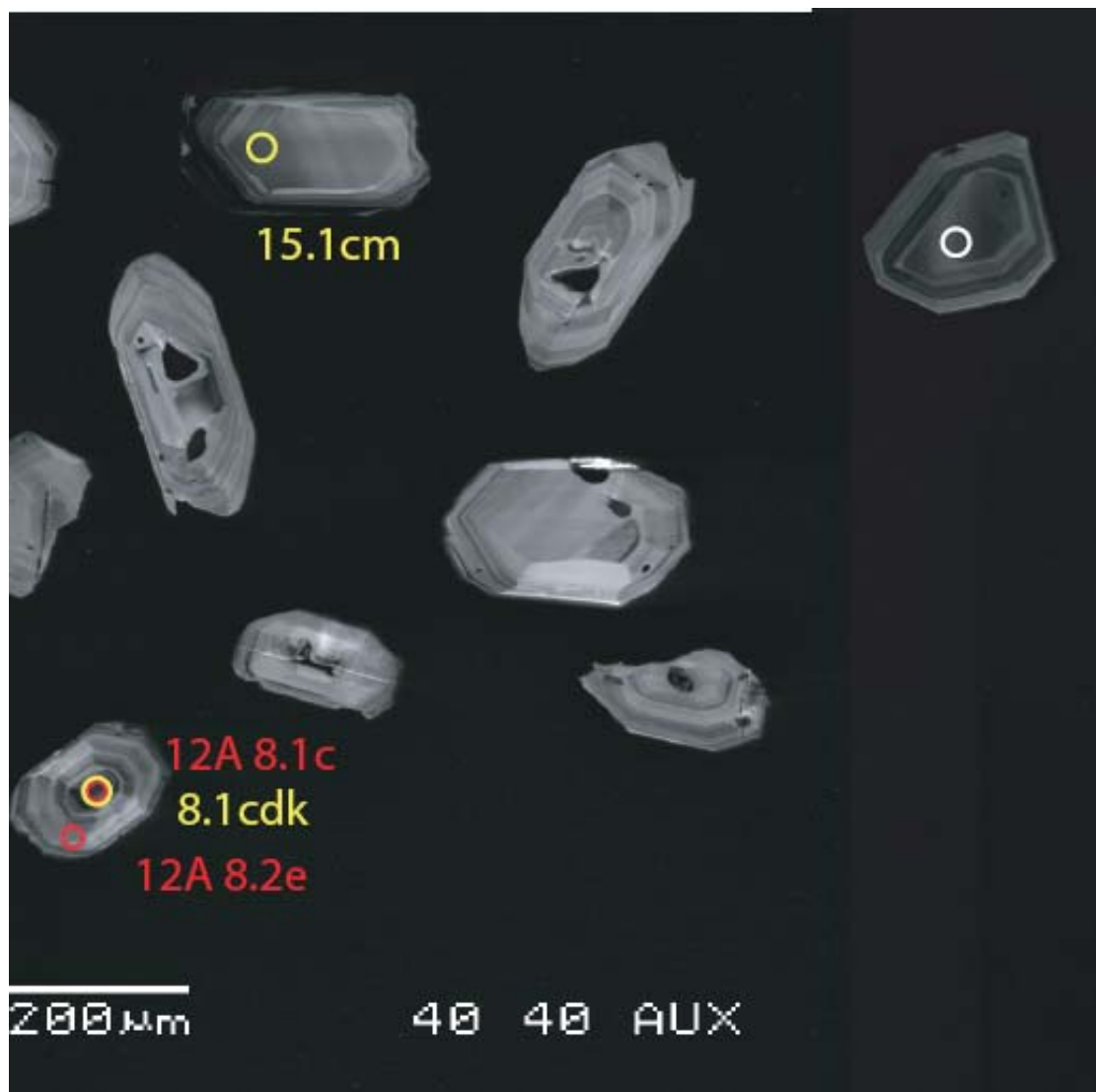












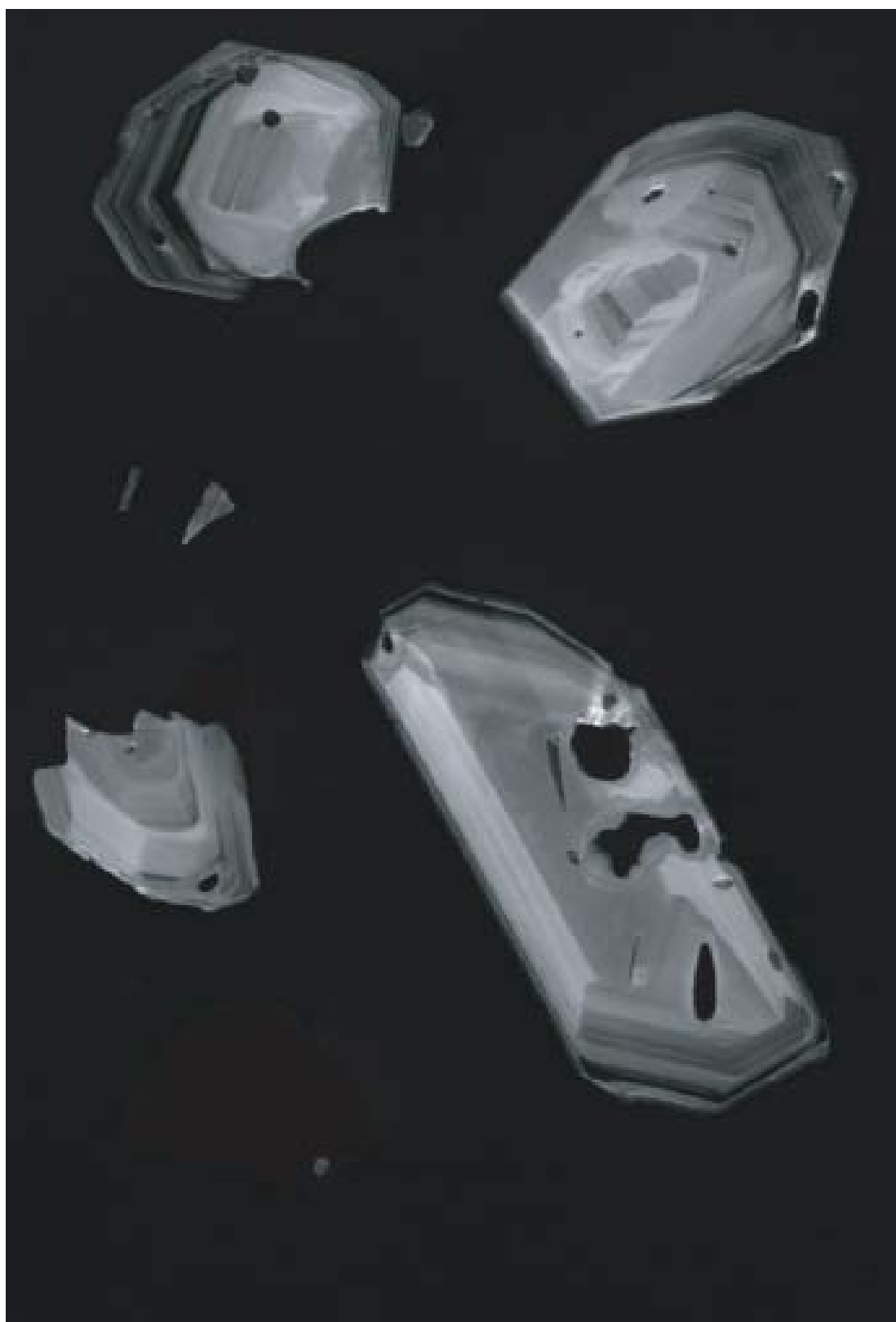
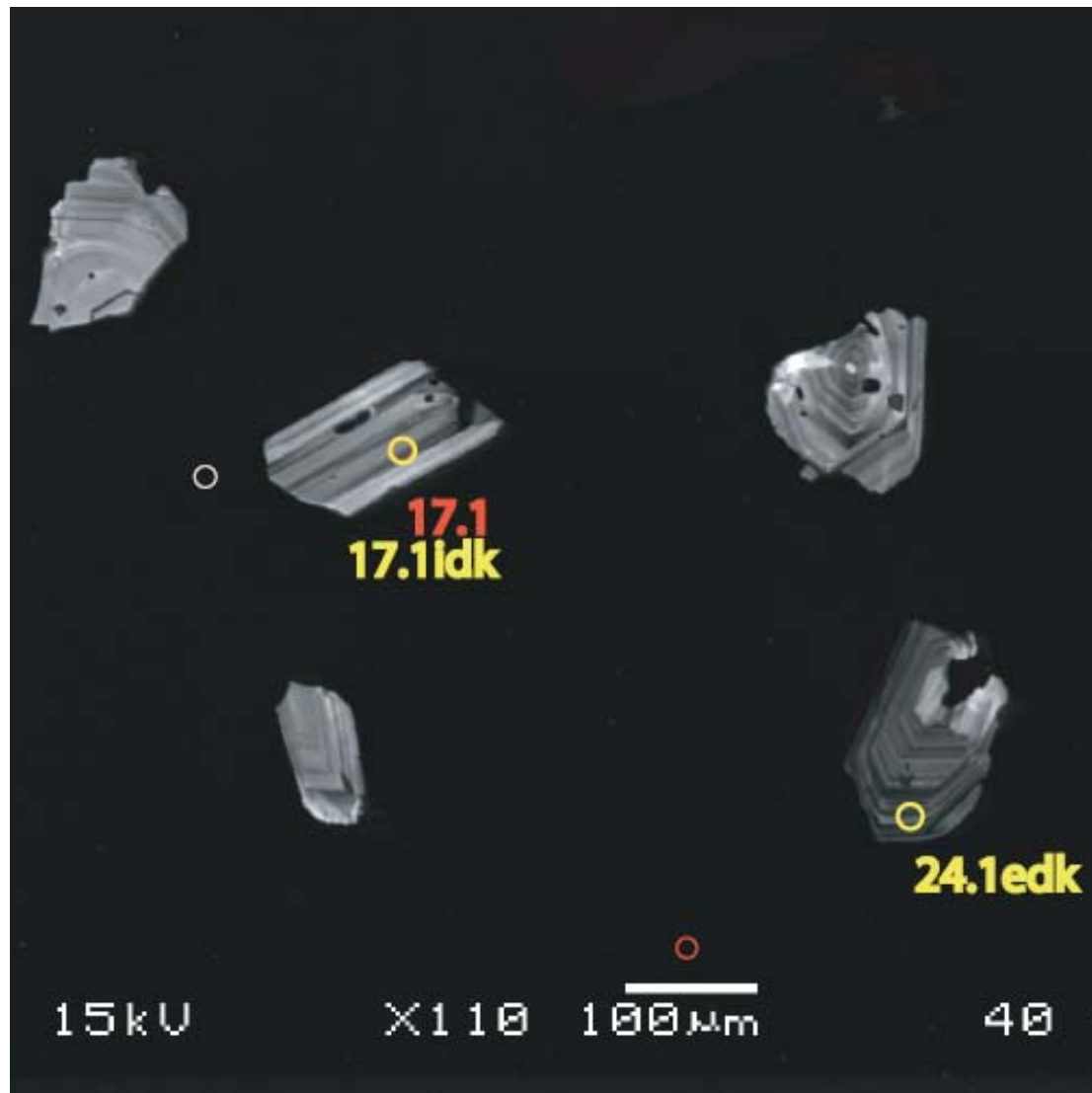
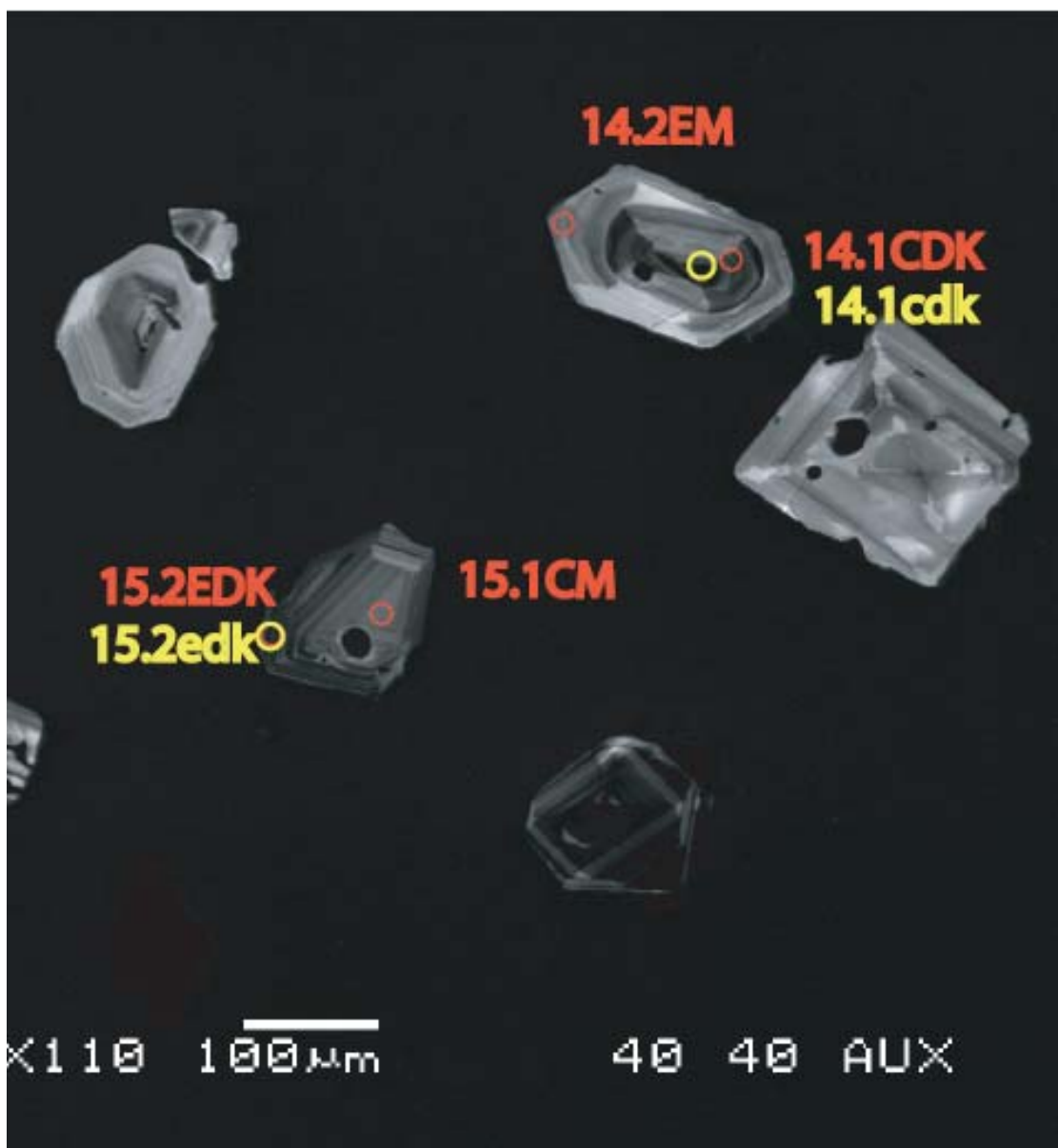


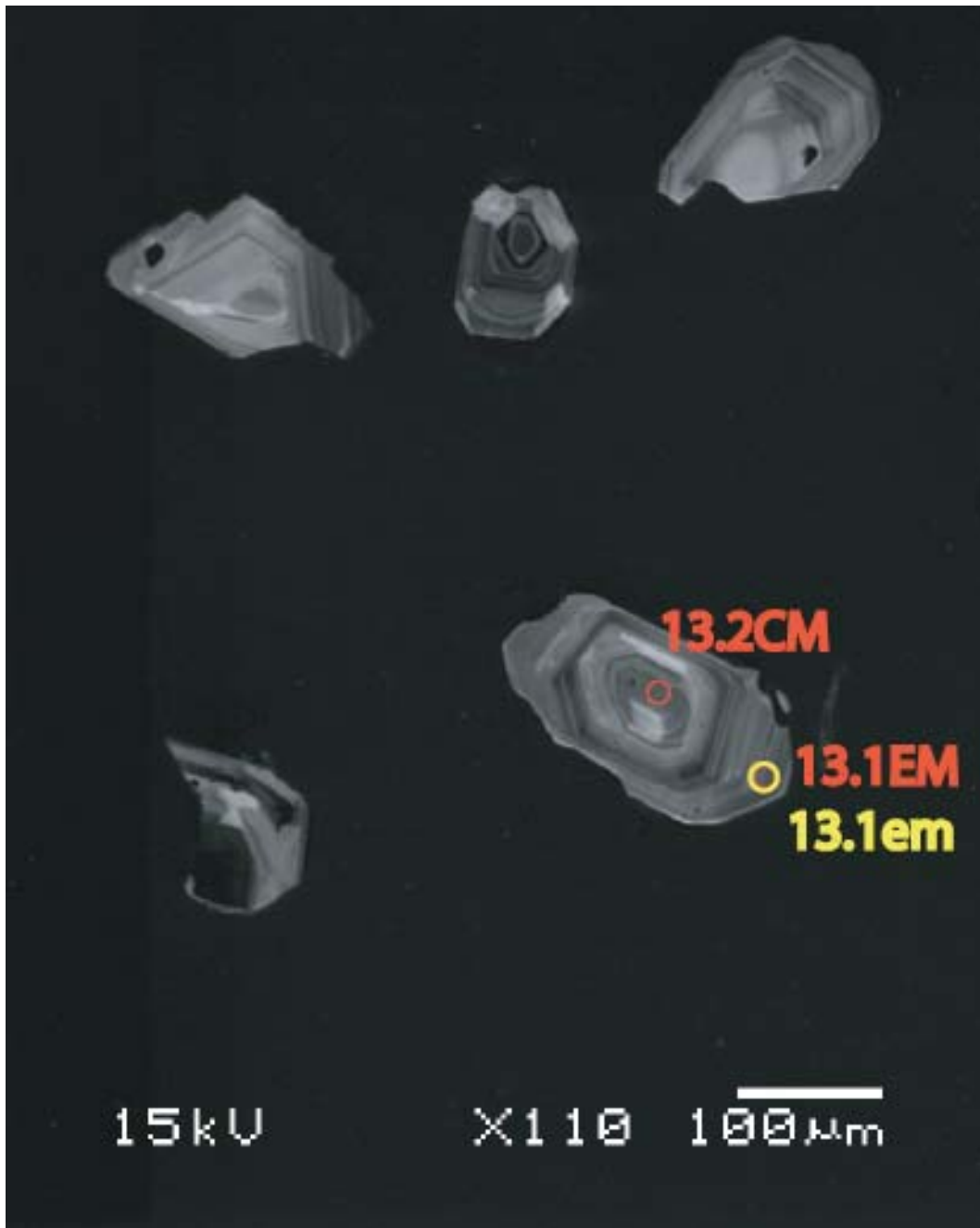
Figure C3:

Cathodoluminescence images of zircons from sampl HRL 14a with spots from U-Pb (yellow) and trace elements (red) SHRIMP-RG analysis marked.

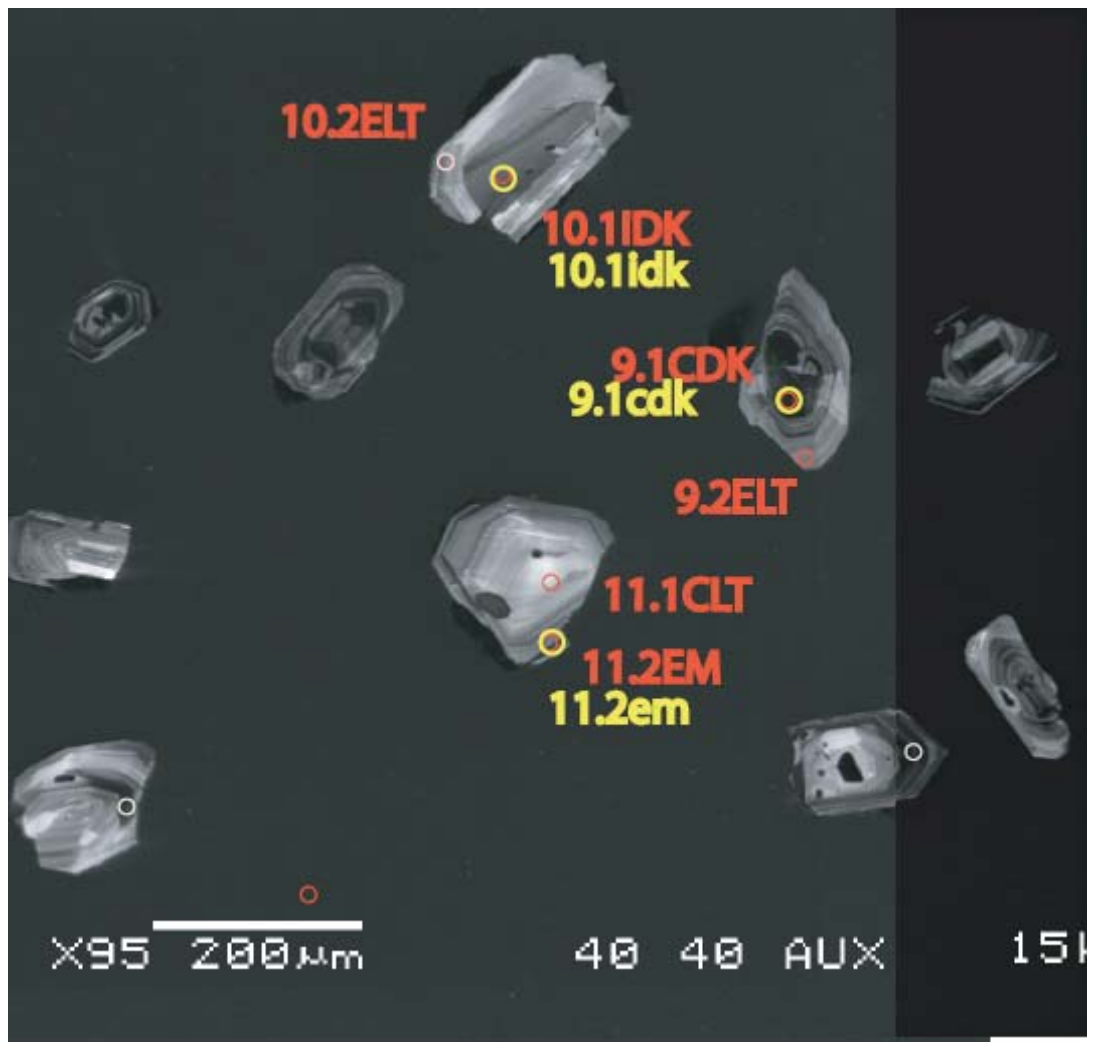


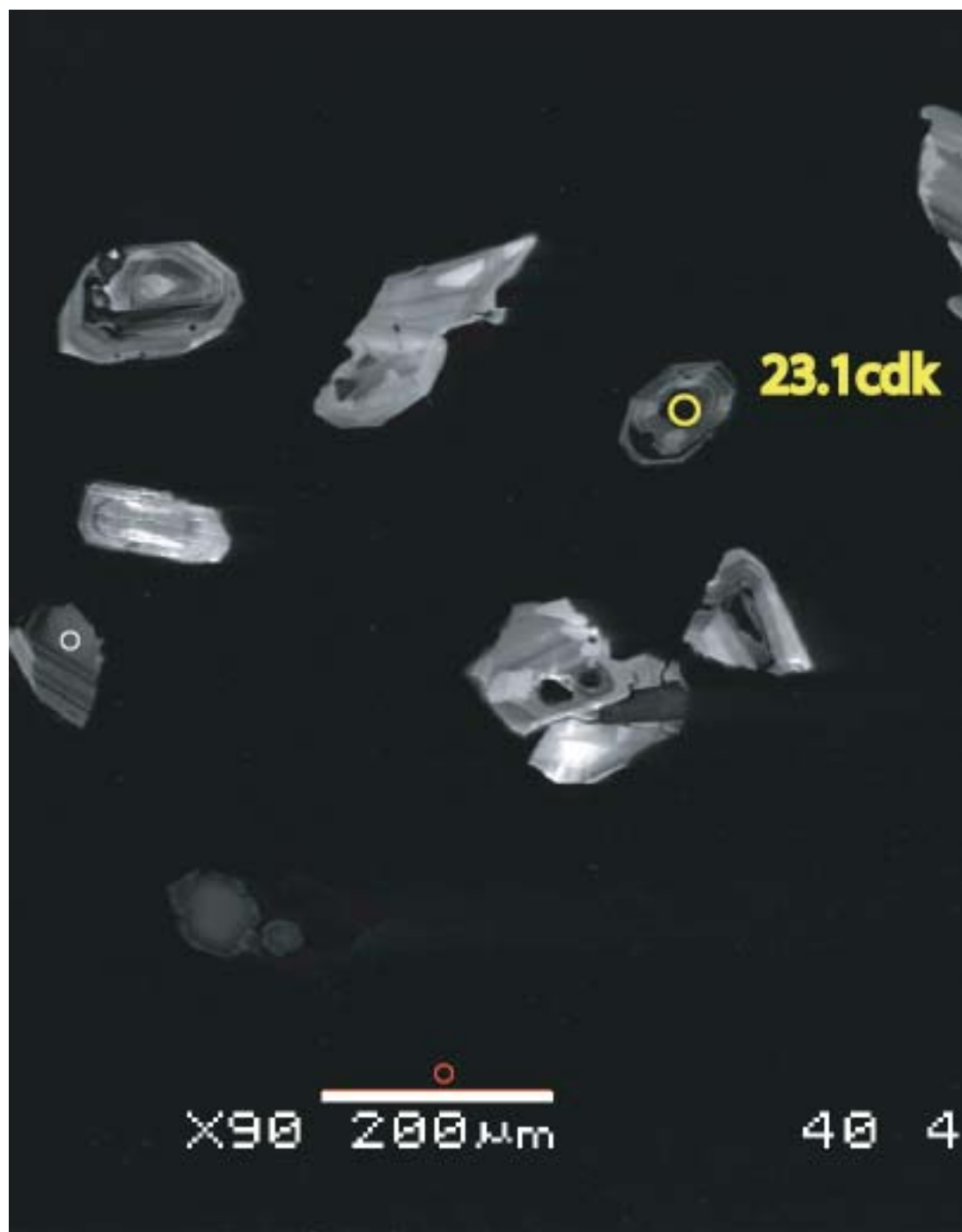






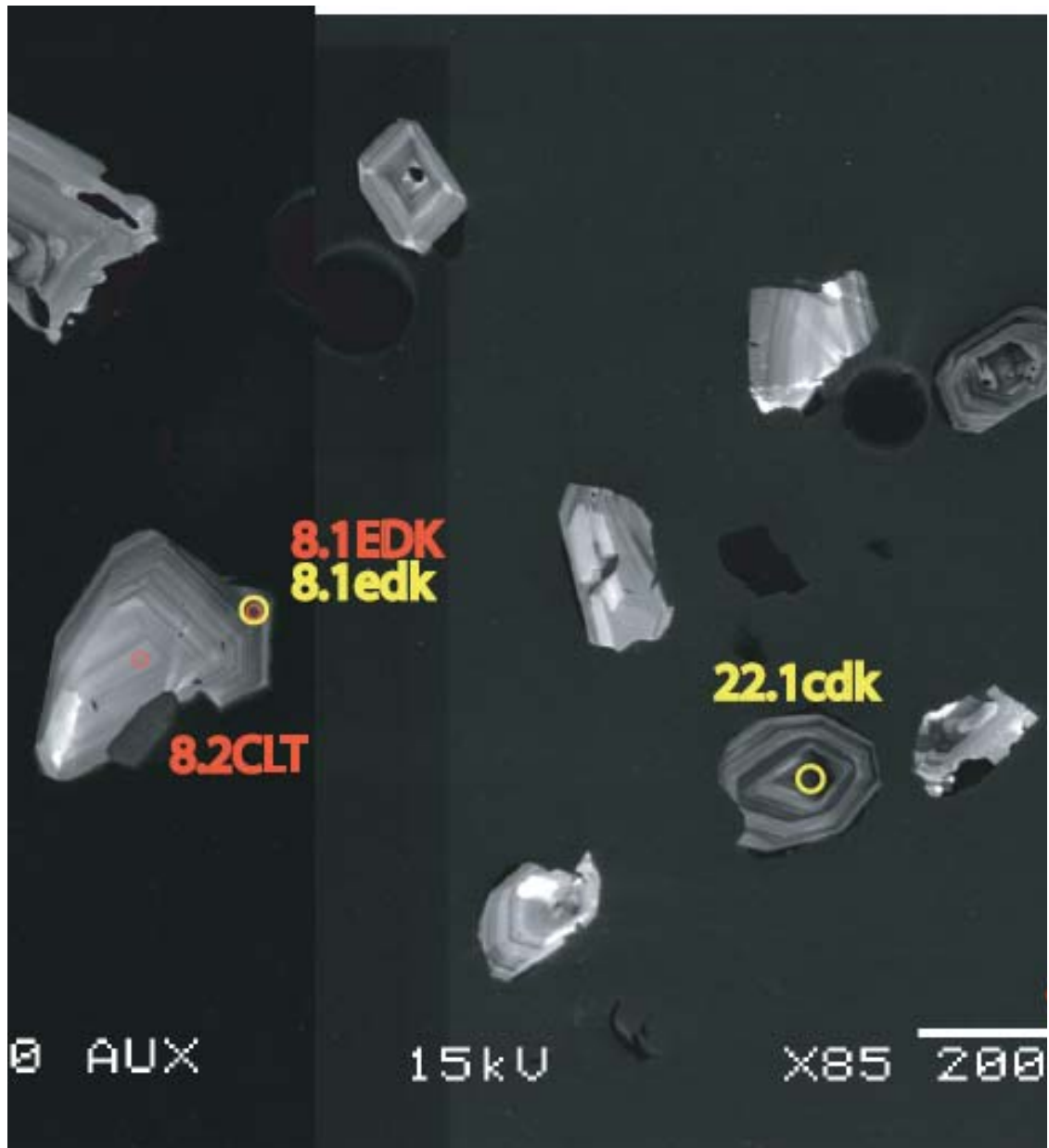




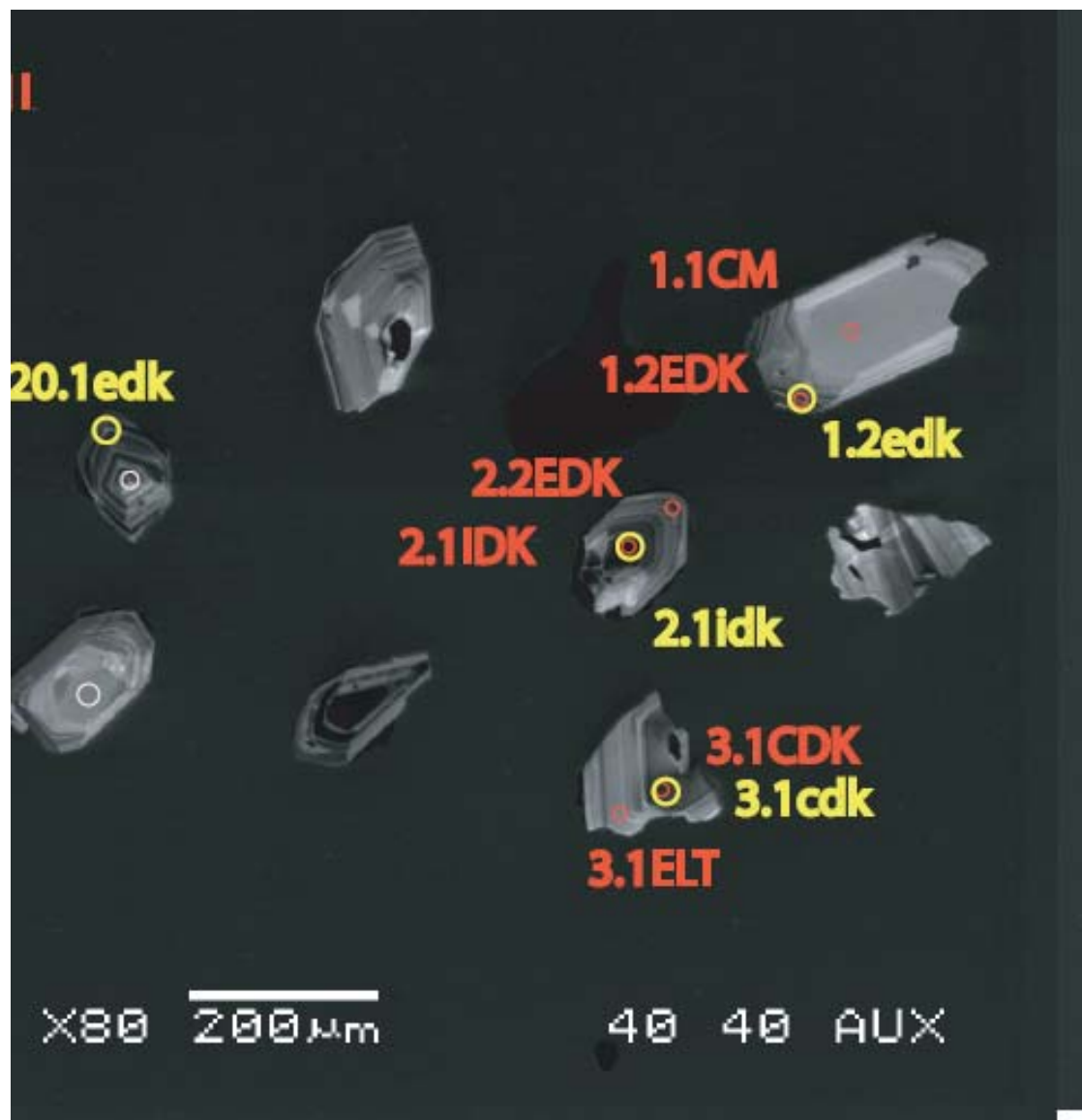


×90 200 μ m

40 4







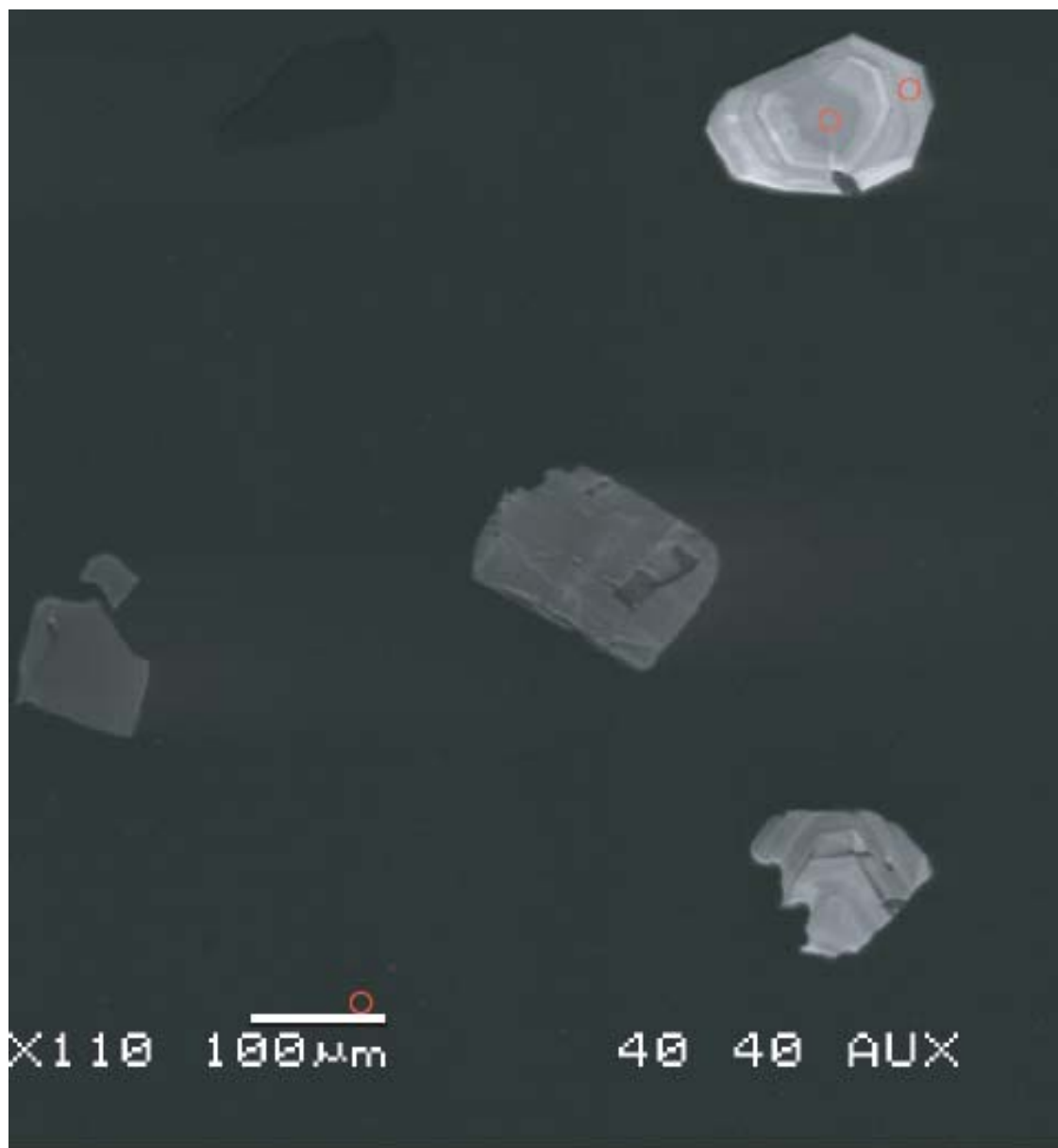
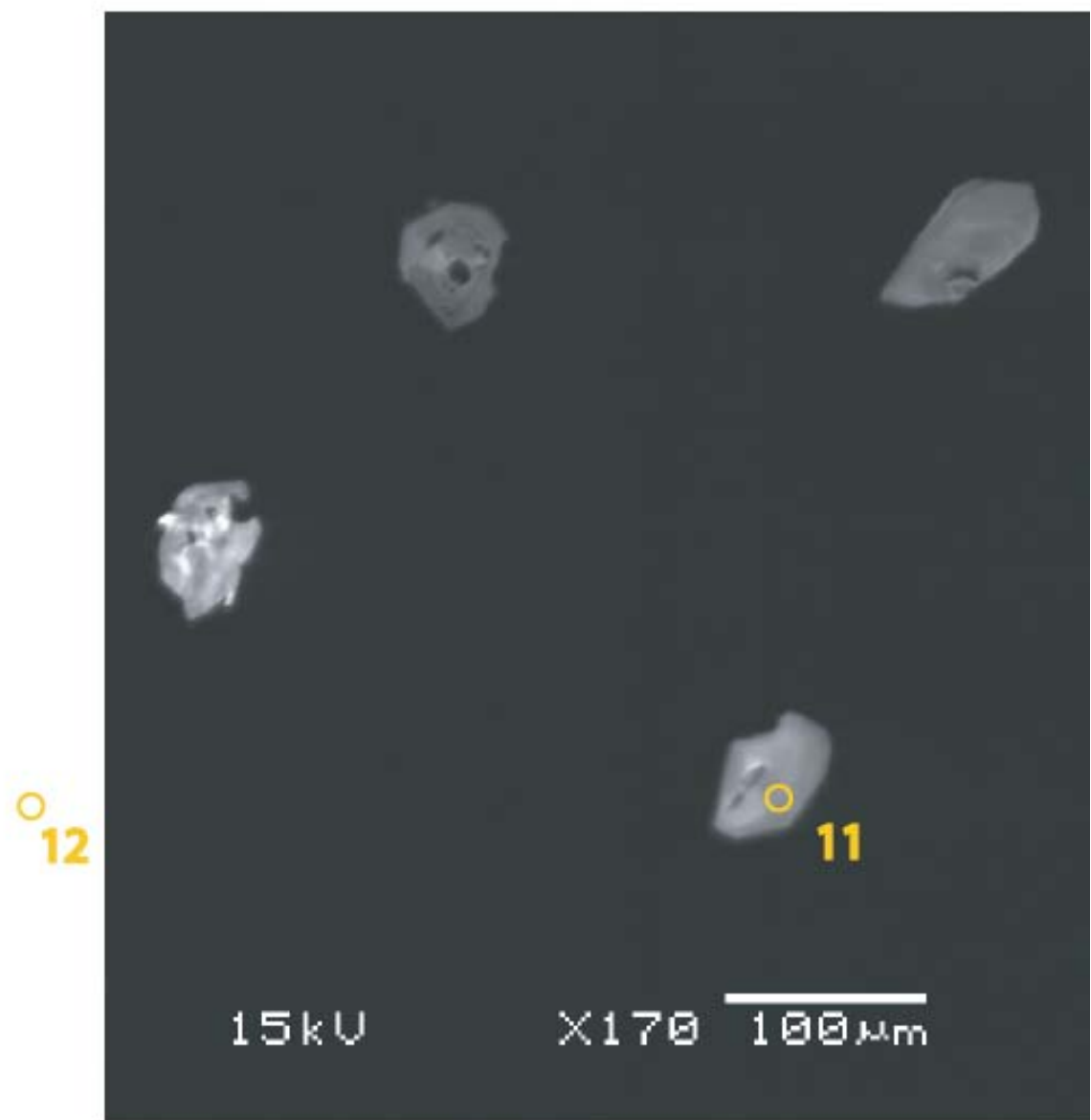
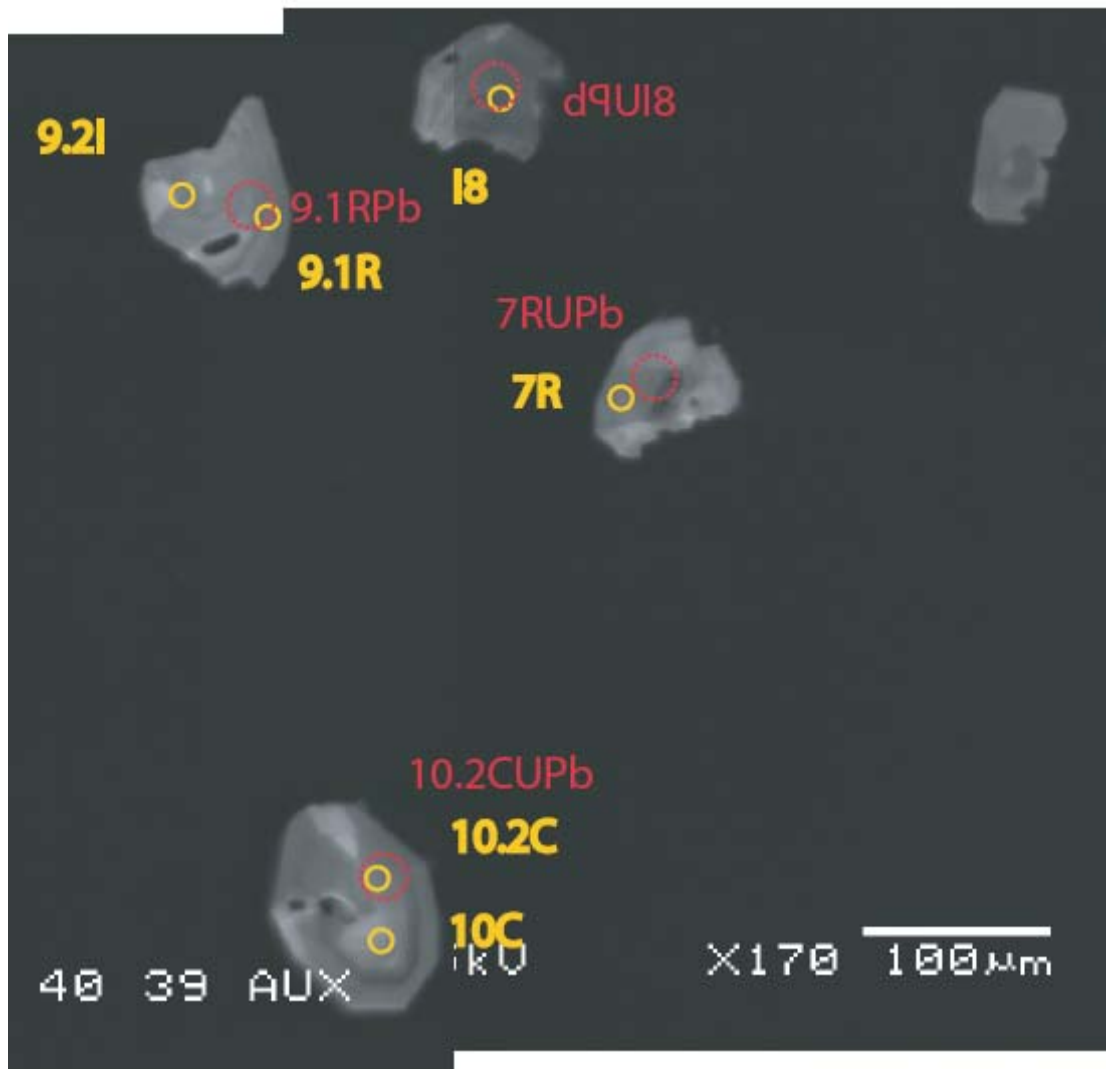


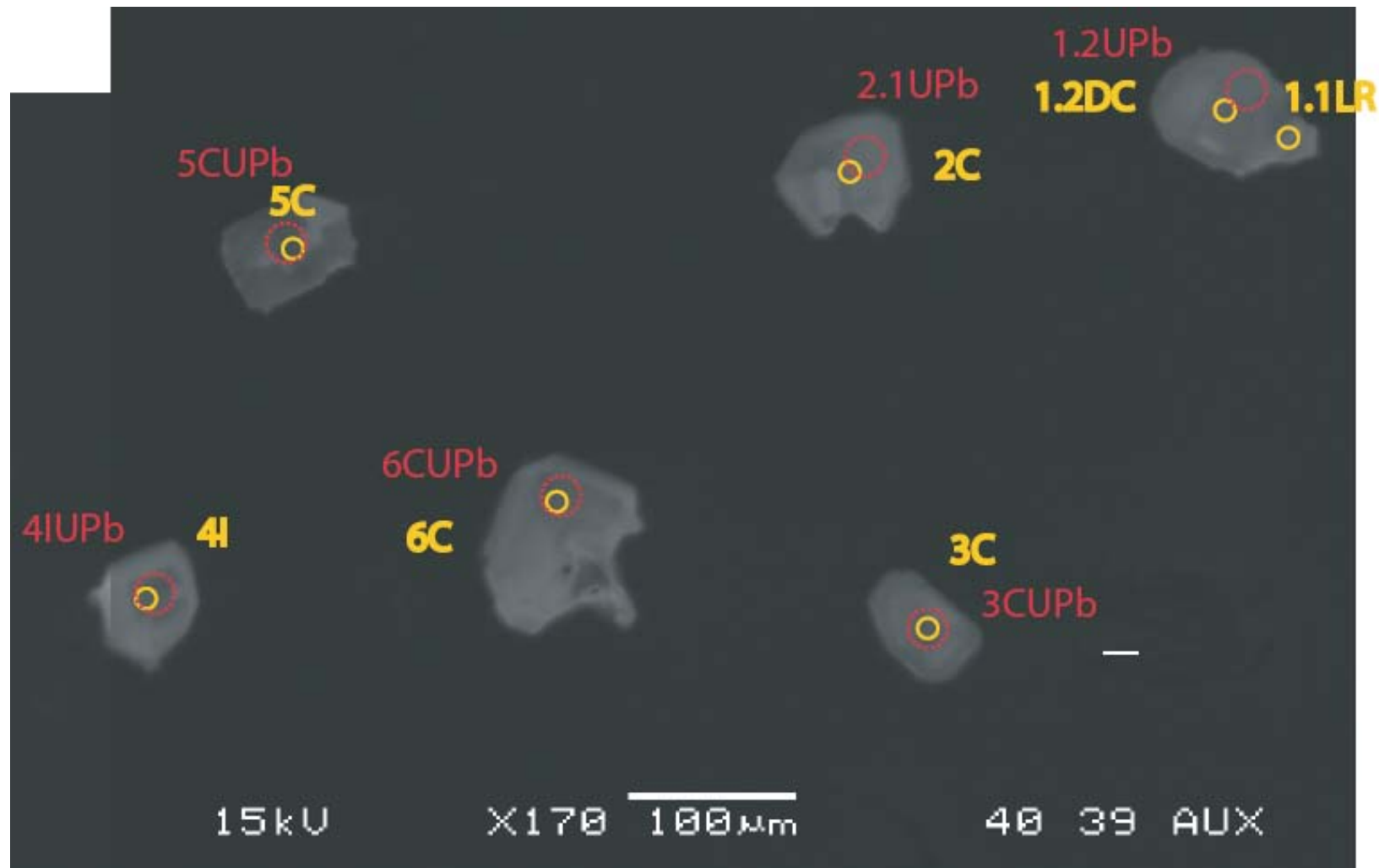
Figure C4:

Cathodoluminescence images of zircons from sampl HRL 27 with spots from U-Pb (yellow) and trace elements (red) SHRIMP-RG analysis marked.





210



APPENDIX D:
Zircon Elemental Data
from the Highland Range Silicic Sequence

Table D1: Trace element data from SHRIMP-RG analysis of zircons from sample HRL 12a of the Highland Range silicic sequence.

Sample Spot	Li ppm Est.	Be9 ppm	B11 ppm	F19 ppm	Na ppm Est.	Mg ppm Est.	Al27 ppm Est.	P31 ppm	S32 Rel.	K39 Rel.
HRL12A-1.1C	0.010	32.91	0.1	24	4.9	1.3	11	242	0.4	1.7
HRL12A-1.2E	0.028	15.33	0.1	19	3.1	2.0	17	264	2.6	8.2
HRL12A-2.1E	0.014	4.44	0.2	16	4.8	1.3	10	255	1.2	1.7
HRL12A-2.2idk	0.005	13.58	0.1	17	4.5	1.0	8	284	0.6	1.5
HRL12A-2.3ilt	0.007	2.16	0.1	18	5.0	1.0	8	303	1.6	1.6
HRL12A-2.4c	0.008	155.61	0.2	22	4.4	1.1	8	669	0.6	1.3
HRL12A-3.1edk	0.005	17.04	0.1	15	4.9	1.6	8	427	2.4	1.4
HRL12A-3.2idk	0.008	38.18	0.1	15	4.3	1.1	8	333	0.6	1.5
HRL12A-3.3e	0.000	3.55	0.1	17	4.8	1.4	8	203	1.4	1.4
HRL12A-4.1ilt	0.005	4.73	0.1	23	5.6	1.2	8	246	0.4	1.7
HRL12A-5.1c	0.028	58.64	0.2	25	8.0	2.7	13	290	1.5	2.5
HRL12A-5.1elt	0.011	5.35	0.1	20	4.6	1.4	9	233	0.8	1.5
HRL12A-6.1cdk	0.025	42.83	0.2	30	5.8	2.0	10	377	0.8	1.6
HRL12A-6.2ilt	0.183	0.53	0.1	22	5.8	1.7	10	594	0.8	1.8
HRL12A-7.1c	0.040	69.13	0.2	22	5.6	2.7	9	265	0.6	1.7
HRL12A-7.2i	0.012	4.33	0.2	13	4.9	1.3	7	218	0.2	1.6
HRL12A-8.1c	0.037	98.18	0.1	26	6.8	1.6	11	448	1.2	1.9
HRL12A-8.2e	0.020	18.58	0.2	20	5.3	1.8	7	299	1.3	1.9
HRL12A-9.1c	0.021	142.33	0.2	34	6.5	2.0	12	549	0.2	1.9
HRL12A-9.2i	0.018	4.47	0.2	21	5.8	1.9	9	222	1.0	1.5
HRL12A-9.3e	0.015	6.83	0.2	18	4.7	1.4	9	268	0.2	1.6
HRL12A-10.1c	0.021	80.99	0.1	20	6.1	1.7	9	391	0.8	1.8
12A-10.2i	0.019	9.94	0.3	27	6.4	1.6	10	269	0.2	1.6
12A-11.1e	1.164	12.30	0.3	17	34.6	2.8	196	209	1.0	159.5
12A-11.2i	0.016	13.51	0.1	19	5.6	1.7	7	278	1.4	1.4
12A-11.3i	0.020	102.77	0.1	18	5.7	2.2	7	364	0.0	1.6
12A-12.1i	0.014	12.54	0.2	95	6.9	2.0	10	530	1.6	1.6
12A-12.2C	0.028	7.64	0.2	27	7.2	1.9	10	239	0.2	1.8
12A-13.1C	0.130	48.33	0.2	294	12.0	2.2	10	1235	2.2	2.1
12A-13.2e	0.024	2.31	0.1	23	8.5	3.4	59	406	0.6	51.5
12A-14.1idk	0.018	3.58	0.2	24	5.2	1.5	8	166	1.0	1.8
HRL12A14.2ilt	0.026	2.70	0.1	27	5.8	1.3	9	349	0.2	1.6
HRL12A14.3edk	0.023	20.63	0.3	22	5.6	1.5	7	171	0.7	1.7

Table D1, continued

Sample Spot	Ca40 ppm Est.	Sc45 ppm	48/49	Ti48 ppm	Ti49 ppm	V51 ppm REL.	Cr Rel.	Mn Rel.	Fe56 ppm	Ge74 Rel.
HRL12A-1.1C	3.4	33	13.8	13.9	13.0	0.54	0.11	0.05	0.9	0.4
HRL12A-1.2E	2.1	57	13.7	12.0	11.3	1.01	0.07	0.05	6.8	0.4
HRL12A-2.1E	3.3	35	13.0	16.3	16.3	0.26	0.07	0.06	1.0	0.1
HRL12A-2.2idk	2.9	34	13.2	11.5	11.3	0.40	0.05	0.05	1.0	0.4
HRL12A-2.3ilt	3.0	48	13.4	21.8	21.1	0.72	0.09	0.05	0.8	0.2
HRL12A-2.4c	2.6	83	13.7	16.1	15.2	2.20	0.07	0.04	0.8	0.2
HRL12A-3.1edk	3.0	39	12.3	10.9	11.5	0.54	0.07	0.04	1.1	0.4
HRL12A-3.2idk	3.2	61	13.2	10.1	9.9	0.27	0.07	0.04	1.0	0.2
HRL12A-3.3e	2.6	33	12.3	8.0	8.4	0.28	0.09	0.05	1.0	0.2
HRL12A-4.1ilt	3.1	41	13.6	16.7	15.8	0.49	0.10	0.06	0.9	0.5
HRL12A-5.1c	4.7	36	13.1	18.3	18.1	0.79	0.10	0.07	1.7	0.3
HRL12A-5.1elt	2.9	33	14.8	12.0	10.5	0.49	0.08	0.05	1.0	0.1
HRL12A-6.1cdk	3.3	37	13.3	6.9	6.7	0.31	0.06	0.05	1.1	0.4
HRL12A-6.2ilt	3.3	47	12.5	7.4	7.7	0.09	0.05	0.07	1.6	0.5
HRL12A-7.1c	3.7	32	13.7	6.8	6.4	0.37	0.06	0.06	1.5	0.2
HRL12A-7.2i	2.9	40	12.9	14.7	14.7	0.22	0.07	0.05	1.0	0.2
HRL12A-8.1c	3.6	71	14.0	6.4	6.0	0.76	0.09	0.11	5.1	0.1
HRL12A-8.2e	3.4	51	14.0	8.9	8.2	0.35	0.08	0.06	1.2	0.4
HRL12A-9.1c	3.4	49	13.4	10.9	10.5	0.69	0.07	0.04	1.7	0.2
HRL12A-9.2i	3.6	40	14.3	12.4	11.2	0.45	0.09	0.04	1.1	0.3
HRL12A-9.3e	2.6	28	14.0	7.4	6.8	0.07	0.04	0.05	1.1	0.3
HRL12A-10.1c	3.0	32	13.5	7.8	7.5	0.77	0.08	0.04	1.3	0.1
12A-10.2i	3.3	60	14.0	15.5	14.4	0.39	0.08	0.06	1.1	0.1
12A-11.1e	4.9	25	13.5	8.0	7.7	0.22	0.12	0.22	7.4	0.1
12A-11.2i	3.1	47	12.2	10.5	11.2	0.54	0.07	0.05	1.1	0.3
12A-11.3i	3.2	48	12.6	13.5	13.9	0.58	0.08	0.07	1.2	0.3
12A-12.1i	87.6	62	13.6	12.2	11.6	0.30	0.11	0.22	2.2	0.5
12A-12.2C	3.7	39	13.9	16.8	15.6	0.37	0.10	0.03	1.1	0.3
12A-13.1C	416.0	50	13.4	13.9	13.5	1.30	0.08	1.22	4.5	0.2
12A-13.2e	6.4	36	13.2	14.6	14.2	124.69	0.06	7.93	28.3	0.3
12A-14.1idk	3.1	26	14.5	10.3	9.1	0.07	0.05	0.05	1.0	0.1
HRL12A14.2ilt	3.0	54	13.0	35.4	35.2	0.30	0.08	0.04	0.8	0.3
HRL12A14.3edk	3.1	51	14.4	6.1	5.5	0.15	0.04	0.04	1.1	0.4

Table D1, continued

Sample Spot	Y89 ppm	Nb93 ppm	Zr94H Rel.	Zr96/Si30 ppm	Zr96/ Zr2O	196/ Si30	Hf ppm	Pb7/6 Est,	Th ppm	U ppm
HRL12A-1.1C	1432	2	1.3	1.97	134	68	8370	0.4167	140	62
HRL12A-1.2E	1362	21	1.9	2.05	97	48	9677	0.0000	183	185
HRL12A-2.1E	771	5	1.5	2.02	118	58	8191	0.0000	144	73
HRL12A-2.2idk	1121	8	1.3	1.99	120	60	9460	0.0000	212	140
HRL12A-2.3ilt	862	4	1.4	2.02	123	61	8478	0.4167	162	84
HRL12A-2.4c	5811	21	1.4	1.97	120	61	7885	0.2469	1383	419
HRL12A-3.1edk	1466	13	1.4	2.01	128	64	9422	0.1639	616	285
HRL12A-3.2idk	1732	19	1.4	2.02	124	61	9744	0.2000	468	290
HRL12A-3.3e	647	5	1.3	1.97	127	65	9261	0.0000	76	60
HRL12A-4.1ilt	1756	3	1.3	1.98	120	61	8232	0.5263	208	82
HRL12A-5.1c	2134	4	1.3	2.00	126	63	8187	0.0000	326	119
HRL12A-5.1elt	673	4	1.4	2.00	130	65	9041	0.5882	68	49
HRL12A-6.1cdk	3098	13	1.4	1.98	127	64	10611	0.0000	538	310
HRL12A-6.2ilt	1119	9	1.3	2.01	120	60	10241	0.2632	203	192
HRL12A-7.1c	2141	7	1.3	1.98	125	63	9976	0.2381	409	225
HRL12A-7.2i	634	4	1.4	1.98	120	60	8355	0.0000	60	41
HRL12A-8.1c	2779	28	1.4	2.01	125	62	11981	0.2459	1123	680
HRL12A-8.2e	1303	18	1.4	2.00	125	63	10279	0.0000	196	187
HRL12A-9.1c	4758	18	1.3	1.97	134	68	9130	0.0000	797	333
HRL12A-9.2i	825	5	1.3	2.00	120	60	9158	0.0000	132	91
HRL12A-9.3e	1102	13	1.5	1.96	118	60	10262	0.0000	383	270
HRL12A-10.1c	2600	10	1.3	1.96	131	67	9989	0.0000	484	263
12A-10.2i	965	7	1.3	1.99	125	63	8420	0.2778	110	84
12A-11.1e	705	10	1.4	1.94	124	64	10917	0.0000	101	106
12A-11.2i	1072	9	1.3	2.02	126	62	9449	0.3846	132	115
12A-11.3i	2626	8	1.3	1.97	125	64	8712	0.0000	407	170
12A-12.1i	1502	15	1.5	2.02	130	64	9922	0.0000	215	183
12A-12.2C	1343	2	1.3	2.03	130	64	9192	0.8333	138	60
12A-13.1C	1968	7	1.3	2.03	133	65	9132	0.6250	304	143
12A-13.2e	904	6	1.5	2.04	120	59	9867	0.3529	107	89
12A-14.1idk	547	4	1.4	2.04	128	63	9361	0.0000	51	43
HRL12A14.2ilt	777	3	1.3	2.01	137	68	7315	1.5385	119	59
HRL12A14.3edk	940	12	1.2	1.99	145	73	10920	0.0000	356	293

Table D1, continued

Sample Spot	Y/Nb	Th/U	Yb/Gd	Yb/Nd	U/Yb	Th/Yb	Ce/Sm	Ce/Lu	U/Ce	Th/Ce
HRL12A-1.1C	697	2.23	7.6	100	0.2	0.4	11.3	1.21	0.8	1.8
HRL12A-1.2E	64	0.99	20.5	298	0.4	0.4	48.2	1.65	1.4	1.4
HRL12A-2.1E	164	1.98	11.8	131	0.3	0.7	26.5	2.15	0.9	1.7
HRL12A-2.2idk	140	1.51	12.4	193	0.4	0.6	30.2	1.78	1.4	2.0
HRL12A-2.3ilt	245	1.95	10.2	138	0.3	0.6	21.0	1.88	1.0	1.9
HRL12A-2.4c	275	3.30	6.5	76	0.3	1.0	14.0	2.01	0.9	2.9
HRL12A-3.1edk	109	2.16	12.2	232	0.7	1.5	28.9	1.85	2.2	4.8
HRL12A-3.2idk	91	1.61	18.6	407	0.5	0.8	41.3	1.44	1.9	3.1
HRL12A-3.3e	127	1.26	15.8	390	0.3	0.3	27.5	1.15	1.2	1.5
HRL12A-4.1ilt	608	2.53	7.8	80	0.2	0.4	8.9	1.03	1.0	2.4
HRL12A-5.1c	608	2.74	7.1	69	0.2	0.5	9.6	1.18	1.0	2.7
HRL12A-5.1elt	181	1.39	14.2	366	0.2	0.3	33.9	1.31	0.9	1.2
HRL12A-6.1cdk	232	1.74	11.2	184	0.4	0.7	13.8	0.92	2.4	4.2
HRL12A-6.2ilt	128	1.06	18.9	607	0.5	0.5	25.0	0.73	3.5	3.7
HRL12A-7.1c	292	1.82	12.5	203	0.3	0.6	14.3	0.80	2.4	4.3
HRL12A-7.2i	179	1.46	12.3	201	0.2	0.3	29.3	1.44	0.8	1.1
HRL12A-8.1c	100	1.65	27.2	414	0.7	1.1	39.9	0.85	4.3	7.0
HRL12A-8.2e	73	1.05	21.1	599	0.4	0.4	39.0	0.99	2.2	2.3
HRL12A-9.1c	262	2.39	7.2	129	0.3	0.7	11.8	1.25	1.4	3.4
HRL12A-9.2i	165	1.45	12.7	251	0.3	0.5	28.8	1.55	1.2	1.7
HRL12A-9.3e	88	1.42	15.7	374	0.8	1.1	36.2	1.40	3.0	4.3
HRL12A-10.1c	252	1.84	10.9	196	0.4	0.7	12.0	0.87	2.4	4.4
12A-10.2i	145	1.31	13.1	230	0.3	0.3	25.4	1.17	1.1	1.4
12A-11.1e	74	0.95	23.9	807	0.4	0.4	36.3	0.99	2.2	2.1
12A-11.2i	119	1.14	16.9	427	0.3	0.4	29.9	1.10	1.5	1.7
12A-11.3i	338	2.40	7.9	105	0.2	0.6	12.6	1.27	1.1	2.6
12A-12.1i	98	1.18	17.1	115	0.4	0.4	35.0	1.27	1.6	1.8
12A-12.2C	662	2.30	7.7	97	0.2	0.4	12.3	1.27	0.7	1.7
12A-13.1C	282	2.13	9.4	43	0.2	0.5	17.2	1.31	1.1	2.2
12A-13.2e	146	1.21	8.9	24	0.3	0.4	76.5	9.80	0.2	0.2
12A-14.1idk	128	1.18	16.1	418	0.2	0.3	36.5	1.47	0.9	1.0
HRL12A14.2ilt	307	2.03	9.0	100	0.3	0.5	15.6	1.33	1.1	2.2
HRL12A14.3edk	77	1.22	25.6	768	0.7	0.9	51.6	1.01	3.6	4.4

Table D1, continued

Sample Spot	Y/Yb	Y/Nb	Yb/Nb	Yb/Sc	Yb/Dy	Dy/Sm	Yb/Nd	Sm/Nd	U/Li
HRL12A-1.1C	4.0	697	175.9	11.0	2.31	22.9	100	1.9	6134
HRL12A-1.2E	3.3	64	19.7	7.3	4.06	37.5	298	2.0	6539
HRL12A-2.1E	3.5	164	47.0	6.3	3.16	21.6	131	1.9	5166
HRL12A-2.2idk	3.4	140	40.9	9.5	3.10	30.8	193	2.0	27173
HRL12A-2.3ilt	3.4	245	72.9	5.4	2.80	22.4	138	2.2	12509
HRL12A-2.4c	4.1	275	66.3	16.8	2.10	19.7	76	1.9	53918
HRL12A-3.1edk	3.6	109	30.4	10.5	2.86	31.8	232	2.5	55010
HRL12A-3.2idk	3.0	91	30.1	9.4	3.74	41.7	407	2.6	38159
HRL12A-3.3e	2.8	127	45.1	6.9	3.94	32.9	390	3.0	
HRL12A-4.1ilt	3.6	608	167.7	11.9	2.45	20.5	80	1.6	15408
HRL12A-5.1c	3.5	608	171.5	16.7	2.39	20.2	69	1.4	4289
HRL12A-5.1elt	3.0	181	59.9	6.7	3.65	36.9	366	2.7	4250
HRL12A-6.1cdk	3.8	232	61.7	22.4	2.86	31.0	184	2.1	12303
HRL12A-6.2ilt	2.8	128	45.2	8.4	4.23	42.7	607	3.4	1048
HRL12A-7.1c	3.2	292	91.4	20.7	3.09	32.9	203	2.0	5691
HRL12A-7.2i	3.3	179	54.2	4.8	2.98	34.8	201	1.9	3305
HRL12A-8.1c	2.7	100	36.6	14.3	5.13	49.5	414	1.6	18408
HRL12A-8.2e	2.8	73	25.9	9.0	4.05	51.7	599	2.9	9374
HRL12A-9.1c	4.2	262	61.8	22.9	1.99	28.6	129	2.3	15942
HRL12A-9.2i	3.1	165	54.0	6.7	3.35	30.1	251	2.5	5134
HRL12A-9.3e	3.2	88	27.9	12.4	3.30	42.6	374	2.7	18345
HRL12A-10.1c	3.5	252	71.6	23.3	2.64	30.7	196	2.4	12420
12A-10.2i	2.9	145	50.4	5.5	3.67	30.3	230	2.1	4513
12A-11.1e	2.7	74	27.5	10.4	4.03	49.9	807	4.0	91
12A-11.2i	2.9	119	41.3	7.8	3.84	36.5	427	3.0	7320
12A-11.3i	3.8	338	88.9	14.2	2.40	23.4	105	1.9	8657
12A-12.1i	3.0	98	32.1	8.0	3.63	40.8	115	0.8	12901
12A-12.2C	3.7	662	178.1	9.3	2.38	23.0	97	1.8	2156
12A-13.1C	3.4	282	82.3	11.6	2.77	26.1	43	0.6	1103
12A-13.2e	3.4	146	43.6	7.4	2.99	13.9	24	0.6	3650
12A-14.1idk	3.1	128	41.1	6.7	3.61	36.6	418	3.2	2445
HRL12A14.2ilt	3.5	307	88.4	4.2	2.97	21.4	100	1.6	2287
HRL12A14.3edk	2.4	77	32.7	7.8	4.90	52.3	768	3.0	12936

Table D1, continued

Sample Spot	La139 ppm	Ce140 ppm	Pr141 ppm	Nd146 ppm	Sm147 ppm	Eu153 ppm	Ho165 ppm	GdO173 ppm	TbO175 ppm	DyO179 ppm	ErO182 ppm	TmO185 ppm	YbO188 ppm	LuO191 ppm
HRL12A-1.1C	0.029	78	0.139	3.63	6.85	2.253	58	48	14.62	157	232	47	362	64
HRL12A-1.2E	0.171	132	0.237	1.41	2.75	0.732	49	20	7.99	103	221	50	419	80
HRL12A-2.1E	0.027	86	0.194	1.69	3.23	0.961	30	19	6.73	70	124	28	221	40
HRL12A-2.2idk	0.012	103	0.173	1.70	3.42	1.160	44	26	9.55	105	198	41	327	58
HRL12A-2.3ilt	0.010	86	0.157	1.86	4.10	1.524	35	25	8.24	92	150	31	256	46
HRL12A-2.4c	0.197	475	1.055	18.34	34.00	10.507	242	215	65.98	668	955	186	1401	237
HRL12A-3.1edk	0.015	129	0.120	1.76	4.48	1.210	59	34	11.76	143	248	52	408	70
HRL12A-3.2idk	0.005	152	0.149	1.41	3.67	1.214	65	31	12.11	153	302	68	573	105
HRL12A-3.3e	0.007	49	0.129	0.59	1.78	0.559	25	15	4.72	58	121	26	230	42
HRL12A-4.1ilt	0.053	86	0.481	6.03	9.67	3.127	72	62	18.46	198	301	60	485	83
HRL12A-5.1c	0.098	120	0.540	8.69	12.50	4.788	89	85	25.55	252	372	75	602	102
HRL12A-5.1elt	0.010	56	0.171	0.61	1.66	0.660	26	16	5.48	61	120	26	223	43
HRL12A-6.1cdk	0.026	128	0.243	4.48	9.29	2.389	117	74	24.83	288	503	103	824	140
HRL12A-6.2ilt	0.027	55	0.117	0.65	2.19	0.592	40	21	7.88	93	202	46	395	75
HRL12A-7.1c	0.029	94	0.193	3.30	6.58	2.099	85	54	19.20	217	398	83	669	118
HRL12A-7.2i	0.014	54	0.115	0.96	1.86	0.796	25	16	5.79	65	108	23	192	38
HRL12A-8.1c	0.160	160	0.182	2.45	4.00	0.890	91	37	14.91	198	465	113	1014	188
HRL12A-8.2e	0.007	86	0.073	0.77	2.20	0.637	50	22	9.14	114	241	55	461	87
HRL12A-9.1c	0.064	233	0.405	8.70	19.69	4.651	203	156	50.71	563	805	154	1121	186
HRL12A-9.2i	0.012	77	0.160	1.08	2.68	0.941	32	21	7.07	80	147	31	269	50
HRL12A-9.3e	0.009	90	0.103	0.93	2.48	0.798	43	22	8.17	106	199	42	349	64
HRL12A-10.1c	0.015	110	0.145	3.77	9.13	2.351	107	68	25.18	280	474	96	738	126
12A-10.2i	0.010	77	0.089	1.45	3.02	1.157	37	26	7.81	91	180	41	335	66
12A-11.1e	0.265	47	0.033	0.33	1.30	0.430	26	11	4.57	65	126	30	262	47
12A-11.2i	0.022	79	0.176	0.87	2.65	0.902	41	22	7.94	97	198	45	371	72
12A-11.3i	0.065	155	0.264	6.57	12.27	3.495	108	87	28.20	287	459	90	690	122
12A-12.1i	3.256	117	0.573	4.30	3.33	1.096	58	29	11.33	136	274	60	493	92
12A-12.2C	0.020	81	0.256	3.71	6.60	2.648	57	47	14.55	152	227	44	361	64
12A-13.1C	10.508	136	1.679	13.41	7.94	3.327	79	61	19.27	207	355	73	575	104
12A-13.2e	3.828	496	2.018	11.40	6.48	3.741	34	30	9.40	90	147	33	270	51
12A-14.1idk	0.010	48	0.095	0.42	1.33	0.511	21	11	4.14	49	94	21	175	33
HRL12A14.2ilt	0.027	55	0.108	2.25	3.52	1.696	29	25	7.24	75	129	27	224	41
HRL12A14.3edk	0.021	80	0.047	0.52	1.56	0.483	35	16	6.08	82	175	45	399	80

Table D2: Trace element data from SHRIMP-RG analysis of zircons from sample HRL 14a of the Highland Range silicic sequence.

Sample Spot	Li ppm Est.	Be9 ppm	B11 ppm	F19 ppm	Na ppm Est.	Mg ppm Est.	Al27 ppm Est.	P31 ppm	S32 Rel.	K39 Rel.
HRL14A-1.1CM	0.88	6.35	0.1	32	7.3	2.2	12	222	0.4	2.3
HRL14A-1.2EDK	2.81	9.98	0.1	25	6.1	4.1	9	164	1.1	1.9
HRL14A-2.1IDK	0.03	1.94	0.1	24	5.1	1.4	7	253	0.4	1.6
HRL14A-2.2EDK	0.03	0.40	0.1	25	6.5	4.6	9	348	0.9	2.3
HRL14A-3.1CDK	0.06	0.12	0.0	22	6.7	2.4	10	523	1.0	1.9
HRL14A-3.2ELT	0.03	0.01	0.1	21	5.8	2.5	8	223	0.4	1.9
HRL14A-4.1I	0.02	0.34	0.2	21	6.8	2.0	15	199	0.4	2.0
HRL14A-5.1I	0.04	0.86	0.1	17	7.3	1.9	15	368	0.8	2.4
HRL14A-6.1EDK	2.05	0.81	0.1	21	7.5	3.5	11	265	0.6	1.9
HRL14A-6.2CM	0.20	0.70	0.1	19	6.7	1.7	11	394	0.2	1.7
HRL14A-7.1CDK	204.4	5.07	0.2	23	6.5	1.9	10	548	1.0	1.9
HRL14A-8.1EDK	0.12	0.22	0.1	15	4.6	5.4	9	205	1.3	1.2
HRL14A-8.2CLT	0.13	1.09	0.2	21	6.7	1.7	8	288	0.8	1.8
HRL14A-9.1CDK	0.26	2.37	0.2	30	50.7	2.6	126	1141	1.0	62.2
HRL14A-9.2ELT	0.02	0.36	0.1	22	6.2	2.2	7	258	0.2	1.8
HRL14A-10.1IDK	0.11	1.80	0.2	23	6.9	3.6	9	267	0.4	2.0
HRL14A-10.2ELT	0.03	1.73	0.1	14	5.7	2.1	8	262	0.4	1.7
HRL14A-11.1CLT	0.02	0.03	0.1	14	5.5	1.8	8	201	0.7	1.6
HRL14A-11.2EM	0.07	2.42	0.3	17	9.1	3.4	12	241	0.4	2.4
HRL14A-12.1EM	0.44	0.28	0.1	21	6.8	20.5	33	162	4.7	4.1
HRL14A-12.2IDK	0.03	0.19	0.1	22	5.4	2.4	9	220	0.9	1.3
HRL14A-12.3CDK	0.08	0.64	0.1	20	4.8	2.7	8	397	0.4	1.7
HRL14A-13.1EM	0.03	0.20	0.2	23	6.6	2.4	8	187	0.6	1.7
HRL14A-13.2CM	0.06	2.74	0.1	22	6.7	2.4	9	333	0.4	2.0
HRL14A-14.1CDK	0.15	1.12	0.2	27	7.1	2.1	11	382	1.4	1.9
HRL14A-14.2EM	0.04	0.04	0.1	21	6.3	2.2	7	302	1.1	1.7
HRL14A-15.1CM	0.09	1.41	0.1	17	6.8	4.5	10	261	1.6	2.2
HRL14A-15.2EDK	0.06	1.19	0.2	17	6.9	3.2	10	219	0.8	2.3
HRL14A-16.1	0.04	1.23	0.1	20	7.1	2.5	10	244	0.2	2.4
HRL14A-17.1	0.07	0.18	0.1	17	6.0	1.5	8	661	0.4	2.0

Table D2, continued

Sample Spot	Ca40 ppm Est.	Sc45 ppm	48/49	Ti48 ppm	Ti49 ppm	V51 ppm REL.	Cr Rel.	Mn Rel.	Fe56 ppm	Ge74 Rel.
HRL14A-1.1CM	3.8	42			16.1	0.05	0.03	0.06	1.2	0.2
HRL14A-1.2EDK	3.5	77			5.0	0.08	0.08	0.07	1.7	0.2
HRL14A-2.1IDK	2.9	78			6.9	0.08	0.07	0.05	1.2	0.2
HRL14A-2.2EDK	3.6	38			10.1	0.47	0.09	0.10	1.8	0.3
HRL14A-3.1CDK	4.1	78			22.1	0.40	0.10	0.05	1.2	0.3
HRL14A-3.2ELT	3.4	31			11.8	0.14	0.04	0.05	1.3	0.3
HRL14A-4.1I	3.1	34			26.4	0.13	0.06	0.07	1.6	0.2
HRL14A-5.1I	4.2	51			30.7	0.50	0.08	0.06	1.8	0.5
HRL14A-6.1EDK	3.8	34			6.0	0.09	0.06	0.06	1.5	0.3
HRL14A-6.2CM	3.8	47			16.2	0.19	0.04	0.04	1.3	0.1
HRL14A-7.1CDK	3.6	75			13.7	0.36	0.05	0.05	1.1	0.3
HRL14A-8.1EDK	2.6	46			7.1	0.28	0.07	0.06	3.7	0.2
HRL14A-8.2CLT	3.5	75			20.5	0.60	0.06	0.08	1.0	0.3
HRL14A-9.1CDK	6.9	113			15.4	0.34	0.04	0.76	204.4	0.3
HRL14A-9.2ELT	3.2	35			9.0	0.43	0.09	0.05	1.4	0.3
HRL14A-10.1IDK	3.5	36			14.2	0.47	0.04	0.04	1.6	0.2
HRL14A-10.2ELT	3.5	54			9.3	0.24	0.06	0.06	1.2	0.2
HRL14A-11.1CLT	2.8	33			26.6	0.22	0.04	0.04	0.8	0.3
HRL14A-11.2EM	4.0	83			5.5	0.06	0.04	0.06	1.5	0.4
HRL14A-12.1EM	4.8	30			14.5	0.21	0.07	0.08	21.7	0.2
HRL14A-12.2IDK	3.3	33			6.0	0.06	0.06	0.07	1.0	0.4
HRL14A-12.3CDK	3.0	57			13.6	0.45	0.05	0.05	3.6	0.2
HRL14A-13.1EM	2.8	22			6.0	0.07	0.05	0.04	1.3	0.2
HRL14A-13.2CM	3.7	39			11.1	0.58	0.08	0.06	1.6	0.4
HRL14A-14.1CDK	3.7	106			6.9	0.14	0.10	0.07	1.0	0.3
HRL14A-14.2EM	3.1	37			12.8	0.28	0.04	0.06	1.3	0.2
HRL14A-15.1CM	3.8	53			15.3	0.29	0.05	0.07	1.4	0.3
HRL14A-15.2EDK	4.0	56			4.5	0.04	0.09	0.08	1.5	0.4
HRL14A-16.1	4.0	33			9.9	0.35	0.04	0.07	1.9	0.2
HRL14A-17.1	3.1	97			10.9	0.32	0.10	0.04	1.0	0.2

Table D2, continued

Sample Spot	Y89 ppm	Nb93 ppm	Zr94H Rel.	Zr96/Si30 ppm	Zr96/ Zr2O	196/ Si30	Hf ppm	Pb7/6 Est,	Th ppm	U ppm
HRL14A-1.1CM	1335	2	1.2	2.00	128	64	8714	0.5263	118	55
HRL14A-1.2EDK	917	19	1.2	1.96	129	66	12384	0.1266	341	305
HRL14A-2.1IDK	1629	42	1.4	1.95	131	67	12159	0.1003	1562	831
HRL14A-2.2EDK	1413	16	1.4	2.00	130	65	9719	0.9091	623	294
HRL14A-3.1CDK	1974	19	1.3	2.00	133	67	8464	0.0000	1687	426
HRL14A-3.2ELT	616	5	1.2	1.94	137	71	8884	0.0000	110	75
HRL14A-4.1I	987	1	1.2	2.00	122	61	7328	1.6667	149	49
HRL14A-5.1I	2122	4	1.2	2.02	132	66	7360	0.0000	459	111
HRL14A-6.1EDK	1163	14	1.2	1.99	130	65	11513	0.1613	449	298
HRL14A-6.2CM	1124	3	1.1	2.00	136	68	8287	0.0000	105	52
HRL14A-7.1CDK	4567	17	1.1	1.98	127	64	8188	0.0000	1094	347
HRL14A-8.1EDK	1011	14	1.4	2.04	118	58	11501	0.2632	362	261
HRL14A-8.2CLT	1163	7	1.1	1.96	126	64	7695	0.0000	105	75
HRL14A-9.1CDK	3433	73	1.1	1.96	129	66	13774	0.1712	1871	1354
HRL14A-9.2ELT	901	8	1.1	1.96	140	72	9409	0.0000	196	126
HRL14A-10.1IDK	2409	5	1.1	2.01	133	66	8179	0.0000	483	192
HRL14A-10.2ELT	1174	14	1.0	1.99	135	68	9831	0.0000	157	144
HRL14A-11.1CLT	446	2	1.1	2.01	125	62	7915	1.8182	47	28
HRL14A-11.2EM	1334	30	1.1	2.01	126	62	12058	0.0000	416	377
HRL14A-12.1EM	624	6	1.3	2.02	118	58	9891	0.0000	72	70
HRL14A-12.2IDK	852	10	1.1	1.96	126	64	11714	0.3226	206	178
HRL14A-12.3CDK	2311	26	1.1	1.97	135	68	9809	0.0000	657	393
HRL14A-13.1EM	739	8	1.1	1.96	127	65	10690	0.3571	139	130
HRL14A-13.2CM	2472	5	1.1	1.98	128	64	8952	0.2083	391	180
HRL14A-14.1CDK	1906	45	1.0	2.02	129	64	12396	0.0901	734	573
HRL14A-14.2EM	893	6	1.0	2.02	139	69	9493	0.3846	223	122
HRL14A-15.1CM	1107	7	1.1	2.01	137	68	8975	0.0000	143	96
HRL14A-15.2EDK	1079	17	1.0	1.98	138	70	13268	0.2410	499	382
HRL14A-16.1	1488	5	1.1	1.99	132	66	9596	0.0000	210	115
HRL14A-17.1	1549	10	1.0	2.01	140	69	8021	0.9091	280	153

Table D2, continued

Sample Spot	Y/Nb	Th/U	Yb/Gd	Yb/Nd	U/Yb	Th/Yb	Ce/Sm	Ce/Lu	U/Ce	Th/Ce
HRL14A-1.1CM	761	2.13	7.2	72	0.2	0.3	6.8	0.90	1.0	2.1
HRL14A-1.2EDK	48	1.12	64.1	1513	0.6	0.7	101.1	0.82	3.7	4.2
HRL14A-2.1IDK	39	1.88	38.6	774	1.2	2.3	88.6	1.27	4.9	9.2
HRL14A-2.2EDK	89	2.12	13.7	234	0.7	1.5	38.2	1.83	2.3	4.8
HRL14A-3.1CDK	105	3.96	8.3	104	0.8	3.2	33.2	3.39	1.5	5.8
HRL14A-3.2ELT	136	1.46	12.1	225	0.4	0.6	34.2	1.85	1.2	1.7
HRL14A-4.1I	798	3.07	9.2	72	0.2	0.5	5.3	0.57	1.4	4.4
HRL14A-5.1I	532	4.12	8.8	97	0.2	0.7	5.7	0.53	1.7	6.9
HRL14A-6.1EDK	81	1.51	19.2	494	0.8	1.1	39.2	1.32	3.0	4.6
HRL14A-6.2CM	380	2.01	9.1	101	0.2	0.4	13.1	1.12	0.8	1.7
HRL14A-7.1CDK	275	3.15	7.3	89	0.3	0.9	14.0	1.61	1.1	3.5
HRL14A-8.1EDK	72	1.38	25.9	476	0.7	1.0	52.7	1.27	2.8	3.9
HRL14A-8.2CLT	167	1.41	13.4	192	0.2	0.3	21.8	1.14	0.9	1.3
HRL14A-9.1CDK	47	1.38	53.1	1240	0.9	1.3	73.3	0.66	7.2	9.9
HRL14A-9.2ELT	107	1.56	14.2	283	0.5	0.7	30.3	1.57	1.6	2.5
HRL14A-10.1IDK	441	2.52	7.4	72	0.3	0.7	10.0	1.22	1.4	3.4
HRL14A-10.2ELT	87	1.09	20.5	490	0.3	0.4	36.5	1.05	1.8	1.9
HRL14A-11.1CLT	196	1.68	9.7	150	0.2	0.4	21.2	1.58	0.7	1.1
HRL14A-11.2EM	45	1.10	41.2	1079	0.6	0.7	60.4	0.81	3.7	4.1
HRL14A-12.1EM	113	1.04	16.9	453	0.3	0.3	35.9	1.29	1.4	1.4
HRL14A-12.2IDK	90	1.16	23.6	646	0.6	0.7	43.5	1.17	2.6	3.0
HRL14A-12.3CDK	87	1.67	13.4	382	0.6	0.9	43.1	1.73	1.8	3.1
HRL14A-13.1EM	87	1.07	17.9	537	0.5	0.6	34.8	1.34	2.2	2.4
HRL14A-13.2CM	512	2.17	8.0	105	0.3	0.6	10.8	1.08	1.5	3.3
HRL14A-14.1CDK	42	1.28	38.8	960	0.7	0.9	77.7	0.99	3.7	4.7
HRL14A-14.2EM	159	1.84	12.0	255	0.4	0.8	27.3	1.74	1.4	2.5
HRL14A-15.1CM	156	1.49	12.8	253	0.3	0.4	28.0	1.52	1.0	1.4
HRL14A-15.2EDK	62	1.31	43.5	741	0.8	1.0	73.3	0.97	3.9	5.1
HRL14A-16.1	289	1.83	10.0	175	0.3	0.5	13.9	1.08	1.5	2.7
HRL14A-17.1	151	1.83	12.8	216	0.3	0.6	28.6	1.54	1.2	2.2

Table D2, continued

Sample Spot	Y/Yb	Y/Nb	Yb/Nb	Yb/Sc	Yb/Dy	Dy/Sm	Yb/Nd	Sm/Nd	U/Li
HRL14A-1.1CM	3.9	761	197.6	8.2	2.30	18.3	72	1.7	63
HRL14A-1.2EDK	1.9	48	25.0	6.1	8.96	65.1	1513	2.6	109
HRL14A-2.1IDK	2.4	39	15.9	8.6	6.40	54.9	774	2.2	31834
HRL14A-2.2EDK	3.5	89	25.4	10.7	3.07	38.8	234	2.0	8461
HRL14A-3.1CDK	3.8	105	27.7	6.7	2.47	24.2	104	1.7	7196
HRL14A-3.2ELT	3.2	136	42.3	6.2	3.37	30.2	225	2.2	2840
HRL14A-4.1I	3.1	798	259.6	9.5	3.12	16.3	72	1.4	1963
HRL14A-5.1I	3.3	532	163.4	12.7	2.94	19.1	97	1.7	2605
HRL14A-6.1EDK	3.0	81	27.5	11.7	3.74	42.1	494	3.1	145
HRL14A-6.2CM	3.8	380	101.2	6.4	2.62	24.1	101	1.6	262
HRL14A-7.1CDK	3.8	275	72.8	16.1	2.26	23.8	89	1.7	2
HRL14A-8.1EDK	2.8	72	25.6	7.9	4.92	41.4	476	2.3	2258
HRL14A-8.2CLT	3.1	167	53.3	5.0	3.58	27.6	192	1.9	563
HRL14A-9.1CDK	2.3	47	20.3	13.0	7.30	78.8	1240	2.2	5253
HRL14A-9.2ELT	3.3	107	32.6	7.8	3.36	31.9	283	2.6	5242
HRL14A-10.1IDK	3.6	441	121.3	18.6	2.41	19.6	72	1.5	1678
HRL14A-10.2ELT	2.7	87	31.8	8.1	4.17	46.0	490	2.6	5274
HRL14A-11.1CLT	3.5	196	56.4	3.9	2.79	24.0	150	2.2	1351
HRL14A-11.2EM	2.1	45	21.1	7.6	7.14	51.7	1079	2.9	5380
HRL14A-12.1EM	3.0	113	37.6	6.9	3.77	39.6	453	3.0	158
HRL14A-12.2IDK	2.7	90	32.9	9.5	4.77	42.3	646	3.2	5161
HRL14A-12.3CDK	3.3	87	26.4	12.2	3.11	45.1	382	2.7	4689
HRL14A-13.1EM	3.0	87	28.7	10.9	3.97	36.8	537	3.7	4757
HRL14A-13.2CM	3.9	512	132.2	16.3	2.38	24.2	105	1.8	3206
HRL14A-14.1CDK	2.3	42	18.3	7.7	6.56	62.6	960	2.3	3875
HRL14A-14.2EM	3.1	159	50.5	7.7	3.07	28.8	255	2.9	3265
HRL14A-15.1CM	3.1	156	50.0	6.6	3.13	31.8	253	2.5	1119
HRL14A-15.2EDK	2.2	62	27.9	8.6	7.11	51.4	741	2.0	6420
HRL14A-16.1	3.5	289	82.7	12.9	2.76	27.3	175	2.3	2853
HRL14A-17.1	3.4	151	44.6	4.7	3.15	32.6	216	2.1	2345

Table D2, continued

Sample Spot	La139 ppm	Ce140 ppm	Pr141 ppm	Nd146 ppm	Sm147 ppm	Eu153 ppm	Ho165 ppm	GdO173 ppm	TbO175 ppm	DyO179 ppm	ErO182 ppm	TmO185 ppm	YbO188 ppm	LuO191 ppm
HRL14A-1.1CM	0.033	56	0.168	4.83	8.25	3.278	55	48	14.61	151	230	46	347	63
HRL14A-1.2EDK	0.009	82	0.072	0.31	0.81	0.211	28	7	3.77	53	165	46	473	100
HRL14A-2.1IDK	0.010	169	0.112	0.87	1.91	0.463	52	17	7.49	105	277	70	670	133
HRL14A-2.2EDK	0.021	130	0.117	1.73	3.41	1.114	55	30	11.74	132	243	50	405	71
HRL14A-3.1CDK	0.030	290	0.342	5.00	8.73	2.833	78	63	20.17	211	323	65	521	86
HRL14A-3.2ELT	0.003	64	0.044	0.85	1.88	0.772	24	16	5.06	57	103	24	191	35
HRL14A-4.1I	0.068	34	0.333	4.45	6.32	3.123	40	35	9.96	103	165	37	321	59
HRL14A-5.1I	0.131	66	0.382	6.69	11.58	6.800	83	74	22.48	221	360	77	651	126
HRL14A-6.1EDK	0.022	98	0.097	0.80	2.49	0.600	43	20	8.58	105	214	47	393	74
HRL14A-6.2CM	0.005	62	0.193	2.96	4.73	1.751	43	33	11.06	114	188	38	299	55
HRL14A-7.1CDK	0.194	315	0.782	13.60	22.47	8.286	191	166	50.67	534	776	153	1209	196
HRL14A-8.1EDK	0.038	94	0.129	0.76	1.78	0.538	36	14	5.63	74	175	41	362	74
HRL14A-8.2CLT	0.037	81	0.120	1.93	3.74	1.776	44	28	9.45	103	206	43	370	71
HRL14A-9.1CDK	0.595	188	0.127	1.19	2.56	0.293	107	28	13.47	202	626	160	1475	283
HRL14A-9.2ELT	0.019	78	0.118	0.97	2.56	0.859	35	19	7.33	82	158	32	274	49
HRL14A-10.1IDK	0.160	140	0.479	9.24	14.02	5.691	97	90	27.54	275	398	82	662	115
HRL14A-10.2ELT	0.016	82	0.103	0.88	2.25	0.787	44	21	8.16	104	216	49	432	78
HRL14A-11.1CLT	0.023	41	0.071	0.86	1.92	0.964	18	13	4.28	46	78	18	129	26
HRL14A-11.2EM	0.017	102	0.098	0.58	1.69	0.388	44	15	6.33	88	245	63	626	126
HRL14A-12.1EM	0.092	50	0.064	0.46	1.39	0.585	24	12	4.42	55	110	24	208	39
HRL14A-12.2IDK	0.005	68	0.090	0.48	1.55	0.456	31	13	5.33	66	148	34	313	58
HRL14A-12.3CDK	0.031	214	0.117	1.83	4.97	1.060	91	52	19.13	224	407	88	698	124
HRL14A-13.1EM	0.007	58	0.033	0.45	1.66	0.440	27	14	5.10	61	126	28	243	43
HRL14A-13.2CM	0.024	119	0.321	6.07	11.07	3.464	99	80	25.64	268	418	85	638	111
HRL14A-14.1CDK	0.012	155	0.127	0.85	2.00	0.401	62	21	8.88	125	348	89	820	157
HRL14A-14.2EM	0.018	88	0.127	1.12	3.22	0.916	36	24	8.17	93	164	34	284	50
HRL14A-15.1CM	0.008	100	0.147	1.40	3.56	1.283	45	28	9.58	113	202	42	355	65
HRL14A-15.2EDK	0.029	97	0.076	0.65	1.33	0.240	34	11	4.61	68	197	51	484	100
HRL14A-16.1	0.018	79	0.191	2.44	5.65	1.879	60	43	13.97	155	261	53	426	73
HRL14A-17.1	0.011	127	0.036	2.11	4.45	1.698	60	36	12.22	145	259	55	457	83

Table D3: Trace element data from SHRIMP-RG analysis of zircons from sample HRL 27 of the Highland Range silicic sequence.

Sample Spot	Li ppm Est.	Be9 ppm	B11 ppm	F19 ppm	Na ppm Est.	Mg ppm Est.	Al27 ppm Est.	P31 ppm	S32 Rel.	K39 Rel.
HLR27-1.1LR	0.012	2.70	0.1	19	4.5	1.1	32	336	0.8	2.0
HLR27-1.2DC	0.009	1.37	0.1	14	3.7	0.7	22	293	0.8	1.5
HLR27-2C	0.005	1.04	0.1	14	3.0	2.0	30	338	0.0	1.3
HLR27-3C	0.006	3.56	0.1	36	3.7	0.9	23	239	1.1	2.2
HLR27-4I	0.002	2.21	0.0	16	3.3	0.4	19	357	1.1	1.4
HLR27-5C	0.005	6.82	0.0	28	2.9	0.6	22	309	0.3	1.5
HLR27-6C	0.001	2.03	0.1	13	3.2	0.5	22	339	0.3	1.4
HLR27-7R	0.009	1.89	0.1	15	5.8	1.5	19	236	1.4	2.0
HLR27-8I	0.008	3.89	0.1	17	3.5	0.5	19	403	0.5	1.4
HLR27-9.1R	0.011	0.87	0.1	13	5.1	1.5	20	270	0.3	2.0
HLR27-9.2I	0.012	0.02	0.1	16	5.9	1.4	28	344	1.6	2.8
HLR27-10C	0.007	0.16	0.0	11	3.1	0.7	20	321	1.0	1.2
HLR27-10.2C	0.004	0.80	0.1	10	2.6	0.6	30	318	0.0	1.0
HLR27-11	0.009	1.62	0.1	14	3.4	3.9	17	234	0.8	1.2
HLR27-12C	0.058	0.02	0.0	11	2.4	0.4	14	179	0.3	1.0

Table D3, continued

Sample Spot	Ca40 ppm Est.	Sc45 ppm	48/49	Ti48 ppm	Ti49 ppm	V51 ppm REL.	Cr Rel.	Mn Rel.	Fe56 ppm	Ge74 Rel.
HLR27-1.1LR	4.2	112	13.4	30.2	30.4	0.19	0.12	0.04	1.0	0.3
HLR27-1.2DC	2.9	89	13.4	28.4	28.7	0.13	0.09	0.03	0.8	0.4
HLR27-2C	2.2	64	13.2	30.3	31.0	0.48	0.05	0.02	0.9	0.3
HLR27-3C	4.4	53	13.8	23.3	22.8	0.28	0.04	0.04	0.9	0.4
HLR27-4I	2.3	84	13.1	31.5	32.5	0.49	0.05	0.02	0.6	0.4
HLR27-5C	2.5	68	13.7	16.5	16.3	0.39	0.06	0.04	0.7	0.4
HLR27-6C	2.5	85	13.7	31.9	31.5	0.33	0.02	0.03	0.6	0.4
HLR27-7R	2.1	57	13.9	24.5	23.7	0.32	0.06	0.04	0.8	0.4
HLR27-8I	2.6	88	13.6	28.8	28.5	0.34	0.08	0.02	0.5	0.4
HLR27-9.1R	3.0	77	13.2	24.1	24.6	0.31	0.09	0.04	0.6	0.2
HLR27-9.2I	4.6	70	13.2	27.1	27.6	0.31	0.06	0.04	2.7	0.2
HLR27-10C	2.4	57	13.3	29.1	29.6	0.18	0.03	0.02	0.6	0.2
HLR27-10.2C	2.6	74	13.8	28.6	27.9	0.28	0.06	0.04	0.6	0.3
HLR27-11	2.6	56	13.4	26.1	26.4	0.28	0.07	0.04	0.9	0.3
HLR27-12C	2.2	26	13.6	15.0	14.9	0.01	0.03	0.02	0.5	0.4

Table D3, continued

Sample Spot	Y89 ppm	Nb93 ppm	Zr94H Rel.	Zr96/Si30 ppm	Zr96/ Zr2O	196/ Si30	Hf ppm	Pb7/6 Est,	Th ppm	U ppm
HLR27-1.1LR	1103	5	2.3	1.74	120	69	7099	0.0000	53	43
HLR27-1.2DC	821	3	2.1	1.74	110	63	7267	1.3333	32	33
HLR27-2C	760	4	2.1	1.79	113	63	7785	0.3077	75	66
HLR27-3C	1161	3	2.2	1.76	119	68	7967	0.5000	93	62
HLR27-4I	1052	5	2.1	1.77	116	66	7774	0.5517	85	78
HLR27-5C	2006	5	2.1	1.75	113	65	8063	0.9756	128	75
HLR27-6C	1025	5	1.9	1.72	113	66	7756	0.2222	85	77
HLR27-7R	828	3	1.8	1.73	121	70	8069	0.0000	61	51
HLR27-8I	2367	5	2.0	1.74	115	66	7298	0.0000	132	73
HLR27-9.1R	1462	6	2.0	1.72	108	63	7955	0.3333	132	86
HLR27-9.2I	1424	4	1.9	1.75	111	63	7606	0.6154	92	56
HLR27-10C	754	3	2.0	1.74	109	63	7592	0.4211	78	58
HLR27-10.2C	914	4	2.0	1.78	118	66	7266	0.0000	52	51
HLR27-11	689	3	1.9	1.76	113	64	8041	0.6154	48	43
HLR27-12C	465	2	2.0	1.81	113	62	7493	0.0675	40	65

Table D3, continued

Sample Spot	La139 ppm	Ce140 ppm	Pr141 ppm	Nd146 ppm	Sm147 ppm	Eu153 ppm	Ho165 ppm	GdO173 ppm	TbO175 ppm	DyO179 ppm	ErO182 ppm	TmO185 ppm	YbO188 ppm	LuO191 ppm
HRL27-1.1LR	0.023	55	0.127	2.01	4.02	2.447	43	29	9.32	109	188	39	321	57
HRL27-1.2DC	0.023	39	0.087	1.82	3.36	2.001	32	25	7.30	77	146	31	255	49
HRL27-2C	0.021	37	0.106	1.62	3.00	1.602	30	20	6.89	75	138	31	264	50
HRL27-3C	0.059	43	0.331	3.79	6.18	2.972	47	41	12.27	115	193	41	318	56
HRL27-4I	0.040	46	0.232	2.05	4.02	1.855	42	27	8.85	88	191	42	346	67
HRL27-5C	0.079	96	0.263	7.32	10.65	5.460	84	77	23.87	240	348	67	509	87
HRL27-6C	0.028	45	0.175	1.99	3.90	1.942	39	27	8.73	92	188	42	345	66
HRL27-7R	0.021	35	0.200	2.34	3.75	1.952	33	27	8.16	91	149	31	258	50
HRL27-8I	0.102	98	0.624	8.47	15.00	8.737	98	98	28.33	281	392	75	584	100
HRL27-9.1R	0.080	73	0.366	4.18	7.05	3.591	59	50	15.66	162	262	54	429	76
HRL27-9.2I	0.100	49	0.283	4.49	7.19	4.121	59	54	15.56	156	250	51	391	71
HRL27-10C	0.024	47	0.136	2.08	3.41	1.923	30	25	7.35	77	135	28	231	43
HRL27-10.2C	0.019	44	0.144	1.87	3.23	1.802	36	23	7.70	90	168	36	296	59
HRL27-11	0.020	34	0.101	1.56	3.07	1.515	26	21	6.42	61	118	25	219	41
HRL27-12C	0.021	15	0.112	1.73	3.59	0.669	19	22	5.88	53	72	15	113	22

APPENDIX E:
Sphene Elemental Data and
Backscatter Electron Images from the
Highland Range Silicic Sequence,
SHRIMP-RG Analysis

Table E1. Rare earth element data from SHRIMP-RG analysis of sphene from the Highland Range silicic sequence.

Sample Spot	La	Ce	Pr	Nd	Sm	Eu	Gd	Tb	Dy	Ho	Er	Tm	Yb	Lu
HRL12A-1.1modZ	4126	13523	1819	7708	1618	133	1473	215	1262	256	686	92.6	544	63.5
HRL12A-1.2ltZ	4166	12183	1509	5693	1034	70	937	137	844	187	536	77.4	479	59.7
HRL12A-2.1ltZ	5332	18551	2774	12805	2957	263	2591	372	2076	392	961	115.2	586	59.5
HRL12A-2.2hvZ	4478	17212	2808	13790	3777	300	3426	496	2731	493	1145	130.0	640	62.3
HRL12A-2.3ltZ	4630	13349	1539	5686	905	91	730	100	580	126	364	53.1	336	43.4
HRL12A-3.1hvZ	4084	14118	2020	9050	2186	152	2018	302	1732	337	839	103.7	558	59.0
HRL12A-3.2modZ	4155	13894	1815	7341	1455	111	1298	195	1180	247	666	88.6	498	57.9
HRL12A-3.3hvZ	4411	16797	2630	12644	3402	206	3174	474	2617	487	1145	131.7	639	65.5
HRL12A-3.4modZ	4182	13919	1855	7547	1554	90	1432	219	1307	277	752	97.7	558	63.6
HRL12A-4.1hvZ	5572	17346	2215	8646	1782	82	1743	272	1687	371	1050	142.9	818	92.0
HRL12A-4.2ltZ	4410	13218	1563	5862	1043	71	904	136	817	182	531	76.7	472	58.7
HRL12A-4.3modZ	4456	14363	1884	7724	1564	121	1397	205	1189	245	655	88.9	494	58.1
HRL12A-5.1hvZ	4020	14042	2015	9062	2172	147	2032	294	1669	325	826	105.9	589	64.8
HRL12A-5.2ltZ	4777	14987	1899	7389	1339	121	1183	170	1011	217	589	78.8	446	51.3
HRL12A-6.1LOZ	4521	14723	1923	7901	1551	129	1398	207	1227	260	712	94.9	542	61.3
HRL12A-6.2MODZ	3971	14171	2146	9875	2353	206	2131	309	1727	337	841	102.8	548	57.5
HRL12A-6.3HIZ	4182	15188	2470	12428	3217	317	3004	419	2283	420	990	113.8	574	59.3
HRL14A-1.1lowZ	3981	13960	2050	9098	2198	130	2165	336	1965	392	999	124.1	668	72.8
HRL14A-1.2hvZ	3820	15139	2552	13119	3857	267	3750	550	3023	541	1256	140.0	669	65.1
HRL14A-2.1lowZ	3891	13488	1808	7423	1682	88	1572	245	1480	305	800	100.4	542	58.8
HRL14A-2.2modZ	5002	17067	2253	8995	1911	102	1780	283	1720	357	952	122.4	670	69.4
HRL14A-3.1hvZ	5153	17111	2252	8665	1830	86	1728	279	1743	373	1012	132.0	721	76.1
HRL14A-3.2lowZ	3847	13321	1753	6883	1466	66	1383	226	1419	304	835	110.4	612	64.9
HRL14A-3.3modZ	4124	14007	1946	8143	1847	90	1769	275	1647	338	886	111.8	610	65.6
HRL14A-3.4hvZ	3769	13921	2087	9661	2460	146	2339	354	2040	395	982	118.9	608	62.1
HRL14A-4.1lowZ	3989	13617	1903	7981	1832	123	1682	257	1483	299	775	96.1	510	53.9
HRL14A-4.2hvZ	5897	19194	2700	11514	2615	187	2261	328	1842	350	868	102.8	539	53.6
HRL14A-4.3modZ	3893	13655	1963	8477	2036	140	1892	290	1703	337	879	108.8	579	61.7
HRL14A-5.1modZ	4168	14314	2025	9024	2117	129	1909	283	1637	323	829	103.4	568	61.5
HRL14A-5.2lowZ	3514	11966	1568	6114	1305	55	1222	194	1203	257	701	92.4	518	58.8

Table E1, continued

230

Sample Spot	La	Ce	Pr	Nd	Sm	Eu	Gd	Tb	Dy	Ho	Er	Tm	Yb	Lu
HRL21-1.1	5197	18021	2287	11755	2760	175.6	2489	351	1893	362	869	101.1	519	57.5
HRL21-1.2D	4637	15698	1840	9649	2036	156.7	1837	255	1394	277	696	85.1	459	54.2
HRL21-2.1DE	4276	13211	1345	6071	1062	83.1	877	125	728	156	441	62.6	401	49.5
HRL21-2.2D	4977	15130	1571	7335	1266	146.9	974	130	737	147	397	54.5	318	39.8
HRL21-2.3DC	4286	15011	1819	9637	2033	226.0	1654	225	1227	235	602	76.1	433	47.4
HRL21-2.4L	4283	15480	1981	10989	2456	268.5	1916	257	1357	251	602	75.1	406	44.1
HRL21-3.1ED	4231	14778	1790	9464	2175	133.4	2027	288	1613	316	792	99.4	509	58.6
HRL21-3.2D	4573	15640	1823	10184	2142	185.5	1817	245	1329	260	660	82.0	437	50.9
HRL21-3.3LC	3844	14714	2209	13743	3943	287.0	3817	517	2695	487	1117	125.0	613	64.7
HRL21-4.1ED	4305	14621	1762	9557	2154	135.7	2010	290	1637	325	811	99.3	528	60.1
HRL21-5.1ED	3618	13172	1832	9310	2475	179.1	2404	364	2062	398	986	118.6	623	66.3
HRL21-5.1ED	3618	13172	1832	9310	2475	179.1	2404	364	2062	398	986	118.6	623	66.3
HRL21-5.2LC	4538	16172	2114	11081	2861	203.6	2552	381	2152	404	985	116.4	610	61.7
HRL21-6..1DE	1654	5550	662	3406	807	54.4	689	106	598	117	307	39.2	218	23.2
HRL21-6.2LC	3879	13976	1908	9618	2487	181.0	2357	354	1997	382	940	114.0	586	65.4
HLR21-6.3LC	5021	17602	2254	11650	2933	209.1	2563	388	2162	417	1000	119.2	617	62.7
HLR21-6.4ED	4157	14456	1933	9226	2231	163.5	2024	303	1708	335	818	102.7	533	56.3
HRL21-7.1ED	4220	14771	2026	9131	2097	128.2	2015	291	1624	318	794	97.8	511	55.4
HRL21-8.1ED	4416	15436	1883	9193	2029	115.7	1787	257	1460	297	748	93.6	497	58.3
HLR21-8.2C	4775	17406	2456	13584	3302	310.9	2842	367	1882	341	778	88.8	441	51.1
HLR21-9.1ED	4299	15015	1926	9097	2019	115.8	1785	259	1461	294	735	91.9	500	57.3
HLR21-9.2LC	4876	18233	2691	14837	4052	293.8	3736	504	2581	458	1004	109.3	505	51.5

Table E1, continued

Sample Spot	La	Ce	Pr	Nd	Sm	Eu	Gd	Tb	Dy	Ho	Er	Tm	Yb	Lu
HLR19A-1.2D	3279	10365	1119	4567	798	54.2	668	97	587	128	375	53.1	336	42.0
HLR19A-1.1L	5882	17930	1799	7569	1265	90.5	965	142	829	177	512	74.6	455	55.9
HLR19A-1.3E	4067	12894	1389	5591	982	70.9	769	114	671	145	421	61.7	382	45.6
HLR19A-1.4D	3925	12491	1378	5615	993	70.4	812	119	704	156	436	62.8	388	47.8
HLR19A-2.1ED	4208	13213	1430	5755	946	73.8	748	107	646	141	399	59.4	372	46.4
HLR19A-2.2L	4966	14839	1679	6542	1083	108.5	869	121	691	147	407	58.1	348	43.1
HLR19A-2.3DC	4410	12509	1468	6313	1184	169.7	946	126	684	133	340	43.5	265	32.0
HLR19A-2.4LC	4910	16629	2160	11425	2524	321.4	2148	287	1505	279	659	79.2	418	48.1
HLR19A-3.1ED	4131	13208	1551	5751	955	68.1	755	113	670	146	425	59.8	380	47.2
HLR19A-3.2L	6118	18536	1955	7587	1250	85.8	1004	146	877	190	549	78.4	501	60.0
HLR19A-3.3DC	3661	11504	1215	5025	878	61.9	743	109	655	145	419	60.9	381	47.1
HLR19A-3.4DE	3988	12447	1363	5526	944	71.3	804	116	690	148	436	63.0	399	49.5
HLR19A-4.1L	6121	18331	2013	7612	1270	89.7	988	142	836	181	516	73.0	458	54.7
HLR19A-4.2D	4454	13733	1444	6176	1068	83.8	891	127	751	162	462	66.7	404	49.7
HLR19A-4.3ED	4092	12807	1298	5890	1044	80.1	895	132	778	166	470	69.0	424	51.6
HLR19A-5.1L	6301	17911	1860	6679	988	69.6	681	96	550	115	332	46.1	284	35.6
HLR19A-5.2ED	3912	12132	1266	5230	881	63.6	694	100	599	131	382	55.3	351	44.8
HLR19A-5.3L	5591	16080	1518	6450	1076	75.1	849	122	704	150	414	58.4	354	41.9
HLR19A-6.1D	4528	13148	1450	5456	835	96.0	635	86	497	106	303	43.7	293	37.4
HLR19A-6.2L	6750	19290	2027	8115	1292	128.6	972	135	761	158	447	60.3	357	43.4
HLR19A-6.3I	4165	12854	1459	5781	1001	87.2	826	120	704	152	437	62.4	396	50.2
HLR19A-6.4D	4324	12899	1364	5496	887	86.6	701	100	583	126	367	54.8	342	43.5
HLR19A-7.1L	6311	18060	1940	6933	1089	77.7	819	115	651	138	382	53.7	327	39.3
HLR19A-7.2D	4033	12531	1367	5501	947	68.9	795	116	682	147	422	62.0	377	45.9
HLR19A-8.1IE	4045	12712	1467	5672	991	73.4	820	123	719	158	440	65.5	407	50.7
HLR19A-8.2L	5552	17145	2132	7272	1237	87.9	999	146	868	186	529	77.7	480	58.4
HLR19A-8.3D	3924	12569	1585	5491	948	68.6	758	111	659	144	412	60.1	365	45.0
HLR19A-9.1IE	4756	14821	1853	6347	1069	81.4	845	121	712	156	442	64.0	394	48.3
HLR19A-9.2D	3931	12440	1561	5414	900	69.1	738	106	635	138	400	58.0	370	46.0
HLR19A-10.1LE	4052	12874	1655	5762	1012	78.3	835	121	717	156	441	64.3	395	48.2
HLR19A-11.1L	5742	17503	2149	7260	1174	86.4	902	130	772	167	485	68.4	425	50.2
HLR19A-11.2IE	4391	13673	1715	5841	985	71.3	797	116	695	149	439	65.0	401	49.0
HLR19A-12.1DE	3895	9790	1070	3553	521	92.4	414	56	313	69	198	29.9	203	28.8
HLR19A-12.2IE	3815	9907	1130	3943	644	105.2	526	70	403	85	235	34.0	228	30.0
HLR19A-12.3LE	4473	15098	2251	9422	1984	233.5	1598	216	1161	223	546	69.7	402	46.0
HLR19A-13.1IE	4530	13904	1764	6234	1060	104.2	867	122	717	153	430	61.9	380	46.8
HLR19A-13.2D	4199	12648	1556	5389	870	79.5	717	99	572	122	345	49.1	314	40.4
HLR19A-13.3I	4120	13874	2013	8397	1785	198.0	1526	206	1080	206	500	60.9	333	36.9
HLR19A-14.1L	4520	13866	1760	6319	1058	110.4	825	113	641	131	367	51.3	305	37.4
HLR19A-14.2I	4605	12060	1425	5143	884	112.7	685	88	480	95	251	33.4	210	27.7

Table E2. Trace element data from SHRIMP-RG analysis of sphene from the Highland Range silicic sequence.

Sample Spot	Li	Be	B	F	Na	Mg	Al	P	Cl	K
HRL12A-1.1modZ	2.13	0.119	0.237	6039	259	320	7576	203	9.23	2.03
HRL12A-1.2ltZ	1.57	0.133	0.000	8565	299	346	8385	165	8.70	1.94
HRL12A-2.1ltZ	5.55	1.209	0.469	2321	438	313	6947	330	4.32	2.65
HRL12A-2.2hvZ	6.15	0.526	0.452	2394	462	342	6630	351	8.32	2.93
HRL12A-2.3ltZ	1.56	0.978	0.078	7203	245	276	7208	194	9.15	3.20
HRL12A-3.1hvZ	2.70	0.157	0.078	5481	280	332	7539	190	6.26	2.82
HRL12A-3.2modZ	2.89	0.041	0.082	5779	279	309	7491	175	8.52	2.66
HRL12A-3.3hvZ	7.49	0.076	0.151	3011	440	345	7108	286	6.50	2.71
HRL12A-3.4modZ	2.85	0.044	0.267	6642	349	366	7647	188	3.83	3.51
HRL12A-4.1hvZ	5.39	0.079	0.315	5037	544	493	7721	350	11.60	3.77
HRL12A-4.2ltZ	2.19	0.149	0.075	7555	330	366	7452	186	6.44	2.00
HRL12A-4.3modZ	1.73	0.651	0.384	6706	268	319	7906	173	11.30	2.55
HRL12A-5.1hvZ	1.72	0.260	0.074	6199	303	365	7578	172	10.06	2.10
HRL12A-5.2ltZ	2.06	0.227	0.304	6151	271	289	7268	191	12.12	1.88
HRL12A-6.1LOZ	2.23	0.072	0.217	5768	226	274	7177	163	13.32	8.50
HRL12A-6.2MODZ	2.60	0.342	0.000	5449	258	307	7993	178	10.28	2.72
HRL12A-6.3HIZ	1.51	0.336	0.149	4999	255	314	8173	1658	31.20	4.49
<hr/>										
HRL14A-1.1lowZ	1.94	0.211	0.254	5812	277	349	7930	197	8.84	2.99
HRL14A-1.2hvZ	5.64	0.277	0.185	3905	369	327	7617	209	4.54	2.50
HRL14A-2.1lowZ	1.96	0.084	0.169	6824	317	330	7451	181	8.82	2.22
HRL14A-2.2modZ	5.15	0.040	0.080	3132	416	282	6710	251	8.87	2.35
HRL14A-3.1hvZ	6.12	0.309	0.177	3661	529	333	7362	676	8.13	2.71
HRL14A-3.2lowZ	3.20	0.723	0.272	5429	441	302	6891	157	5.00	2.79
HRL14A-3.3modZ	3.03	0.447	0.163	4942	352	343	7262	187	13.48	2.73
HRL14A-3.4hvZ	0.34	0.000	0.163	6430	297	340	7809	167	13.04	3.03
HRL14A-4.1lowZ	0.01	0.116	0.772	5686	250	277	7186	194	10.43	2.26
HRL14A-4.2hvZ	9.17	0.466	0.544	2707	382	389	7534	348	12.41	24.79
HRL14A-4.3modZ	0.02	0.000	0.000	7102	248	306	8058	176	8.03	2.71
HRL14A-5.1modZ	1.34	0.196	0.000	6387	342	376	7278	187	7.24	2.18
HRL14A-5.2lowZ	2.49	0.276	0.000	7703	359	358	7328	182	9.07	3.60

Table E2, continued

Sample Spot	Ca	Sc	Ti	V	Cr	Mn	Fe	Co	Ni	Zn
HRL12A-1.1modZ	211082	58.8	230658	318	18.9	2261	19218	0.151	0.873	20.2
HRL12A-1.2ltZ	217837	85.6	232207	244	3.54	2782	22992	0.169	0.837	41.2
HRL12A-2.1ltZ	209067	25.6	230876	370	9.64	1783	18312	0.111	0.738	45.4
HRL12A-2.2hvZ	195919	23.9	227271	379	10.70	1753	19004	0.153	0.697	33.3
HRL12A-2.3ltZ	214340	68.5	231700	314	9.35	2142	18679	0.139	0.849	32.8
HRL12A-3.1hvZ	210435	41.3	233737	297	13.57	2046	19771	0.143	0.509	38.2
HRL12A-3.2modZ	215538	47.7	234883	268	7.97	2138	18866	0.124	0.756	22.8
HRL12A-3.3hvZ	207870	32.0	232453	268	7.18	1980	19038	0.144	0.864	36.9
HRL12A-3.4modZ	212756	59.6	232828	202	2.38	2655	20515	0.168	0.701	14.5
HRL12A-4.1hvZ	208825	85.3	227772	196	12.06	3579	22817	0.179	0.930	31.1
HRL12A-4.2ltz	210229	83.3	227913	243	4.86	2834	20693	0.122	0.723	26.1
HRL12A-4.3modZ	212353	71.0	223410	306	10.14	2267	21755	0.154	0.725	30.3
HRL12A-5.1hvZ	202589	46.2	228972	313	17.64	2335	20596	0.131	0.895	22.5
HRL12A-5.2ltZ	212302	54.3	231458	325	4.37	1952	19056	0.147	0.688	33.5
HRL12A-6.1LOZ	208494	44.3	230113	300	7.18	2182	19721	0.155	0.841	30.3
HRL12A-6.2MODZ	210940	36.2	230810	368	13.21	1896	20513	0.143	0.405	33.6
HRL12A-6.3HIZ	209983	40.9	225088	417	9.35	1744	20538	0.146	0.913	29.5
<hr/>										
HRL14A-1.1lowZ	213224	49.3	234166	241	18.16	2179	20555	0.133	0.751	29.5
HRL14A-1.2hvZ	216901	29.0	235594	363	14.63	2014	20801	0.157	0.564	32.2
HRL14A-2.1lowZ	209430	50.8	228108	119	1.60	2463	20501	0.174	0.466	35.3
HRL14A-2.2modZ	210086	38.7	234289	104	0.23	2475	17710	0.077	0.775	33.6
HRL14A-3.1hvZ	218381	44.6	237056	85	0.22	2802	19418	0.064	0.574	34.9
HRL14A-3.2lowZ	217483	43.4	242522	83	0.30	2851	18316	0.119	0.820	29.4
HRL14A-3.3modZ	210988	47.4	230317	137	2.68	2602	19031	0.099	0.577	35.9
HRL14A-3.4hvZ	211836	42.3	231431	253	7.56	2158	20371	0.112	0.515	28.5
HRL14A-4.1lowZ	207696	44.9	218426	186	0.47	2074	20370	0.119	0.791	37.7
HRL14A-4.2hvZ	207643	30.7	229071	242	1.95	1965	17399	0.126	0.904	48.8
HRL14A-4.3modZ	212339	45.2	225216	199	0.56	2102	20539	0.149	0.651	35.7
HRL14A-5.1modZ	207361	53.2	226047	242	7.18	2484	20556	0.105	0.743	32.9
HRL14A-5.2lowZ	212290	58.3	227548	105	1.65	2905	21063	0.133	0.527	40.7

Table E2, continued

Sample Spot	Ga	Ge	Sr	Y	Zr	Zr	Zr	Nb	Sn	Ba
HRL12A-1.1modZ	3.68	4.04	15.1	5943	698	701	698	2721	313	1.02
HRL12A-1.2ltZ	3.93	4.41	6.03	4882	742	754	742	2715	391	0.43
HRL12A-2.1ltZ	3.28	3.15	26.67	8235	769	763	763	3633	392	0.34
HRL12A-2.2hvZ	3.33	4.05	24.58	9899	834	823	823	3748	397	0.00
HRL12A-2.3ltZ	3.25	4.43	13.49	3336	651	635	635	2627	277	0.34
HRL12A-3.1hvZ	3.63	3.58	15.86	7617	741	741	741	2536	320	0.20
HRL12A-3.2modZ	3.47	4.83	11.50	5955	693	682	682	2754	341	0.02
HRL12A-3.3hvZ	3.44	3.26	10.25	10168	754	739	739	3211	391	0.19
HRL12A-3.4modZ	3.56	4.67	4.95	6696	650	626	626	2927	383	0.27
HRL12A-4.1hvZ	4.19	4.23	5.43	8834	925	914	914	6975	779	0.47
HRL12A-4.2ltz	3.70	4.43	5.59	4822	719	691	691	3390	408	0.24
HRL12A-4.3modZ	3.96	4.43	9.85	5948	781	770	770	2480	352	0.28
HRL12A-5.1hvZ	3.56	3.51	13.10	7097	805	814	805	2610	394	0.17
HRL12A-5.2ltZ	3.25	3.47	12.98	5114	939	942	939	1946	310	0.11
HRL12A-6.1LOZ	3.49	4.47	11.98	6024	700	700	700	2293	371	0.28
HRL12A-6.2MODZ	3.46	2.87	18.88	7343	734	730	730	2068	316	0.11
HRL12A-6.3HIZ	3.64	2.31	36.18	8294	909	915	909	1772	283	0.41
<hr/>										
HRL14A-1.1lowZ	3.65	3.19	10.83	8288	747	727	727	2821	342	0.10
HRL14A-1.2hvZ	3.75	2.86	17.14	10714	753	740	740	2414	315	0.06
HRL14A-2.1lowZ	3.59	4.20	4.88	7133	626	608	608	2980	373	0.23
HRL14A-2.2modZ	3.48	3.56	4.04	8402	616	575	575	4658	533	0.07
HRL14A-3.1hvZ	3.57	4.39	2.73	8986	732	708	708	6258	684	0.31
HRL14A-3.2lowZ	3.25	5.84	2.16	7526	546	513	513	4251	551	0.25
HRL14A-3.3modZ	3.36	5.25	3.45	7772	618	586	586	3252	394	0.37
HRL14A-3.4hvZ	3.58	3.41	8.18	8593	668	646	646	2430	350	0.09
HRL14A-4.1lowZ	3.50	3.32	7.92	6723	688	674	674	2945	326	0.27
HRL14A-4.2hvZ	3.14	4.91	16.28	7663	828	839	828	4755	398	0.13
HRL14A-4.3modZ	3.51	6.20	7.45	7609	709	707	707	2434	359	0.25
HRL14A-5.1modZ	3.58	4.76	7.99	7613	697	695	695	2656	351	0.05
HRL14A-5.2lowZ	3.78	4.59	2.79	6807	630	612	612	3369	449	0.53

Table E2, continued

Sample Spot	Hf	Ta	^{208}Pb	Th	U
HRL12A-1.1modZ	44.9	272		332	29.7
HRL12A-1.2ltZ	58.7	277		325	28.5
HRL12A-2.1ltZ	48.4	580		427	22.9
HRL12A-2.2hvZ	52.1	563		349	21.4
HRL12A-2.3ltZ	39.9	219		329	27.3
HRL12A-3.1hvZ	49.4	220		242	20.6
HRL12A-3.2modZ	47.9	254		262	20.7
HRL12A-3.3hvZ	46.3	371		315	18.0
HRL12A-3.4modZ	44.7	258		302	22.1
HRL12A-4.1hvZ	98.6	946		686	42.5
HRL12A-4.2ltz	50.5	296		353	32.3
HRL12A-4.3modZ	50.7	242		344	29.3
HRL12A-5.1hvZ	54.7	242		332	26.7
HRL12A-5.2ltZ	53.6	180		265	22.3
HRL12A-6.1LOZ	47.9	212		311	25.0
HRL12A-6.2MODZ	45.5	205		290	23.6
HRL12A-6.3HIZ	50.8	194		270	20.8
HRL14A-1.1lowZ	54.3	272		288	23.3
HRL14A-1.2hvZ	44.7	263		228	17.7
HRL14A-2.1lowZ	43.2	285		262	22.5
HRL14A-2.2modZ	47.5	563		493	26.8
HRL14A-3.1hvZ	60.8	869		542	29.8
HRL14A-3.2lowZ	44.3	404		317	23.1
HRL14A-3.3modZ	46.2	315		293	22.2
HRL14A-3.4hvZ	41.7	223		246	20.5
HRL14A-4.1lowZ	45.3	289		279	27.4
HRL14A-4.2hvZ	58.4	630		410	23.1
HRL14A-4.3modZ	48.3	242		308	25.2
HRL14A-5.1modZ	44.4	247		289	24.2
HRL14A-5.2lowZ	48.3	311		255	23.7

Table E2, continued

236

Sample Spot	Li	Be	B	F	Na	Mg	Al	P	Cl	K
HRL21-1.1	2.5	3.7	0.4	6698	512	874	8015	273	14	7
HRL21-1.2D	1.9	3.5	0.3	9858	381	878	9169	184	9	2
HRL21-2.1DE	1.0	0.0	0.1	5816	205	229	7193	148	7	1
HRL21-2.2D	0.9	0.0	0.2	5292	175	249	6797	184	7	1
HRL21-2.3DC	0.8	2.5	0.4	5070	213	302	7845	227	7	2
HRL21-2.4L	0.9	0.0	0.1	3393	179	287	6762	235	7	1
HRL21-3.1ED	4.4	3.5	0.3	10292	391	869	9526	178	7	2
HRL21-3.2D	3.2	2.3	0.1	8999	351	848	9198	219	11	3
HRL21-3.3LC	3.0	2.5	0.4	9366	395	1068	9873	230	8	3
HRL21-4.1ED	4.2	1.2	0.6	8830	408	864	9013	185	15	2
HRL21-5.1ED	1.9	3.6	0.1	5535	207	338	8149	188	11	3
HRL21-5.1ED	1.9	3.6	0.1	5535	207	338	8149	188	11	3
HRL21-5.2LC	3.3	3.6	0.4	3399	301	325	7173	276	22	3
HRL21-6..1DE	2.5	44.2	12.9	2103	2383	167	27282	87	66	15545
HRL21-6.2LC	2.3	1.2	0.2	5309	225	341	7704	242	9	2
HLR21-6.3LC	3.7	8.4	0.0	3365	304	327	7318	346	8	1
HLR21-6.4ED	2.6	6.4	0.2	5059	265	326	7572	168	12	1
HRL21-7.1ED	6.3	3.7	0.4	8780	562	856	8483	163	7	3
HRL21-8.1ED	3.5	3.4	0.3	8991	349	853	8709	185	10	2
HLR21-8.2C	4.2	5.1	0.3	8813	409	895	9266	3384	80	2
HLR21-9.1ED	3.4	2.0	0.4	8915	363	834	8522	176	10	2
HLR21-9.2LC	8.6	2.2	0.6	6820	608	906	9504	262	12	2

Table E2, continued

Sample Spot	Ca	Sc	Ti	V	Cr	Mn	Fe	Co	Ni	Zn
HRL21-1.1	191874	73.6	219072	119	2	2598	21353			
HRL21-1.2D	203591	99.6	221487	121	1	2356	22954			
HRL21-2.1DE	198129	70.3	225182	125	4	1977	17467			
HRL21-2.2D	204021	37.0	228494	148	20	1484	16632			
HRL21-2.3DC	207901	37.8	230566	129	24	1340	18062			
HRL21-2.4L	179541	31.3	213632	126	28	1158	16156			
HRL21-3.1ED	201388	82.1	217343	120	1	3013	23683			
HRL21-3.2D	197168	93.5	217357	124	2	2101	21345			
HRL21-3.3LC	206557	75.9	217052	121	8	1784	23770			
HRL21-4.1ED	190255	83.5	220024	123	1	2809	22719			
HRL21-5.1ED	197497	42.6	219312	124	1	1834	21367			
HRL21-5.1ED	197497	42.6	219312	124	1	1834	21367			
HRL21-5.2LC	189389	37.2	219020	125	0	1756	18853			
HRL21-6..1DE	77406	18.9	89872	47	1	816	8040			
HRL21-6.2LC	195282	42.0	219855	138	1	1812	20056			
HLR21-6.3LC	188922	37.5	222193	129	0	1776	18911			
HLR21-6.4ED	201015	42.6	226244	119	1	1920	19712			
HRL21-7.1ED	206859	70.1	225731	132	2	3019	21643			
HRL21-8.1ED	182591	79.3	208201	142	1	2778	22178			
HLR21-8.2C	204263	80.0	221442	121	3	2069	22175			
HLR21-9.1ED	181241	79.3	207526	111	1	2720	21612			
HLR21-9.2LC	207942	63.2	231427	114	1	2559	22145			

Table E2, continued

Sample Spot	Ga	Ge	Sr	Y	Zr	Zr	Zr	Nb	Sn	Ba
HRL21-1.1			5	7791	1184	1159		3196		13
HRL21-1.2D			7	6103	1178	1155		2605		17
HRL21-2.1DE			9	3953	634	579		2718		13
HRL21-2.2D			33	3544	690	616		1957		16
HRL21-2.3DC			42	5082	809	788		2382		17
HRL21-2.4L			48	5855	905	797		2348		10
HRL21-3.1ED			4	7068	1018	980		2366		17
HRL21-3.2D			11	6102	1306	1353		2117		15
HRL21-3.3LC			19	9408	1494	1400		1879		17
HRL21-4.1ED			5	7366	1116	1086		2833		18
HRL21-5.1ED			11	8498	861	843		2180		15
HRL21-5.1ED			11	8498	861	843		2180		15
HRL21-5.2LC			13	9151	1133	1087		3722		8
HRL21-6..1DE			6	2986	325	344		1279		5
HRL21-6.2LC			12	8426	943	928		3198		15
HLR21-6.3LC			12	9686	1185	1146		4315		9
HLR21-6.4ED			12	7409	749	648		2751		14
HRL21-7.1ED			5	6753	936	940		3003		17
HRL21-8.1ED			4	7248	1068	1052		2561		12
HLR21-8.2C			19	7286	1474	1560		1906		13
HLR21-9.1ED			4	7032	1005	990		2704		9
HLR21-9.2LC			8	8778	1380	1393		2485		12

Table E2, continued

Sample Spot	Hf	Ta	208Pb	Th	U
HRL21-1.1	69.5	288	3.4	445	24
HRL21-1.2D	67.2	210	3.0	351	27
HRL21-2.1DE	50.2	262	3.3	500	39
HRL21-2.2D	37.4	198	2.4	413	32
HRL21-2.3DC	52.4	286	2.8	391	37
HRL21-2.4L	49.9	283	1.9	360	30
HRL21-3.1ED	70.9	164	3.4	304	25
HRL21-3.2D	72.1	170	2.8	331	25
HRL21-3.3LC	89.4	191	3.7	363	29
HRL21-4.1ED	72.3	209	3.7	343	25
HRL21-5.1ED	57.9	277	2.7	287	24
HRL21-5.1ED	57.9	277	2.7	287	24
HRL21-5.2LC	75.6	474	3.1	384	21
HRL21-6..1DE	20.3	123	3.7	141	13
HRL21-6.2LC	64.9	363	3.1	321	25
HLR21-6.3LC	89.1	729	2.8	437	23
HLR21-6.4ED	52.9	272	2.4	317	24
HRL21-7.1ED	51.7	250	4.3	307	23
HRL21-8.1ED	62.8	181	3.3	326	23
HLR21-8.2C	76.1	167	3.5	297	22
HLR21-9.1ED	60.2	190	2.8	324	24
HLR21-9.2LC	72.3	258	3.1	283	17

Table E2, continued

Sample Spot	Li	Be	B	F	Na	Mg	Al	P	Cl	K
HLR19A-1.2D	0.7	2.1	0.5	5859	236	250	7341	170	13	1
HLR19A-1.1L	1.8	3.1	0.2	3227	311	242	6288	303	15	1
HLR19A-1.3E	0.8	1.0	0.3	6338	204	236	6974	135	16	1
HLR19A-1.4D	0.4	1.0	0.2	5884	214	277	6650	208	8	1
HLR19A-2.1ED	0.9	0.0	0.3	5107	185	218	6323	138	8	1
HLR19A-2.2L	0.7	1.0	0.2	6098	184	231	7604	149	11	2
HLR19A-2.3DC	1.0	0.0	0.2	4927	126	212	6582	194	9	2
HLR19A-2.4LC	1.0	1.0	0.3	4615	185	296	7890	218	6	1
HLR19A-3.1ED	1.0	0.0	0.1	5394	255	225	6803	151	9	1
HLR19A-3.2L	1.8	3.2	0.2	4145	405	294	7489	354	14	1
HLR19A-3.3DC	0.6	0.0	0.2	6604	244	278	7738	183	16	3
HLR19A-3.4DE	0.7	2.1	0.2	7271	232	265	7597	155	10	2
HLR19A-4.1L	2.1	2.0	0.5	3245	351	261	6265	282	10	2
HLR19A-4.2D	0.9	1.0	0.1	5955	247	235	6755	196	10	1
HLR19A-4.3ED	0.8	0.0	0.2	8351	222	259	8158	142	12	2
HLR19A-5.1L	1.5	2.0	0.2	3199	252	206	6030	255	5	3
HLR19A-5.2ED	0.8	0.0	0.3	6364	219	240	6845	163	11	1
HLR19A-5.3L	1.6	1.0	0.1	4979	329	243	8013	244	9	2
HLR19A-6.1D	0.7	0.0	0.0	5152	141	206	6884	176	5	1
HLR19A-6.2L	1.5	1.0	0.3	2788	297	234	6253	310	13	2
HLR19A-6.3I	0.9	1.0	0.2	6595	195	246	7337	170	12	2
HLR19A-6.4D	0.7	0.0	0.7	6204	161	219	7113	168	12	1
HLR19A-7.1L	1.5	1.9	0.1	4167	319	244	7320	264	13	1
HLR19A-7.2D	0.9	0.0	0.3	7459	215	273	7076	175	12	2
HLR19A-8.1IE	0.8	1.0	0.3	8024	222	262	7980	129	9	2
HLR19A-8.2L	2.1	2.1	0.2	3793	399	274	6940	262	8	1
HLR19A-8.3D	0.9	0.0	0.2	6320	214	234	6949	148	11	1
HLR19A-9.1IE	1.1	2.0	0.0	5749	262	249	7095	188	7	1
HLR19A-9.2D	0.8	1.0	0.0	7270	221	255	7178	166	6	1
HLR19A-10.1LE	0.8	1.0	0.1	7749	209	261	7820	133	12	1
HLR19A-11.1L	1.6	0.9	0.1	3653	314	241	6043	291	13	1
HLR19A-11.2IE	0.8	0.9	0.3	5878	267	236	6931	189	13	1
HLR19A-12.1DE	0.7	0.0	0.1	5721	136	199	7023	229	11	2
HLR19A-12.2IE	0.8	0.0	0.4	5495	126	204	6959	220	14	1
HLR19A-12.3LE	1.0	1.0	0.2	4109	197	282	7654	223	10	2
HLR19A-13.1IE	0.8	0.0	0.1	7254	192	245	8055	143	8	2
HLR19A-13.2D	0.5	0.0	0.1	6866	185	211	7390	169	7	2
HLR19A-13.3I	0.6	1.0	0.1	4141	146	172	6899	187	8	1
HLR19A-14.1L	0.8	0.9	0.3	5935	174	225	7036	158	13	3
HLR19A-14.2I	0.9	1.9	0.0	5612	161	209	6806	206	12	2

Table E2, continued

Sample Spot	Ca	Sc	Ti	V	Cr	Mn	Fe	Co	Ni	Zn
HLR19A-1.2D	197403	81.5	222495	121	0	2294	17923			
HLR19A-1.1L	184098	66.5	216785	114	0	2084	16350			
HLR19A-1.3E	189590	75.1	218247	115	1	2074	17583			
HLR19A-1.4D	191591	98.5	221210	116	0	2096	19131			
HLR19A-2.1ED	187388	63.4	219297	111	2	1991	15884			
HLR19A-2.2L	203646	51.4	229616	114	11	1708	17899			
HLR19A-2.3DC	190991	33.5	222063	112	9	1416	14645			
HLR19A-2.4LC	197164	56.2	225682	110	4	1377	18012			
HLR19A-3.1ED	197605	65.9	224123	108	0	2162	16331			
HLR19A-3.2L	211009	80.0	229940	110	0	2378	19285			
HLR19A-3.3DC	212353	98.8	225124	114	0	2263	20508			
HLR19A-3.4DE	210160	82.0	230572	114	1	2260	18942			
HLR19A-4.1L	193827	66.8	221888	105	1	2083	16736			
HLR19A-4.2D	201843	77.5	224316	106	1	2087	18167			
HLR19A-4.3ED	208081	87.7	228423	112	1	2166	20427			
HLR19A-5.1L	176852	50.3	213973	98	0	1968	12955			
HLR19A-5.2ED	192834	76.6	219817	109	0	2102	16926			
HLR19A-5.3L	205217	55.0	225912	103	1	2281	15759			
HLR19A-6.1D	195618	45.6	223981	111	16	1517	15292			
HLR19A-6.2L	200403	42.0	229893	100	9	1613	15557			
HLR19A-6.3I	203659	65.6	228751	110	7	1950	17971			
HLR19A-6.4D	203492	55.6	229282	105	14	1697	16867			
HLR19A-7.1L	196449	55.8	223500	93	0	2158	15090			
HLR19A-7.2D	201480	94.0	225756	94	1	2164	19829			
HLR19A-8.1E	205042	85.7	224810	88	1	2204	19712			
HLR19A-8.2L	211529	69.6	233200	92	0	2278	17389			
HLR19A-8.3D	194387	76.3	221100	100	0	2129	17301			
HLR19A-9.1E	205317	77.3	231854	93	2	2185	17683			
HLR19A-9.2D	200570	82.8	222465	83	1	2146	18142			
HLR19A-10.1LE	205186	81.2	225561	94	1	2155	19402			
HLR19A-11.1L	190795	64.3	221646	89	0	2050	16148			
HLR19A-11.2IE	195427	77.1	220378	89	0	2150	17265			
HLR19A-12.1DE	206516	32.2	230990	95	8	1515	13855			
HLR19A-12.2IE	207044	34.8	231094	97	8	1555	13921			
HLR19A-12.3LE	207543	42.6	233459	90	22	1438	16886			
HLR19A-13.1IE	220212	57.6	238898	92	15	1879	18597			
HLR19A-13.2D	201984	87.2	223843	89	2	1686	19030			
HLR19A-13.3I	195642	57.0	223069	90	20	1424	16542			
HLR19A-14.1L	200647	54.6	225109	90	15	1660	16733			
HLR19A-14.2I	211081	38.6	233679	86	12	1609	15493			

Table E2, continued

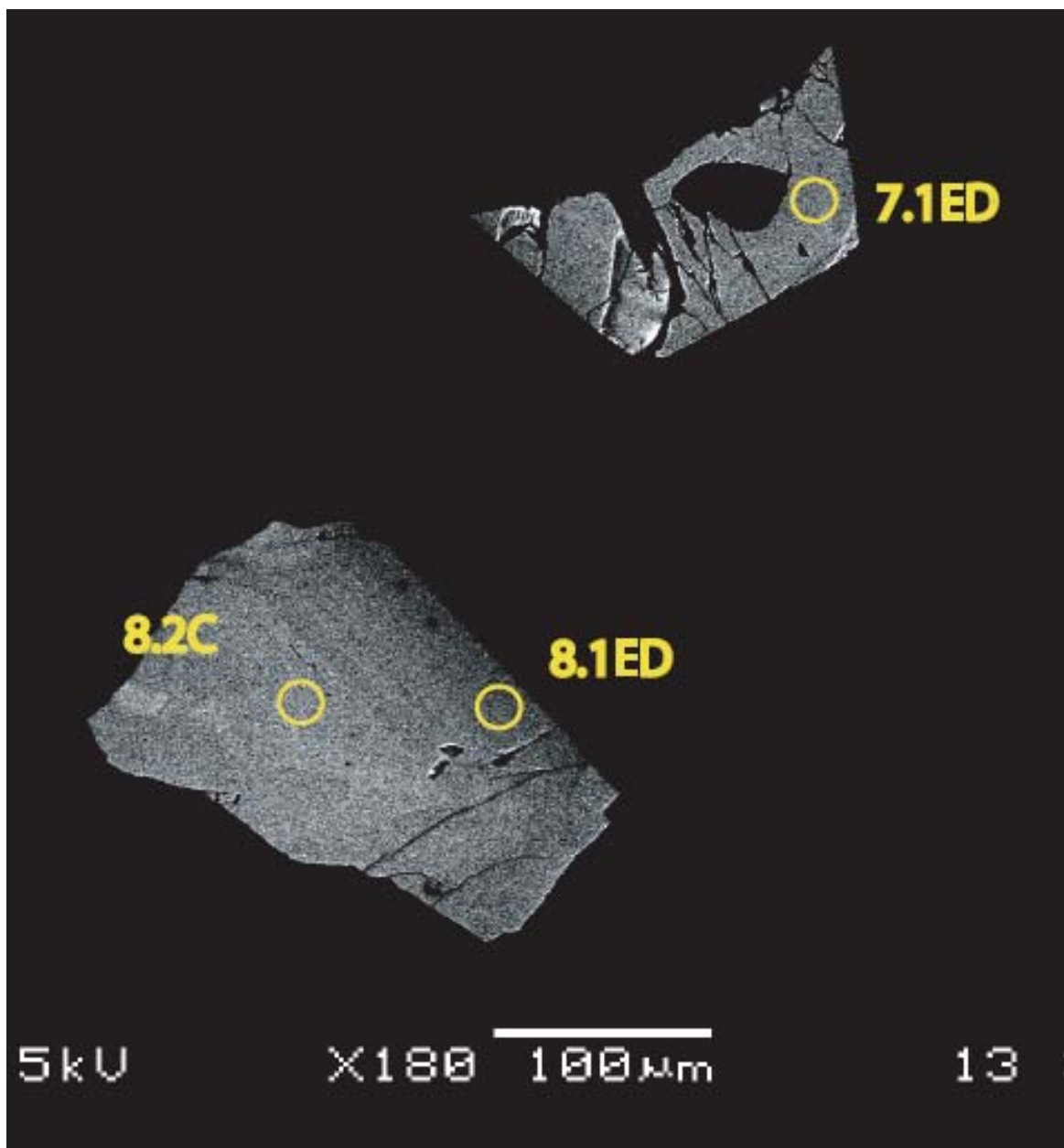
Sample Spot	Ga	Ge	Sr	Y	Zr	Zr	Zr	Nb	Sn	Ba
HLR19A-1.2D			5	3350	621	610		3321		12
HLR19A-1.1L			7	5022	987	979		7916		10
HLR19A-1.3E			6	4144	650	631		2694		9
HLR19A-1.4D			5	4218	742	727		3603		8
HLR19A-2.1ED			6	3884	591	551		3233		12
HLR19A-2.2L			17	3632	684	657		2247		10
HLR19A-2.3DC			39	3185	751	715		1628		11
HLR19A-2.4LC			50	5799	935	936		1623		12
HLR19A-3.1ED			5	4120	688	666		3801		10
HLR19A-3.2L			6	5069	1298	1307		10275		11
HLR19A-3.3DC			7	3740	1071	1006		3932		18
HLR19A-3.4DE			8	3783	646	581		3241		15
HLR19A-4.1L			8	4928	1009	986		7460		10
HLR19A-4.2D			8	4121	963	946		3962		11
HLR19A-4.3ED			8	4089	640	616		2508		12
HLR19A-5.1L			7	3488	732	702		5730		4
HLR19A-5.2ED			6	3692	633	607		3281		11
HLR19A-5.3L			8	3776	831	838		5768		14
HLR19A-6.1D			21	2921	646	622		2504		12
HLR19A-6.2L			20	4058	812	766		4373		7
HLR19A-6.3I			13	3831	646	619		2935		11
HLR19A-6.4D			15	3309	655	632		2859		10
HLR19A-7.1L			9	3730	831	850		5880		8
HLR19A-7.2D			8	3872	680	657		3278		11
HLR19A-8.1IE			7	4103	640	646		2523		11
HLR19A-8.2L			7	4840	839	811		6247		9
HLR19A-8.3D			6	3990	668	644		3423		8
HLR19A-9.1IE			8	4248	862	817		4171		10
HLR19A-9.2D			8	3712	624	596		3116		9
HLR19A-10.1LE			7	4093	644	615		2543		12
HLR19A-11.1L			7	4706	745	737		5070		8
HLR19A-11.2IE			7	4079	858	835		3798		8
HLR19A-12.1DE			34	1870	660	652		1769		9
HLR19A-12.2IE			33	2213	658	650		1742		9
HLR19A-12.3LE			45	5028	754	720		2231		6
HLR19A-13.1IE			16	3756	647	609		2405		15
HLR19A-13.2D			10	3110	740	732		2641		10
HLR19A-13.3I			23	4718	946	918		2907		6
HLR19A-14.1L			19	3481	624	597		2460		9
HLR19A-14.2I			27	2321	675	638		2103		12

Table E2, continued

Sample Spot	Hf	Ta	^{208}Pb	Th	U
HLR19A-1.2D	42.4	327	2.5	364	38
HLR19A-1.1L	64.3	818	3.6	884	58
HLR19A-1.3E	41.4	250	2.2	468	38
HLR19A-1.4D	63.6	292	3.2	570	43
HLR19A-2.1ED	44.3	332	3.2	483	40
HLR19A-2.2L	49.6	224	2.8	444	38
HLR19A-2.3DC	42.4	158	2.6	391	26
HLR19A-2.4LC	47.4	180	3.0	368	22
HLR19A-3.1ED	48.9	373	2.9	505	40
HLR19A-3.2L	96.2	951	4.1	1006	68
HLR19A-3.3DC	177.8	390	2.6	435	40
HLR19A-3.4DE	53.3	321	3.7	482	40
HLR19A-4.1L	77.8	1132	3.8	881	52
HLR19A-4.2D	93.0	557	3.1	521	43
HLR19A-4.3ED	49.2	277	3.2	484	40
HLR19A-5.1L	55.3	667	3.4	651	38
HLR19A-5.2ED	43.1	317	2.7	448	39
HLR19A-5.3L	66.0	568	5.1	715	47
HLR19A-6.1D	37.9	243	2.1	423	38
HLR19A-6.2L	52.9	669	3.5	699	39
HLR19A-6.3I	45.4	303	2.9	437	39
HLR19A-6.4D	42.5	275	2.0	427	38
HLR19A-7.1L	61.5	599	4.9	722	43
HLR19A-7.2D	45.6	349	3.7	507	41
HLR19A-8.1IE	49.6	287	3.8	478	40
HLR19A-8.2L	68.9	907	4.5	850	52
HLR19A-8.3D	44.9	287	3.2	473	40
HLR19A-9.1IE	78.6	591	3.3	556	43
HLR19A-9.2D	43.1	305	2.8	459	38
HLR19A-10.1LE	47.7	258	2.6	460	39
HLR19A-11.1L	50.5	630	3.9	816	45
HLR19A-11.2IE	77.3	482	3.2	535	44
HLR19A-12.1DE	34.0	155	3.0	418	33
HLR19A-12.2IE	34.8	147	2.3	389	32
HLR19A-12.3LE	44.5	244	3.4	361	31
HLR19A-13.1IE	45.0	254	3.0	442	37
HLR19A-13.2D	72.7	312	2.9	495	41
HLR19A-13.3I	66.6	383	2.7	351	26
HLR19A-14.1L	37.6	236	3.2	433	34
HLR19A-14.2I	32.5	192	3.0	444	31

Figure E1:

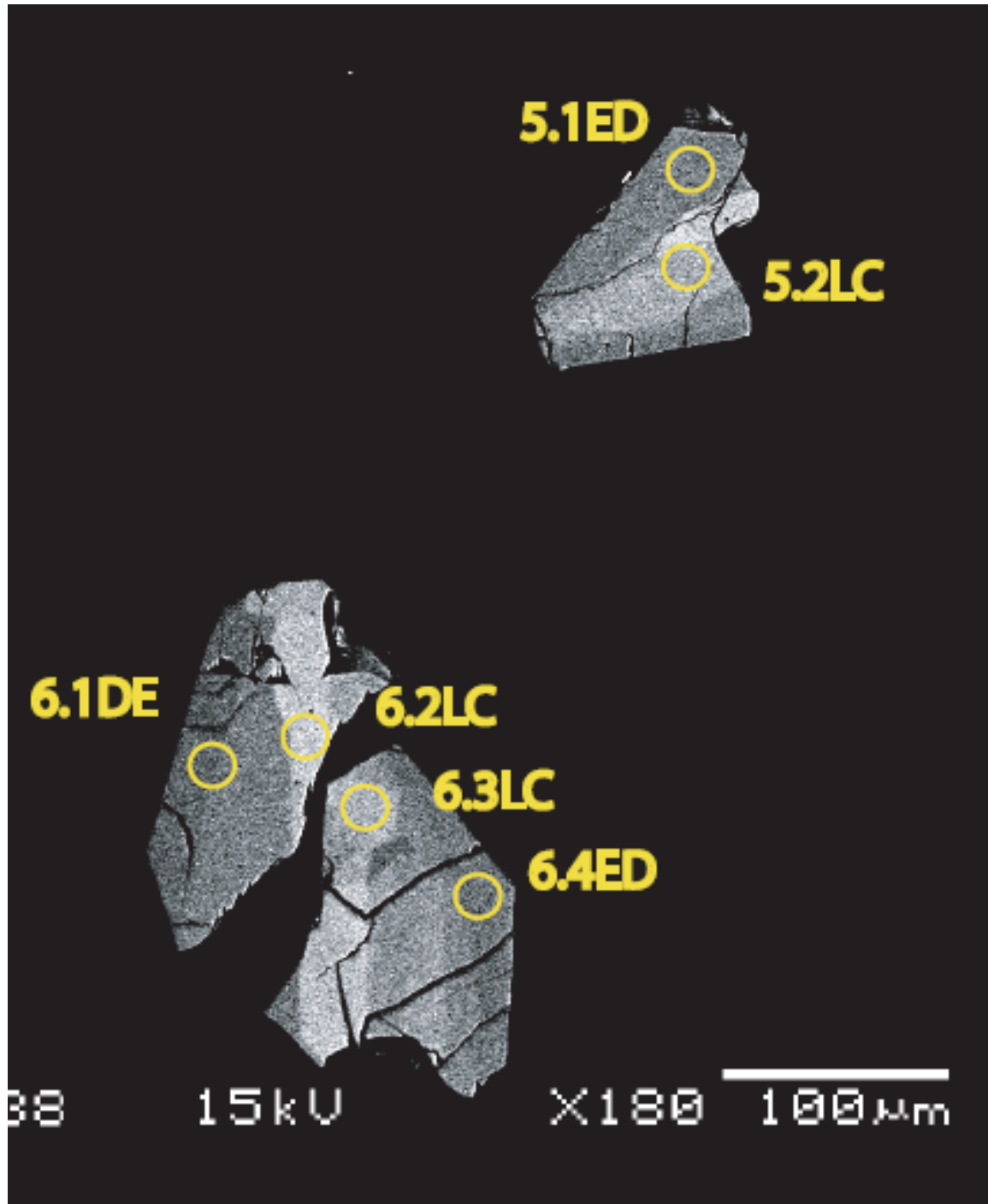
Backscatter electron images of sphene from sample HRL 21 with spots from Trace Element SHRIMP-RG analyses marked.



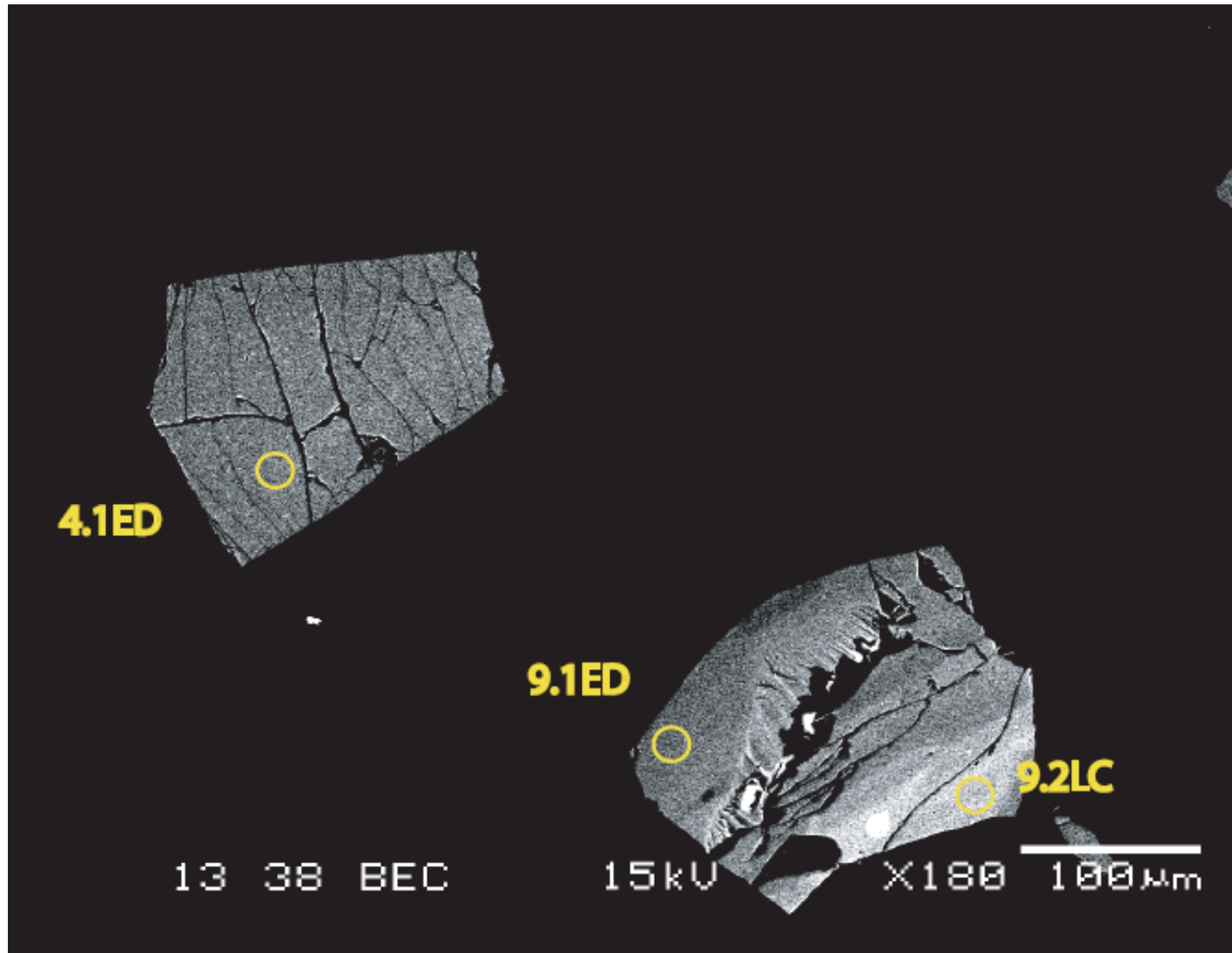
5kV

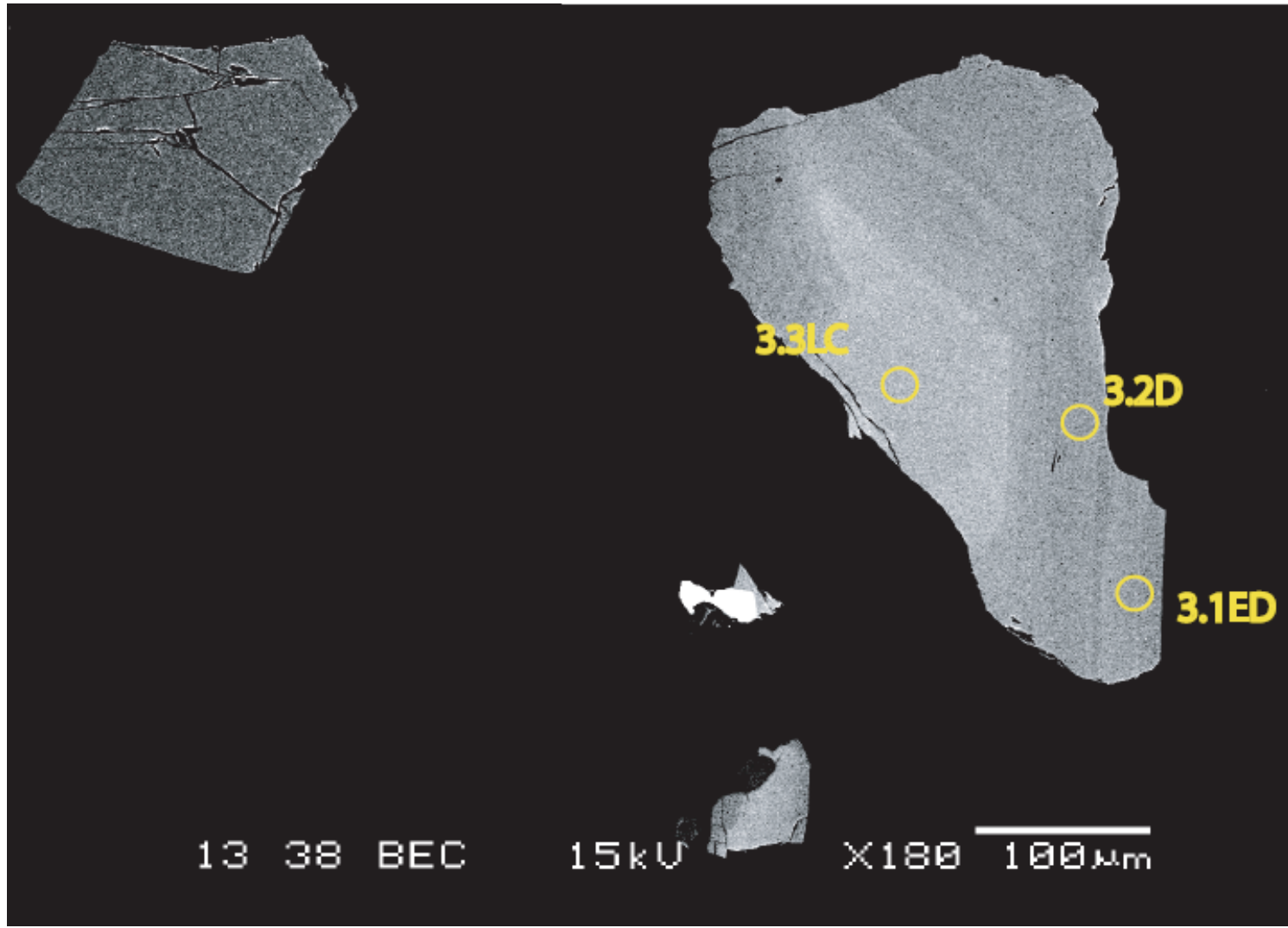
×180 100 μm

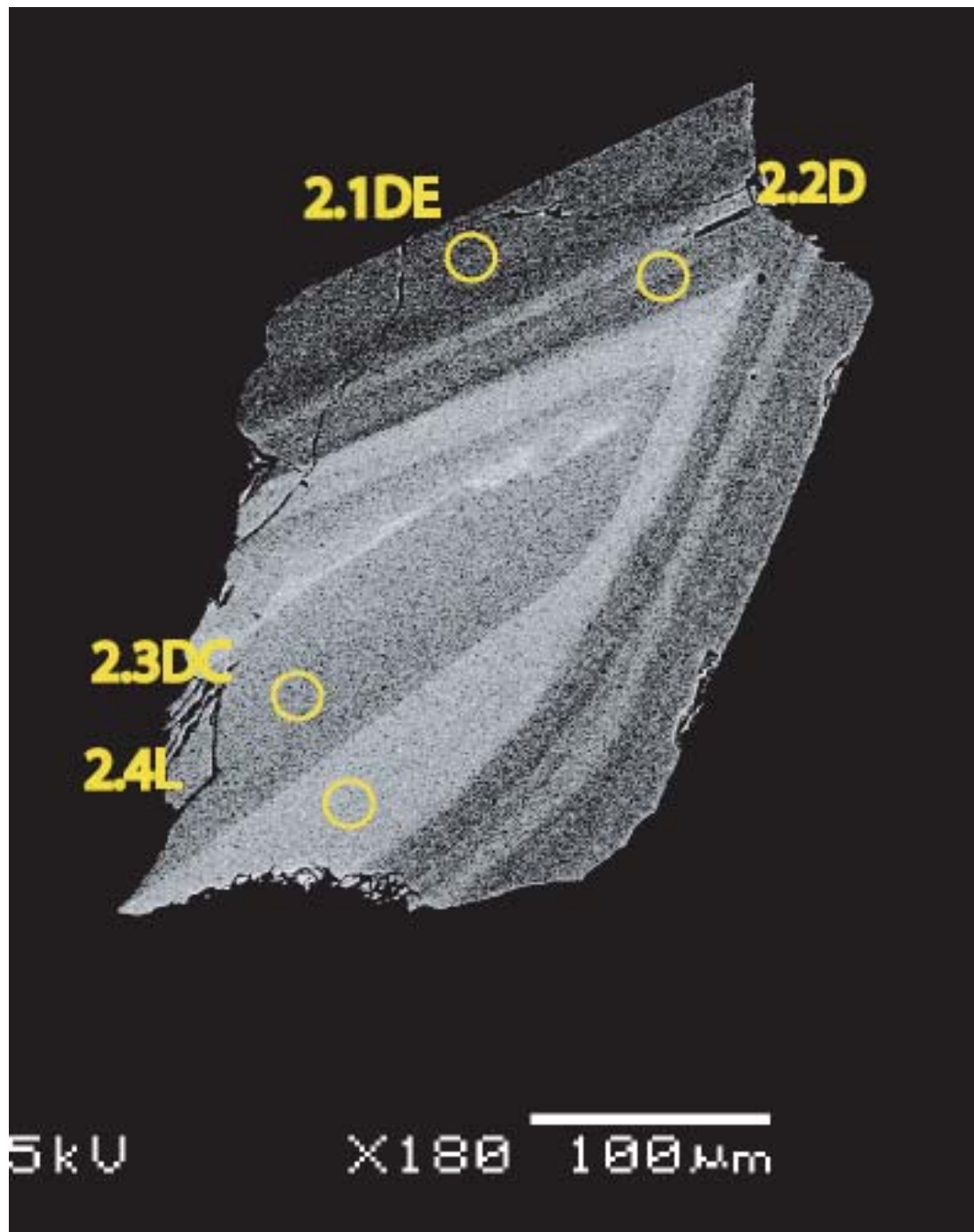
13



247







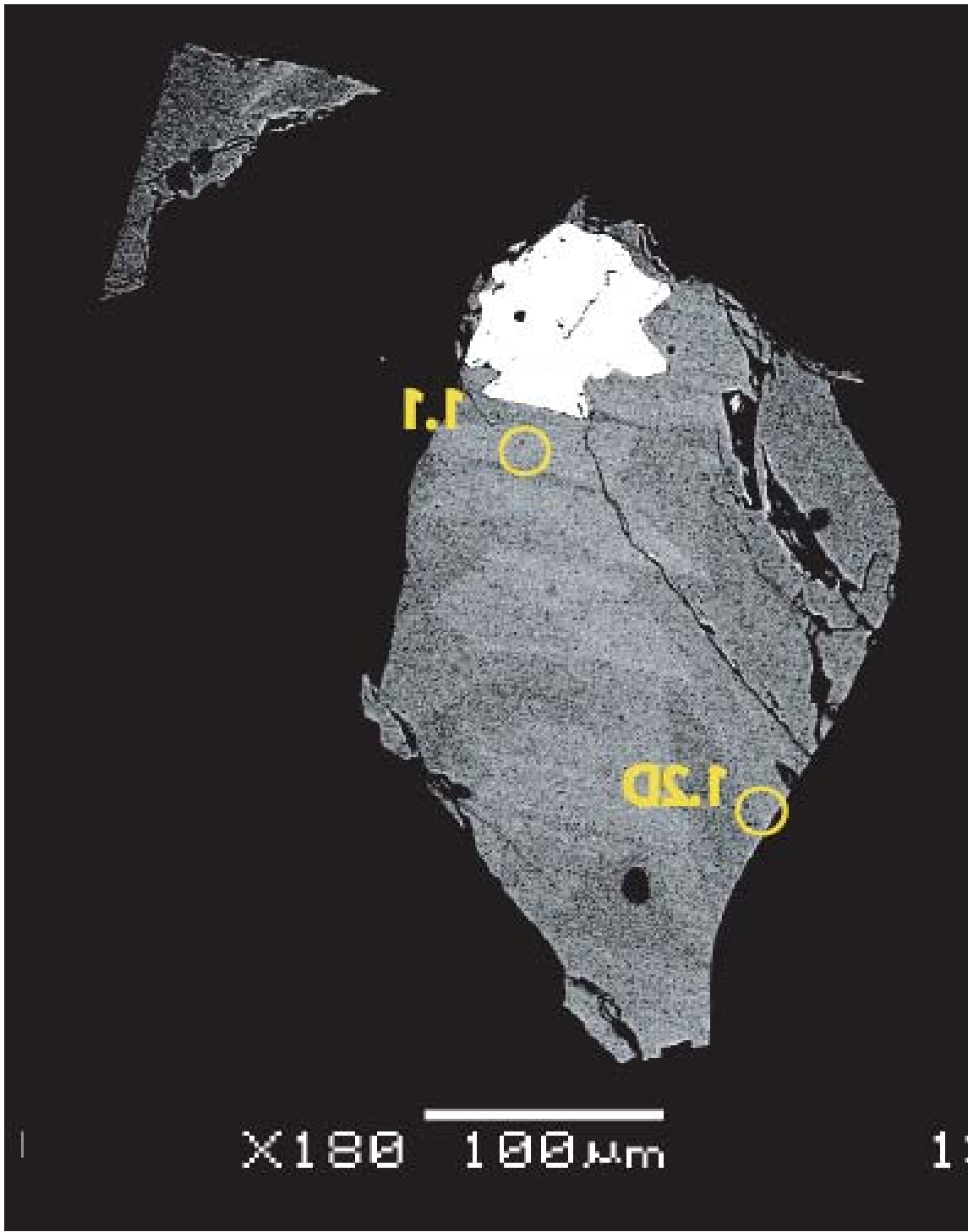
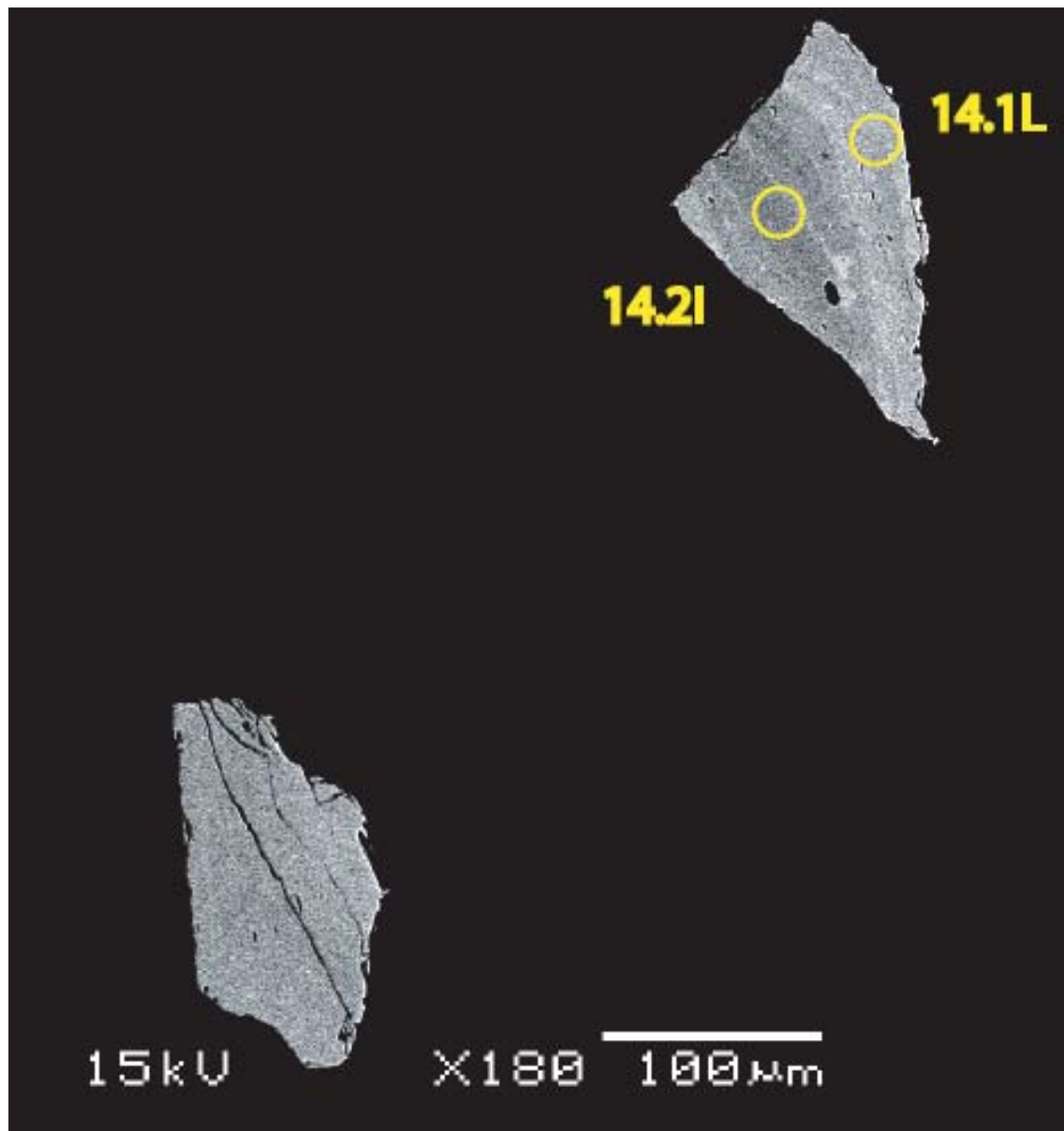
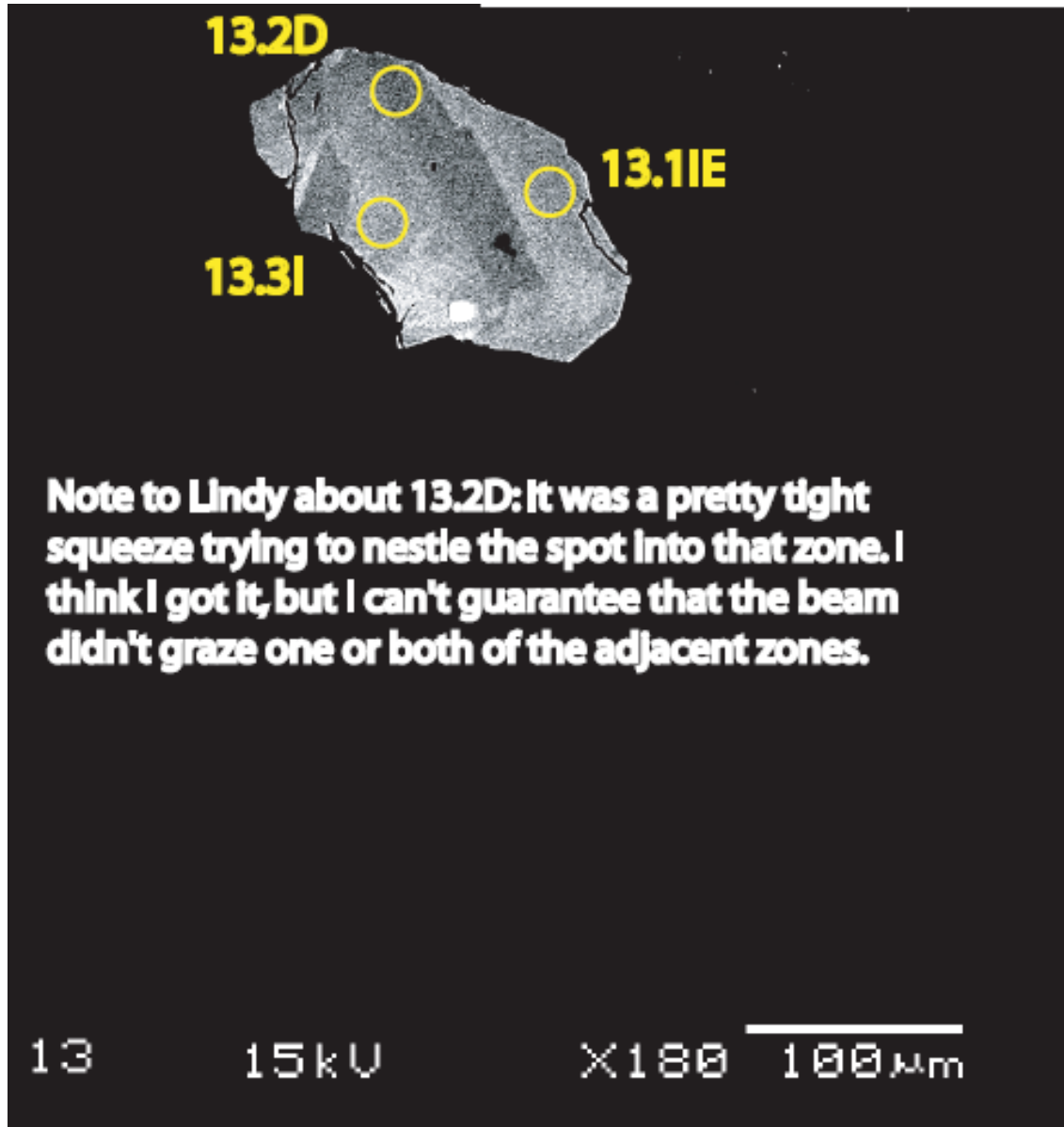


Figure E2:

Backscatter electron images of sphene from sample HRL 19a with spots from Trace Element SHRIMP-RG analyses marked.





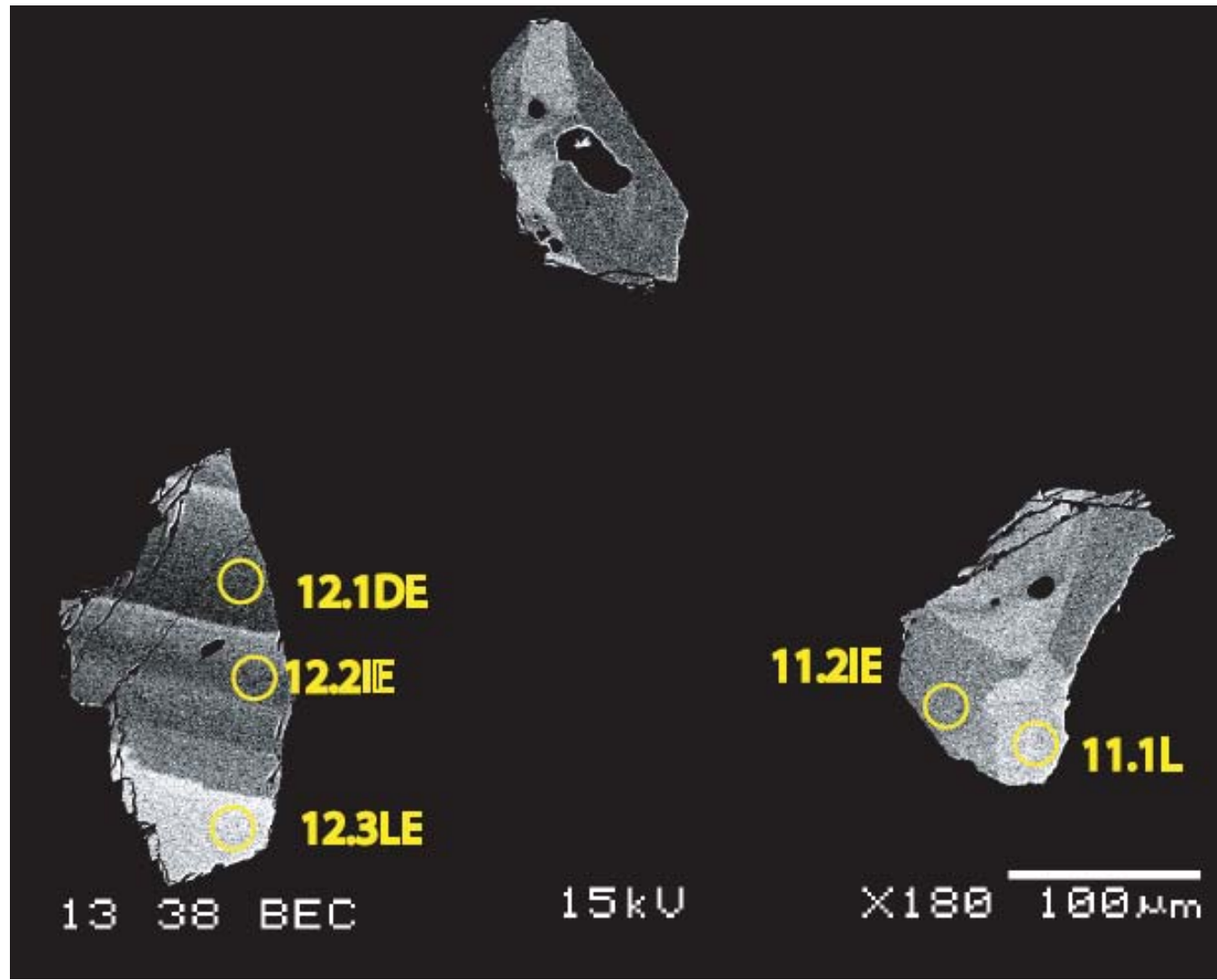
Note to Lindy about 13.2D: It was a pretty tight squeeze trying to nestle the spot into that zone. I think I got it, but I can't guarantee that the beam didn't graze one or both of the adjacent zones.

13

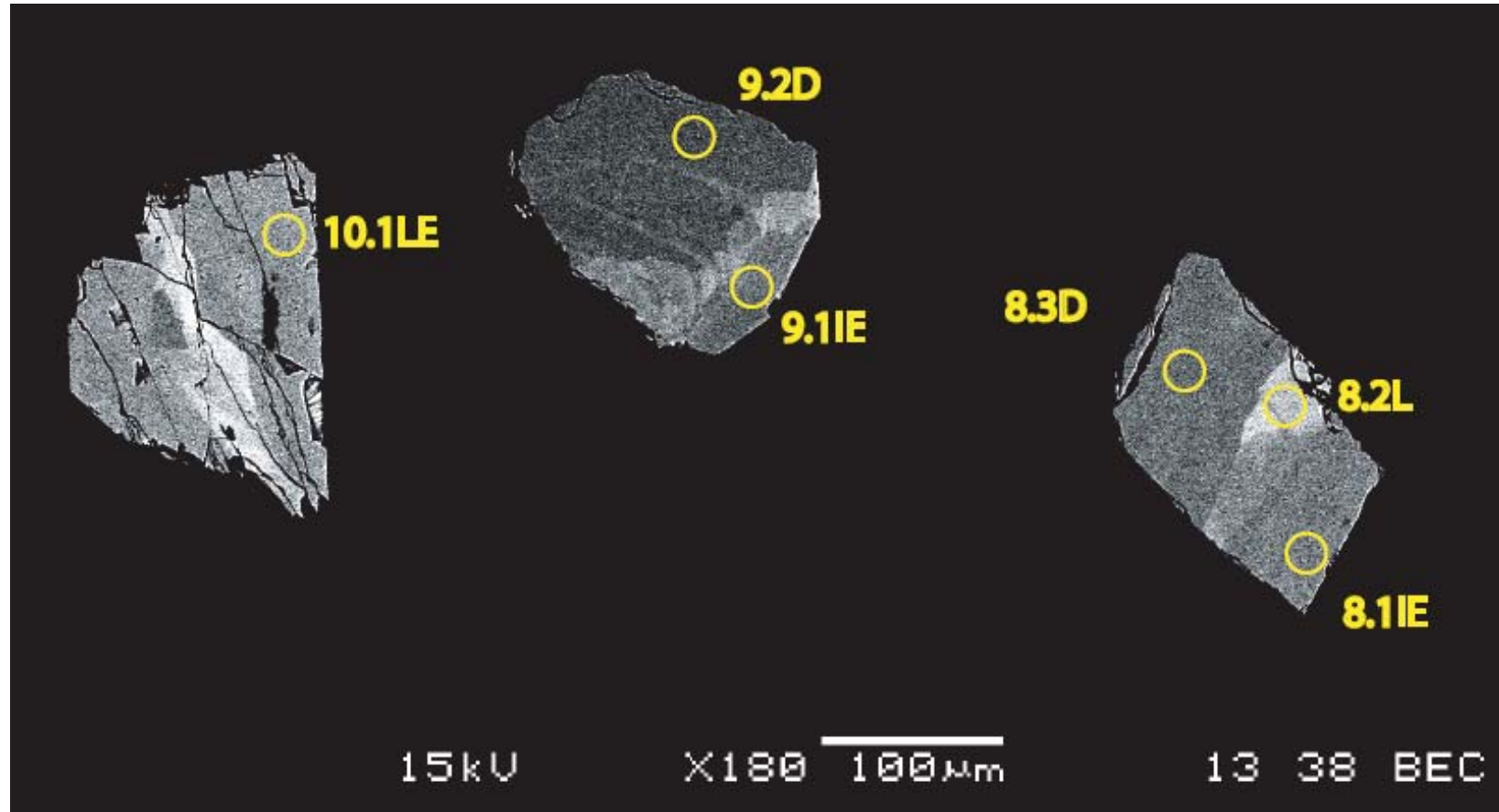
15 kV

×180

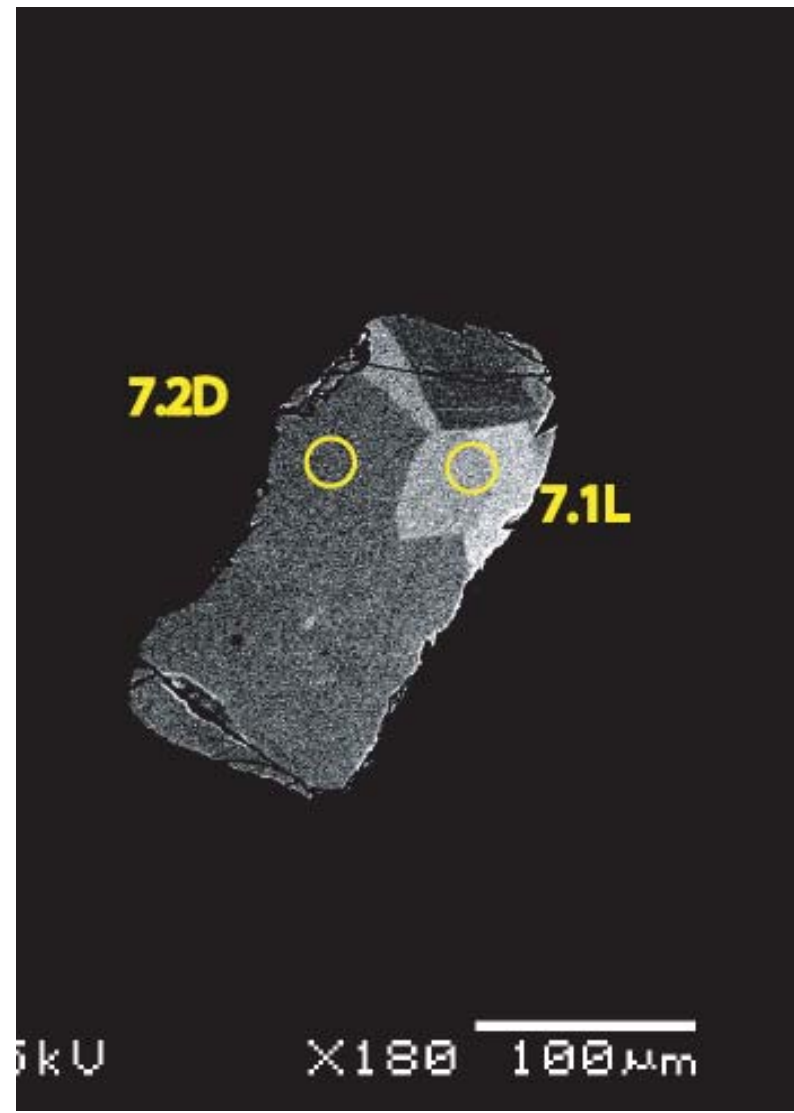
100 µm

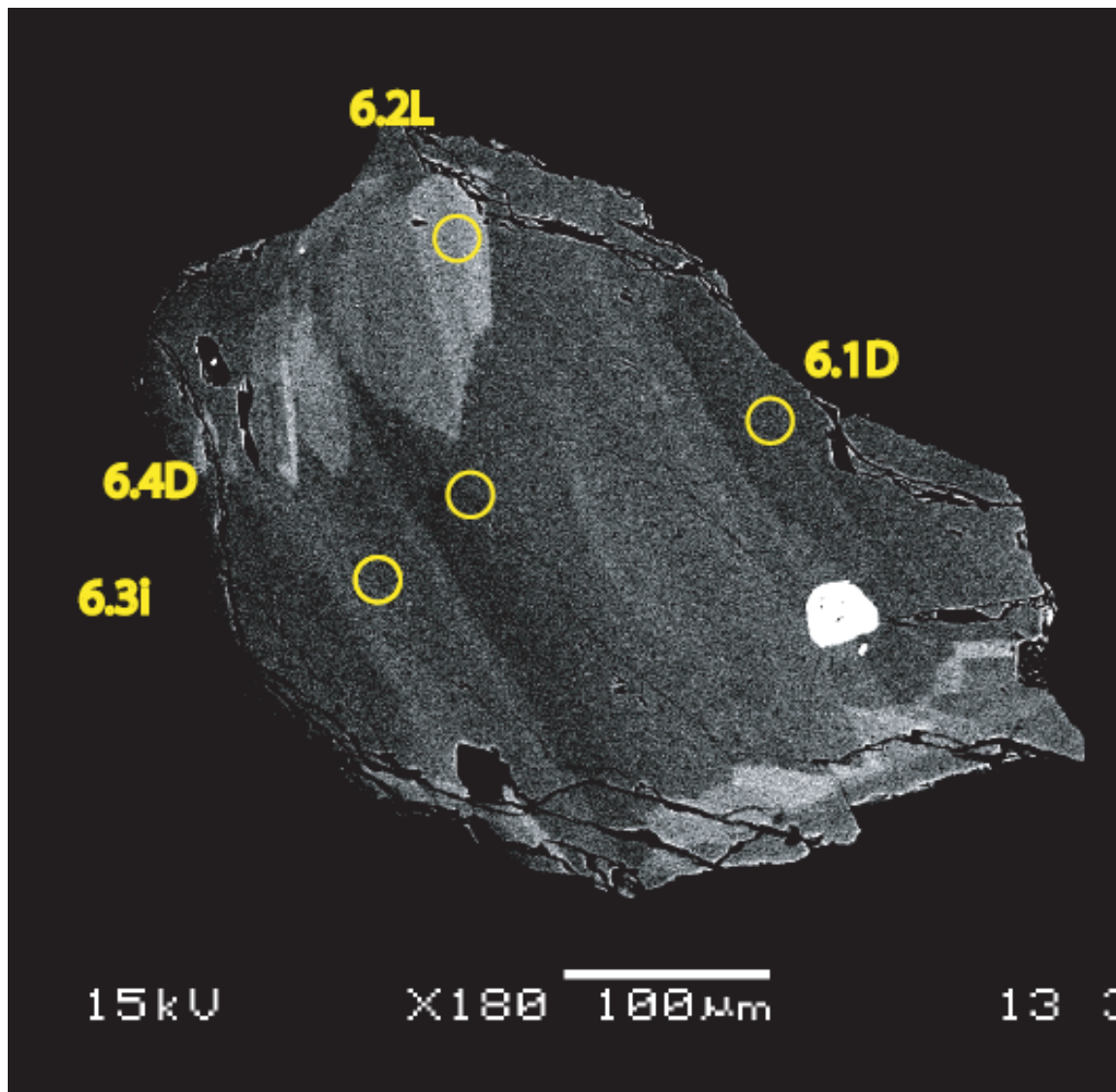


255

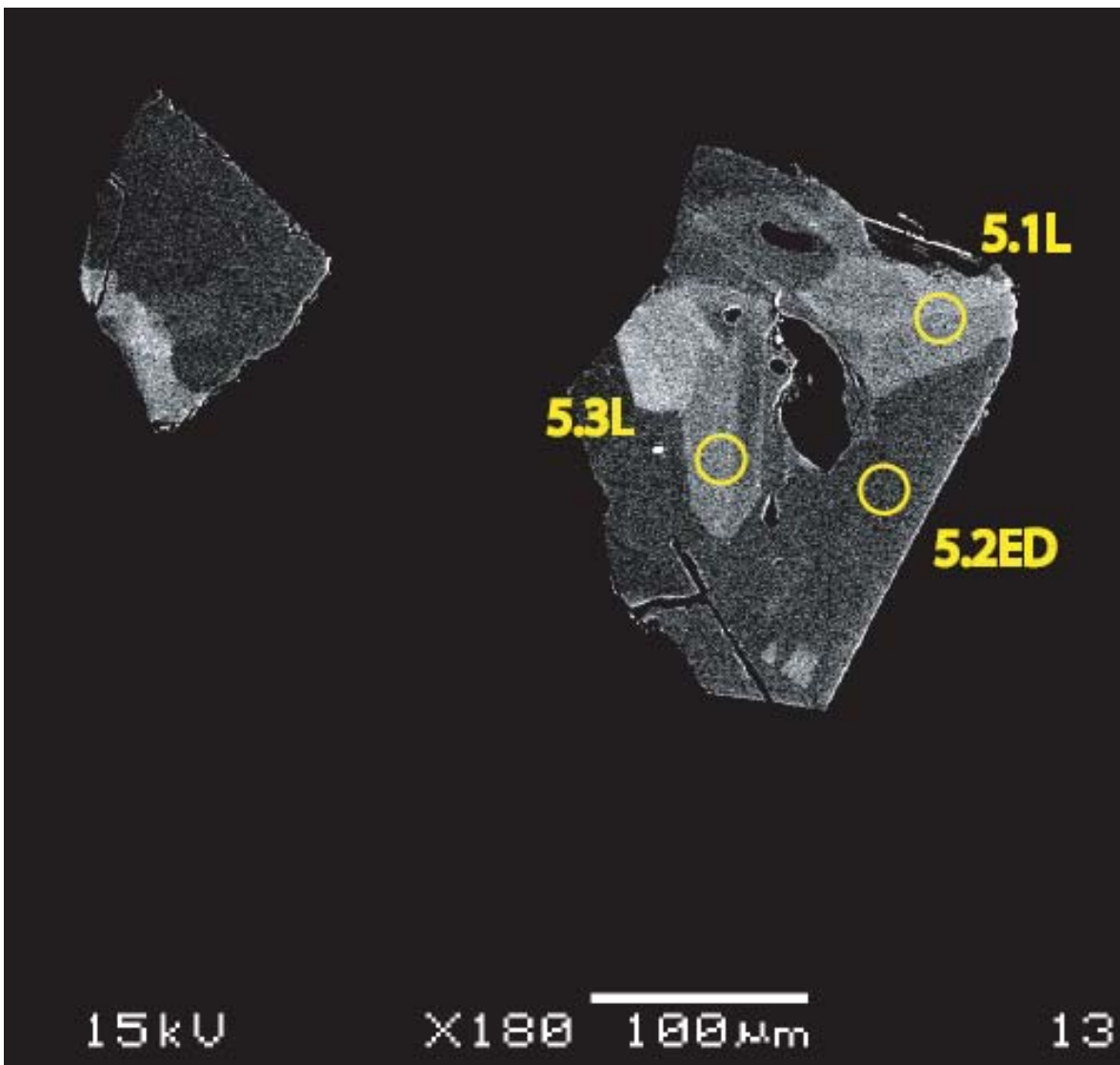


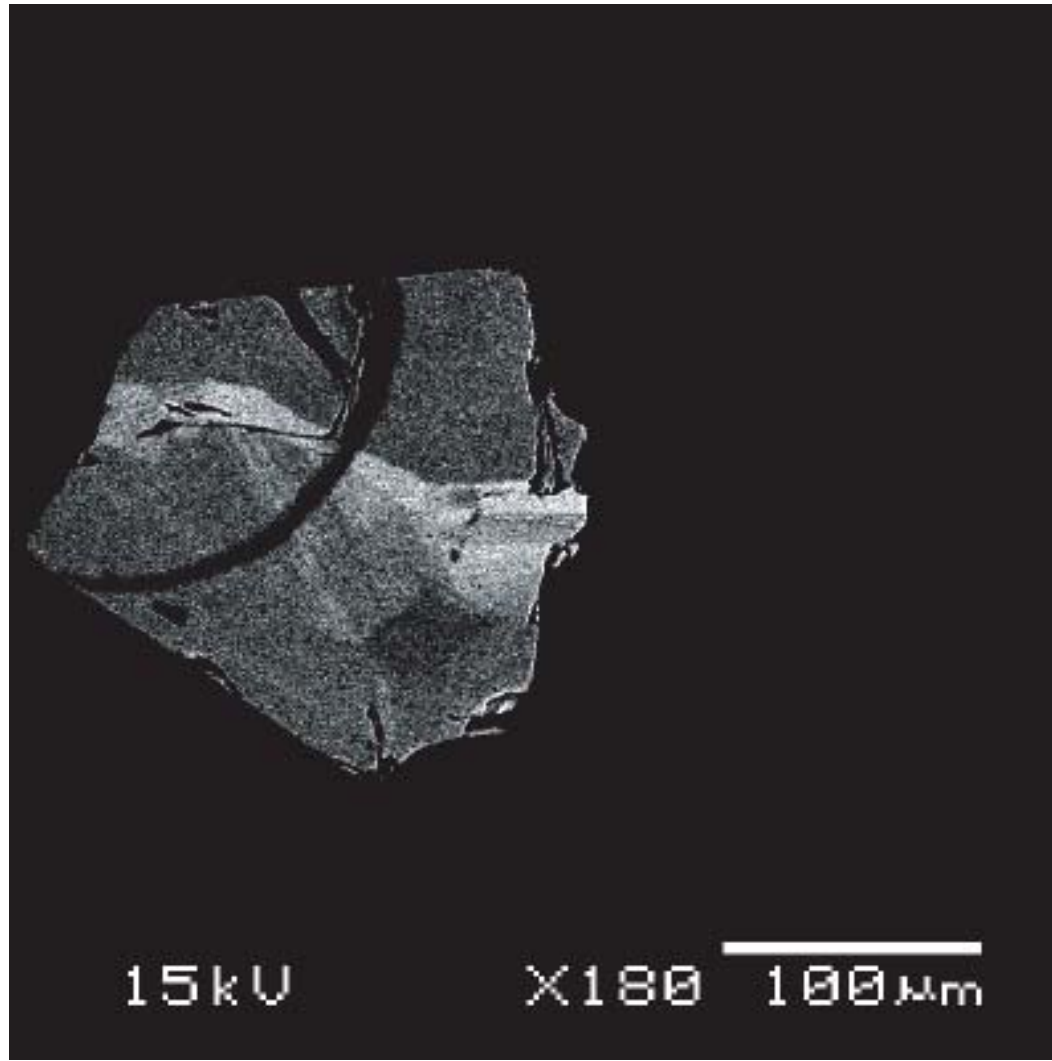
256





258

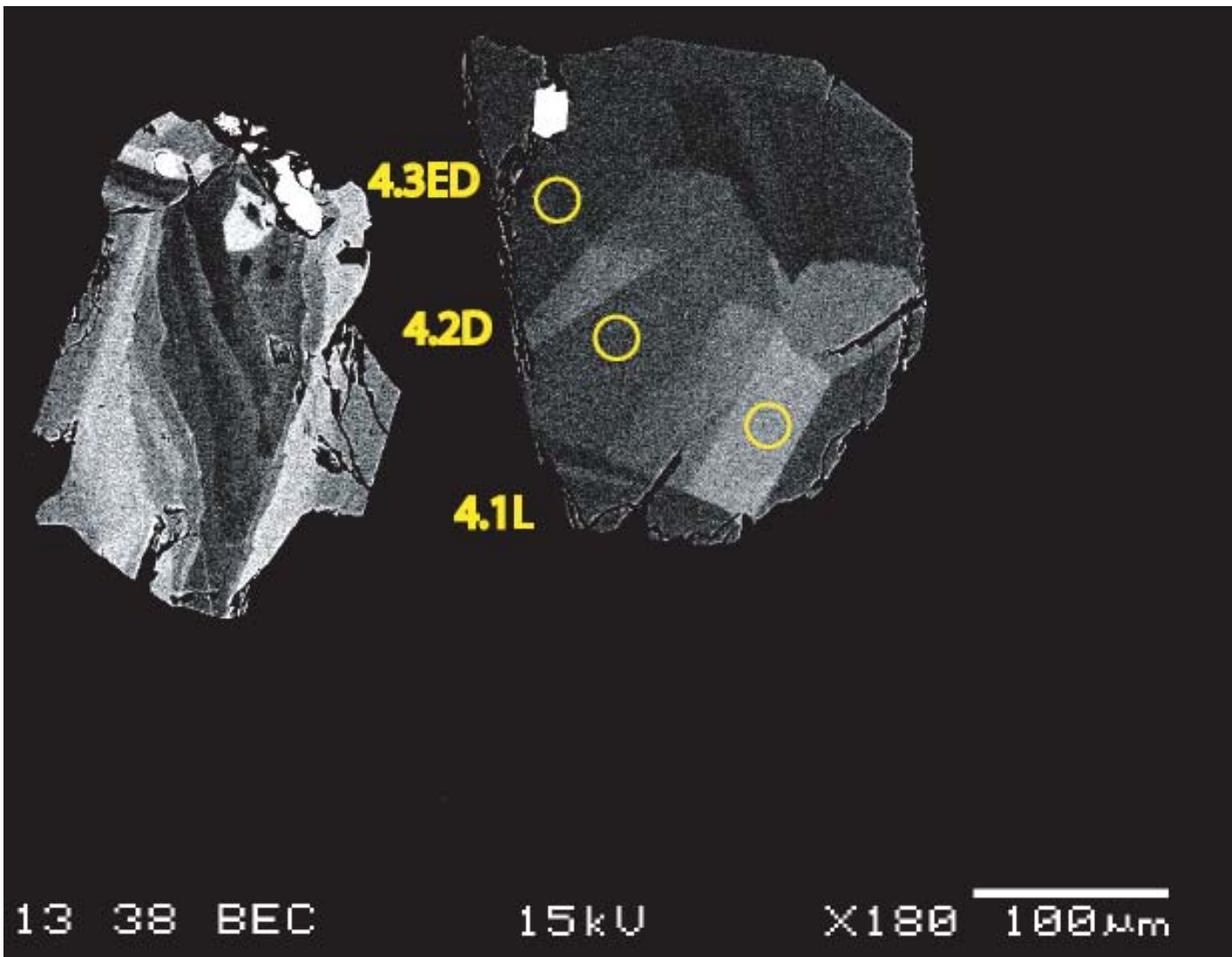




15kV

X180 100 μm

260



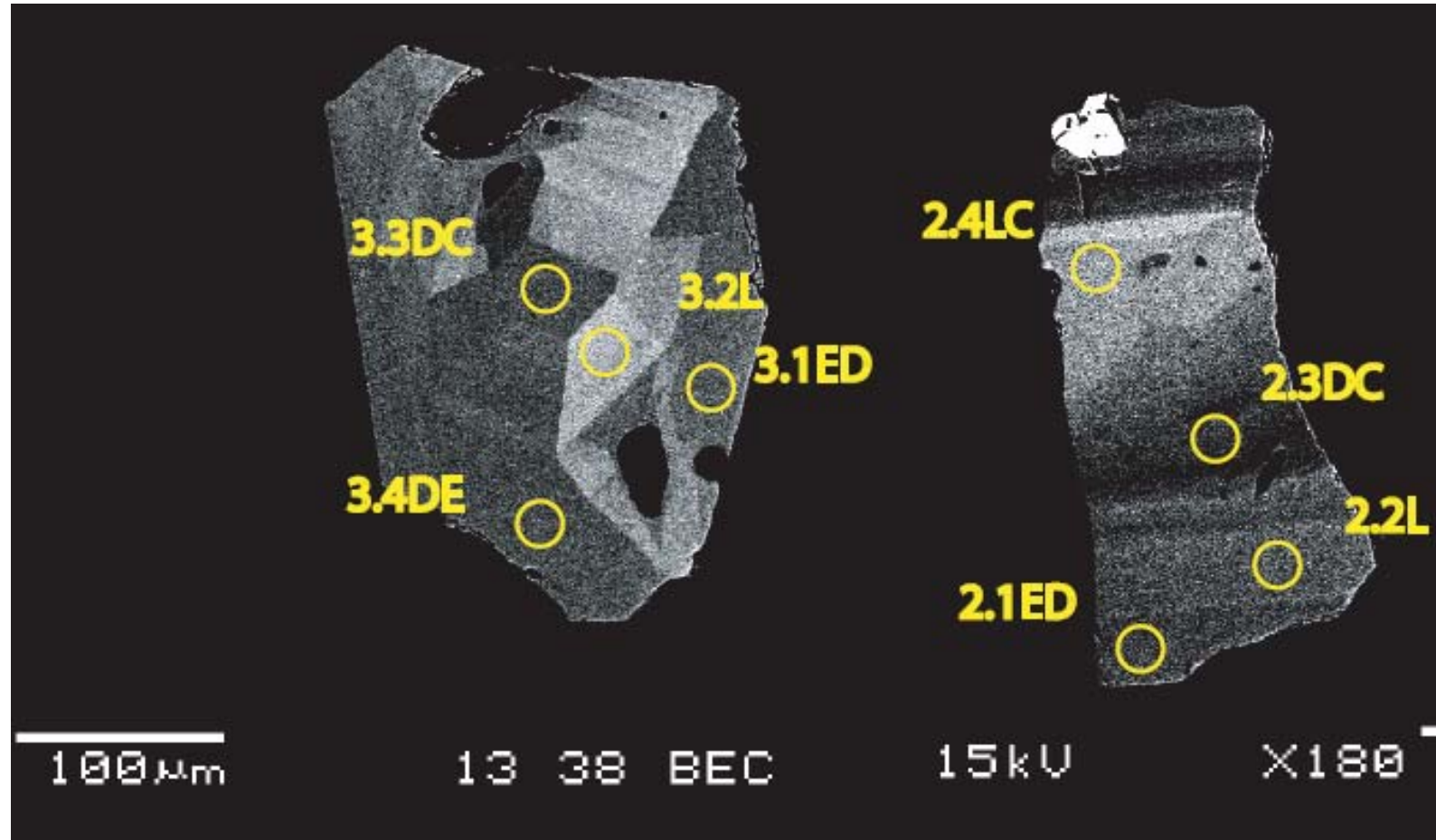
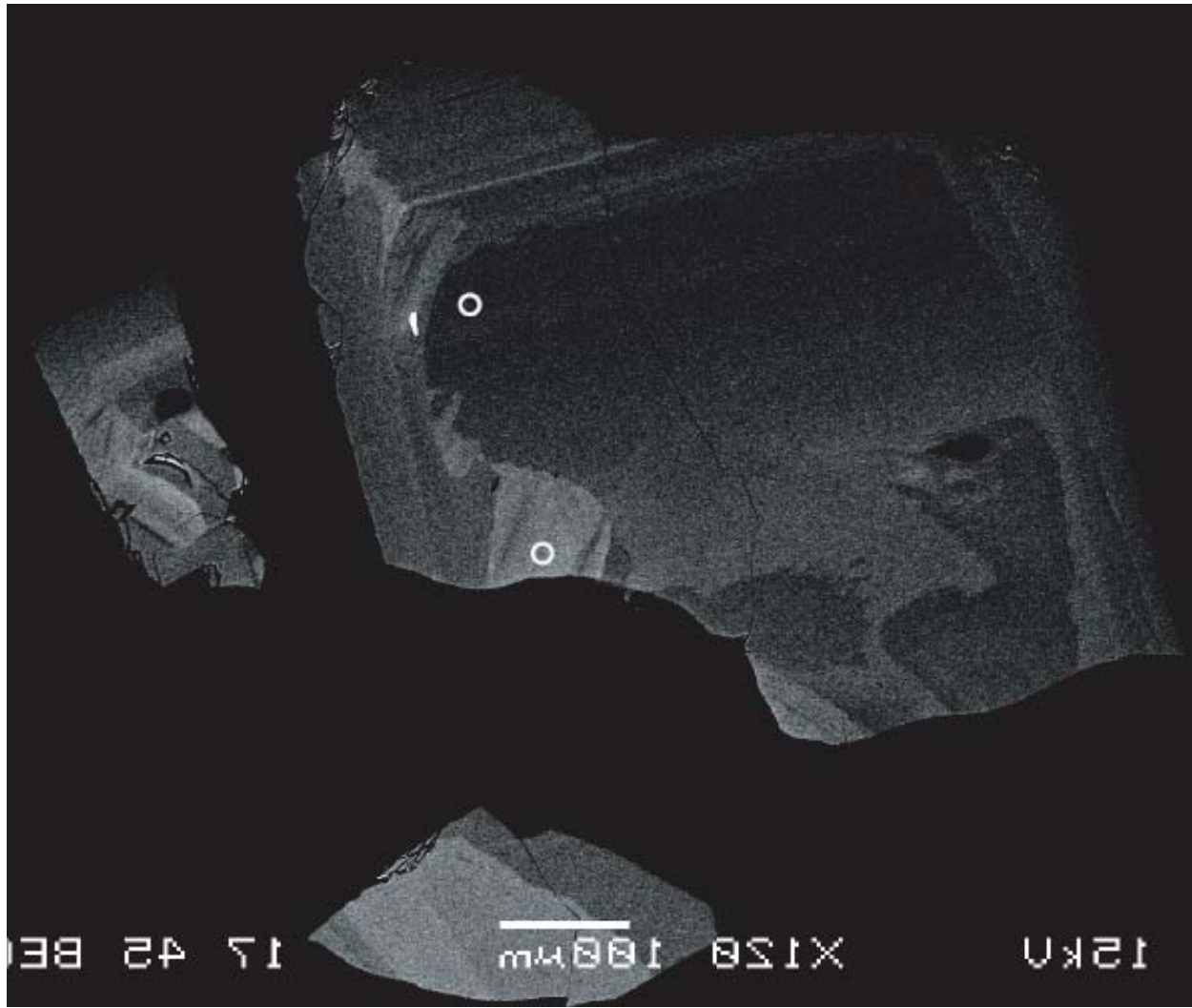


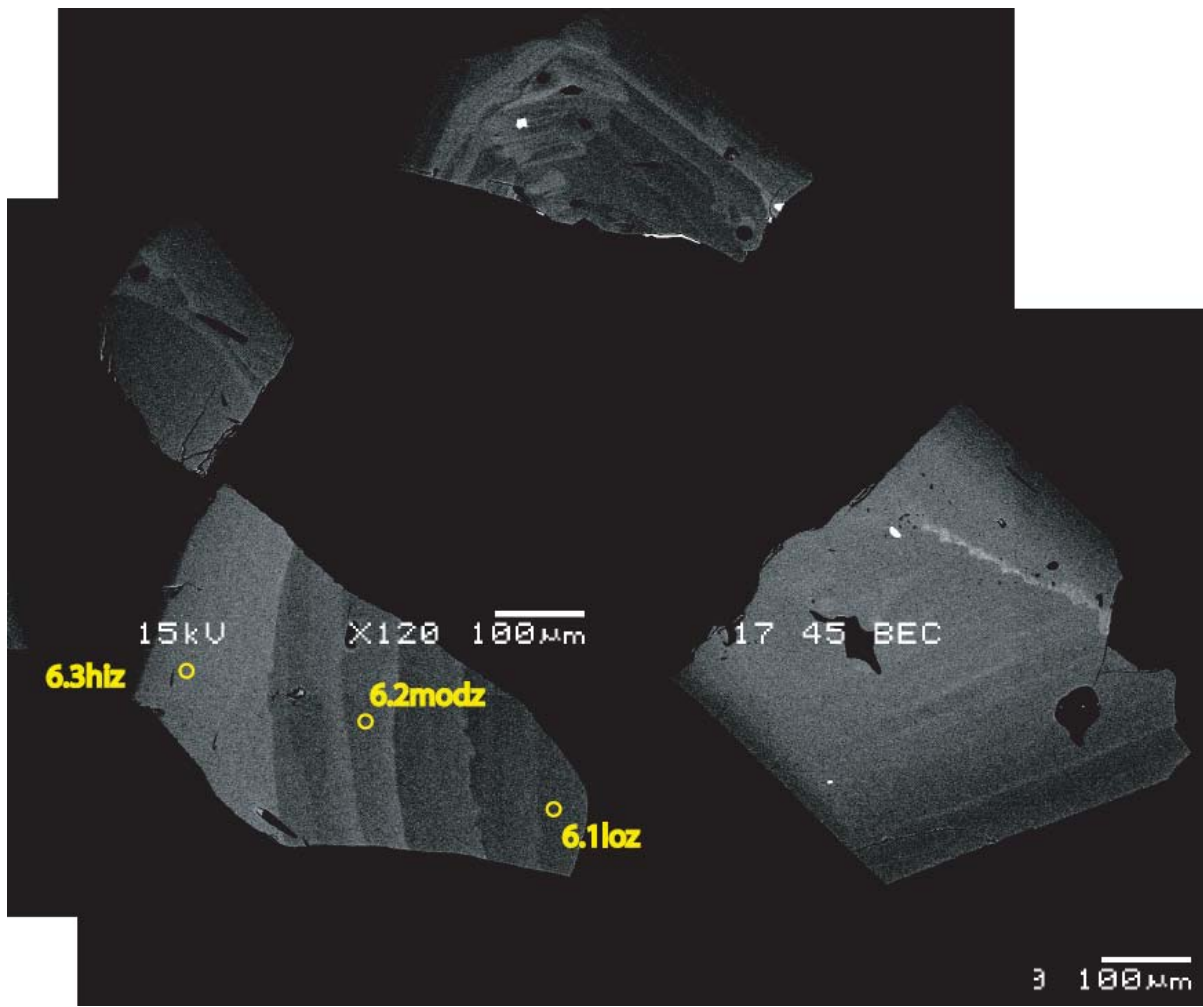
Figure E2:

Backscatter electron images of sphene from sample HRL 12a with spots from Trace Element SHRIMP-RG analyses marked.

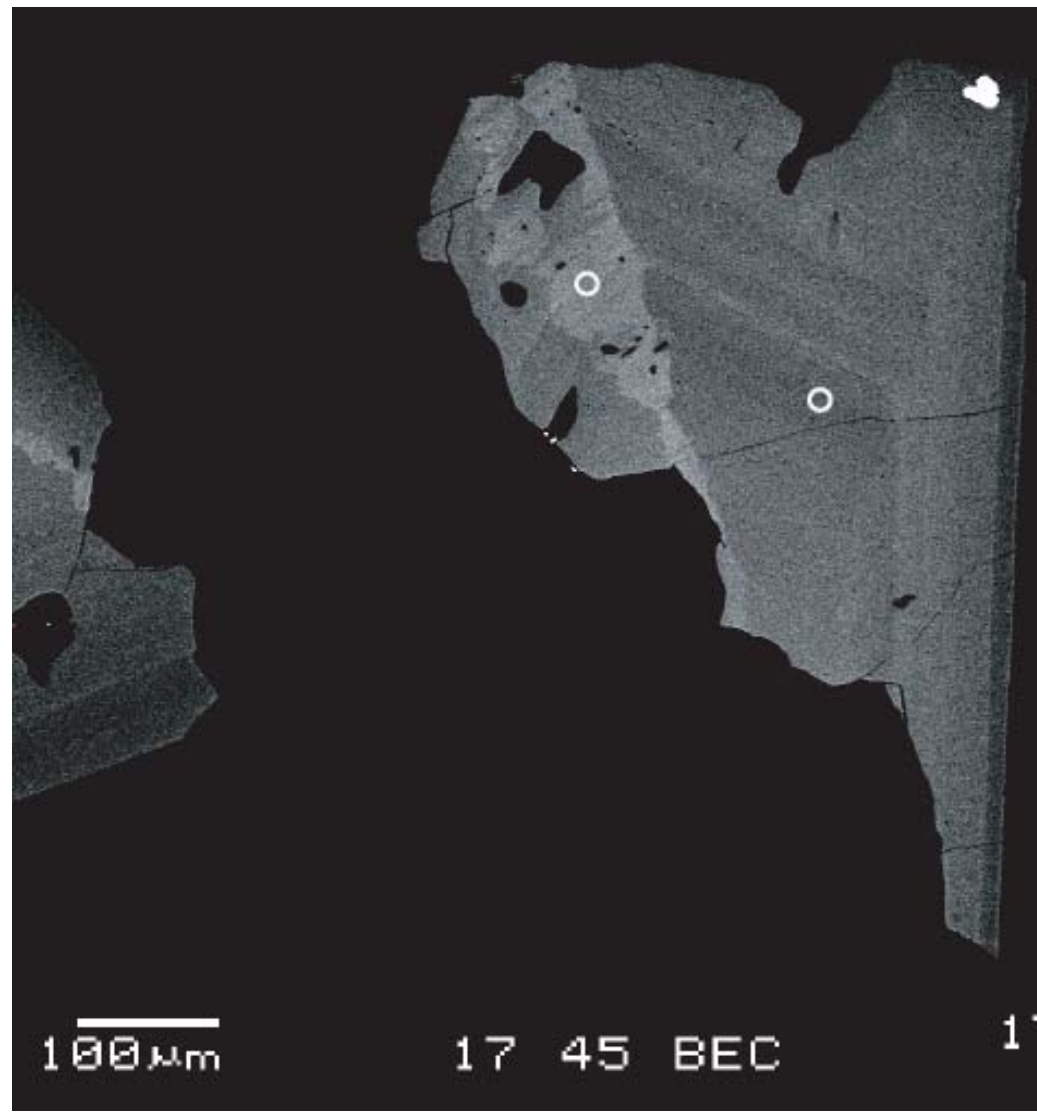
263

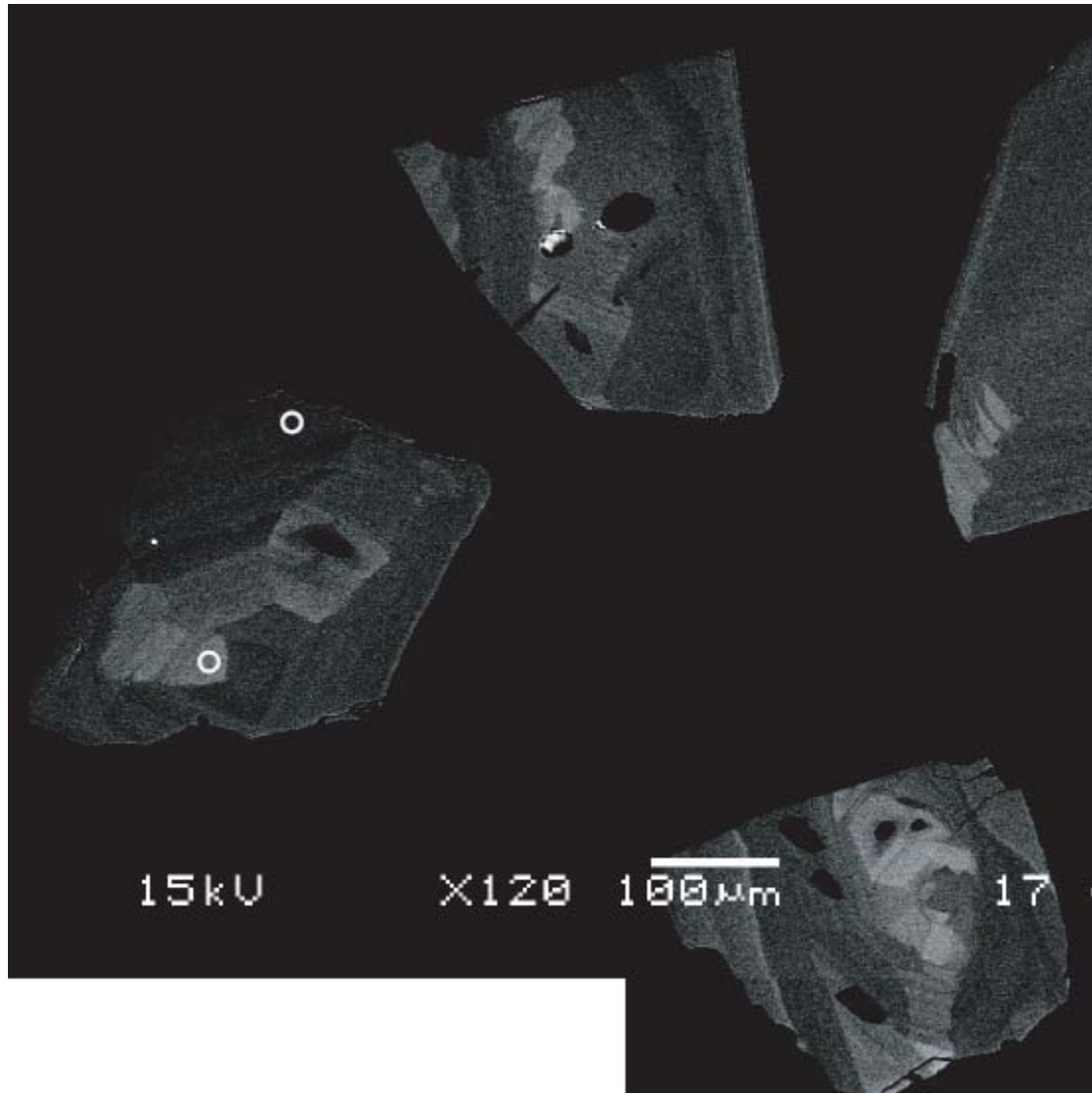


264

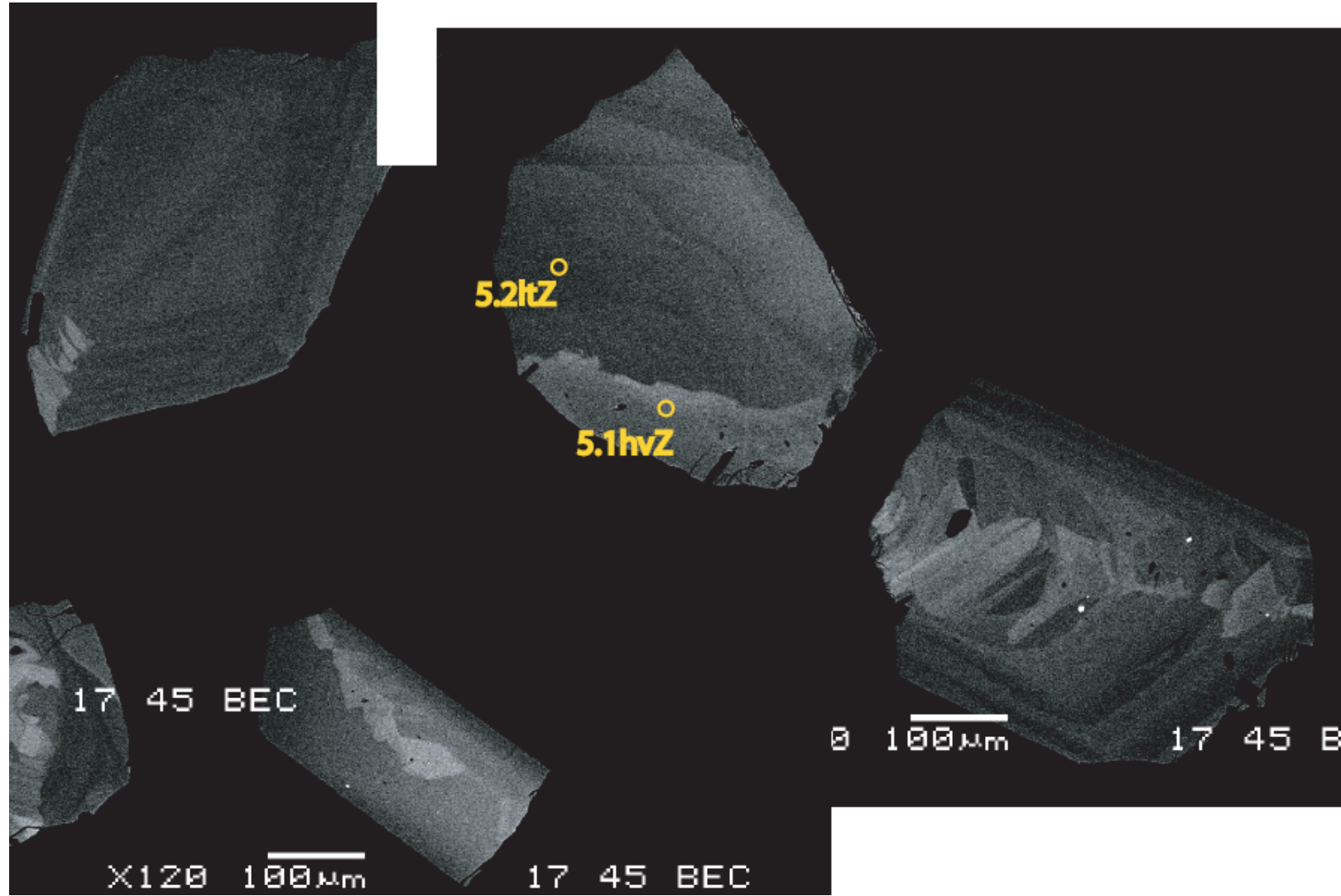


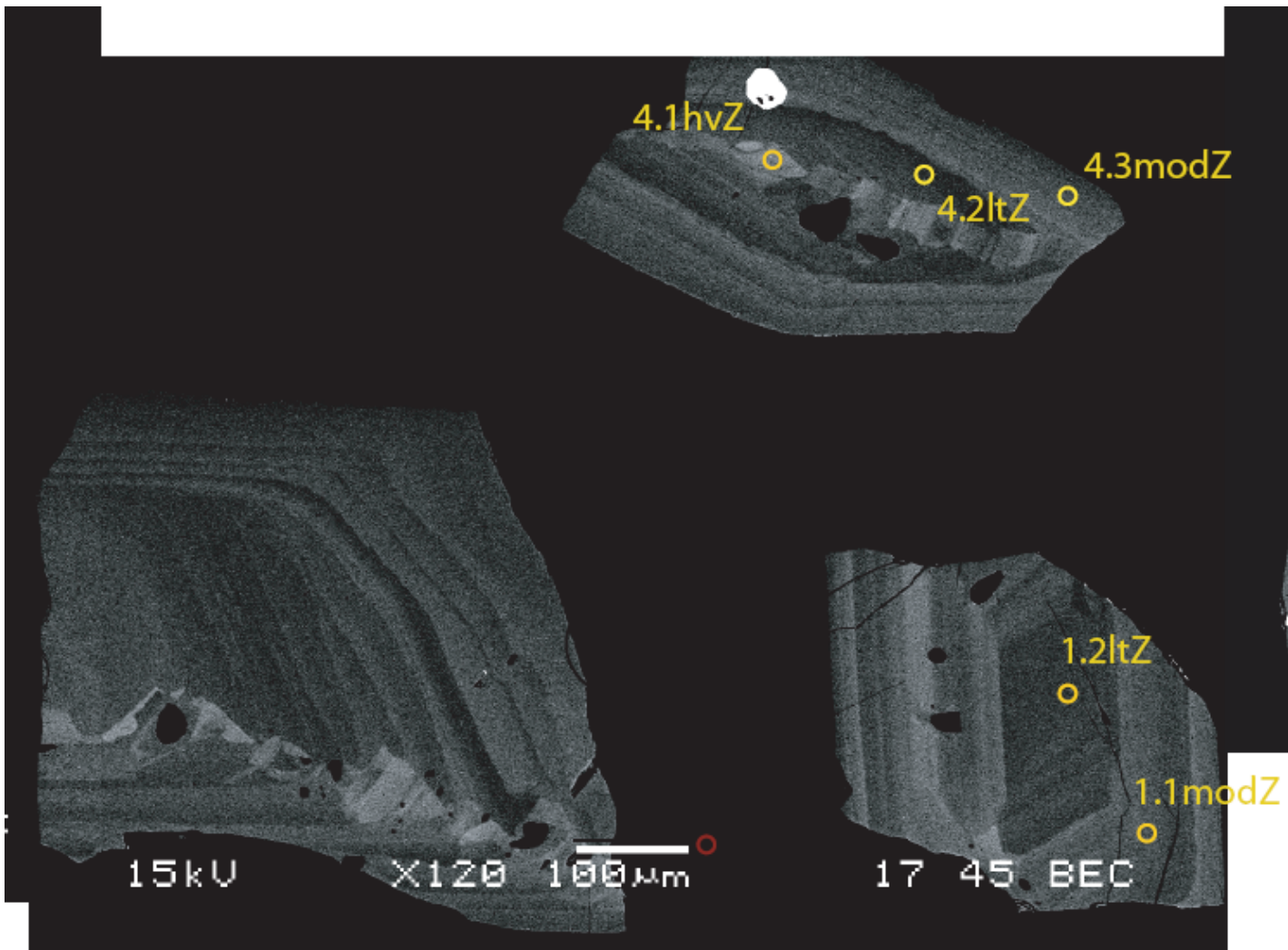
265



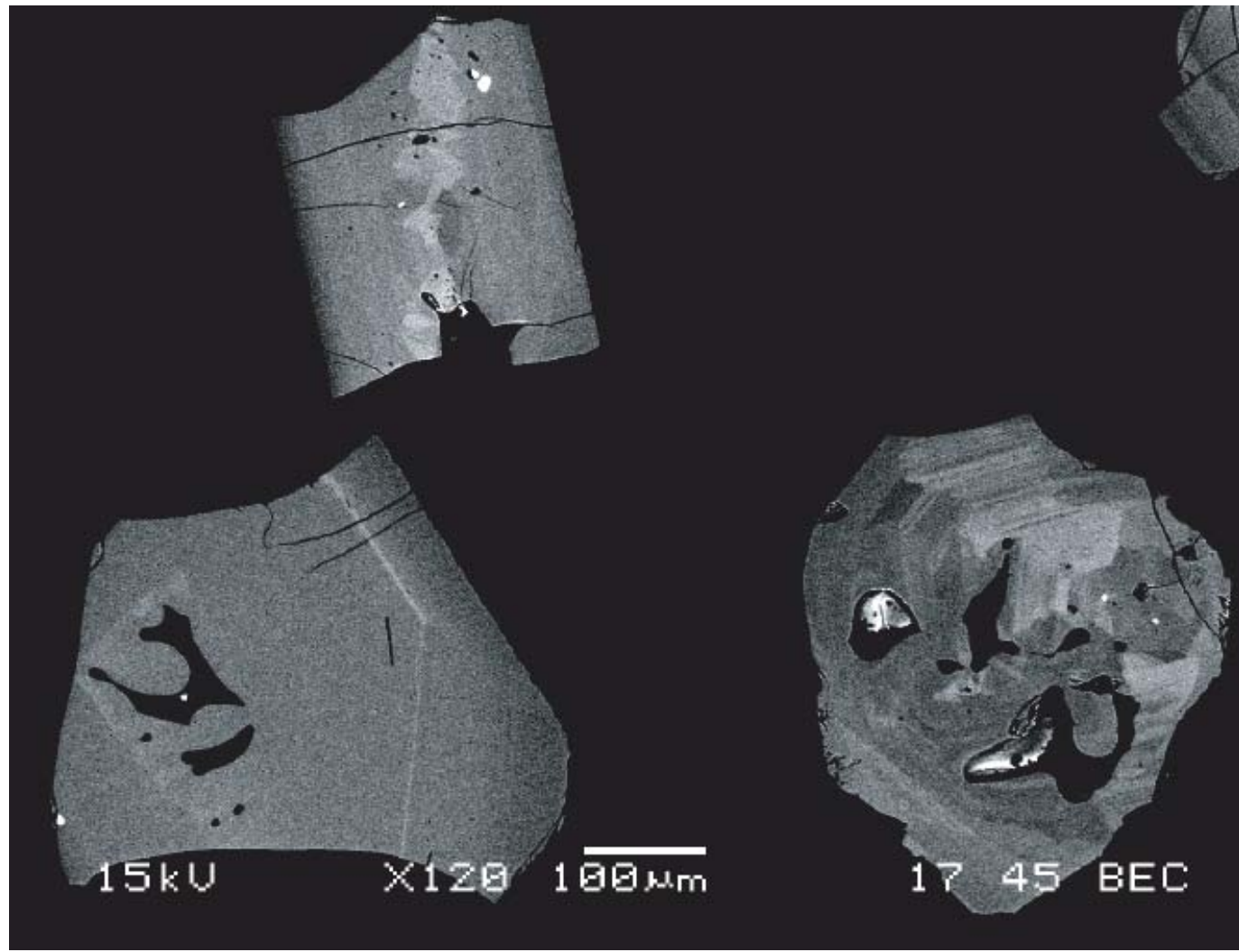


267

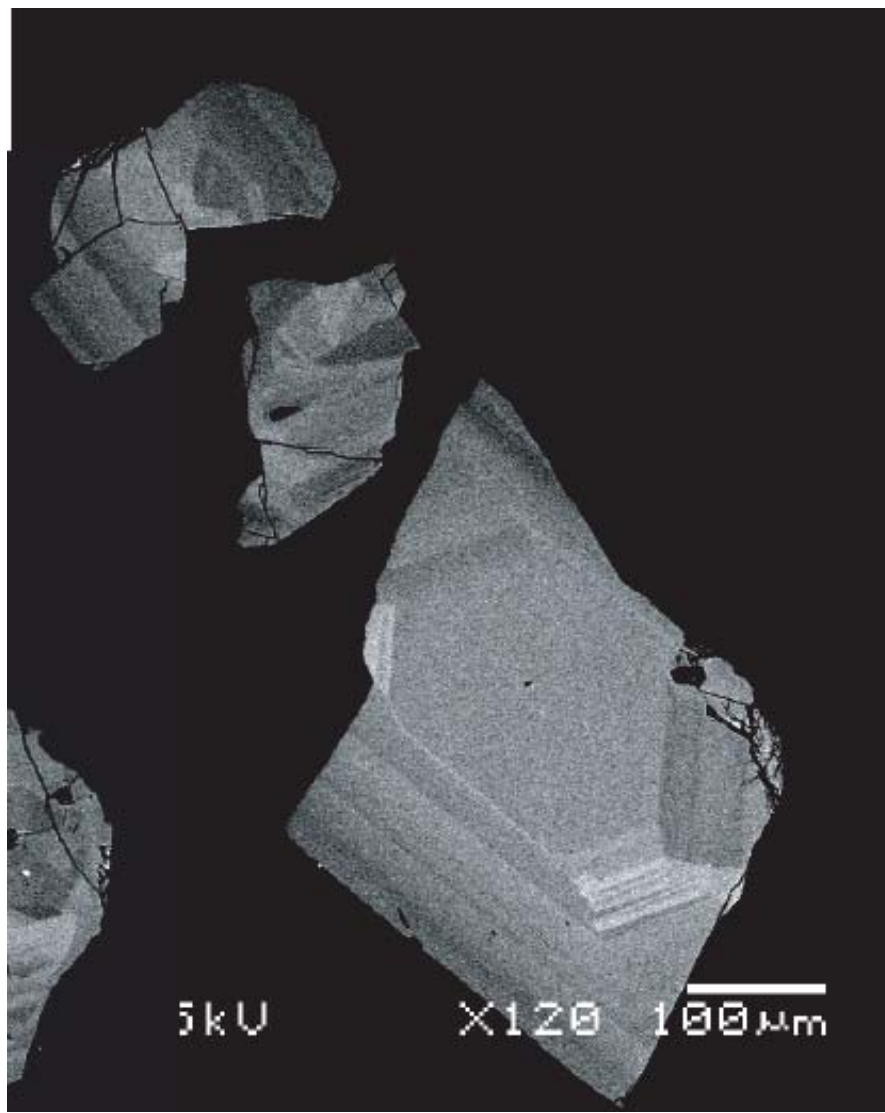




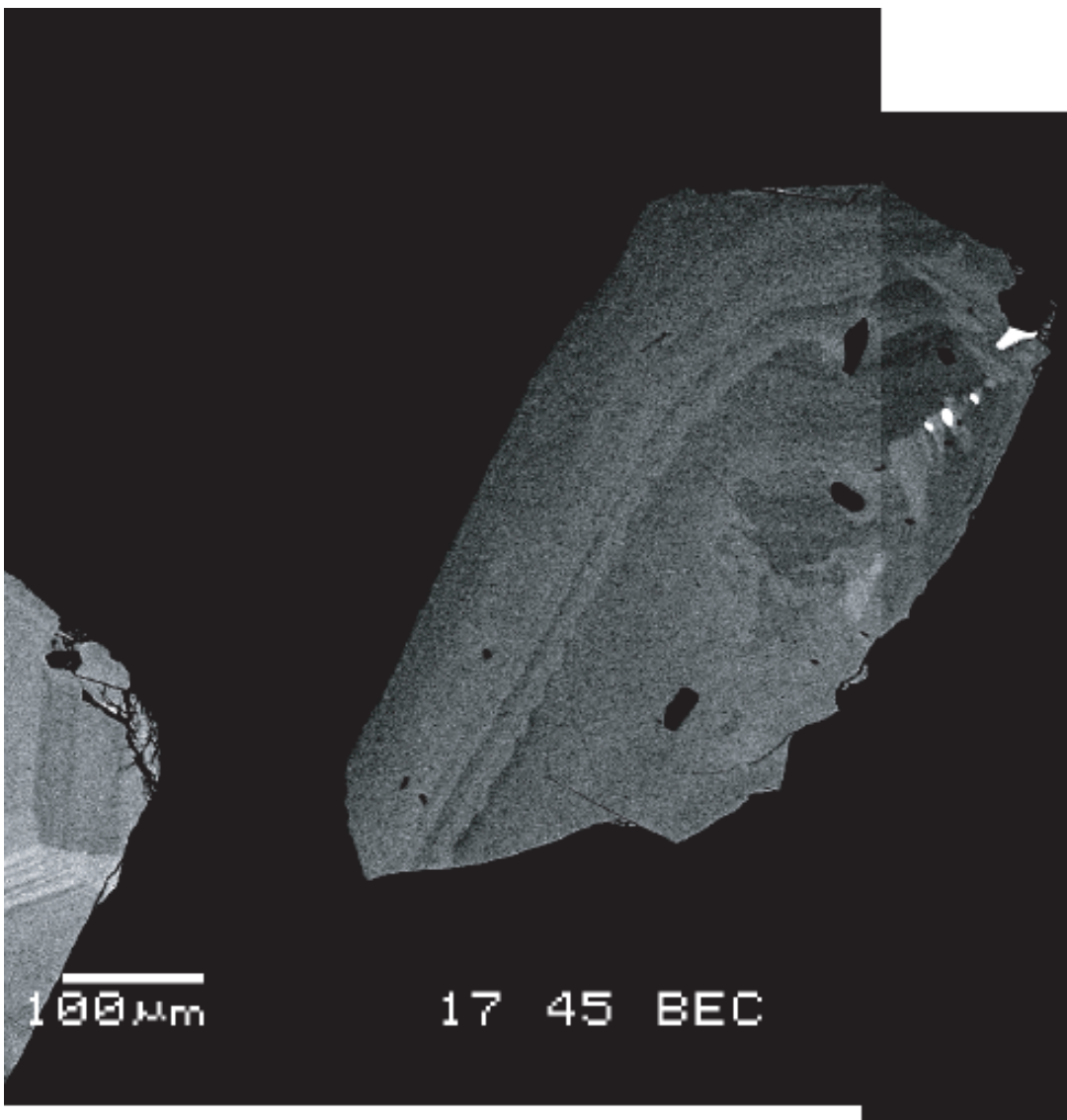
269



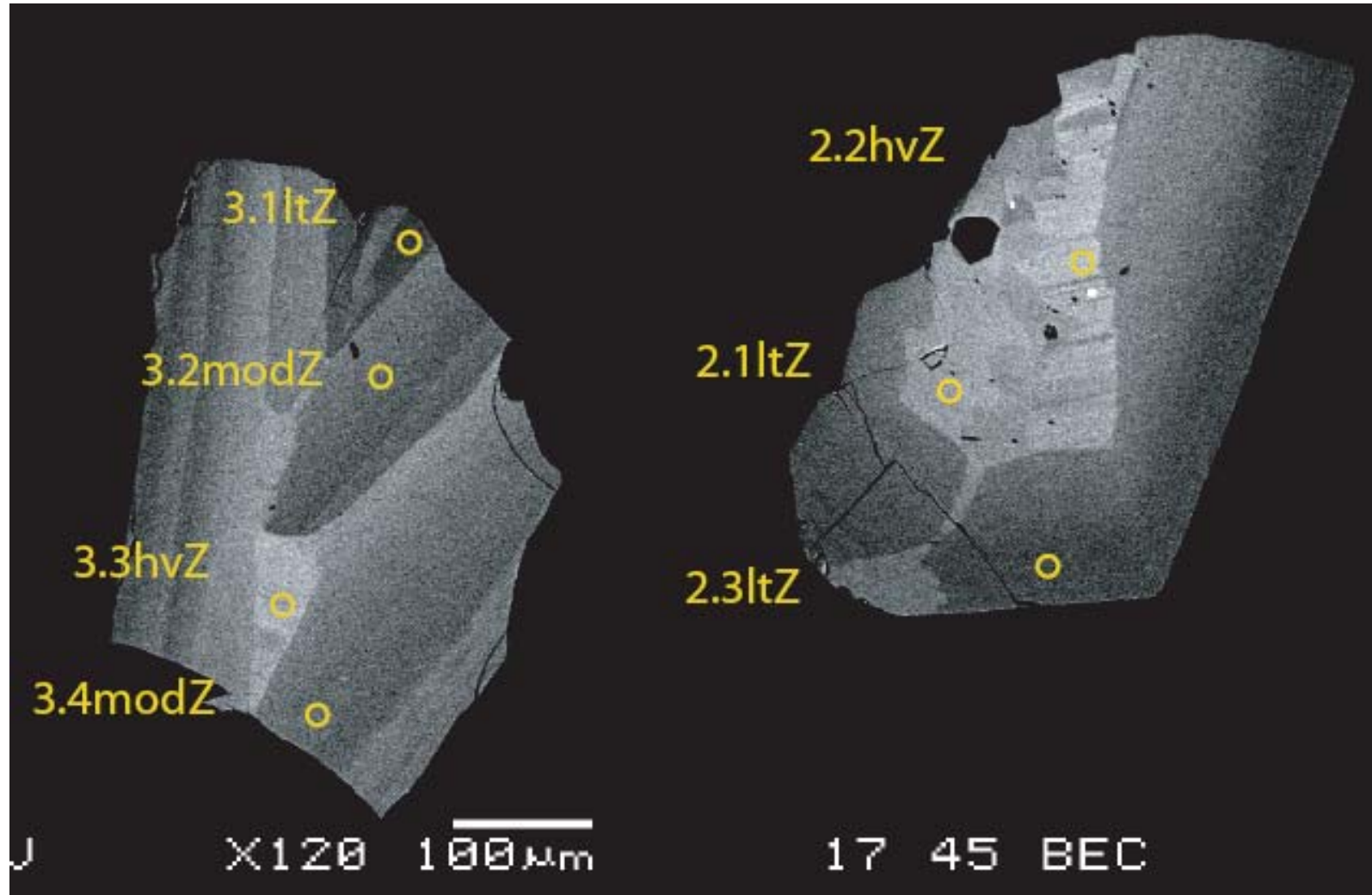
270



271



272



273

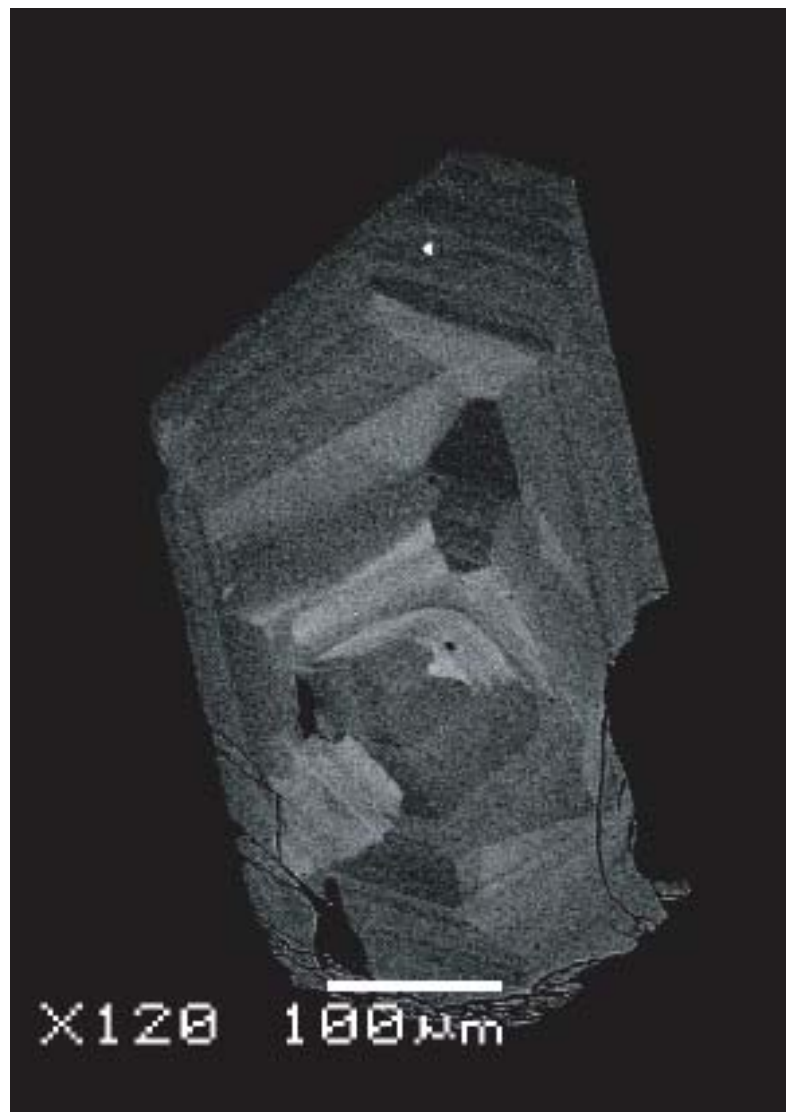
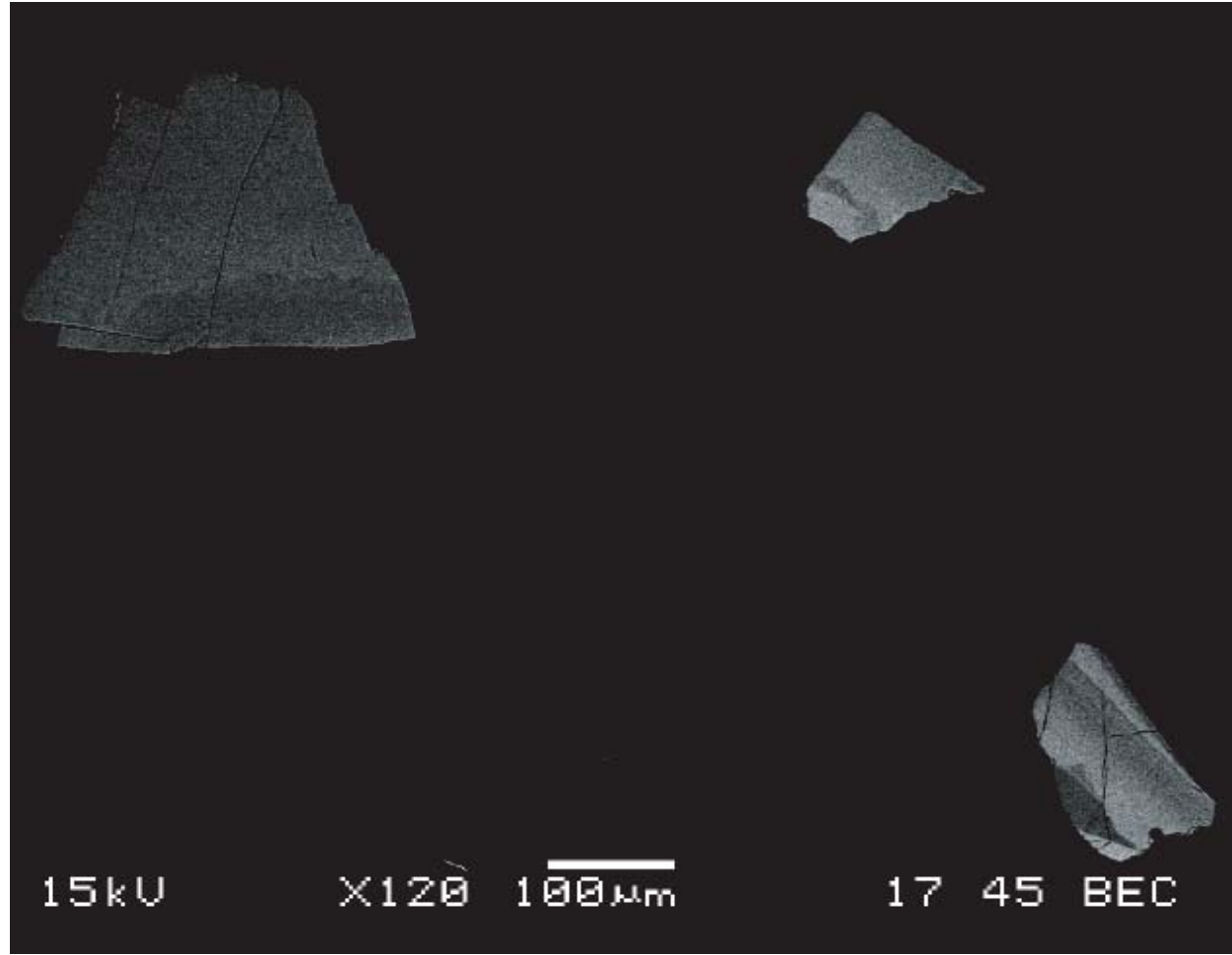


Figure E2:

Backscatter electron images of sphene from sample HRL 14a with spots from Trace Element SHRIMP-RG analyses marked.

275

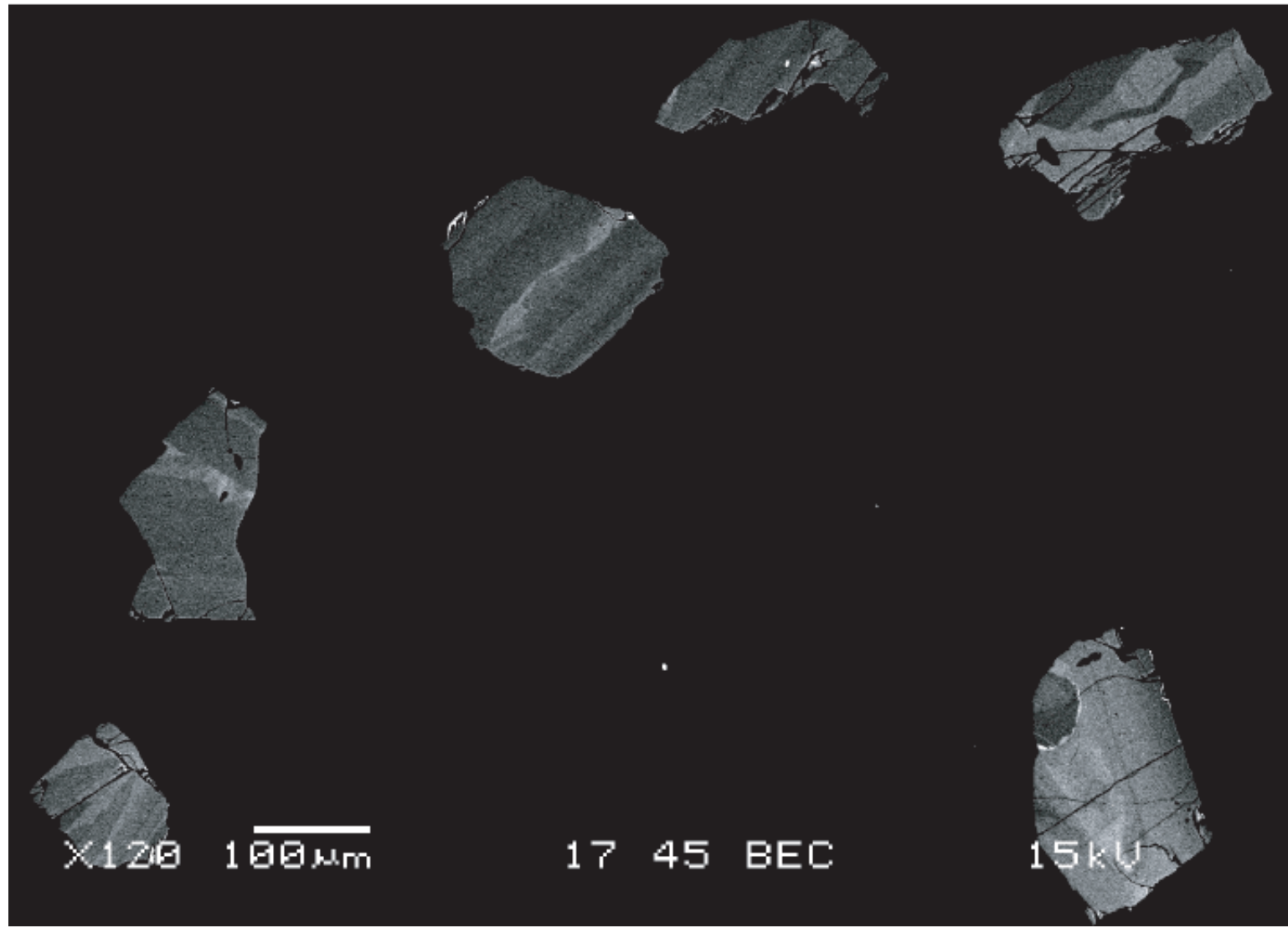


15kV

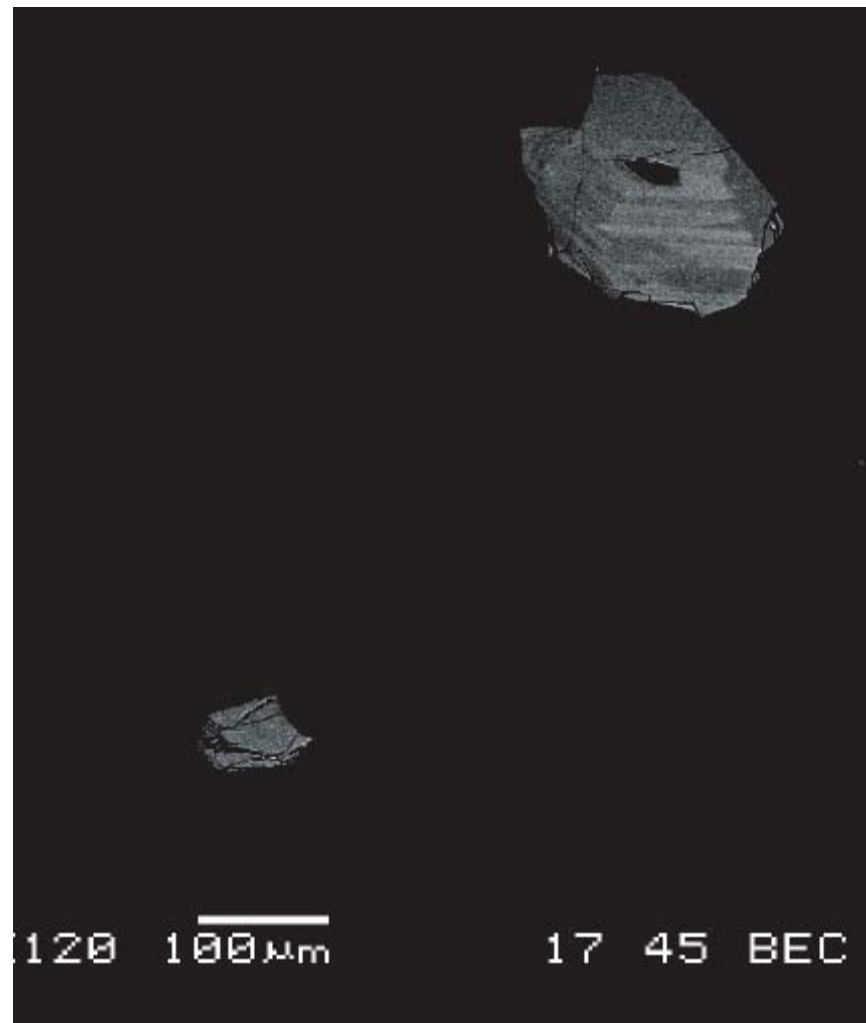
×120 100 μm

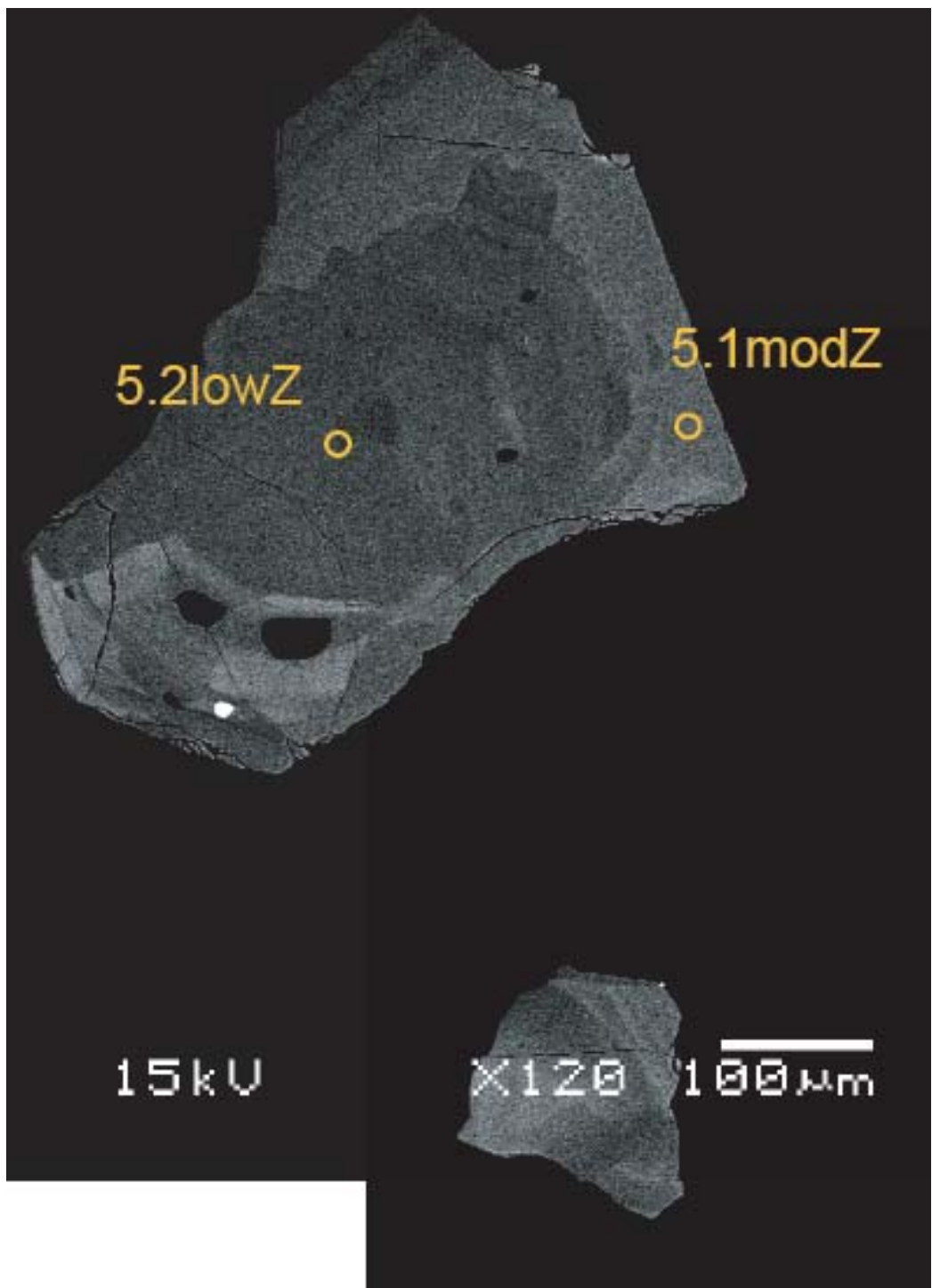
17 45 BEC

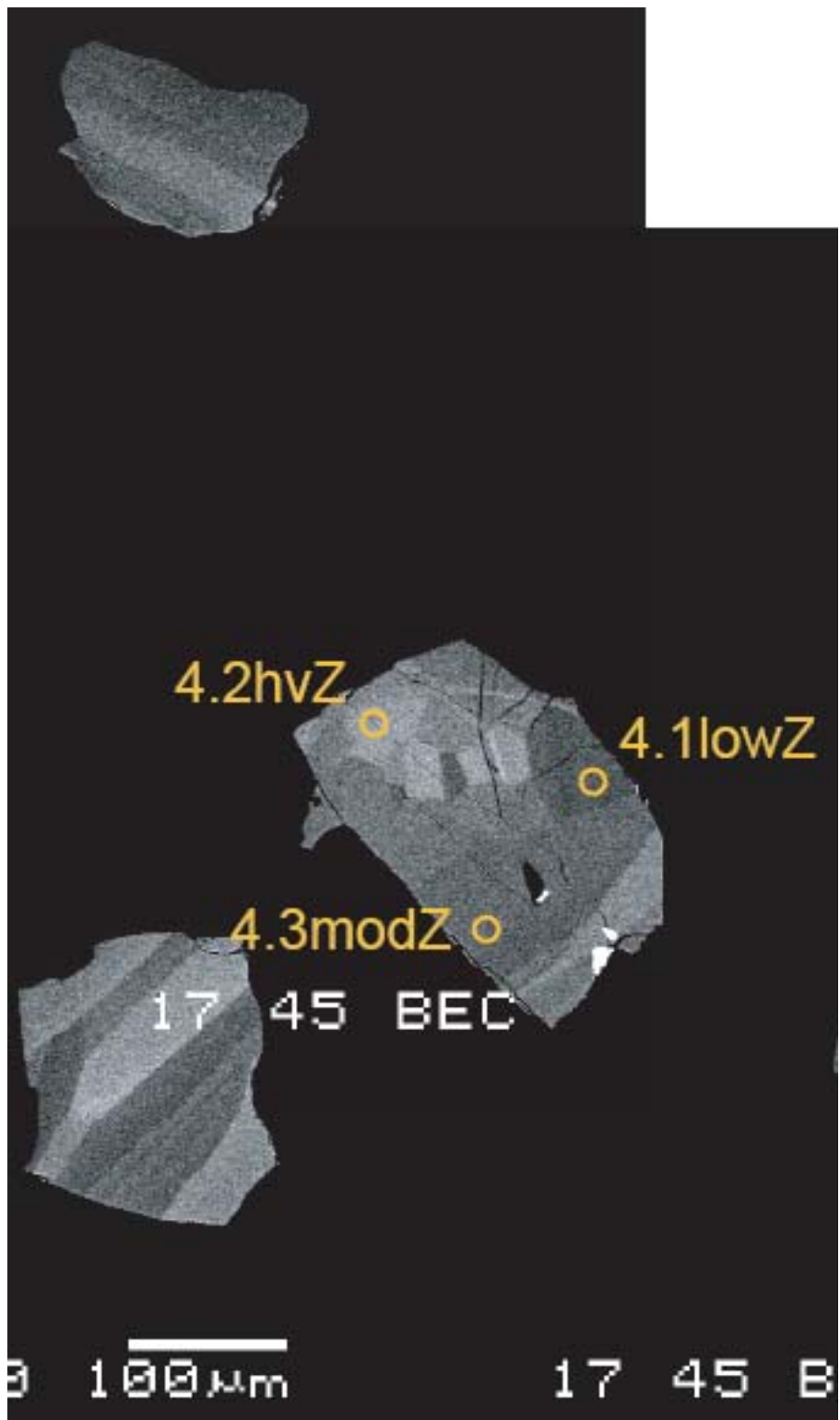
276



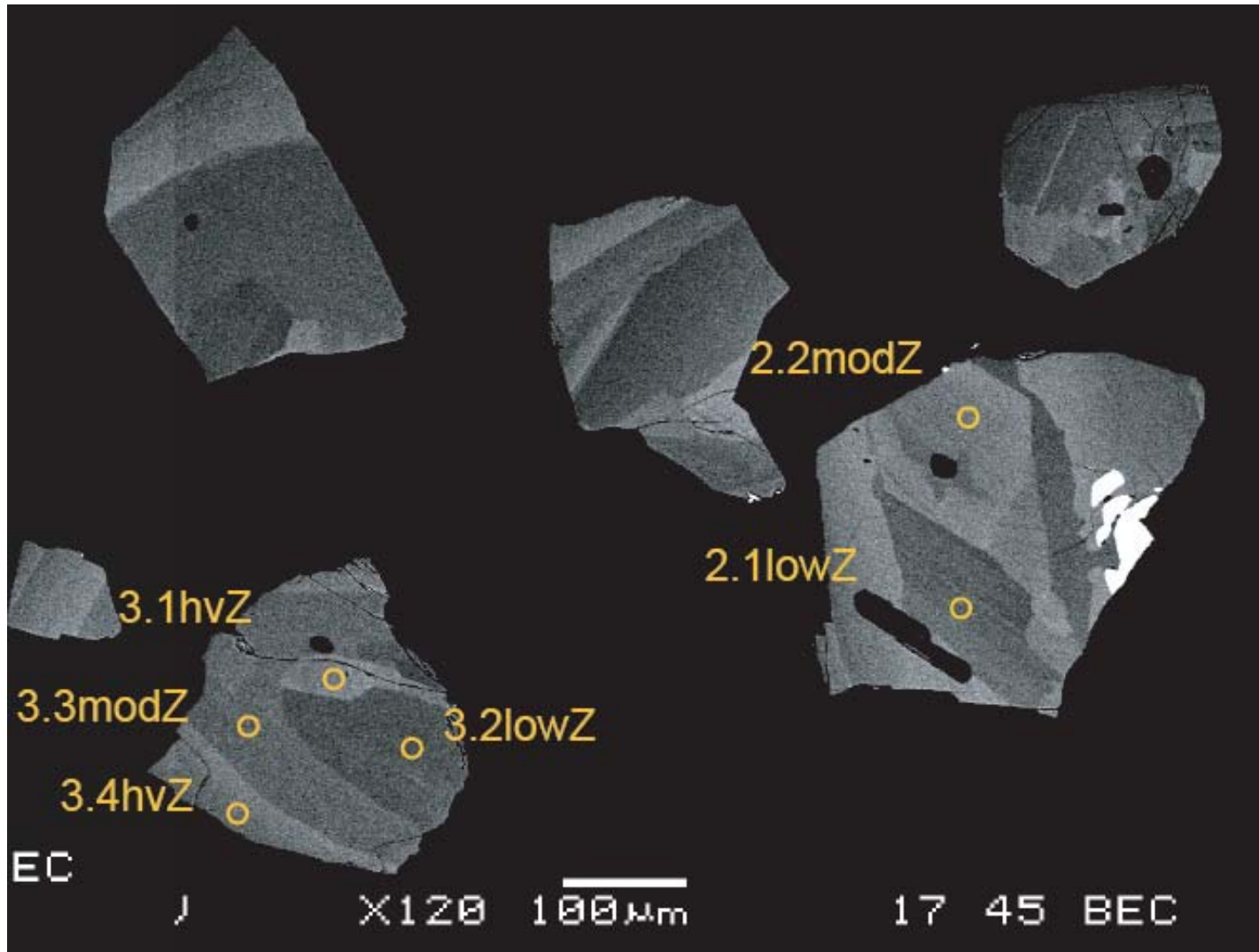
277



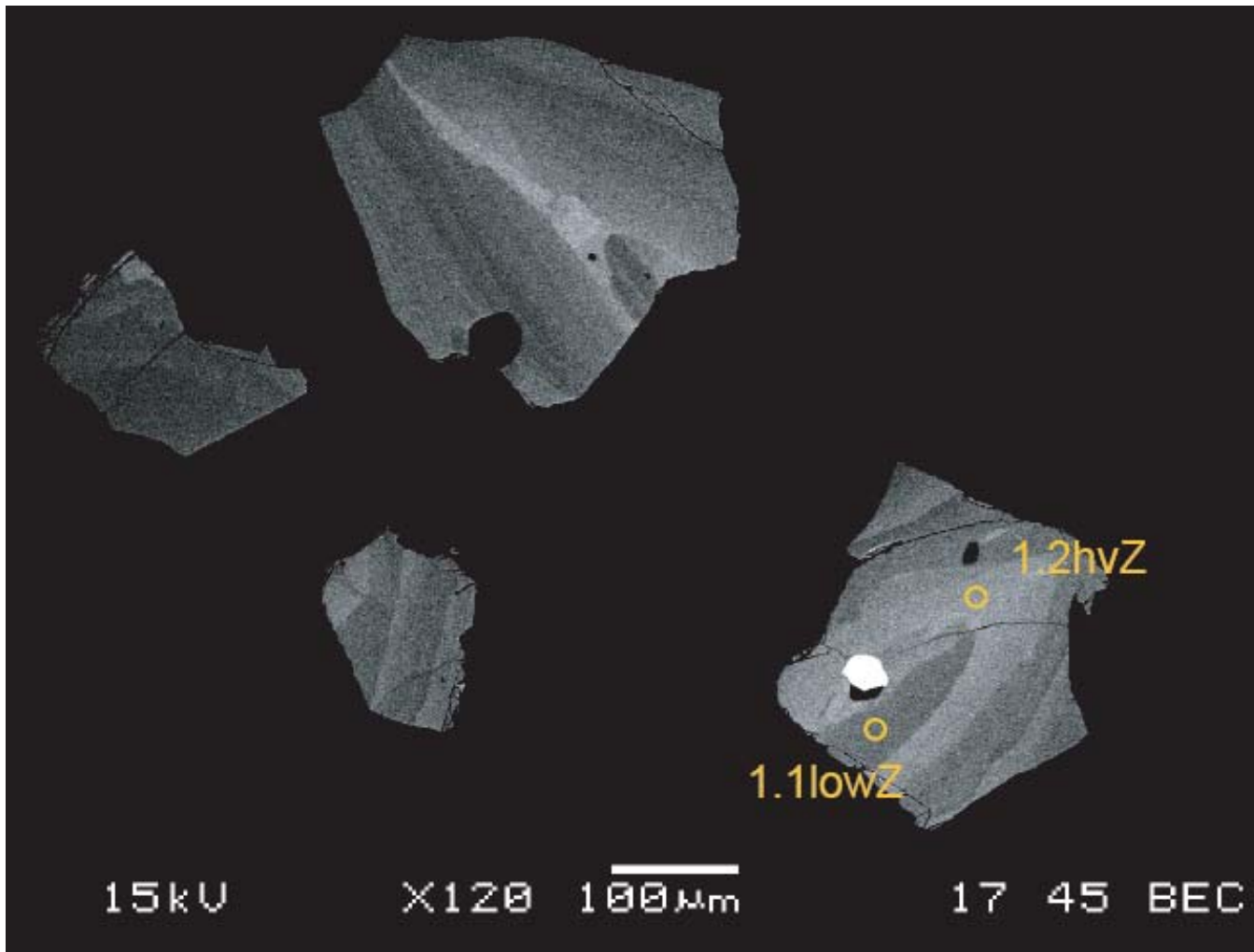


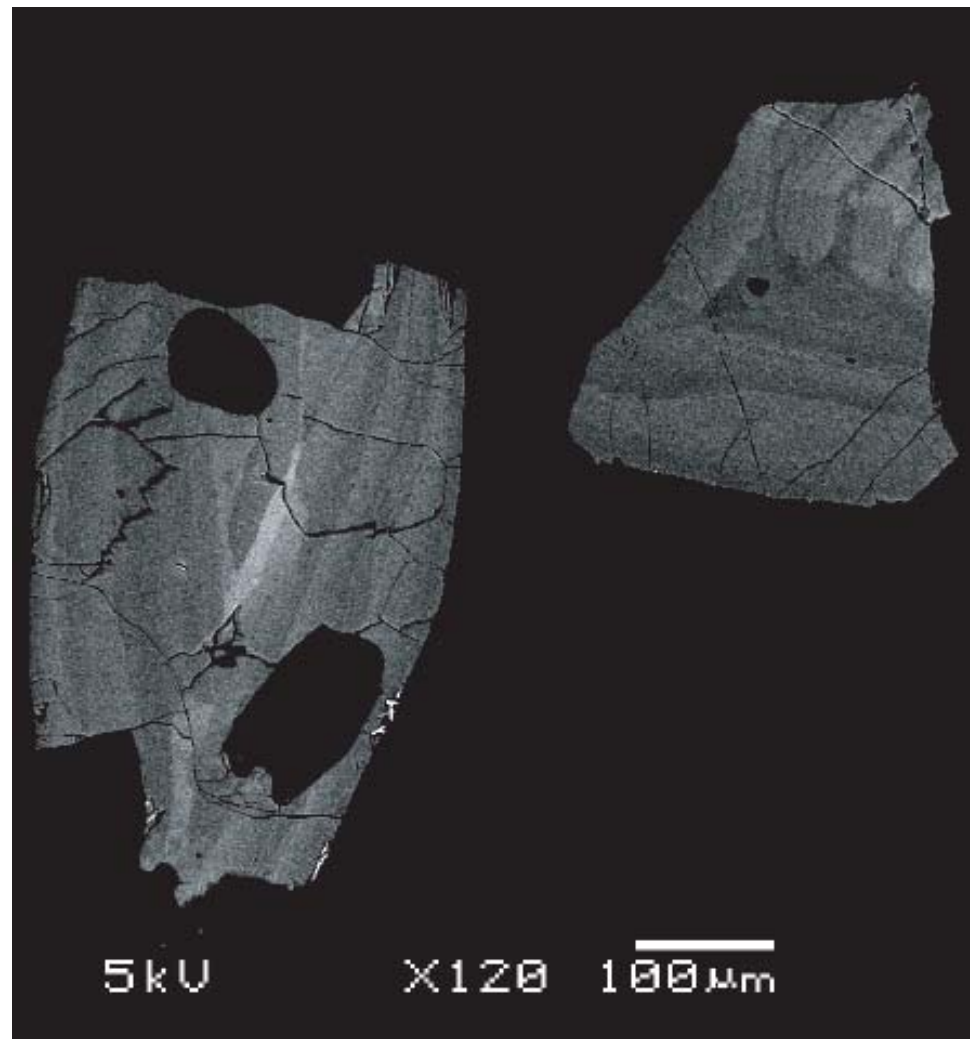


280

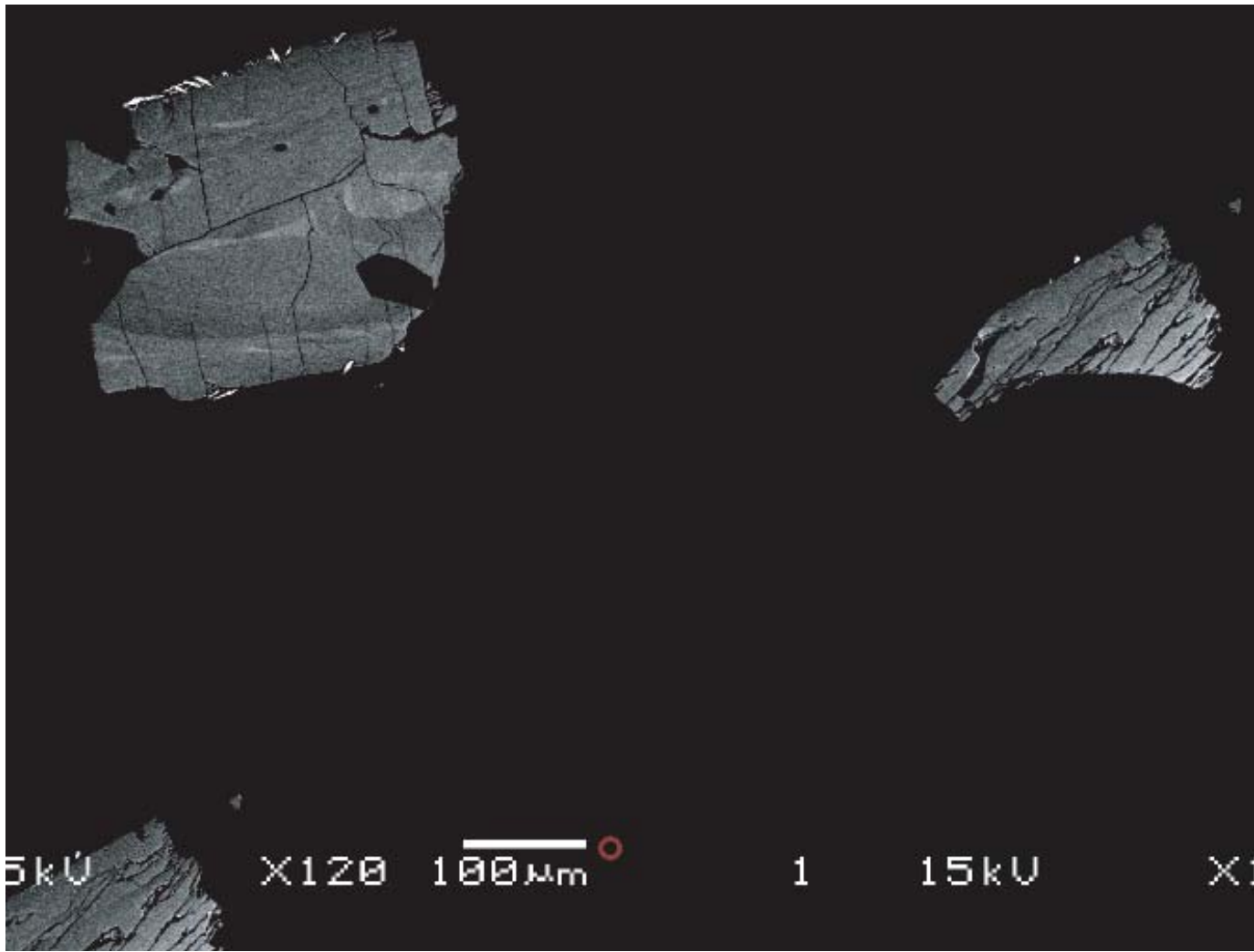


281





283



APPENDIX F:
Ar-Ar Data and Method
of the Highland Range silicic sequence

Table F1: Ar-Ar data and results for samples HRL 12a, HRL 14a, HRL 26, HRL 27, HRL 31 from the Highland Range silicic sequence.

ID	$^{40}\text{Ar}/^{39}\text{Ar}$	$^{37}\text{Ar}/^{39}\text{Ar}$	$^{36}\text{Ar}/^{39}\text{Ar}$	$^{39}\text{Ar}_K$ ($\times 10^{-3}$)	K/Ca	$^{40}\text{Ar}^*$ (%)	Age (Ma)	$\pm 1\sigma$: (Ma)
HRL-12A , Sanidine, J=0.0008082±0.05%, D=1.0014±0.001, NM-221P, Lab#=58750								
08	14.58	0.0088	12.08	16.265	57.8	75.5	15.985	0.058
04	11.65	0.0087	2.120	7.507	58.4	94.6	16.007	0.048
15	11.61	0.0105	1.965	4.086	48.5	95.0	16.008	0.069
01	11.66	0.0142	2.150	12.829	35.8	94.6	16.010	0.038
05	11.18	0.0099	0.4272	17.081	51.3	98.9	16.045	0.031
12	11.21	0.0084	0.4798	12.608	60.4	98.7	16.062	0.038
06	11.21	0.0084	0.4920	8.885	60.6	98.7	16.069	0.043
14	13.04	0.0108	6.654	5.217	47.3	84.9	16.070	0.071
02	11.21	0.0088	0.4535	14.502	58.0	98.8	16.074	0.035
09	11.65	0.0093	1.896	6.725	54.6	95.2	16.091	0.046
13	11.46	0.0088	1.251	7.026	58.3	96.8	16.095	0.046
10	11.56	0.0131	1.526	12.481	38.9	96.1	16.121	0.036
07	11.24	0.0100	0.4342	9.265	51.0	98.9	16.135	0.043
11	11.34	0.0079	0.7457	2.954	64.3	98.1	16.137	0.079
03	11.24	0.0096	0.3650	9.628	53.2	99.0	16.153	0.042
Mean age ± 2σ	n=15	MSWD=1.24		53.2 ±16.0		16.072		0.029
HRL-14A , Sanidine, J=0.0008083±0.05%, D=1.0014±0.001, NM-221P, Lab#=58751								
15	11.20	0.0128	0.6189	10.950	39.9	98.4	15.993	0.037
03	11.54	0.0134	1.731	8.332	38.0	95.6	16.011	0.043
08	11.13	0.0086	0.3433	5.134	59.1	99.1	16.017	0.055
10	11.06	0.0121	0.0914	6.864	42.1	99.8	16.027	0.041
04	11.44	0.0094	1.341	4.726	54.5	96.5	16.029	0.056
11	11.22	0.0087	0.6045	8.808	58.9	98.4	16.036	0.039
12	12.72	0.0104	5.642	9.243	49.2	86.9	16.043	0.052
01	11.12	0.0082	0.2237	2.866	62.3	99.4	16.045	0.087
07	11.15	0.0090	0.3234	4.426	57.0	99.1	16.055	0.058
09	11.15	0.0124	0.2973	6.306	41.2	99.2	16.057	0.043
06	11.10	0.0087	0.1255	5.485	58.6	99.7	16.064	0.050
05	11.07	0.0094	0.0347	10.567	54.5	99.9	16.064	0.036
02	14.03	0.0094	10.01	5.339	54.2	78.9	16.072	0.080
14	11.54	0.0098	1.556	5.608	51.8	96.0	16.084	0.053
13	11.13	0.0125	0.1260	5.834	40.9	99.7	16.103	0.048
Mean age ± 2σ	n=15	MSWD=0.41		50.8 ±16.5		16.043		0.029

Table F1, continued

ID	$^{40}\text{Ar}/^{39}\text{Ar}$	$^{37}\text{Ar}/^{39}\text{Ar}$	$^{36}\text{Ar}/^{39}\text{Ar}$ ($\times 10^{-3}$)	$^{39}\text{Ar}_K$ ($\times 10^{-15}$ mol)	K/Ca	$^{40}\text{Ar}^*$ (%)	Age (Ma)	$\pm 1\sigma$ (Ma)
HRL-26 , Alkali feldspar J=0.0008095±0.05%, D=1.0014±0.001, NM-221P, Lab#=58752								
06	12.75	0.2189	5.260	0.416	2.3	88.0	16.31	0.52
08	11.59	0.0924	1.171	1.321	5.5	97.1	16.36	0.18
03	11.70	3.375	2.270	0.187	0.15	96.7	16.5	1.0
05	11.64	0.0405	0.7857	1.888	12.6	98.0	16.58	0.12
15	11.60	0.0546	0.5898	1.111	9.4	98.5	16.62	0.20
13	12.13	0.7343	2.487	0.370	0.69	94.4	16.67	0.55
09	11.60	0.0399	0.4528	1.750	12.8	98.9	16.67	0.12
14	11.54	0.1196	0.1560	1.153	4.3	99.7	16.72	0.18
02	13.30	1.971	6.530	0.374	0.26	86.7	16.79	0.58
01	12.48	0.3975	3.124	1.810	1.3	92.9	16.86	0.13
12	11.68	0.1577	-0.1345	0.672	3.2	100.5	17.06	0.30
07	21.24	0.5674	32.27	0.645	0.90	55.3	17.09	0.42
10	11.52	0.3131	-1.4064	0.564	1.6	103.8	17.39	0.38
11	12.84	1.796	2.464	0.138	0.28	95.5	17.8	1.4
Mean age ± 2σ	n=14		MSWD=1.03		4.0 ± 9.0	16.69	0.11	
HRL-27 , Alkali feldspar J=0.000811±0.05%, D=1.0014±0.001, NM-221P, Lab#=58753								
15	12.76	3.568	12.04	0.087	0.14	74.4	13.9	2.3
11	12.06	3.053	6.764	0.093	0.17	85.5	15.1	2.0
09	12.41	5.221	6.999	0.228	0.098	86.8	15.75	0.87
05	16.10	3.998	18.31	0.236	0.13	68.4	16.09	0.91
14	12.30	1.291	4.030	0.427	0.40	91.2	16.35	0.50
06	14.26	0.1490	10.23	1.564	3.4	78.9	16.39	0.17
01	11.65	0.0324	1.047	1.969	15.7	97.4	16.52	0.13
12	11.49	0.0344	0.5079	3.248	14.8	98.7	16.523	0.079
02	11.82	0.4823	1.563	0.984	1.1	96.4	16.61	0.22
03	11.65	0.2159	0.8717	0.989	2.4	97.9	16.62	0.21
13	11.44	1.505	0.5028	0.248	0.34	99.8	16.64	0.84
10	11.72	0.2053	0.9093	1.221	2.5	97.9	16.70	0.18
07	11.87	0.2851	1.313	1.206	1.8	96.9	16.75	0.17
08	14.86	1.655	11.02	0.457	0.31	79.0	17.12	0.49
04	14.91	4.512	9.987	0.055	0.11	82.7	18.0	3.5
Mean age ± 2σ	n=15		MSWD=0.58		2.9 ± 10.3	16.55	0.10	

Table F1, continued

ID	$^{40}\text{Ar}/^{39}\text{Ar}$	$^{37}\text{Ar}/^{39}\text{Ar}$	$^{36}\text{Ar}/^{39}\text{Ar}$ (x 10 ⁻³)	$^{39}\text{Ar}_K$ (x 10 ⁻¹⁵ mol)	K/Ca	$^{40}\text{Ar}^*$ (%)	Age (Ma)	$\pm 1(1)$ (Ma)
HRL-31 , Alkali feldspar, J=0.0008121±0.05%, D=1.0014±0.001, NM-221P, Lab#=58754								
15	18.35	2.408	27.51	0.156	0.21	56.8	15.2	1.3
09	13.21	2.155	9.317	0.367	0.24	80.5	15.54	0.64
14	12.69	1.635	6.420	0.488	0.31	86.1	15.96	0.44
01	18.92	3.791	27.73	0.375	0.13	58.4	16.15	0.60
13	11.52	0.6671	1.644	0.501	0.76	96.3	16.18	0.42
05	11.51	0.4103	1.110	0.746	1.2	97.4	16.36	0.27
12	11.96	0.4638	2.401	0.824	1.1	94.4	16.48	0.26
11	17.33	3.832	21.31	0.299	0.13	65.5	16.60	0.70
02	11.65	0.3890	0.8250	1.256	1.3	98.2	16.68	0.16
06	12.12	0.2569	2.388	2.092	2.0	94.4	16.68	0.11
07	11.86	0.4786	1.520	1.302	1.1	96.5	16.70	0.18
08	11.54	0.6579	0.3571	0.643	0.78	99.6	16.76	0.32
04	11.78	1.079	1.210	0.574	0.47	97.7	16.81	0.37
03	11.80	1.201	1.283	0.928	0.42	97.6	16.82	0.23
10	12.17	0.9334	1.997	0.629	0.55	95.8	17.01	0.32
Mean age ± 2(1)		n=15	MSWD=0.90		0.71 ± 1.07	16.64	0.13	

Notes:

Isotopic ratios corrected for blank, radioactive decay, and mass discrimination, not corrected for interfering Errors quoted for individual analyses include analytical error only, without interfering reaction or J uncertainty Mean age is weighted mean age of Taylor (1982). Mean age error is weighted error

of the mean (Taylor, 1982), multiplied by the root of the MSWD where MSWD>1, and also incorporates uncertainty in J factors and irradiation correction uncertainties.

Decay constants and isotopic abundances after Steiger and Jäger (1977).

symbol preceding sample ID denotes analyses excluded from mean age calculations.

Ages calculated relative to FC-2 Fish Canyon Tuff sanidine interlaboratory standard at 28.02 Ma

Decay Constant (LambdaK (total)) = 5.543e-10/a

Correction factors:

$$(^{39}\text{Ar}/^{37}\text{Ar})_{\text{Ca}} = 0.00068 \pm 5\text{e-}05$$

$$(^{36}\text{Ar}/^{37}\text{Ar})_{\text{Ca}} = 0.00028 \pm 2\text{e-}05$$

$$(^{38}\text{Ar}/^{39}\text{Ar})_K = 0.0125$$

$$(^{40}\text{Ar}/^{39}\text{Ar})_K = 0 \pm 0.0004$$

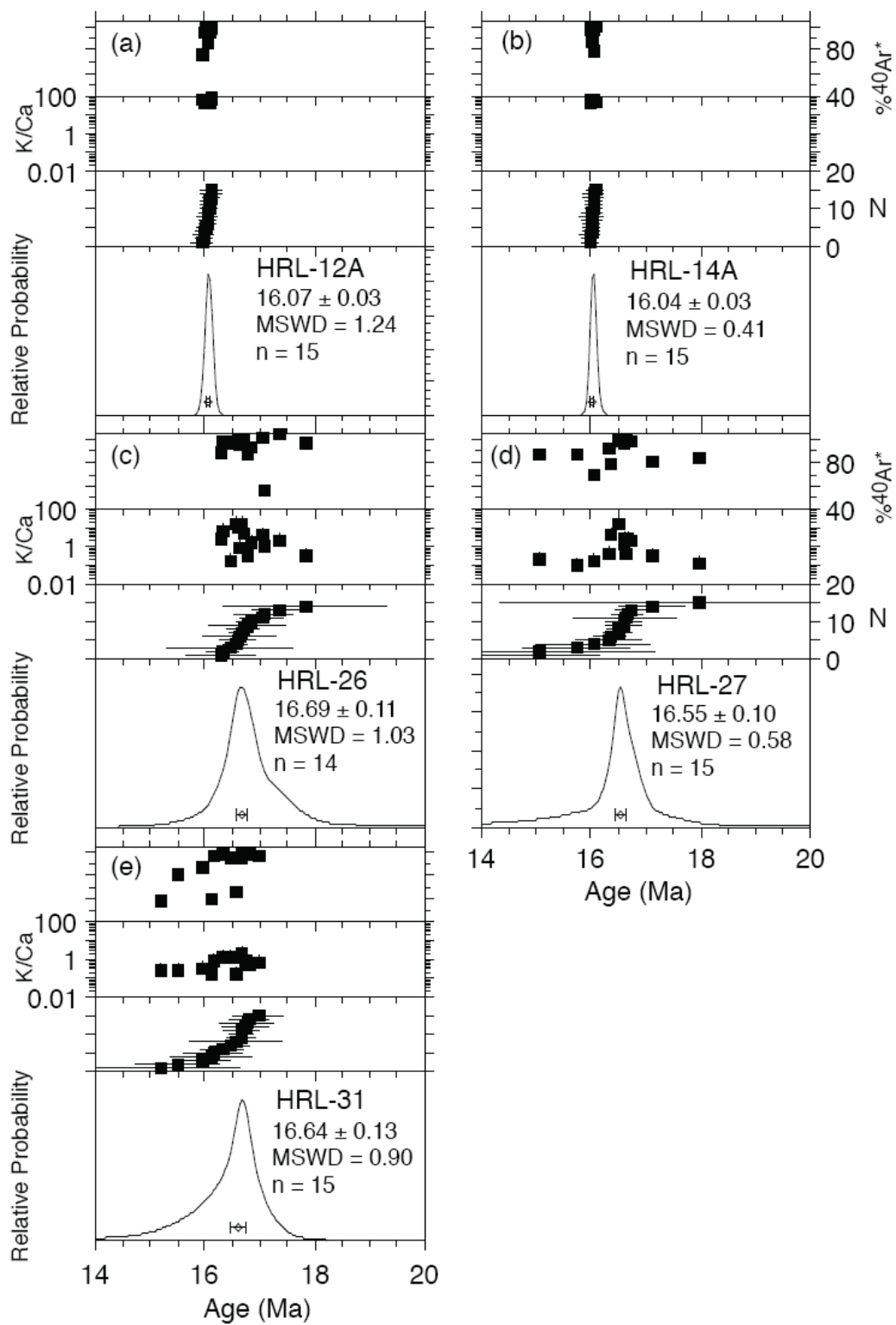


Figure F1. Ar-Ar probability graphs by sample from the Highland Range silicic sequence.

APPENDIX G:
Glass Major Elemental Data
of the Highland Range silicic sequence,
Electron Microprobe Analyses

Table G1. Major elemental data from electron microprobe analysis of glass from the Highland Range silicic sequence. Spot analyses that were not of pure glass were removed.

Sample	P2O5	SiO2	TiO2	Al2O3	MgO	CaO	MnO	FeO	Na2O	K2O	Total
HRL 14a-gl-3	0.17	71.11	0.69	13.52	0.00	0.41	0.01	0.68	3.18	6.41	96.19
HRL 14a-gl-4	0.32	69.90	0.65	13.60	0.36	0.84	0.03	1.09	3.15	6.45	96.38
HRL 14a-gl-7	0.13	70.50	0.76	13.49	0.02	0.31	0.02	0.56	3.11	6.36	95.25
HRL 14a-gl-8	0.09	70.86	0.77	13.45	0.02	0.30	0.01	0.78	3.11	6.52	95.90
HRL 14a-gl-9	0.08	70.73	0.71	14.00	0.01	0.35	0.00	0.49	3.27	6.29	95.93
HRL 14a-gl-11	0.13	70.27	0.70	13.47	0.16	0.53	0.02	1.35	3.17	6.31	96.12
HRL 16-gl-1	0.01	73.30	0.11	11.79	0.05	0.41	0.06	0.56	2.52	5.88	94.69
HRL 16-gl-2	0.00	73.52	0.12	11.78	0.03	0.42	0.05	0.55	2.52	5.91	94.92
HRL 16-gl-3	0.01	74.54	0.11	11.93	0.04	0.47	0.02	0.60	2.99	5.36	96.08
HRL 16-gl-5	0.00	74.40	0.10	11.93	0.04	0.41	0.03	0.59	3.10	5.21	95.80
HRL 16-gl-6	0.00	74.23	0.11	12.09	0.03	0.45	0.07	0.56	3.07	5.18	95.78
HRL 16-gl-7	0.00	74.01	0.10	12.00	0.07	0.47	0.06	0.53	3.17	5.29	95.69
HRL 21-gl-1	0.00	74.01	0.11	11.76	0.06	0.45	0.03	0.58	3.07	5.03	95.11
HRL 21-gl-3	0.01	73.70	0.09	11.78	0.05	0.49	0.01	0.52	3.05	4.92	94.62
HRL 21-gl-4	0.01	74.23	0.14	11.87	0.05	0.42	0.01	0.53	3.15	4.93	95.35
HRL 21-gl-5	0.04	73.71	0.09	11.85	0.05	0.45	0.04	0.58	3.19	4.98	94.97
HRL 21-gl-7	0.00	73.47	0.14	11.83	0.04	0.48	0.04	0.46	3.05	5.14	94.65
HRL 10b-gl-1	0.03	67.27	0.00	13.94	0.35	2.05	0.00	0.00	1.57	3.69	88.91
HRL 10b-gl-2	0.01	88.56	0.14	4.39	0.22	0.19	0.04	0.68	1.07	2.13	97.44
HRL 10b-gl-3	0.00	63.30	0.22	10.95	0.44	1.19	0.06	1.39	1.03	5.62	84.19
HRL 10b-gl-5	0.06	64.12	0.00	13.16	0.33	2.05	0.03	0.07	1.79	4.04	85.65
HRL 10b-gl-6	0.00	67.91	0.00	13.86	0.32	1.86	0.01	0.00	1.89	4.58	90.42
HRL 10b-gl-7	0.02	67.35	0.02	13.68	0.29	1.79	0.01	0.09	1.73	4.66	89.64
HRL 10b-gl-8	0.05	64.45	0.04	13.02	0.29	1.55	0.00	0.35	1.70	4.91	86.35
HRL-27-gl-1	0.00	72.59	0.30	13.63	0.02	0.28	0.04	0.31	4.01	4.90	96.08
HRL-27-gl-2	0.00	72.27	0.27	13.51	0.00	0.29	0.03	0.26	3.49	5.62	95.73
HRL-27-gl-3	0.00	71.43	0.26	13.29	0.00	0.26	0.02	0.26	3.78	5.04	94.34
HRL-27-gl-4	0.03	70.59	0.25	13.20	0.01	0.30	0.00	0.23	4.00	4.98	93.61
HRL-27-gl-5	0.02	70.93	0.27	13.48	0.00	0.30	0.02	0.26	3.87	5.00	94.15
HRL-27-gl-6	0.02	72.60	0.27	13.54	0.00	0.26	0.03	0.23	4.04	4.97	95.95
HRL-12a-gl-1	0.00	88.72	0.06	5.84	0.08	0.18	0.03	0.24	1.35	3.03	99.53

Table G2. Averages of normalized major elemental data from electron microprobe analysis of glass from the Highland Range silicic sequence. Note that samples HRL 10b or HRL 12a were not averaged or used in calculations.

Sample	HRL 14a Average	HRL 16 Average	HRL 21 Average	HRL 27 Average
P ₂ O ₅	0.16	0.00	0.01	0.01
SiO ₂	73.53	77.49	77.76	75.53
TiO ₂	0.74	0.11	0.12	0.28
Al ₂ O ₃	14.16	12.48	12.45	14.15
MgO	0.10	0.05	0.05	0.00
CaO	0.47	0.46	0.48	0.30
MnO	0.02	0.05	0.03	0.02
FeO	0.86	0.59	0.56	0.27
Na ₂ O	3.30	3.03	3.27	4.07
K ₂ O	6.66	5.73	5.27	5.35
Total	100	100	100	100

APPENDIX H:
Operating Conditions,
Trace Elemental Data of Glass
from the Highland Range Silicic Sequence,
Laser Ablation – Inductively Coupled Plasma Mass Spectrometer

Table H1. Operating conditions for LA-ICP-MS analysis on samples from the Highland Range silica sequence.

Table F1. LA-ICP-MS Operating Conditions (after Luo and Ayers, 2007)	
<i>Perkin-Elmer Sciex ELAN 6100 DRCII</i>	
Forward Power	1350-1400 W
Gas Flow Rate	
Nebulizer	0.75 L min ⁻¹
Auxiliary	0.65-1.00 L min ⁻¹
Plasma	~15.0 L min ⁻¹
Lens Voltage	10.5 V
Auto Lens	OFF
<i>New Wave 213 Laser Ablation System</i>	
Wavelength	213 nm
Energy (26-30 kV, 10 Hz)	~6 J cm ²
Laser Frequency	10 Hz
Laser Output	80%
Spot Size	60 µm
He Carrier Gas Flow	0.85 L min ⁻¹
Pulse Duration	20 ns
<i>Data acquisition</i>	
Data Acquisition Protocol	Time resolved analysis
Scanning Mode	Peak hopping, 1 pt/peak
Dwell Time	~60 s
Analysis Time	60 s
Final Dwell Time	~60 s
Replicates	1

Table H2. Rare earth element data from LA-ICPMS analysis of glass from samples HRL 16, HRL 21, HRL 10b, and HRL 27. Note that the data from HRL 10b is usable but not reliable.

Analyte Element (ppm)	La139 La	Ce140 Ce	Pr141 Pr	Nd143 Nd	Sm147 Sm	Eu151 Eu	Gd155 Gd	Tb159 Tb	Dy163 Dy	Ho165 Ho	Er166 Er	Tm169 Tm	Yb173 Yb	Lu175 Lu
028_13Apr2009_HRL16	38.1	45.0	4.91	11.4	1.28	0.25	0.94	0.20	1.31	0.38	1.16	0.19	1.58	0.21
097_14Apr2009_HRL16	31.3	46.9	3.57	9.08	1.68	0.18	1.17	0.16	1.38	0.30	1.06	0.21	1.86	0.29
Average	34.7	46.0	4.24	10.2	1.48	0.22	1.06	0.18	1.35	0.34	1.11	0.20	1.72	0.25
St Dev/Average	14%	3%	22%	16%	19%	26%	15%	16%	4%	18%	6%	8%	12%	23%

Table H2, continued

Analyte Element (ppm)	La139 La	Ce140 Ce	Pr141 Pr	Nd143 Nd	Sm147 Sm	Eu151 Eu	Gd155 Gd	Tb159 Tb	Dy163 Dy	Ho165 Ho	Er166 Er	Tm169 Tm	Yb173 Yb	Lu175 Lu
036_13Apr2009_HRL21	29.7	47.3	4.15	10.8	1.67	0.18	1.41	0.24	1.51	0.31	0.81	0.15	1.64	0.21
037_13Apr2009_HRL21	31.2	51.0	4.30	11.2	1.68	0.13	1.51	0.18	1.09	0.32	1.31	0.17	1.44	0.21
039_13Apr2009_HRL21	34.7	54.5	4.92	12.5	2.30	0.23	1.13	0.28	1.60	0.36	1.33	0.23	1.71	0.32
040_13Apr2009_HRL21	35.2	55.9	4.47	12.6	1.81	0.13	1.53	0.18	1.67	0.34	1.55	0.22	1.83	0.25
041_13Apr2009_HRL21	35.3	56.3	4.55	13.0	1.69	0.30	1.47	0.34	1.42	0.38	1.14	0.33	1.75	0.25
042_13Apr2009_HRL21	34.5	55.3	4.92	13.3	1.37	0.18	2.08	0.29	1.36	0.45	1.17	0.28	1.87	0.22
043_13Apr2009_HRL21	34.3	56.6	4.40	11.0	2.47	0.26	1.55	0.20	1.95	0.45	1.23	0.16	1.58	0.25
044_13Apr2009_HRL21	34.0	55.5	4.58	13.0	1.84	0.25	1.28	0.21	2.04	0.37	1.26	0.28	1.37	0.31
045_13Apr2009_HRL21	33.6	56.6	4.36	13.8	1.57	0.35	1.90	0.27	1.91	0.42	1.19	0.21	2.03	0.23
Average	33.6	54.3	4.52	12.3	1.82	0.22	1.54	0.24	1.62	0.38	1.22	0.22	1.69	0.25
St Dev/Average	6%	6%	6%	9%	19%	34%	19%	23%	19%	14%	16%	27%	12%	16%

Table H2, continued

Analyte Element (ppm)	La139 La	Ce140 Ce	Pr141 Pr	Nd143 Nd	Sm147 Sm	Eu151 Eu	Gd155 Gd	Tb159 Tb	Dy163 Dy	Ho165 Ho	Er166 Er	Tm169 Tm	Yb173 Yb	Lu175 Lu
059_14Apr2009_HRL10b	2.59	7.20	0.40	1.18	0.13 <0.040		0.21	0.01 <0.089		0.02 <0.059		0.08	0.26	0.03
060_14Apr2009_HRL10b	5.99	7.33	0.65	2.34	0.40	0.08	0.23	0.05	0.12	0.04	0.09 <0.018		0.23	0.05
061_14Apr2009_HRL10b	123	27.5	15.5	32.4	3.69	0.43	3.57	0.26	1.53	0.25	0.74	0.10	0.65	0.38
062_14Apr2009_HRL10b	6.70	12.8	1.11	26.8	0.80 <0.075		0.52	0.10	0.14 <0.035		0.13 <0.023		0.29	0.02
063_14Apr2009_HRL10b	4.42	86.3	0.79	2.56 <0.128		0.04	0.35	0.04	0.51	0.07	0.45	0.09	0.87	0.25
064_14Apr2009_HRL10b	7.20	13.7	0.88	2.64	0.44	0.08	0.39 <0.028	<0.137		0.05	0.09	0.03	0.34	0.31
065_14Apr2009_HRL10b	9.07	14.1	1.10	3.04	0.58	0.06	0.36	0.04	0.15 <0.032	<0.045		0.05	0.43	0.10
066_14Apr2009_HRL10b	3.10	9.55	0.46	1.61	0.53 <0.064		0.11 <0.032	0.16 <0.027	<0.09	<0.09	<0.025		0.40	0.11
067_14Apr2009_HRL10b	9.88	10.2	1.42	3.25	0.98 <0.056	<0.19		0.06	0.33	0.08	0.20 <0.027		0.26	0.23
068_14Apr2009_HRL10b	4.36	6.37	0.59	1.58	0.27 <0.062	<0.161		0.02 <0.098		0.02	0.05 <0.023		0.34	0.21
Average	17.6	19.5	2.29	7.74	0.87	0.14	0.72	0.07	0.42	0.08	0.25	0.07	0.41	0.17
St Dev/Average	210%	124%	203%	150%	125%	119%	161%	110%	121%	105%	102%	43%	50%	73%

Table H2, continued

Analyte Element (ppm)	La139 La	Ce140 Ce	Pr141 Pr	Nd143 Nd	Sm147 Sm	Eu151 Eu	Gd155 Gd	Tb159 Tb	Dy163 Dy	Ho165 Ho	Er166 Er	Tm169 Tm	Yb173 Yb	Lu175 Lu
079_14Apr2009_HRL27	72.1	135	13.5	47.5	7.85	0.99	5.08	0.75	4.29	0.83	2.25	0.37	2.00	0.33
080_14Apr2009_HRL27	80.0	146	14.9	51.9	7.29	0.91	5.39	0.78	4.93	0.90	2.86	0.36	2.22	0.48
081_14Apr2009_HRL27	78.1	143	14.4	54.5	7.91	1.36	6.23	0.72	3.88	0.96	2.51	0.36	3.08	0.27
082_14Apr2009_HRL27	78.6	145	14.9	52.6	7.15	1.05	5.44	0.78	4.89	0.80	2.11	0.32	2.84	0.36
083_14Apr2009_HRL27	79.1	145	15.0	53.4	7.93	1.06	4.94	0.80	4.96	0.89	2.52	0.35	2.93	0.42
084_14Apr2009_HRL27	77.7	145	14.9	51.4	7.86	1.05	5.34	0.62	4.16	0.83	2.35	0.26	3.27	0.30
085_14Apr2009_HRL27	77.8	144	15.2	50.1	7.93	0.95	5.83	0.92	4.55	0.95	2.57	0.30	2.03	0.27
086_14Apr2009_HRL27	77.9	146	14.1	51.1	8.52	0.97	6.30	0.81	4.30	0.88	2.26	0.34	2.36	0.35
087_14Apr2009_HRL27	81.6	147	15.3	53.9	8.20	0.93	6.08	0.88	5.41	0.86	2.55	0.36	2.82	0.31
088_14Apr2009_HRL27	81.3	155	15.9	57.2	8.47	1.14	5.92	0.83	4.90	0.91	2.50	0.33	3.33	0.35
112_14Apr2009_HRL27	82.3	149	14.7	54.8	8.52	1.37	6.27	0.78	5.23	0.88	2.74	0.36	2.74	0.36
113_14Apr2009_HRL27	82.5	154	15.6	55.6	8.55	1.35	5.83	0.83	4.74	0.99	2.48	0.36	2.91	0.40
115_14Apr2009_HRL27	80.2	148	15.4	51.3	8.67	1.19	5.90	0.87	3.80	0.97	2.47	0.34	2.38	0.42
Average	79.2	146	14.9	52.7	8.07	1.10	5.73	0.80	4.62	0.90	2.47	0.34	2.69	0.36
St Dev/Average	3%	3%	4%	5%	6%	15%	8%	9%	11%	7%	8%	9%	17%	17%

Table H3. Trace element data from LA-ICPMS analysis of glass from samples HRL 16, HRL 21, HRL 10b, and HRL 27. Note that the data from HRL 10b is usable but not reliable.

Analyte Element (ppm)	Mg24 Mg	Al27 Al	Si29 Si	P31 P	Ca42 Ca	Sc45 Sc	Ti49 Ti	V51 V	Cr52 Cr
028_13Apr2009_HRL16	276	61908	362219 <17.06		3132	1.82	484	0.52 <2.15	
097_14Apr2009_HRL16	308	58281	362219 <28.36		3302	1.34	498	0.62 <2.18	
Average	292	60095	362219 #DIV/0!		3217	1.58	491	0.57 #DIV/0!	
St Dev/Average	8%	4%	0% #DIV/0!		4%	21%	2%	12% #DIV/0!	

Table H3, continued

Analyte Element (ppm)	Mn55 Mn	Fe57 Fe	Co59 Co	Ni60 Ni	Cu65 Cu	Zn66 Zn	Ga71 Ga	Rb85 Rb	Sr88 Sr
028_13Apr2009_HRL16	275	3627	<0.184	<0.90	0.72	19.9	17.6	177	26.8
097_14Apr2009_HRL16	289	3845	0.20	<0.70	1.74	19.6	15.9	168	19.1
Average	282	3736	0.20	#DIV/0!	1.23	19.8	16.7	172	22.9
St Dev/Average	3%	4%	#DIV/0!	#DIV/0!	59%	1%	7%	4%	24%

Table H3, continued

Analyte Element (ppm)	Y89 Y	Zr90 Zr	Nb93 Nb	Cs133 Cs	Ba137 Ba	Hf179 Hf	Ta181 Ta	Pb208 Pb	Th232 Th	U238 U
028_13Apr2009_HRL16	11.2	57.7	22.1	2.51	42.6	2.80	1.30	30.3	19.9	3.92
097_14Apr2009_HRL16	11.2	62.1	22.7	2.51	25.2	2.98	1.34	27.6	20.9	4.14
Average	11.2	59.9	22.4	2.51	33.9	2.89	1.32	29.0	20.4	4.03
St Dev/Average	0%	5%	2%	0%	36%	4%	2%	7%	3%	4%

Table H3, continued

Analyte Element (ppm)	Mg24 Mg	Al27 Al	Si29 Si	P31 P	Ca42 Ca	Sc45 Sc	Ti49 Ti	V51 V	Cr52 Cr
036_13Apr2009_HRL21	417	49843	363481	<38.18	3398	1.22	555	0.99	<3.42
037_13Apr2009_HRL21	673	56456	363481	<28.18	4506	1.60	615	1.63	<2.74
039_13Apr2009_HRL21	366	57702	363481	27.1	3695	1.39	611	1.31	<2.64
040_13Apr2009_HRL21	323	58530	363481	<23.79	3660	2.42	619	1.33	3.58
041_13Apr2009_HRL21	318	59459	363481	31.2	3716	2.16	615	1.47	<2.81
042_13Apr2009_HRL21	325	57938	363481	28.6	3923	1.50	623	1.68	<2.71
043_13Apr2009_HRL21	317	57411	363481	<20.72	3643	1.59	631	1.59	<2.63
044_13Apr2009_HRL21	314	57295	363481	22.7	3665	2.13	623	1.71	2.56
045_13Apr2009_HRL21	321	57393	363481	31.7	3514	1.77	617	1.16	3.08
Average	375	56892	363481	28.2	3747	1.75	612	1.43	3.07
St Dev/Average	31%	5%	0%	13%	9%	23%	4%	17%	17%

Table H3, continued

Analyte Element (ppm)	Mn55 Mn	Fe57 Fe	Co59 Co	Ni60 Ni	Cu65 Cu	Zn66 Zn	Ga71 Ga	Rb85 Rb	Sr88 Sr	
036_13Apr2009_HRL21	254	4199		0.23 <1.10	<0.68		16.2	14.9	177	12.2
037_13Apr2009_HRL21	255	3958		0.20 <0.71		1.61	21.1	15.1	203	12.8
039_13Apr2009_HRL21	287	4131		0.24 <1.23	<0.98		20.5	15.0	193	13.1
040_13Apr2009_HRL21	287	4256		0.23 <1.26	<0.99		24.9	13.1	184	13.0
041_13Apr2009_HRL21	292	4271	<0.21	<1.00	<0.74		26.5	14.5	182	13.4
042_13Apr2009_HRL21	284	4236		0.38 <0.79	<1.05		21.4	15.5	204	13.2
043_13Apr2009_HRL21	291	4277		0.35 <1.02		0.82	21.5	15.8	176	12.7
044_13Apr2009_HRL21	288	4264		0.18 <1.07	<0.79		25.7	15.4	179	13.4
045_13Apr2009_HRL21	290	4339		0.33 <1.41		1.21	22.2	15.8	193	13.3
Average	281	4214		0.27 #DIV/0!		1.21	22.2	15.0	188	13.0
St Dev/Average	5%	3%		28% #DIV/0!		33%	14%	6%	6%	3%

Table H3, continued

Analyte Element (ppm)	Y89 Y	Zr90 Zr	Nb93 Nb	Cs133 Cs	Ba137 Ba	Hf179 Hf	Ta181 Ta	Pb208 Pb	Th232 Th	U238 U
036_13Apr2009_HRL21	10.8	73.3	22.0	2.46	15.9	2.62	1.28	21.8	19.8	4.07
037_13Apr2009_HRL21	12.2	78.7	22.8	3.23	16.0	2.71	1.56	23.1	22.6	4.56
039_13Apr2009_HRL21	13.3	82.6	23.5	2.93	16.4	3.31	1.64	27.3	24.1	5.20
040_13Apr2009_HRL21	12.2	80.2	23.8	3.17	19.0	3.40	1.56	27.0	24.4	5.04
041_13Apr2009_HRL21	12.8	80.1	24.7	3.08	18.4	3.14	1.66	28.7	24.5	5.12
042_13Apr2009_HRL21	13.0	81.8	25.2	3.13	20.4	3.23	1.53	27.7	23.7	5.11
043_13Apr2009_HRL21	12.4	79.8	23.8	3.08	20.0	3.14	1.78	27.7	23.7	5.09
044_13Apr2009_HRL21	12.9	80.4	23.6	2.89	19.7	3.02	1.62	28.5	24.2	4.91
045_13Apr2009_HRL21	12.1	79.0	23.5	3.17	17.1	3.22	1.54	28.1	23.8	5.21
Average	12.4	79.5	23.6	3.02	18.1	3.09	1.57	26.6	23.4	4.92
St Dev/Average	6%	3%	4%	8%	10%	9%	9%	9%	6%	8%

Table H3, continued

Analyte Element (ppm)	Mg24 Mg	Al27 Al	Si29 Si	P31 P	Ca42 Ca	Sc45 Sc	Ti49 Ti	V51 V	Cr52 Cr
059_14Apr2009_HRL10b	2956	43427	350580 <28.99		9218	4.79	959	0.53	<2.23
060_14Apr2009_HRL10b	2975	58193	350580 <25.77		12705	3.58	898	<0.35	<2.10
061_14Apr2009_HRL10b	2849	61508	350580 49.8		11247	3.66	809	1.68	<2.29
062_14Apr2009_HRL10b	2940	60841	350580 <22.90		11788	2.57	730	<0.39	3.71
063_14Apr2009_HRL10b	3663	67235	350580 <26.12		12109	3.99	971	<0.51	4.19
064_14Apr2009_HRL10b	3310	61577	350580 <23.88		12381	4.35	1038	0.94	3.53
065_14Apr2009_HRL10b	2556	62737	350580 <18.79		11024	3.43	769	0.75	3.19
066_14Apr2009_HRL10b	2408	60305	328329 25.3		11740	2.42	690	0.58	<2.50
067_14Apr2009_HRL10b	2805	60413	328329 38.1		11207	3.75	830	1.21	3.01
068_14Apr2009_HRL10b	3220	53559	328329 <17.13		12432	4.01	898	0.62	2.98
Average	2968	58980	343904	37.7	11585	3.66	859	0.90	3.44
St Dev/Average	12%	11%	3%	32%	9%	20%	13%	46%	14%

Table H3, continued

Analyte Element (ppm)	Mn55 Mn	Fe57 Fe	Co59 Co	Ni60 Ni	Cu65 Cu	Zn66 Zn	Ga71 Ga	Rb85 Rb	Sr88 Sr
059_14Apr2009_HRL10b	207	8327	0.16	3.33	4.32	49.6	24.3	215	90.7
060_14Apr2009_HRL10b	162	6918	<0.172	2.90	1.89	44.6	16.1	231	145
061_14Apr2009_HRL10b	232	6611	<0.24	5.75	2.84	39.9	15.3	232	126
062_14Apr2009_HRL10b	202	5930	0.27	2.61	2.76	51.8	19.0	230	129
063_14Apr2009_HRL10b	346	7816	0.53	4.74	3.02	47.7	17.8	223	141
064_14Apr2009_HRL10b	152	7584	<0.20	3.58	2.28	49.7	15.2	231	132
065_14Apr2009_HRL10b	120	5674	0.27	4.12	1.63	32.8	18.4	232	118
066_14Apr2009_HRL10b	112	5821	<0.173	<1.45	1.93	30.8	15.8	220	123
067_14Apr2009_HRL10b	120	6595	<0.28	4.60	1.91	42.3	15.0	214	127
068_14Apr2009_HRL10b	156	6253	0.21	2.61	2.08	34.3	13.8	229	129
Average	181	6753	0.29	3.80	2.47	42.3	17.1	226	126
St Dev/Average	39%	13%	50%	28%	33%	18%	18%	3%	12%

Table H3, continued

Analyte Element (ppm)	Y89 Y	Zr90 Zr	Nb93 Nb	Cs133 Cs	Ba137 Ba	Hf179 Hf	Ta181 Ta	Pb208 Pb	Th232 Th	U238 U
059_14Apr2009_HRL10b	0.60	61.9	21.4	6.85	4.10	2.52	1.13	5.78	12.2	4.13
060_14Apr2009_HRL10b	0.86	91.8	21.0	7.00	5.94	4.08	1.91	4.86	13.2	4.47
061_14Apr2009_HRL10b	9.17	87.6	22.3	8.22	8.11	4.39	1.80	7.55	91.2	4.95
062_14Apr2009_HRL10b	1.38	71.8	19.3	6.32	6.67	3.26	1.82	5.62	39.5	4.57
063_14Apr2009_HRL10b	1.95	89.7	27.5	7.40	7.69	5.73	1.86	55.6	29.6	4.91
064_14Apr2009_HRL10b	0.92	84.8	25.9	8.36	7.56	4.24	1.59	7.80	18.8	4.83
065_14Apr2009_HRL10b	0.77	74.8	20.9	6.85	7.60	4.00	1.50	6.65	18.0	4.27
066_14Apr2009_HRL10b	0.60	79.1	18.3	7.32	3.77	4.55	1.72	4.44	19.6	3.66
067_14Apr2009_HRL10b	1.15	90.8	24.8	7.43	5.37	4.24	1.85	5.55	29.0	4.37
068_14Apr2009_HRL10b	0.57	89.8	21.6	7.83	4.58	3.87	1.81	3.29	12.4	4.37
Average	1.80	82.2	22.3	7.36	6.14	4.09	1.70	10.7	28.3	4.45
St Dev/Average	146%	12%	13%	9%	26%	20%	14%	148%	84%	9%

Table H3, continued

Analyte Element (ppm)	Mg24 Mg	Al27 Al	Si29 Si	P31 P	Ca42 Ca	Sc45 Sc	Ti49 Ti	V51 V	Cr52 Cr
079_14Apr2009_HRL27	1175	56695	353057 <33.70		4094	3.20	1536	7.80	<2.97
080_14Apr2009_HRL27	932	61532	353057	63.0	4213	3.29	1625	7.48	<2.41
081_14Apr2009_HRL27	911	63904	353057	40.1	4464	3.49	1585	7.79	<2.43
082_14Apr2009_HRL27	890	61491	353057	69.9	4214	3.56	1601	7.52	2.26
083_14Apr2009_HRL27	927	61273	353057	61.7	4061	3.81	1591	7.75	2.39
084_14Apr2009_HRL27	1572	59518	353057	86.2	4392	3.86	1617	9.70	<2.01
085_14Apr2009_HRL27	788	61434	353057	67.8	3894	3.28	1608	7.33	2.40
086_14Apr2009_HRL27	765	62127	353057	49.1	3652	2.94	1615	7.44	<2.24
087_14Apr2009_HRL27	909	64458	353057	76.6	4028	3.23	1606	8.14	<2.22
088_14Apr2009_HRL27	872	64504	353057	192	4509	3.17	1573	7.06	<2.46
112_14Apr2009_HRL27	977	61712	353057	38.6	4760	2.93	1624	7.93	<2.19
113_14Apr2009_HRL27	1080	63503	353057	173	4261	3.74	1597	7.08	<2.15
115_14Apr2009_HRL27	1122	63212	353057	61.1	4285	3.28	1728	11.9	<2.41
Average	994	61951	353057	81.6	4217	3.37	1608	8.07	2.35
St Dev/Average	21%	3%	0%	60%	7%	9%	3%	16%	3%

Table H3, continued

Analyte Element (ppm)	Mn55 Mn	Fe57 Fe	Co59 Co	Ni60 Ni	Cu65 Cu	Zn66 Zn	Ga71 Ga	Rb85 Rb	Sr88 Sr
079_14Apr2009_HRL27	368	8101	0.67 <0.72		3.02	35.2	17.3	173	49.4
080_14Apr2009_HRL27	407	8552	0.70 <1.02		1.25	33.0	18.6	177	58.3
081_14Apr2009_HRL27	389	8574	0.64 <1.37		1.70	37.6	15.9	175	79.4
082_14Apr2009_HRL27	376	8014	0.68 <0.66		1.65	36.2	19.0	190	53.8
083_14Apr2009_HRL27	359	7539	0.30 <1.08		2.81	34.6	18.4	190	49.3
084_14Apr2009_HRL27	396	9392	0.82 <0.73		6.86	35.1	17.8	206	51.6
085_14Apr2009_HRL27	362	7619	0.72 <1.12		1.22	38.0	17.5	174	53.7
086_14Apr2009_HRL27	362	7650	0.42 1.04	0.97		39.5	17.6	172	51.3
087_14Apr2009_HRL27	373	7996	0.58 <0.85	<0.94		36.9	20.0	179	50.3
088_14Apr2009_HRL27	387	7550	0.30 <1.35	<1.19		32.6	18.5	171	49.4
112_14Apr2009_HRL27	425	8254	0.70 0.96		2.87	35.8	17.8	186	50.8
113_14Apr2009_HRL27	378	8021	0.52 <0.94		3.79	33.8	18.9	215	65.9
115_14Apr2009_HRL27	414	10275	0.62 <1.20		2.83	39.1	19.5	229	50.5
Average	384	8272	0.59	1.00	2.63	36.0	18.2	187	54.9
St Dev/Average	6%	10%	27%	6%	64%	6%	6%	10%	16%

Table H3, continued

Analyte Element (ppm)	Y89 Y	Zr90 Zr	Nb93 Nb	Cs133 Cs	Ba137 Ba	Hf179 Hf	Ta181 Ta	Pb208 Pb	Th232 Th	U238 U
079_14Apr2009_HRL27	22.5	262	26.4	2.38	518	6.36	1.47	25.6	16.2	3.26
080_14Apr2009_HRL27	25.3	279	27.2	2.45	611	8.30	1.58	28.2	18.1	3.21
081_14Apr2009_HRL27	24.0	268	26.7	2.35	722	7.63	1.54	28.7	17.7	3.47
082_14Apr2009_HRL27	24.7	275	26.8	2.55	550	8.32	1.63	28.4	17.8	3.65
083_14Apr2009_HRL27	24.7	281	27.8	2.61	549	8.20	1.73	29.0	18.5	3.64
084_14Apr2009_HRL27	23.5	274	27.9	3.02	533	8.01	1.67	28.1	18.4	3.83
085_14Apr2009_HRL27	24.7	277	27.3	2.61	551	7.87	1.61	28.3	18.6	3.95
086_14Apr2009_HRL27	25.0	278	27.0	2.48	576	7.57	1.62	28.6	18.9	3.76
087_14Apr2009_HRL27	25.3	279	27.8	2.80	560	7.06	1.57	29.5	19.0	3.88
088_14Apr2009_HRL27	26.4	271	27.5	2.64	551	6.97	1.60	29.2	17.5	3.81
112_14Apr2009_HRL27	25.0	276	28.6	2.47	549	6.86	1.67	29.3	18.8	3.72
113_14Apr2009_HRL27	26.0	281	28.0	2.75	719	8.43	1.66	28.7	18.5	3.79
115_14Apr2009_HRL27	24.8	281	27.6	2.85	565	8.88	1.57	27.7	17.9	3.73
Average	24.8	276	27.4	2.61	581	7.73	1.61	28.4	18.1	3.67
St Dev/Average	4%	2%	2%	8%	11%	10%	4%	3%	4%	6%

APPENDIX I:
Estimated Temperatures for Zircon and Sphene
Spot Analyses of the Highland Range Silicic Sequence

Table I1. Estimated temperatures for spot analyses of sphene grains from the Highland Range silicic sequence.

Sample Spot T (Celsius)	Sample Spot T (Celsius)	Sample Spot T (Celsius)	
HRL12A-1.1modZ	721	HRL21-1.1	749
HRL12A-1.2ltZ	724	HRL21-1.2D	749
HRL12A-2.1ltZ	726	HRL21-2.1DE	709
HRL12A-2.2hvZ	730	HRL21-2.2D	712
HRL12A-2.3ltZ	716	HRL21-2.3DC	727
HRL12A-3.1hvZ	724	HRL21-2.4L	726
HRL12A-3.2modZ	720	HRL21-3.1ED	739
HRL12A-3.3hvZ	724	HRL21-3.2D	759
HRL12A-3.4modZ	715	HRL21-3.3LC	759
HRL12A-4.1hvZ	736	HRL21-4.1ED	745
HRL12A-4.2ltZ	720	HRL21-5.1ED	731
HRL12A-4.3modZ	726	HRL21-5.1ED	731
HRL12A-5.1hvZ	729	HRL21-5.2LC	745
HRL12A-5.2ltZ	737	HRL21-6..1DE	685
HRL12A-6.1LOZ	721	HRL21-6.2LC	736
HRL12A-6.2MODZ	723	HRL21-6.3LC	748
HRL12A-6.3HIZ	735	HRL21-6.4ED	714
		HRL21-7.1ED	737
		HRL21-8.1ED	743
		HRL21-8.2C	768
		HRL21-9.1ED	740
		HRL21-9.2LC	760

Table I1, continued

Sample Spot T (Celsius)	Sample Spot T (Celsius)
HLR19A-1.2D	713
HLR19A-1.1L	740
HLR19A-1.3E	715
HLR19A-1.4D	723
HLR19A-2.1ED	707
HLR19A-2.2L	717
HLR19A-2.3DC	721
HLR19A-2.4LC	737
HLR19A-3.1ED	718
HLR19A-3.2L	756
HLR19A-3.3DC	740
HLR19A-3.4DE	709
HLR19A-4.1L	740
HLR19A-4.2D	737
HLR19A-4.3ED	713
HLR19A-5.1L	720
HLR19A-5.2ED	712
HLR19A-5.3L	731
HLR19A-6.1D	714
HLR19A-6.2L	725
HLR19A-6.3I	713
HLR19A-6.4D	715
	HLR19A-7.1L
	HLR19A-7.2D
	HLR19A-8.1IE
	HLR19A-8.2L
	HLR19A-8.3D
	HLR19A-9.1IE
	HLR19A-9.2D
	HLR19A-10.1LE
	HLR19A-11.1L
	HLR19A-11.2IE
	HLR19A-12.1DE
	HLR19A-12.2IE
	HLR19A-12.3LE
	HLR19A-13.1IE
	HLR19A-13.2D
	HLR19A-13.3I
	HLR19A-14.1L
	HLR19A-14.2I

Table I2. Estimated temperatures for spot analyses of zircon grains from the Highland Range silicic sequence.

Sample Spot T (Celsius)	Sample Spot T (Celsius)	Sample Spot T (Celsius)	
HRL12A-1.1C	808	HRL27-1.1LR	862
HRL12A-1.2E	793	HRL27-1.2DC	855
HRL12A-2.1E	832	HRL27-2C	864
HRL12A-2.2idk	793	HRL27-3C	830
HRL12A-2.3ilt	861	HRL27-4I	870
HRL12A-2.4c	824	HRL27-5C	794
HRL12A-3.1edk	795	HRL27-6C	866
HRL12A-3.2idk	779	HRL27-7R	834
HRL12A-3.3e	763	HRL27-8I	855
HRL12A-4.1ilt	829	HRL27-9.1R	838
HRL12A-5.1c	844	HRL27-9.2I	851
HRL12A-5.1elt	785	HRL27-10C	859
HRL12A-6.1cdk	742	HRL27-10.2C	852
HRL12A-6.2ilt	755	HRL27-11	846
HRL12A-7.1c	737	HRL27-12C	784
HRL12A-7.2i	821		
HRL12A-8.1c	731		
HRL12A-8.2e	761		
HRL12A-9.1c	785		
HRL12A-9.2i	792		
HRL12A-9.3e	744		
HRL12A-10.1c	753		
12A-10.2i	818		
12A-11.1e	755		
12A-11.2i	792		
12A-11.3i	815		
12A-12.1i	796		
12A-12.2C	827		
12A-13.1C	811		
12A-13.2e	817		
12A-14.1idk	772		
HRL12A14.2ilt	924		
HRL12A14.3edk	723		

REFERENCES

- Bachl, C.A., Miller, C.F., Miller, J.S., and Faulds, J.E. (2001). Construction of a pluton: Evidence from an exposed cross section of the Searchlight pluton, Eldorado Mountains, Nevada. *Geological Society of America Bulletin*, 113, 1213-1228.
- Bachmann, O. & Bergantz, G.W., (2003). Rejuvenation of the Fish Canyon magma body: A window into the evolution of large-volume silicic magma systems, *Geology*, vol. 31, pg. 789-792.
- Bachmann, O. & Bergantz, G.W. (2008a). Rhyolites and their source mushes across tectonic settings, *Journal of Petrology*, vol. 49, pg. 2277-2285.
- Bachmann, O., Dungan, M.A., and Bussy, F., (2005). Insights into shallow magmatic processes in large silicic magma bodies: the trace element record in the Fish Canyon magma body, Colorado. *Contributions to Mineralogy and Petrology*, vol. 149, pg. 338-349.
- Bachmann, O., Miller, C.F., and de Silva, S.L. (2007). The volcanic-plutonic connection as a stage for understanding crustal magmatism. *Journal of volcanology and geothermal research*, 167, 1-23.
- Blundy, J. & Wood, B. (1994). Prediction of crystal-melt partition coefficients from elastic moduli, *Nature*, vol. 372, pg. 452-454.
- Buttner, R., Dellino, P., and Zimanowski, B., (1999). Identifying magma-water interaction from the surface features of ash particles. *Nature*, vol. 401, pg. 688-690.
- Cas, R.F. & Wright, J.V., (1987). *Volcanic Successions Modern and Ancient*. London, UK: Allen & Unwin Ltd.
- Claiborne, L.L., Miller, C.F., Walker, B.A., Wooden, J.L., Mazdab, F.K., and Bea, F., (2006). Tracking magmatic processes through Zr/Hf ratios in rocks and Hf and Ti zoning in zircons: An example from the Spirit Mountain batholith, Nevada. *Mineralogical Magazine*, 70, 517-543.
- Claiborne, L.L., Miller, C.F., Wooden, J.L., and Mazdab, F.K. (2009). Trace Element Composition of Igneous Zircon: A Thermal and Compositional Record of the Accumulation and Evolution of a Large Silicic Batholith, Spirit Mountain, Nevada. Manuscript submitted for publication.
- Dodge, M.C. Miller, J.S., Faulds, J.E., and Miller, C.F. (2005). An erupted record from the Miocene Searchlight Pluton, Nevada. *Abstract with Programs – GSA*, 37, 66.

- Dolfi, D., de Rita, D., Cimarelli, C., Mollo, S., Soligo, M., and Fabbri, M. (2007). Dome growth rates, eruption frequency and assessment of volcanic hazard: Insights from new U/Th dating of the Panarea and Basiluzzo dome lavas and pyroclastics, Aeolian Islands, Italy, *Elsevier*, vol. 132-136, pg. 182-194.
- Duffield, W.A., Bacon, C.R., and Delany, P.T., (1986). Deformation of poorly consolidated sediment of a basalt sill, Coso Range, California, *Bulletin of Volcanology*, vol. 48, pg. 97-107.
- Faulds, J.E., Feuerbach, D.L., Miller, C.F., and Smith, E.I. (2001). Cenezoic evolution of the northern Colorado River extensional corridor, southern Nevada and northwest Arizona. *Guidebook – Pacific Section American Association of Petroleum Geologists Publication*, 78, 239-271.
- Faulds, J.E., Olson, E.L., Harlan, S.S., and McIntosh, W.C. (2002a). Miocene extension and fault-related folding in the Highland Range, southern Nevada: a three-dimensional perspective. *Journal of Structural Geology*, 24, 861-886.
- Faulds, J.E., Bell, J.W., and Olson, E.L. (2002b). *Geologic Map of the Nelson SW Quadrangle, Clark County, Nevada*. U.S. Geological Survey Nelson SW 7.5' Quadrangle.
- Faulds, J.E., Bell, J.W. and Olson, E.L., (2002c). Stratigraphic and Structural Framework of the Nelson SW Quadrangle, Clark County, Nevada, *Text and reverences for Nevada Bureau of Mines and Geology Map 134*, pg. 1-15.
- Ferry, J.M. & Watson, E.B. (2007). New thermodynamic models and revised calibrations for the Ti-in-zircon and Zr-in-rutile thermometers. *Contrib Mineral Petrol*, 154, 429-437.
- Fisher, R.V., (1984). *Pyroclastic Rocks*, Germany: Springer-Verlag Berlin Heidelberg
- Gioncada, A., Mazzuoli, R., and Milton, A.J. (2005). Magma mixing at Lipari (Aeolian Islands, Italy): Insights from textural and compositional features of phenocrysts, *Elsevier*, vol. 145, pg. 97-118.
- Glazner, A.F., Coleman, D.S. and Bartley, J.M. (2008). The tenuous connection between high-silica rhyolites and granodiorite plutons. *Geology*, vol. 36, pg. 183-186.
- Green, T.H. & Pearson, N.J. (1987). An experimental study of Nb and Ta partitioning between Ti-rich minerals and silicate liquids at high pressure and temperature, *Geochimica et Cosmochimica Acta*, vol. 51, pg. 55-62.

- Griffen, W.L., Powell, W.J., Pearson, N.J. and O'Reilly, S.Y. (2008). Appendix A2: GLITTER: Data Reduction Software for Laser Ablation ICP-MS, Mineralogical Association of Canada Short Course, Vancouver, B.C., vol. 40, pg. 308-311.
- Harper, B.E., Miller, C.F., Koteas, G.C., Cates, N.L., Wiebe, R.A., Lazzareschi, D.S., and Cribb, J.W. (2004). Granites, dynamic magma chamber processes and pluton construction: the Aztec Wash pluton, Eldorado Mountains, Nevada, USA, *Transactions of the Royal Society of Edinburgh: Earth Sciences*, vol. 95, pg. 277-295.
- Hawkins, D.P. & Wiebe, R.A., (2004). Discrete stoping events in granite plutons: A signature of eruptions from silicic magma chambers?, *Geology*, vol. 32, pg. 1021-1024.
- Hayden, L.A. & Watson, B.E., (2007). Rutile saturation in hydrous siliceous melts and its bearing on Ti-thermometry of quartz and zircon. *Earth and Planetary Science Letters*, 258, 561-568.
- Hayden, L.A., Watson, E.B., & Wark, D.A., (2008). A thermobarometer for sphene (titanite), *Contributions to Mineralogy and Petrology*, vol. 155, pg. 529-540.
- Leslie, S., Miller, J., Miller, C., Wooden, J., and Fualds, J., (2007). Magmatic construction of the Searchlight magmatic system (Eldorado-Newberry Mountains, Nevada) as revealed through zircon geochemistry and Ti-in-zircon geothermometry, *Eos Trans. AGU*, 88(52), Fall Meet. Suppl., Abstract V51C-0707.
- Luo, Y. and Ayers, J.C., (2007). Instructions for in-situ LA-ICPMS analysis, Version 2. Vanderbilt University Department of Earth and Environmental Sciences.
- Lucchi, F., Tranne, C.A., De Astis, G., Keller, J., Losito, R., and Morche, W. (2008). Stratigraphy and significance of Brown Tuffs on the Aeolian Islands (southern Italy), *Journal of Volcanology and Geothermal Research*, vol. 177, pg. 79-70.
- Mastin, L.G. (2005). The controlling effect of viscous dissipation on magma flow in silicic conduits, *Journal of Volcanology and Geothermal Research*, vol. 143, pg. 17-28.
- Mazdab, F.K., Wooden, J.L., and Barh, A.P. (2007) Trace element variability in titanite from diverse geologic environments, *GSA Abstracts with Programs*, 39(6): 406.
- McDowell, F.W., McIntosh, W.C., and Farley, K.A., (2004). A precise ^{40}Ar - ^{39}Ar reference age for the Durango apatite (U-Th)/He and fission-track dating standard, *Chemical Geology*, vol. 214, pg. 249-263.

- McPhie, J., Doyle, M., and Allen, R. (1993). Volcanic Textures: A guide to the interpretation of textures in volcanic rocks. Printing Authority of Tasmania: Tasmania.
- Metcalf, R.V., (2004). Volcanic-plutonic links, plutons as magma chambers and crust-mantle interaction: a lithospheric scale view of magma systems. *Transactions of the Royal Society of Edinburgh: Earth Sciences*, 95, 357-374.
- Miller, C.F. & Miller, J.S. (2002). Contrasting stratified plutons exposed in tilt blocks, Eldorado Mountains, Colorado River Rift, NV, USA. *Lithos*, 61, 209-224.
- Miller, J.S., Faulds, J.E., Miller, C.F., Wooden, J.L., Dodge, M., Bazar, D., Leslie, S., Aggarwal, J. (2007). Growth, eruption, solidification, fractionation, and rejuvenation of a large felsic magmatic system, Eldorado-Newberry Mountains, Nevada (USA). *IUGG-International Association of Volcanology and Chemistry*, Abstract.
- Olson, E.L., Faulds, J.E., and Harlan, S.S., (1999). *Miocene extension and extension-related folding in the Highland Range, southern Nevada: Implications for hydrocarbon exploration*, Cenozoic Geology of the Northern Colorado River Extensional Corridor, Southern Nevada and Northwestern Arizona: Economic Implications of Regional Segmentation Structures, Nevada Petroleum Society 1999 Field Trip Guidebook, pg. 97-114.
- Pallister, J.S., Hoblitt R.P., Reyes A.G. (1992). A basalt trigger for the 1991 eruptions of Pinatubo volcano? *Nature*, 256, 426- 428.
- Perrault, D.S., Miller, C.F., Furbish, D.J., Faulds, J.E., and Miller, J.S., Giant country rock blocks within the Searchlight pluton, southern Nevada: *Geological Society of America Bulletin*, in review.
- Platz, T., Cronin, S.J., Cashman, K.V., Stewart, R.B., and Smith, I.E.M. (2007). Transition from effusive to explosive phases in andesite eruptions - A case-study from the AD1655 eruption of Mt. Taranaki, New Zealand, *Journal of Volcanology and Geothermal Research*, vol. 161, pg. 15-34.
- Prowatke, S. and Klemme, S., (2006). Rare earth element partitioning between titanite and silicate melts: Henry's law revisited, *Geochimica et Cosmochimica Acta*, vol. 70, pg. 4997-5012.
- Rollinson, H., (1993). Using geochemical data: evaluation, presentation, interpretation. Longman Group: England.

- Scandone, R., Cashman, K.V., and Malone, S.D., (2007). Magma supply, magma ascent and the style of volcanic eruptions. *Earth and Planetary Science Letters*, 253, 501-529.
- Simmons, E. C. and Hedge, C.E., (1978). Minor-Element and Sr-Isotope Geochemistry of Tertiary Stocks, Colorado Mineral Belt. *Contributions to Mineralogy and Petrology*, vol. 67, pg. 379-396.
- Walker Jr., B.A., Miller, C.F., Claiborne, L.L., Wooden, J.L., and Miller, J.S. (2007). Geology and geochronology of the Spirit Mountain batholith, southern Nevada: Implications for timescales and physical processes of batholith construction, *Journal of Volcanology and Geothermal Research*, vol. 167, pg. 239-262.
- Watson, E.B., Hoblitt R.P., Reyes A.G. (2006). Crystallization thermometers for zircon and rutile. *Contrib. Mineral Petrol*, vol. 151, 413-433.
- Watson, E.B. and Harrison, T.B., (1983). Zircon saturation revisited: Temperature and composition effects in a variety of crustal magma types, *Earth and Planetary Science Letters*, vol. 64, pg. 295-304.